



Exploring the Influence of Adipokines on Neuronal Function in Alzheimer's Disease

Neha Santoshkumar Tomar

School of Science, Engineering and Environment

The University of Salford, U.K.

Submitted in partial fulfilment of the requirements of the Degree of
Doctor of Philosophy (Ph.D.), 2021

DECLARATION

I certify that the thesis submitted to the University of Salford as partial fulfilment of the requirements for a Degree of Doctor of Philosophy, is a presentation of my own research work. Wherever contributions of others are involved, every effort is made to indicate this clearly with due reference to the literature and acknowledgement of collaborative research and discussions. The content of this thesis has not been submitted for a higher degree at this or any other university.

Contents

DECLARATION	1
ACKNOWLEDGMENT.....	13
Abbreviations	14
Abstract	18
CHAPTER 1. INTRODUCTION	19
1.1 DEMENTIA.....	19
1.1.1 Dementia epidemiology	19
1.1.2 Types of dementia	19
1.2. ALZHEIMER’S DISEASE.....	21
1.2.1 History and epidemiology: Alzheimer’s disease	21
1.2.2 Pathology of AD	23
1.2.3 Types of AD.....	24
1.2.3.1 EOAD.....	24
1.2.3.1 LOAD.....	24
1.2.4 Risk factors for AD	25
1.2.4.1 Genetic Risk Factors	25
1.2.4.2 Environmental and other risk factors	27
1.2.5 Molecular biology and pathology of AD	27
1.2.5.1 Amyloid cascade hypothesis	28
1.2.5.2 Tau cascade hypothesis	30
1.2.5.3 Inflammation hypothesis.....	32
1.2.5.4. Oxidative stress hypothesis	32
1.2.6 Therapeutic intervention	34
1.2.6.1 Current drugs.....	34
1.2.6.2 Drugs in trial	37

1.2.6.3 Risk reduction approaches	37
1.3 OBESITY	38
1.3.1 Classification & epidemiology.....	39
1.3.2 Association with dementia	40
1.4 ADIPOSE TISSUE AND ADIPOKINES.....	42
1.4.1 The normal role of adipose tissue	42
1.4.2 Adipokines	44
1.4.2.1 Leptin	45
1.4.2.2 Resistin.....	45
1.4.2.3 Chemerin.....	46
1.4.3 Adipose tissues and adipokines in obesity	47
1.4.4 Adipose tissue and adipokines in neurodegeneration	50
1.5 OXIDATIVE STRESS	52
1.5.1 Oxidative stress in obesity	53
1.5.2 Oxidative stress in Alzheimer’s disease.....	54
1.6 CELLULAR MODELS: Exploring AD, obesity & oxidative stress relation.....	55
1.6.1 H ₂ O ₂ induced oxidative stress.....	55
1.6.2 SHSY5Y cells	56
1.6.3 3T3-L1 cells	58
1.6.4 Skin-derived fibroblasts cells.....	58
AIM OF THE STUDY	59
OBJECTIVES	59
Chapter 2. Materials and Methods	60
2.1 Materials.....	60
2.2. Methods.....	65
2.2.1. Cell culture.....	65

2.2.1.1 Image Analysis:.....	66
2.2.2. Cell culture maintenance.....	67
2.2.2.1. Thawing of frozen cells.....	67
2.2.2.2. Sub-culturing.....	67
2.2.2.3. Cryopreservation.....	68
2.2.3. Establishing an adipocyte-like cell culture model.....	68
2.2.3.1. Maintenance and expansion of 3T3-L1.....	69
2.2.3.2. Differentiation of 3T3-L1 to adipocyte-like cells.....	69
2.2.3.3. Confirmation of 3T3-L1 differentiation.....	70
2.2.4. Establishing neuronal-like cell culture model.....	70
2.2.4.1 Maintenance and expansion of SHSY5Y cells.....	71
2.2.4.2 Differentiation of SHSY5Y cells into neuronal-like cells.....	71
2.2.4.3. Optimization: Differentiation protocols.....	73
2.2.4.4. Confirmation of neuronal-like phenotype.....	73
2.2.4.5 Optimisation: primary/secondary Ab ratio.....	75
2.2.5 Establishing fibroblast cell culture.....	75
2.2.5.1 Maintenance and expansion of fibroblast cells.....	76
2.2.6 Measuring cell viability of cultured cells.....	76
2.2.6.1 General MTT assay protocol.....	76
2.2.6.2 Dose dependent assay on SHSY5Y cells using H ₂ O ₂	77
2.2.6.2.1 H ₂ O ₂ dose dependent assay on undifferentiated SHSY5Y cells.....	77
2.2.6.2.2 H ₂ O ₂ dose dependent assay on differentiated SHSY5Y cells.....	78
2.2.6.2.3 H ₂ O ₂ dose dependent assay on skin derived fibroblast cells.....	79
2.2.6.3 Investigating the effect of co-treatment using CM from 3T3-L1 cells on SHSY5Y cell viability.....	79
2.2.6.4 Effect of co-treatment using adipocyte-like and pre-adipocyte (3T3-L1) derived CM on oxidative stress induced cytotoxicity in differentiated and undifferentiated SHSY5Y cells.....	80

2.2.6.5 Investigating the co-treatment effect of commercial adipokines under oxidative stress on SHSY5Y cells response	82
2.2.6.6 Investigating the effect of commercial chemerin response on fibroblast cells	82
2.3 STATISTICAL ANALYSIS	83
Chapter 3. RESULTS	84
3.1 Cell culture	84
3.1.1 3T3-L1 cell culture	84
3.1.2 SHSY5Y cell culture	85
3.1.3 Fibroblasts cell culture	86
3.2 Differentiation of cell lines	88
3.2.1. 3T3-L1 differentiation: pre-adipocytes into adipocyte-like cells	88
3.2.1.1 Determination of differentiated 3T3-L1 by Oil-Red-O staining	90
3.2.1.1.1. PBS wash	90
3.2.1.1.2 Fixative solution	91
3.2.2 SHSY5Y differentiation:	93
3.2.2.1 Optimization of SHSY5Y cells differentiation protocol	93
3.2.2.1.1 Cell density	93
3.2.2.1.2 Ethanol concentration	94
3.2.2.1.3 Assessment of RA stability	95
3.2.2.2. Optimization of ICC to confirm SHSY5Y differentiation	97
3.2.2.3. SHSY5Y differentiation: 10-days protocol	101
3.2.2.3.1 Determination of differentiated SHSY5Y by ICC: 10-day protocol	104
3.2.2.4 SHSY5Y differentiation: 21-day protocol	107
3.2.2.4.1 Determination of differentiated SHSY5Y by ICC: 21-day protocol	109
3.2.2.5 Comparing 10-day and 21-day protocol for differentiation	112
3.3 Estimation of cell viability in oxidative stress	113

3.3.1. Optimization of H ₂ O ₂ dose on SHSY5Y cells	113
3.3.1.1. Effect of variable H ₂ O ₂ concentration on differentiated SHSY5Y cell viability at 12 hrs and 24 hrs	114
3.3.1.2 Effect of variable H ₂ O ₂ concentration on undifferentiated SHSY5Y cell viability at 12 hrs and 24 hrs	115
3.3.2 Exploring the effect of co-treatment using differentiated and undifferentiated (3T3-L1) derived conditioned media on oxidative stress induced cytotoxicity in differentiated and undifferentiated SHSY5Y cells.....	116
3.3.3. Exploring the effect of co-treatment using stressed adipocyte and pre-adipocyte (3T3-L1) derived CM on oxidative stress induced cytotoxicity in differentiated and undifferentiated SHSY5Y cells	118
3.3.4. Exploring the effect of co-treatment using stressed adipocyte and pre-adipocyte (3T3-L1) derived half CM change on oxidative stress induced cytotoxicity in differentiated and undifferentiated SHSY5Y cells.....	121
3.3.5. Understanding the effect of commercial adipokines on SHSY5Y cell viability	123
3.3.5.1 Effect of chemerin on differentiated and undifferentiated SHSY5Y cell viability in the presence and absence of H ₂ O ₂ induced oxidative stress	124
3.3.5.2 Effect of leptin on differentiated and undifferentiated SHSY5Y cell viability in the presence and absence of H ₂ O ₂ induced oxidative stress	125
3.3.5.3 Effect of resistin on differentiated and undifferentiated SHSY5Y cell viability in the presence and absence of H ₂ O ₂ induced oxidative stress	127
3.3.6 Understanding the effect of commercial chemerin on human skin derived fibroblast cell viability	128
3.3.6.2 Comparing the effect of chemerin (10nM) on non-AD and AD donors skin derived fibroblasts under H ₂ O ₂ induced oxidative stress.....	130
3.3.6.3 Comparing the effect of chemerin (20nM) on non-AD and AD patient skin derived fibroblasts under H ₂ O ₂ induced oxidative stress.....	131
Chapter 4. DISCUSSION	132
4.1. Consideration of the cellular models used in this study.....	135

4.2. Consideration of different concentrations of H ₂ O ₂ to induce oxidative stress	139
4.3. Considering use of conditioned media technique to evaluate the role of an adipokine rich environment on cultured neuronal cell viability under H ₂ O ₂ induced oxidative stress	141
4.3.1. Does conditioned media from adipocyte-like possess neuroprotective effects against H ₂ O ₂ induced oxidative stress in neuronal -like cells?.....	142
4.3.2. What is the effect of conditioned media from H ₂ O ₂ stressed-adipocyte-like on the viability of neuronal-like cells under oxidative stress?	144
4.3.3 Do adipokines in half condition media change from adipocyte-like possess neuroprotective effect in co-treatment with neuronal-like cells under oxidative stress?.....	146
4.4 Do commercial adipokines have neuroprotective potential under oxidative stress?	148
4.5. Does commercial chemerin have protective effect in AD-like condition under oxidative stress?	151
Future Work	153
APPENDIX.....	155
5.1. Understanding the impact of H ₂ O ₂ on cell viability in oxidative stress.....	155
5.1.1. Pre-treatment:.....	156
5.1.2. Post-treatment	157
5.1.3 Understanding the effect of CM from differentiated 3T3-L1 cells after recovery from H ₂ O ₂ induced stressed on the differentiated SHSY5Y cells.	158
5.2 To estimate the cytometric responsiveness of chemerin on SHSY5Y cells	160
5.3 Impact of H ₂ O ₂ induced oxidative stress on mitochondrial function using dichlorodihydrofluorescein diacetate (DCFDA) assay in undifferentiated SHSY5Y cells.....	162
REFERENCES.....	164

List of Figures

Figure 1.1 Types of dementia	20
Figure 1.2 Neurodegenerative disease causes dementia	20
Figure 1.3 Early and late stage sketches of neurofibrillary tangles	22
Figure 1.4 Atypical atrophy pattern in AD	23
Figure 1.5 Alzheimer's disease related genes	25
Figure 1.6 APOE plays vital role in AD pathogenesis	26
Figure 1.7 Amyloid cascade hypothesis	28
Figure 1.8 Amyloid precursor protein processing showing 3 cleavage sites	29
Figure 1.9 Toxic forms of A β	30
Figure 1.10 Tau hyperphosphorylation.	31
Figure 1.11 Hypothetical presentation of neuronal death in AD due to oxidative stress	33
Figure 1.12 Molecular mechanism and pathology of AD due to oxidative stress	34
Figure 1.13 The epitome location on the A β sequence.....	35
Figure 1.14 The aetiological factors of AD and the therapeutic intervention points	36
Figure 1.15 Prevalence of obesity	39
Figure 1.16 Glycotoxins induces hyperproduction of advanced glycation end products.....	41

Figure 1.17 AT acts as an endocrine organ and regulate various metabolic pathways44

Figure 1.18 Change in adipose tissue in the lean and obese condition with their physiological effects.....47

Figure 1.19 Increased resistin levels48

Figure 1.20 Chemerin in obesity condition49

Figure 1.21 Mid-life obesity as risk factor for AD development.....51

Figure 1.22 Oxidative stress induced mitochondrial dysfunction lead to metabolic disorders and AD53

Figure 2.1 Schematic diagram represents the general steps involved in the CM technique.....80

Figure 2.2 Three different co-treatment conditions were used with CM from 3T3-L1 cells on the SHSY5Y cells (differentiated and undifferentiated)81

Figure 3.1 Observation of 3T3-L1, pre-adipocyte cell culture.....85

Figure 3.2 Progression of SHSY5Y cell culture confluency: SHSY5Y cells.....85

Figure 3.3 Cell morphology of skin derived fibroblasts from non-AD donors after 48 hrs of culture.....86

Figure 3.4. Cell morphology of skin derived fibroblast from AD donors after 48 hrs of cell culture.87

Figure 3.5 Microscopic overview of 3T3-L1 cell culture progressive differentiation from pre-adipocytes into mature adipocytes over 3 weeks89

Figure 3.6 Optimization of Oil-Red-O staining90

Figure 3.7 Optimisation of Oil Red-O staining.....92

Figure 3.8 Optimizing the initial cell density required for SHSY5Y differentiation after 48 hrs.....	94
Figure 3.9 Microscopic images of SHSY5Y cells displayed the impact of prepared RA on the viability of SHSY5Y cells.....	95
Figure 3.10 Microscopic images of SHSY5Y showing the impact of exposure of differentiation media to direct light on SHSY5Y cells	96
Figure3.11 Optimized immunofluorescence images of differentiated SHSY5Y cells are presented for NF.....	98
Figure 3.12 Optimized immunofluorescence images of differentiated SHSY5Y cells are presented for MAP2.....	99
Figure 3.13 Optimized immunofluorescence images of differentiated SHSY5Y cells are presented for NSE.....	100
Figure 3.14 Morphological changes in SHSY5Y cells during the neuronal differentiation progression when 10-day protocol was followed, in presence of RA (10µM).	102
Figure 3.15 Immunofluorescence images representation after RA-mediated 10-days differentiation.....	105
Figure 3.16. Morphological changes in SHSY5Y cells during the RA mediated neuronal differentiation (21-day protocol).....	108
Figure 3.17. Immunofluorescence images after RA mediated 21-days differentiation.....	110
Figure 3.18 Impact of H ₂ O ₂ dose on cell viability in differentiated SHSY5Y cells (12 hrs and 24 hrs incubation)	114
Figure 3.19 The impact of H ₂ O ₂ dose on cell viability of undifferentiated SHSY5Y cells (12hrs and 24hrs incubation)	115
Figure 3.20 To explore the impact of co-treatment using differentiated and undifferentiated 3T3-L1 derived CM on oxidative stress induced cytotoxicity in differentiated and undifferentiated SHSY5Y cells	117

Figure 3.21 To explore the impact co-treatment using differentiated 3T3-L1 (or non-stressed in this study), stressed differentiated 3T3-L1 and undifferentiated 3T3-L1 derived CM on oxidative stress induced cytotoxicity in differentiated (neuronal-like) and undifferentiated (non-neuronal) SHSY5Y cells.	120
Figure 3.22 To investigate the effect of co-treatment using half media change condition derived from differentiated 3T3-L1 (or non-stressed in this study), stressed differentiated 3T3-L1 and undifferentiated 3T3-L1 on oxidative stress induced cytotoxicity in differentiated and undifferentiated SHSY5Y cells.	122
Figure 3.23 Exploring the impact of commercially available chemerin on differentiated SHSY5Y cell viability.....	124
Figure 3.24 Exploring the impact of commercially available leptin on H ₂ O ₂ induced oxidative stress in differentiated (neuronal-like) and undifferentiated (non-neuronal) SHSY5Y cells.....	126
Figure 3.25 Exploring the impact of commercially available resistin on differentiated (neuronal-like) and undifferentiated (non-neuronal) SHSY5Y cells with and without H ₂ O ₂ induced oxidative stress.....	127
Figure 3.26. Exploring the impact of different doses of H ₂ O ₂ for 15 mins to induce oxidative stress in fibroblast cells.....	129
Figure 3.27. Exploring the impact of chemerin with and without H ₂ O ₂ induced oxidative stress for 15 mins using AD patient derived and non-AD fibroblast cells.....	130
Figure 3.28. Exploring the impact of chemerin with and without H ₂ O ₂ induced oxidative stress for 15 mins using AD patient derived and non-AD fibroblast cells.....	131
Figure 5.1 Impact on SHSY5Y cell viability after induction of oxidative stress H ₂ O ₂ as pre-treatment and CM was added after 24 hrs.....	156
Figure 5.2 Impact on SHSY5Y cell viability using CM (added before 24 hrs) and subsequent induction of oxidative stress as post-treatment with H ₂ O ₂	157
Figure 5.3 The impact of recovered CM after being oxidised with H ₂ O ₂ for 24 hrs on the differentiated SHSY5Y cells in comparison to the control.....	159
Figure 5.4 The anti-apoptotic properties of chemerin (5nM) was explored.....	161

Figure 5.5. Fluorescence images of undifferentiated cells using DCFDA assay.....163

List of Tables

Table 1.1 Illustrates comparative difference between types of adipose tissues.....43

Table 2.1 The table below enlists the experimental materials used in this research.....60

Table 2.2. The skin derived fibroblast cells were used in this study and presented in the given table.....66

Table 2.3 Optimization of primary and secondary Ab using different dilutions or ratios trialled to obtain the accurate combination for ICC protocol75

Table 3.1 Final antibody ratio used for the concluding ICC SOP followed by SHSY5Y differentiation101

Table.3.2. The table below compares the features and results obtained from RA-mediated 10- and 21-day protocols in the efficacy to achieve neuronal differentiation.....112

ACKNOWLEDGMENT

Firstly, I would like to thank my supervisors Dr. Sarah Withers and Dr. Gemma Lace-Perrin, without which this PhD would not have been possible and for the countless outstanding opportunities they offered me regarding both research and scientific communications opportunities, such as conference and science festival engagements. I would like to thank them for their continuous help, support, and encouragement through really difficult times. I would not have gained so many skills and have completed my PhD without them.

Additionally, I would like to thank Rumana Rafiq, Manishadevi Patel, Dr. Muna Abubaker and Helen Bradshaw for their help in the laboratory, for providing reagents and guidance on how to use different laboratory equipment as well as academics Dr. Athar Aziz, Dr. Arijit Mukhopadhyay, Dr. Geoff Hide and Dr. Niroshini Nirmalan who have supported me throughout my PhD. I would like to convey my special thanks to my TDL family for motivating and cheering me up in my bad times and above all believing in me. I would like to extend my special thanks to Dr. Priyanka P. Patel for her continuous motivation, emotional support and advices for research and personal life, who is like elder sister to me more than just my flatmate.

Thanks to all Ph.D. colleagues and Postdocs from TM lab who helped and supported me specially Dr. Marco and Dr. Gloria and everyone in the laboratory who helped me with different techniques and obtaining results. I would also like to thank Dr. Ashutosh Pathak, Dr. Diana M. Stan, Dr. Bader Alawfi Louisa Barbato, Richard Heale, Dr. Gary Kerr, Sowmya Chinta, Toby Aarons, Dr. Natasha H., Toni Dewhurst, Nazila, Nayab and Dr. Ayed for their unconditional friendship and continuous emotional support. I would also like to thank Dr. Sara Rollinson from the University of Manchester for helping me with the differentiation training and sharing relevant research ideas.

I dedicate this thesis to my parents especially my father, because of them I am here today. I would like to thank my family above all, for their continued support throughout my tough times, who offered unconditional mental, emotional, and financial support as well as motivating me to never give up and get to where I am today. I would like to dedicate my achievement to my father Santoshkumar, my mother Shashibala, my sisters Swati and Neha, my brothers Aman and Bhushan, and my nieces Vibhuti and Aditi and niece Advik.

Abbreviations

A β	Amyloid-beta
AChE	Acetylcholinesterase
AD	Alzheimer's diseases
AGEs	Advanced glycation end products
Akt	Protein kinase B
ALDH2	Aldehyde dehydrogenase 2
APP	Amyloid precursor protein
AT	Adipose tissues
ATCC	American type culture collection
BACE	Beta secretase
BBB	Blood-brain barrier
Bcl-2	B-cell lymphoma
BDNF	Brain-derived neurotrophic factor
BeAT	Beige adipose tissue
BK	Bradykinin
BSA	Bovine serum Albumins
CCL2	Chemokine ligand receptor 2
ChEIs	Cholinesterase inhibitors
CMKLR2	Chemerin chemokine-like receptor 2
CM	Conditioned media
CNS	Central nervous system
CO ₂	Carbon dioxide

Conc ⁿ	Concentration
dH ₂ O	Distilled water
DAPI	4',6-diamidino-2-phenylindole
DMEM	Dulbecco's modified eagle's medium
DMSO	Dimethyl sulphoxide
DNA	Deoxyribonucleic acid
EOAD	Early onset Alzheimer's disease
ECACC	European collection of cell cultures
FBS	Fetal bovine serum
FCS	Fetal calf serum
FTDP	Frontotemporal dementia with Parkinsonism
GAP-43	Growth- associated protein-43
GLP-1	Glucagon like peptide 1
GLUT4	Glucose transporter type 4
GPR1	G-protein coupled receptor 1
hASC	Human adipocyte derived mesenchymal cells
Hrs	Hours
HRP	Horseradish peroxidase
H&L	Heavy and light chain
H ₂ O ₂	Hydrogen peroxide
IBMX	Isobutylmethylxanthine
ICC	Immunocytochemistry

IDO	Indoleamines 2,3-dioxygenase
IFN- γ	Interferon gamma
IgA	Immunoglobulin A
IgG	Immunoglobulin G
IgM	Immunoglobulin M
IHC	Immunohistochemistry
IL	Interleukin
IR	Insulin resistance
IRS2	Insulin receptor substrate 2
JAK2	Janus kinase2
LOAD	Late onset Alzheimer's disease
MAP 2	Microtubule associated protein 2
MEM	Minimum Essential Medium
MP1	Metalloproteinase
NADPH	Nicotinamide adenine dinucleotide phosphate
NFTs	Neurofibrillary tangles
NIA	National Institute of Aging
NK cells	Natural killer cells
NMDA	N-methyl-D-aspartate
NO	Nitric oxide
NSE	Neuron specific enolase
PBS	Phosphate buffer saline

PCR	Polymerase chain reaction
PE	Phycoerythrin
PHF	Paired helical filaments
PPAR- γ	Peroxisome proliferator activated receptors gamma
P/S	Penicillin/Streptomycin
PKA	Protein kinase A
RA	Retinoic acid
RNS	Reactive nitrogen species
ROS	Reactive oxygen species
ROM	Reactive oxygen metabolites
sAPP β	Soluble APP-beta peptides
SAG	Surface antigen
SIRT-1	Sirtuin- 1
STAT3	Signal transducer & activator of transcription3
SV2	Synaptic vesicle protein II
SYN	Synaptophysin
TGF- β 1	Transforming growth factor- beta 1
TLRs	Toll-Like Receptors
TNF- α	Tumor necrosis factor alpha
TREM2	Triggering receptor expressed on myeloid cells 2
TRP	Transient receptor potential
UK	United Kingdom
VEGF	Vascular endothelial growth factor

Abstract

Alzheimer's disease (AD) is one of the major causes of dementia. Alzheimer's disease is an irreversible, slow neurodegenerative disease leading to memory and language impairment and amyloid- β plaques and intraneuronal neurofibrillary tangles are the characteristic pathology of AD. Studies have shown that obesity is major risk factor in Alzheimer's disease. While obesity related modulation has been suggested to influence AD pathogenesis, the molecular mechanisms involved are still unclear. Recent research has shown that adipocytes can actively secrete adipokines and these adipokines may possess the ability to influence AD pathology, but it remains poorly understood how adipokines impact neural functioning. The current study was focused on the potential neuroprotective effect of adipokines on the neurons during hydrogen peroxide (H_2O_2) induced oxidative stress and cell death. In this study, human neuroblastoma SHSY5Y cells were differentiated using retinoic acid to demonstrate neuronal-like characteristics which was confirmed by immunocytochemistry (ICC). The pre-adipocytes 3T3-L1 cells, were chemically differentiated to exhibit adipocyte-like characteristics (determined by Oil-Red-O staining). To understand the potential rescue effect of conditioned media from adipocyte-like cells on neuronal-like cells, and commercially available adipokines (chemerin, leptin and resistin) on neuronal-like cells and effect of chemerin on human skin fibroblast cells derived from AD and non-AD donors, MTT assay was performed in the presence and absence of H_2O_2 induced oxidative stress. Conclusively, the conditioned media and commercial adipokines showed protective effects on the neuronal-like cells (* $p < 0.05$, ** $p < 0.01$, *** $p < 0.001$) in comparison to the non-neuronal cells and chemerin showed no protective effect in AD patient derived cells under H_2O_2 induced oxidative stress in comparison to the non-AD donors derived fibroblast cells. Neuroprotection was not observed in the obesity mimicked induced oxidative stress condition. Our findings suggested that the adipokines might play vital role in neuronal-like cellular metabolic protection against oxidative stress and warrants further investigation of the role of adipokines dysregulation in Alzheimer's disease.

CHAPTER 1. INTRODUCTION

1.1 DEMENTIA

Dementia is a clinical syndrome affecting 47 million people worldwide and this number is expected to increase to 131 million by 2050 (Arvanitakis et al., 2019). It is caused by a number of diseases, the most common of which is Alzheimer's disease (Rossor et al., 2010). Dementia is characterised by behavioural, cognitive, and psychological symptoms such as memory loss, confusions, agitation, apathy, disinhibition, delusions, hallucination, sleep, or appetite changes (Weller & Budson, 2018).

1.1.1 Dementia epidemiology

850,000 people in the United Kingdom (UK) are living with dementia and this figure is estimated to increase approximately to 1 million by 2025 (ARUK, dementiastatistics, 2021). Dementia is leading cause of death in UK and the total cost to the UK economy is £13.9 billion each year (Public Health England, 2018). Dementia is the only condition among top 10 causes of mortality without a treatment to prevent, cure or slow disease progression. A higher prevalence of dementia has been observed in the aging population, with 1 in 14 people over the age of 65 and 1 in 6 over the age of 80 (ARUK, dementiastatistics, 2021). This substantial socioeconomical impact on society, as well as the personal impact on dementia patients and families, highlights the urgent need for the development of new therapeutic interventions.

1.1.2 Types of dementia

Dementia is an umbrella term used to describe a set of heterogenous conditions caused by a number of diseases, including AD, dementia with Lewy bodies (LBD), vascular dementia (VaD), alcohol related brain damage, mixed Alzheimer's/vascular dementia, dementia in Parkinson's disease, posterior clinical atrophy and Huntington's disease. Out of these dementia types, the percentage of occurrence is higher in the population of some of them, including: AD, VaD, mixed Alzheimer's/vascular dementia, LBD and dementia in Parkinson's disease (DementiaUK, 2017), as shown in figure 1.1.

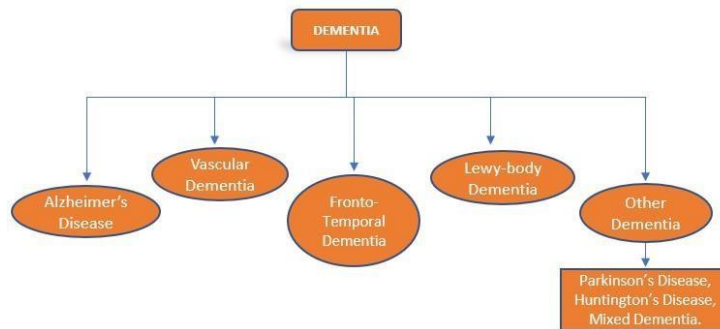


Figure 1.1. Types of dementia. Two-thirds of dementia patients are diagnosed with AD. Other types of dementia include vascular dementia, dementia with Lewy body, mixed dementia, when Alzheimer’s disease is diagnosed with vascular dementia or Lewy body dementia or both are diagnosed, Parkinson’s disease, Huntington’s disease. Adapted from ARUK, dementiastatistics, (2021).

Alzheimer’s disease is the most common form of dementia, being reported to underlie 62% dementia cases in the UK (approximately 505,813 people) as shown in figure 1.2. The second most common form of dementia is vascular dementia, that contributes 17% of dementia cases and affecting around 138,691 people in the UK. 10% of cases are a result of mixed dementia, and following this, 4% and 2% cases recorded were diagnosed with LBD and frontotemporal dementia, respectively. Whereas dementia with Parkinson’s disease affects approximately 16,317 people i.e., 2% out of overall dementia cases (Alzheimer’s society, 2016).

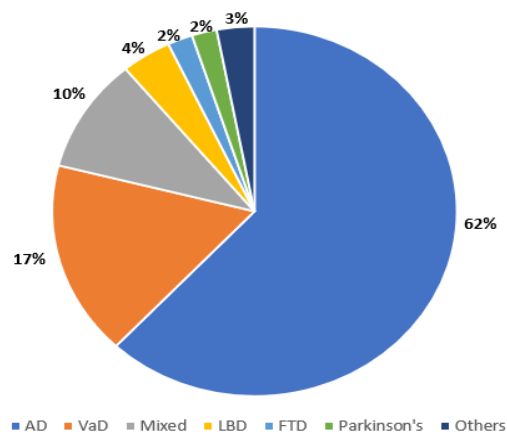


Figure 1.2. Neurodegenerative disease causes dementia. Alzheimer’s disease is most common diagnosis following the vascular dementia, mixed dementia, LBD, frontotemporal dementia, dementia with Parkinson’s disease and other neurodegenerative disease. AD- Alzheimer’s disease, VaD- Vascular dementia, LBD- Lewy body dementia, FTD- Frontotemporal dementia. Adapted from Alzheimer’s society, (2016).

1.2. ALZHEIMER'S DISEASE

AD is the most common cause of dementia and is symptomatically characterized by the progressive decline in cognitive function alongside personality and behavioural changes.

Typically, AD progresses in three stages: mild (early-stage), moderate (middle-stage), and severe (late-stage) (ARUK, dementia statistics, , 2021). The early-stage symptoms are marked as depression, difficulty in understanding language and memory impairment. At the moderate stage of AD, the basic daily activities of life become affected and symptoms such as dyspraxia, reduced decision-making skills may develop. In the severe/late stage of AD, symptoms get worsen and further progresses to social withdrawal, severe behavioural changes, and psychotic symptoms (Wattmo et al., 2016). In this disease, death can occur due to lack of nutrition, lost memory for the basic life survival activities (such as swallowing) but infection (such as pneumonia) is the most common cause of death in AD (Bird, 2015).

The standard diagnosis for AD is made through examination of patient's history in relation to the cognitive and functional changes over the time, as well as a full physical examination including a neurological examination to rule out other causes of present symptoms (Dubois et al., 2016).

Despite much being known about the molecular biology of AD, there are still no disease modifying therapies and this is likely a consequence of complexity of the disorder and the variety of genetic and environmental risk factors associated with this disease. Understanding how each of these risk factors contributes to the disease is vital while new therapeutic approaches are to be developed which can be prevented.

1.2.1 History and epidemiology: Alzheimer's disease

AD was named after a German clinical psychiatrist and neuroanatomist, Alois Alzheimer, a lecturer at the Munich University Hospital. On November 3, 1906, at 37th Meeting of South-West German Psychiatrists held in Tubingen, Germany, he reported 'a peculiar severe disease process of cerebral cortex' of an in-patient suffering from paranoia.

Mr. Alzheimer's gave a lecture on the distinguishing plaques and neurofibrillary tangles in the brain histology report from a 50-year-old female patient, Auguste Deter. His colleague published an article on 'Alzheimer's disease' in 1910 describing Alois Alzheimer's text report in the 3rd edition of *Psychiatrie*, crediting him by coining this term (Hippius & Neundörfer, 2003).

In year 1911, the female patient died aged 55 and Alois published a paper presenting the post-mortem brain histology sketches of the patient by using then new silver staining histological technique (Bondi et al., 2017). As shown in figure 1.3, the morphological changes of neuronal cells was published during the early and late stage of AD derived from patient Auguste Deter by Mr. Alzheimer. Different stages of neuronal damage was observed and represented the level of brain damage occurred due the diseased condition.

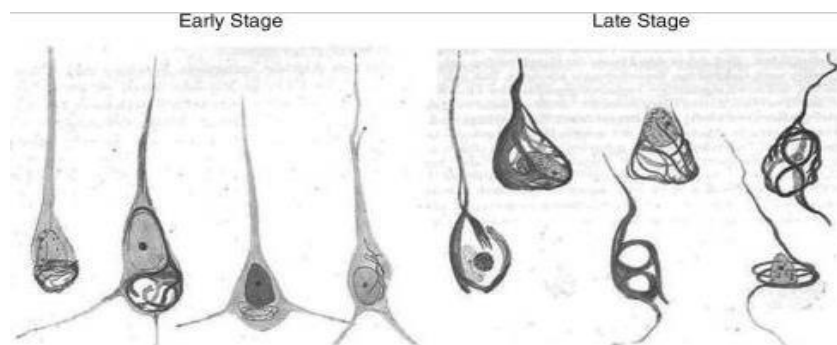


Figure 1.3 Early and late-stage sketches of neurofibrillary tangles. The morphology of neurofibrillary tangles from the patient Auguste Deter drawn by Alois Alzheimer in paper published in 1911. Adapted from Bondi, (2017).

In the UK, approximately two thirds of all dementia cases (approximately 850,000 people) have Alzheimer's disease, affecting approximately 500,000 people (ARUK, dementiastatistics, 2021). Globally, it is estimated that by 2050, 115.4 million people will be living with dementia, out of which 60-70% of the population will be affected with AD (Li & Liu, 2016). According to World Health Organisation (WHO), each year nearly 10 million new cases are being registered, out of which higher percentage of cases are occurring in low-income countries with poor medical facilities (WHO, 2020). Efforts are being made by the government towards dementia research funding and it is estimated that between 2012-15, approximately £60 million a year was funded (ARUK, dementiastatistics, 2021).

1.2.2 Pathology of AD

Two main pathological hallmarks of AD are amyloid-beta ($A\beta$)-containing senile plaques and the intracellular tau neurofibrillary tangles that interfere in normal synaptic signalling leading to reduced neuronal function and results in neuronal loss (Querfurth & Laferla, 2010). This neuronal loss leads to the cortical atrophy, reduced brain volume and subsequent loss of brain function, as shown in figure 1.4. The diagnosis of AD by assessment of atrophy patterns and vascular lesions using recorded neuroimaging is becoming a popular and useful tool as a systematic approach (Vernooij & Buchem, 2020).

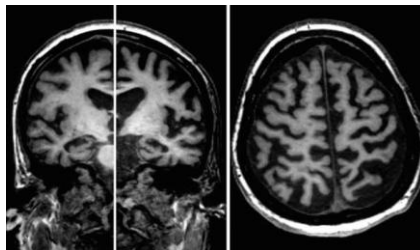


Figure 1.4. Atypical atrophy pattern in AD. The T1-weighted brain image of 70-year-old female clinically diagnosed with dementia is shown, with clear signs of bilateral cortical atrophy which is typical sign of late onset stage of AD. Adapted from Vernooij & Buchem, (2020).

Glial cells are non-neuronal cells which are present in the close vicinity of neuronal cells providing support and protection. These cells are a heterogenous mixture of microglial cells, astrocytes and oligodendrocyte lineage cells (Jäkel & Dimou, 2017). The coordinated interaction between neuronal and glial cells is important for synaptic homeostasis. However, in past few decades evidence of glial dysfunction in AD is increasing which influences the neuronal and glial receptors by mediating the $A\beta$ toxicity (Iqbal et al., 2016; Nordengen et al., 2019). Accumulating evidence confirms that apart from the neuropathological symptoms, the progression of AD is closely linked to the limbic systems, neocortical regions as well as basal forebrain, damages of synapses, degradation of axons and eventually the dendritic atrophy (Crews & Masliah, 2010; Perlson et al., 2010; Grutzendler et al., 2007; Serrano-Pozo et al., 2011). In early AD, microglial cells act as a protective factor by enhancing the neuronal repair, digesting the oligomers of $A\beta$. However, the hyper-activated microglia also increase the release of pro-inflammatory factors and enhance the oxidative stress by induction of ROS leading to neuropathologies (Pan et al., 2011; Guo et al., 2020). The impact of oxidative stress on the neuropathology will be discussed in detail later in section 1.5.

1.2.3 Types of AD

AD can be sub-divided in two types: early-onset AD, also known as EOAD and late-onset AD, also called as LOAD (Iqbal et al., 2014). The development of EOAD and LOAD is slow and eventually result in severe symptoms. In both cases of EOAD and LOAD, the neuropathological changes involves the progression of brain region and neuronal damage resulting into irreversible loss of function (Bekris et al., 2010).

1.2.3.1 EOAD

The onset of AD at the age less than 65 years has been considered as EOAD and only 1% - 2% of AD cases are accounted to EAOD, also known as familial AD (Zhu et al., 2015). In EOAD, mutation in 3 genes: *amyloid precursor protein (APP)*, *presenilin 1 (PSEN1)* and *presenilin 2 (PSEN2)* were attributed to genetic mutation (Reitz et al., 2020). *APP* mutations have been reported and observed in less than 1% of EAOD cases, *PSEN1* mutations in 6% and *PSEN2* mutations in 1% of total EOAD cases (Cacace et al., 2016). These mutations affect (*APP, PSEN 1&2*) the amyloidogenic pathway which results in the inappropriate sequential cleavage of APP protein and increased generation of A β leading to accumulation of amyloid plaques (Ayodele et al., 2021). The physiological role of these genes, their associated proteins and implication in AD will be explored in the discussion section in relation to the skin derived fibroblast cells.

1.2.3.1 LOAD

LOAD onset cases are more frequent and common among AD patients and usually affect patients over 65 years (Rosenthal & Kamboh, 2014). LOAD is also known as sporadic AD and out of overall AD cases, high number of cases falls under this category and affects nearly 90-95% of elderly people (Zhang et al., 2020).

Studies have shown that the polygenic mutation may cause the occurrence of LOAD, instead of single gene mutation (Dai et al., 2017). Polymorphism in the *apolipoprotein E (APOE)* genotype, which encodes brain's major cholesterol transporter protein APOE, is the major risk factor for LOAD onset (detailed in section 1.2.4.1). A study demonstrated that mutation in 3 alleles of *APOE* contributes

towards increased risk of AD development and their frequency of occurrence worldwide are: $\epsilon 2$ (8.4%), $\epsilon 3$ (77.9%) and $\epsilon 4$ (13.4%) (Gu et al., 2013). Another identified LOAD-related gene is *triggering receptor expressed on myeloid cells2 (TREM2)*, but its exact role in relation to LOAD is unknown (Bagyinszky et al., 2014).

1.2.4 Risk factors for AD

1.2.4.1 Genetic Risk Factors

AD causative genetic mutations and risk enhancing gene polymorphisms have been reported on four different chromosomes, each locus being named as AD1, AD2, AD3 and AD4, as shown in figure 1.5. The *APP* gene is located on chromosome 21q21, the *APOE* gene is positioned on chromosome 19q13.32, *PSEN1* is present on chromosome 14q24.2 and the *PSEN2* gene is located on chromosome 1q42.13 (Bekris et al., 2010).

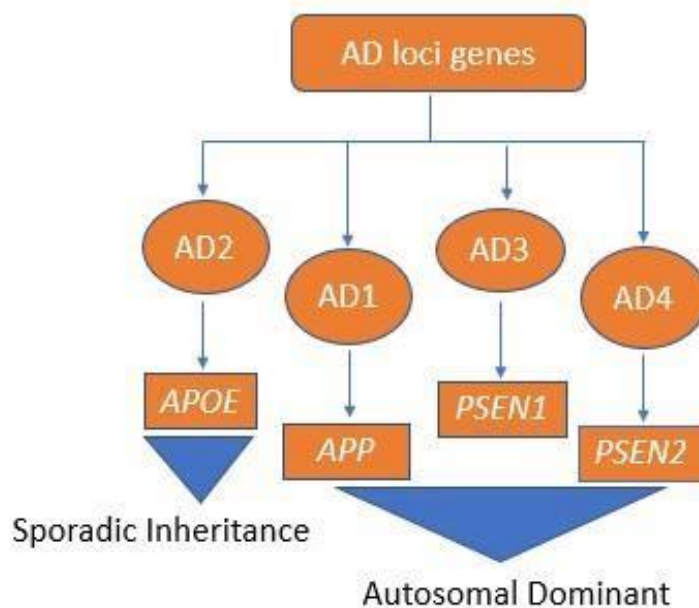


Figure 1.5. AD related genes. The mutative loci genes responsible to cause AD are AD1, AD2, AD3 and AD4. AD2 mutation in *APOE* results in development of sporadic inherited AD and AD 1,3 and 4 mutation results in *APP*, *PSEN1* and *PSEN2* which increases risk of autosomal dominant AD. Adapted from Bekris et al., (2010).

Amyloid- β serves as an important contributor to the repair function of neuronal cells, for example, any synaptic damage repair, recovery from neuronal injury or infection; these roles are supported by in-vitro as well as in-vivo studies (Brothers et al., 2018). *APP*, *PSEN1* and *PSEN2* mutations alter the processing of APP which results in increased production of the toxic A β 42 fragment, which aggregates extracellularly and interferes with normal neuronal functioning (Lanoiselée et al., 2017). The process of toxic A β 42 fragment generation will be explored in detail in section 1.2.5.1.

APOE is a major cholesterol carrier implicated in lipid transport, repair in the brain and *APOE* polymorphic alleles are the main genetic determinants for AD (Liu et al., 2013). It exists in three isoforms: E2 encoded by $\epsilon 2$ gene, E3 encoded by $\epsilon 3$ gene and E4 encoded by $\epsilon 4$ gene of the chromosome. Individuals carrying two copies of the $\epsilon 4$ alleles having the strongest genetic risk of AD, whereas the $\epsilon 2$ alleles are known to decrease the risk (Harold et al., 2009). The mechanism by which APOE genotype impacts AD risk is varied and complex, as indicated in figure 1.6, since theories of both toxic gain and loss of function have been proposed. Interestingly, some studies have supported synergistic effects of APOE genotype and obesity in relation to AD risk (Jones et al., 2018) and this concept will be explored in more detail in discussion chapter.

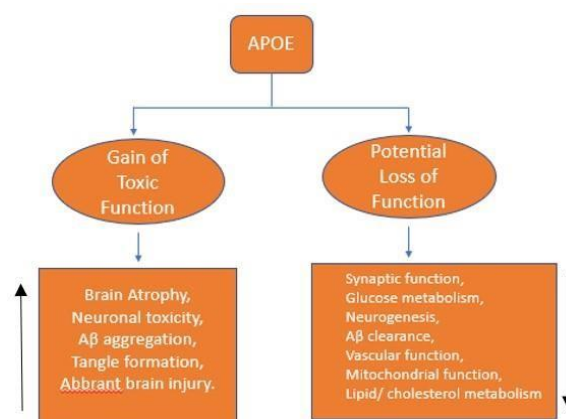


Figure 1.6. APOE plays vital role in AD pathogenesis. APOE mutation leads to the increased brain atrophy, neurofibrillary tangles formation and tau phosphorylation, loss of synaptic and mitochondrial function. Adapted from Liu et al., (2013).

In an animal study, it has been documented that the triplication of chromosome 21 (also known as Trisomy 21) upregulates the neurofibrillary tangle formation and neurodegeneration induced by excess A β accumulation. Therefore, individuals with trisomy 21 are at higher risk of developing dementia with increased age (Wiseman et al., 2018).

The duplication of APP without trisomy 21 also causes the EOAD (Rovelet-Lecrux et al., 2006). TREM2 is myeloid cell surface receptor which is vital for the signal transduction regulating major microglial function such as phagocytosis, autophagy, inflammation, and others. A knockout AD mouse model study has depicted that mutation in TREM2 inhibits the microglial clustering around amyloid which causes disruption in microglial activation and related signalling pathway (Hall-Roberts et al., 2020; Wang et al., 2016; Koth et al., 2010).

1.2.4.2 Environmental and other risk factors

Various environmental factors have been implicated in AD risk with nine modifiable risk factors including early life education, midlife hypertension, obesity, hearing loss, old-age smoking, depression, physical inactivity, diabetes, and social isolation (Livingston et al., 2017; Gabin et al., 2017; Chatterjee & Muther, 2018; Gu et al., 2010) have been identified. In addition, people from low-income countries are at greater risk in comparison to those from developed countries. Traumatic brain injury and cerebrovascular disease has also been shown to impact dementia risk (Ramos-Cejudo et al., 2018; Reitz & Mayeux, 2014). Related role of obesity and diabetes in relation to neurodegeneration development will be explored in detail in section 1.3, with a particular focus on obesity in line with aim of this thesis.

1.2.5 Molecular biology and pathology of AD

Given the understanding of various genetic mutations and the understanding of the abnormal protein accumulations that are damaging to brain cells in AD, there have been a number of attempts to ‘explain’ the underlying pathogenesis of AD. Whilst next section explores some of the main theories, it should be acknowledged that the most common consensus is that AD is multifactorial, and the disease process and progression varies in different individuals and populations. Consideration of the research describing various contributions of factors such as toxic A β generation, tau accumulation, inflammation, and oxidative stress helps shed light on where hope for the development of new drugs might lie. The neurological symptoms of AD development are considered to be result of gradual but progressive loss of neurons in the cholinergic and glutamatergic neural systems as well as the irregular functioning of the remaining neurons, such as deficits in neurotransmitter acetylcholine, imbalanced Ca⁺ influx (Wenk, 2006).

1.2.5.1 Amyloid cascade hypothesis

In 1992, Hardy & Higgins suggested for very first time that A β accumulation in the brain was the main fundamental trigger to the etiology of AD (Ricciarelli & Fedele, 2017; Hardy & Higgins, 1992). As shown in figure 1.7, the amyloid cascade hypothesis suggested that aggregation of A β primarily triggers the formation of soluble A β oligomers (also monomers such as fibrillar and protofibrils) and neurofibrillary tangle formation due to A β triggers results in synaptic dysfunction and neuronal death in AD (Evin & Weidemann, 2002).

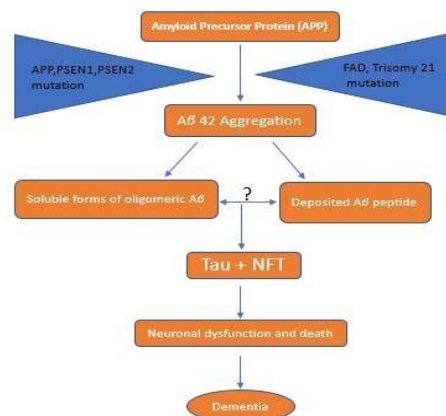


Figure 1.7. Amyloid cascade hypothesis. The flow chart describes the hypothesis proposing that the formation of A β 42 aggregates initiate the senile plaque formation which progresses to neurofibrillary tangle formation and finally dementia development. Adapted from Reitz & Mayeux, (2014).

As shown in the figure 1.7, the aggregation and formation of senile plaques extracellularly is one of the histopathological hallmarks of AD (Cheignon et al., 2017). In the central core of senile plaques, A β 42 proteins are abnormally arranged in a radial fashion. Multiple studies have shown that these structures as well as soluble, oligomeric forms of A β can interfere with normal neuronal functioning and contribute to cell death (Perlson et al., 2010; Sengoku, 2020; Singh et al., 2016). In the amyloid cascade hypothesis, A β 42 accumulation drives AD pathogenesis and subsequent cell death through a variety of mechanisms. However, therapeutic interventions aiming to inhibit the amyloidogenic pathway or clearance of toxic A β , e.g., via beta secretase (BACE) inhibition or A β immunization have not proved successful in human trials so far. This led researchers to investigate the role of other contributory disease factors, such as pathogenic tau, oxidative stress, and neuroinflammation in addition to other miscellaneous targets and how these components might interact in AD affected brain (Gupta et al., 2016; Athar et al., 2021).

Amyloid precursor protein, the protein from which A β is derived, undergoes sequential cleavage to produce various forms of A β , as shown in figure 1.8. In the non-amyloidogenic pathway, α -secretase cleaves APP to form a nontoxic fragment whereas in the amyloidogenic pathway, sequential cleavage of APP by β -secretase and γ -secretase yields the toxic A β 42 fragment (Bekris et al., 2010). The toxic forms of A β have a few detrimental cellular effects such as hyperactivation of microglia and tau pathology (Gupta et al., 2016). Amyloid precursor protein processing shows 3 cleavage sites namely α -secretase, β -secretase, and γ -secretase. A β 42 fragments cleaved by γ secretase is associated with AD (O'Brien & Wong, 2011).

BACE1, a transmembrane aspartic protease cleaves the APP at +1 and +11 sites of A β and releases soluble APP-beta peptides (sAPP β) which is followed by the γ -secretase complex cleavage at several sites between +41 to +44 resulting in release of A β peptides and intracellular APP. Understanding of the APP processing has given molecular characterisation of the secretases involved in A β production and accelerated the advanced efforts to model AD pathogenesis in animal model (Thinakaran & Koo, 2008).

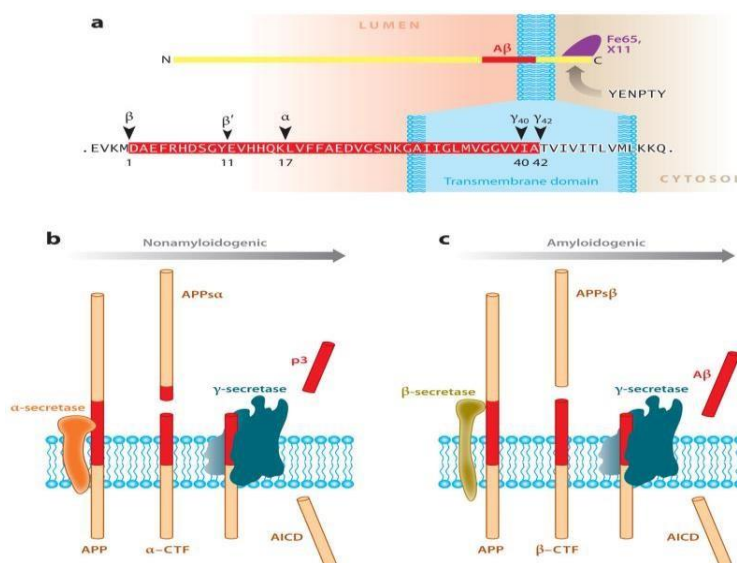


Figure 1.8. Amyloid precursor protein recruitment and processing. There are two ways for the consecutive cleavage of APP. **A.** the position of A β is demonstrated which includes a large and a short domain that initiates from the ectodomain into the transmembrane domain. The cleavage sites of α , β and γ -secretase are located between position 1-42. **B.** α -secretase and then γ -secretase mediates the cleavage of APP in the non-amyloidogenic processing. **C.** the sequential cleavage of APP in the amyloidogenic cleavage processing facilitated by β -secretase and then γ -secretase. Adapted from O'Brien & Wong, (2011).

1.2.5.2 Tau cascade hypothesis

Tau proteins are highly soluble microtubule associated proteins (MAP), which is physiologically important for the regulation of axonal transport and cytoskeletal maintenance (Kametani & Hasegawa, 2018). Historically, there has been debate regarding whether progressive accumulation of A β triggers the tau phosphorylation and aggregation, or vice versa (Selkoe & Hardy, 2016). Whilst the given evidence in the previous chapters indicates a key role of A β in the initiation of a pathogenic cascade in AD development, another research have demonstrated a clear role of tau in gradual AD development. The aggregated A β and neurofibrillary tangles (NFT) are the hallmarks of AD, as shown in histopathological section in figure 1.9 (Maccioni et al., 2010).

Interest in tau protein began when tau mutations were found to be directly pathogenic, giving rise to frontotemporal dementia with Parkinsonism (FTDP-17) linked to chromosome 17 (Spillantini et al., 1998). Tau pathology, also known as ‘tauopathies’ is a feature of numerous neurodegenerative disorders which is characterised by the abnormal accumulation of tau proteins in the brain. Over the years, there is gaining interest in therapeutics which disrupt the formation of tau lesions for better understanding of its role in AD (Congdon & Sigurdsson, 2018).

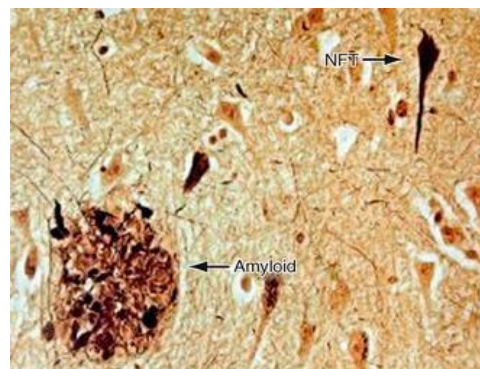


Figure 1.9. Histopathological hallmarks of AD pathology. The extracellular amyloid plaques and intracellular neurofibrillary tangles (NFT) are shown in the figure above. Adapted from Ridha & Yousry, (2016).

Apart from the helical filament phosphorylation, some of the factors are involved in tau hyperphosphorylation such as glycogen synthase kinase 3 β (GSK-3 β), cyclin-dependent kinase (cdk5) or exposure to polyanions involving protein kinase B (Akt), protein kinase A (PKA) and MAP kinase (MAPK) signalling pathway are present (Mazanetz & Fischer, 2007), as shown in figure 1.10.

This abnormally phosphorylated tau has been shown to sequester the normal tau, MAP1, MAP2 and ubiquitin into paired helical filaments resulting in microtubule destabilization and disruption of axonal transport (Mohandas et al., 2009).

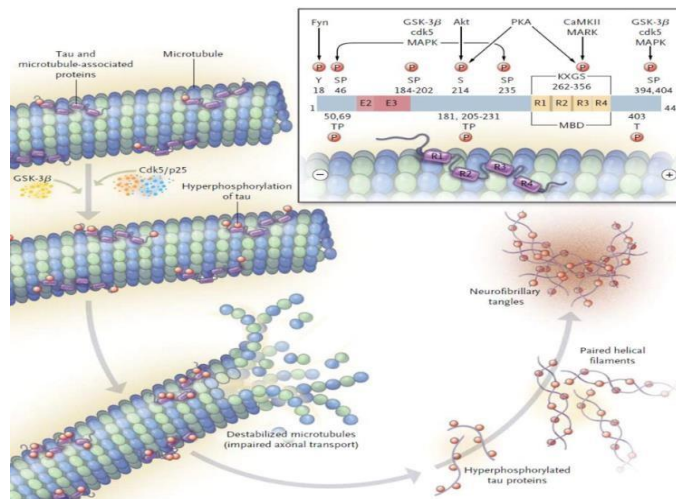


Figure 1.10. Tau hyperphosphorylation. Hyperphosphorylated tau sequesters into a number of aggregates including the neurofibrillary tangles with various factors and signalling pathways involved. Abbreviations: cdk- cyclin dependent kinase, GSK- glycogen synthase kinase, PKA- phosphorylated kinase, TP-tau phosphorylation, MBD- microtubule binding domain. CaMK- calcium dependent kinase, KXGS-serine motifs. Adapted from Querfurth & Laferla, (2010).

The tau protein family consists of 6 isoforms consisting 352-441 amino acids which are differentially expressed during development (Lace et al., 2009). The microtubule binding and subsequent functional properties of tau are regulated via phosphorylation and in AD, tau becomes abnormally hyperphosphorylated and forms abnormal intracellular paired helical filament of tau (PHF-tau) and neurofibrillary tangles (Ridha & Yousry, 2016). A cell culture and animal model study has confirmed that the soluble forms of tau have also shown toxicity and increasing accumulation of tau lesions correlates with increased cognitive impairment, more significantly than the accumulation of A β plaques (Šimić et al., 2016). The relationship between tau and A β is now understood to be complex with each protein exerting an influence on the other protein (Miao et al., 2019). With the advancement of neuroimaging studies, it is now understood that A β accumulates for many years prior to clinical symptom manifestation suggesting that both tau and A β have a role in early disease pathogenesis (Van der Kant et al., 2020). Tau and A β proteins have been linked to increase neuroinflammation and brain oxidative stress (Agostinho et al., 2010). The next section of this thesis will explore the role of these factors in AD pathogenesis development.

1.2.5.3 Inflammation hypothesis

Inflammation is known to play a key role in development of AD pathogenesis as well as in other neurodegenerative disorders such as Parkinson's disease (Alam et al., 2016). Neuroinflammation and reactive gliosis are commonly seen in the AD brain (Rogers et al., 2007).

A study has confirmed that inflammatory mediators are released during innate immune response which leads to glial dependent neuroinflammation (Van Eldik et al., 2016). TREM2 variation is a known risk factor for AD, which further supports a direct involvement of glial cells in cascade of AD disease development (Gratuze et al., 2018). In addition, studies have demonstrated a relationship between tau pathology and inflammation. Tau can induce inflammation, and chronic inflammation can further influence tau aggregation (Laurent et al., 2018).

Additionally, A β accumulation has been linked to neuroinflammation by promoting the release of free radicals and chemokines that contribute to further production and accumulation of A β (Cai et al., 2014). Release of inflammatory mediators were observed to be increased in AD and decreases the neuronal networking/communication in the AD condition (Hong et al., 2016). Finally, it is known that disorders that subject the body to chronic inflammation, such as metabolic syndrome and obesity, are known to increase development of AD risk.

1.2.5.4. Oxidative stress hypothesis

The oxidative stress hypothesis describes how oxidative damage, and the subsequent generation of reactive oxygen species (ROS) can contribute to the series of events that results in the development of AD, as shown in figure 1.11 (Tönnies et al., 2017; Markesbery, 1997). Under certain physiological conditions, such as head trauma, ischemia, and increased heavy metal exposure, free radical production is initiated due to peroxidation of oxygen and the disruption of membrane potential.

In addition, due to brain tissue damaging events, such as trauma, ischemia, toxicity, and cognitive condition including Parkinson's disease, AD, multiple sclerosis, lipofuscinosis, and accumulation of ROS increases over the period of time (Llanos-González et al., 2020; Misrani et al., 2021).

The central nervous system (CNS) also produces some damaging metabolic by products, as part of normal biochemical reactions such as superoxide, hydroxyl free radicals and hydrogen peroxide, sometimes collectively known as reactive oxygen metabolites (ROM) (Tümmler et al., 2017). Therefore, limiting the production of ROS and ROM, or the damage inflicted by ROS/ROM has a therapeutic potential in AD (Fiuza-Luces et al., 2019).

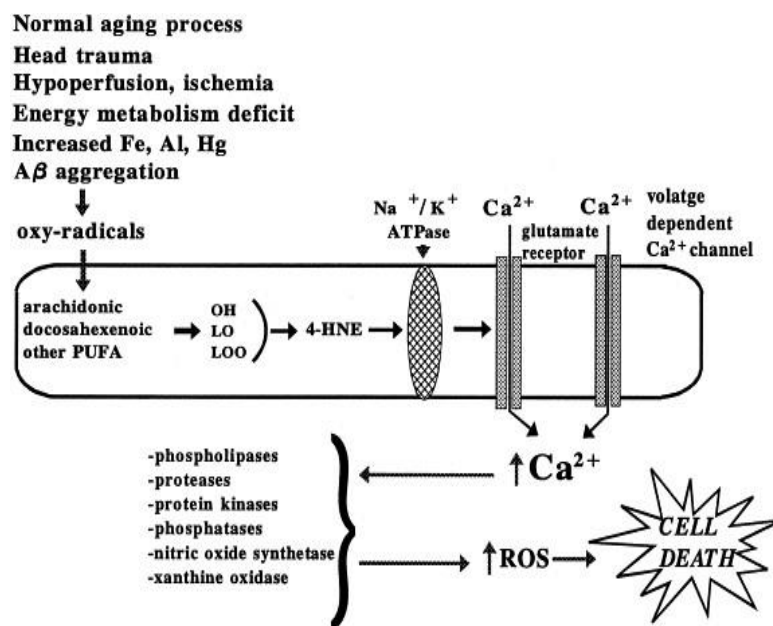


Figure 1.11. Hypothetical presentation of neuronal death in AD due to oxidative stress. Abbreviations used: Fe- iron, Al- aluminium, Hg- mercury, PUFA- polyunsaturated fatty acid, OH- hydroxide, LO/LOO- lipid peroxidases, 4-HNE- 4 hydroxynonenal, Na⁺- sodium ion, K⁺- potassium ion, Ca⁺- calcium ion. Adapted from Markesbery, (1997).

Some versions of the oxidative stress hypothesis postulated that genetic mutations, such as *APP* or *PSEN1* mutation, causes the formation of Aβ plaques which cause oxidative stress, and accumulative oxidative stress also contributes to the formation of the Aβ plaques, as shown in figure 1.12. Oxidative stress in turn, has been shown to modulate the activity of β and γ- secretase enzymes causing increased Aβ plaque formation and soluble, oligomeric Aβ generation (Praticò, 2008; Guglielmotto et al., 2010; Jo et al., 2010). Oxidative stress have depicted to induce tau hyperphosphorylation directly and through the activation of several protein kinases. This creates a positive feedback system resulting in further ROS generation and inflammatory response, irreversible neuronal damage, and ultimately neuronal death.

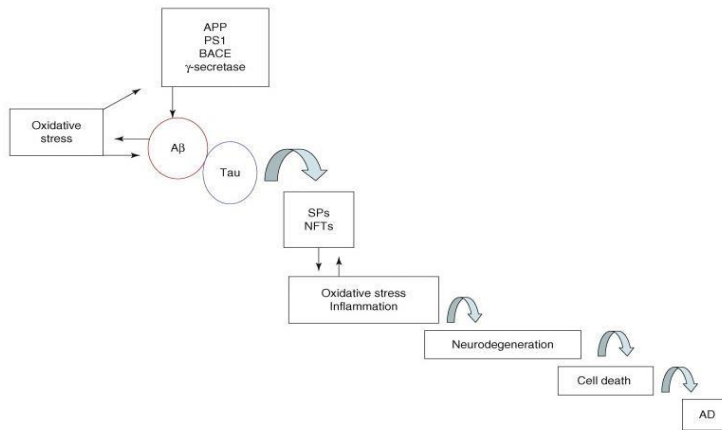


Figure.1.12. Molecular mechanism and pathology of AD due to oxidative stress. Mutation in APP and PSEN lead to the aggregation of A β and NFT and progress to neurodegeneration or AD development. Abbreviations: PS1-presenilin plaques, SP1-senile plaques. Adapted from Praticò, (2008).

Another factor known to increase oxidative stress levels is obesity and research studies have suggested that this might underlie the increased dementia especially AD and vascular dementia risk for those individuals defined as overweight or obese during midlife (Xu et al., 2011). In addition, overweight and central obesity is risk factor, causing dementia in population more than 50 year of age. However, the exact underlying mechanism of action is still unclear in relation to the development of AD pathologies with time (Ma et al., 2020). The link between obesity, oxidative stress and AD will be explored in more detail in section 1.3 and 1.4.

1.2.6 Therapeutic intervention

1.2.6.1 Current drugs

The US food and drugs administration (FDA) recently (June-2021) approved first novel drug since 2003 following a series of failed clinical trials and immunisation strategies. This drug is called Aducanumab or Aduhelm, which is targeted towards the clearance of amyloid plaques in AD patients with early or mild symptoms in a time and dose dependent manner. In spite of continued reduction in amyloid plaques results in clinical trials, the drug (aduhelm) failed to show primary end point in the second phase of third clinical trial. However, based on the clinical benefits of the drug to the patients, immediate need of treatment, and anticipated post approval trials for verification of drug, FDA permitted the drug for the benefit of the patients (Dunn et al., 2021; FDA, 2021; Mahase, 2021).

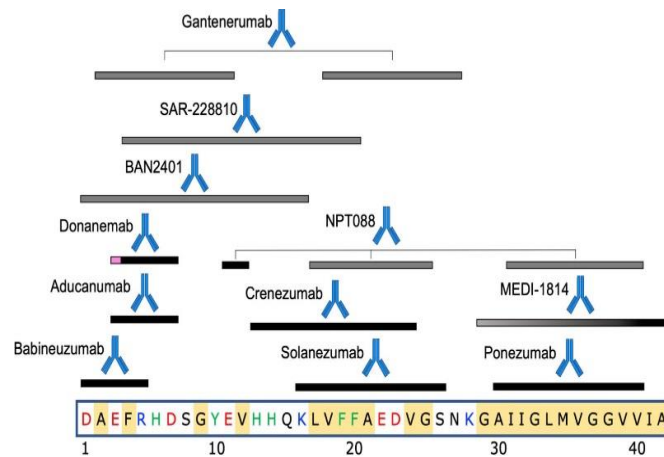


Figure 1.13. The epitome location on the A β sequence. The black bars represent epitome location, grey bars indicates presumptive epitomes presence, gradient filling for MEDI-1814 showed the incompletely epitope characterisation with A β specificity, Gantenerumab and NPT088 are an irregular epitome on A β sequence, pink coloured region in Donanemab pyroglutamate at amino acid position 3. Adapted from Plotkin & Cashman, (2020).

In figure 1.13, current drugs in clinical trials are based on the A β passive immunization which targets the epitome location on the primary A β sequence for antibodies generation (Plotkin & Cashman, 2020) to reduce or clear the accumulation of amyloid plaques and its subsequent consequences such as neuroinflammation, synaptic blockage, neuronal oxidative stress, and others (Crehan & Lemere, 2016).

Apart from the recently approved aduhelm, there are five other FDA-approved medical treatments available for the AD patients; however, these act only to control the symptoms instead of altering the course of the disease, as shown in figure 1.14 (Briggs et al., 2016). The current available treatments includes cholinesterase inhibitors (donepezil, rivastigmine and galantamine) and NMDA (N-methyl-D-aspartate) receptor antagonists (memantine) (Tan et al., 2014).

Cholinesterase inhibitors (ChEIs) such as donepezil, rivastigmine and galantamine are the factors that prevent the degradation of the acetylcholine from neurotransmission into acetyl and choline (Singh & Sadiq, 2021). However, pooled trial data suggested that ChEIs produces only minimal and short-lived benefits in cognitive impairment in dementia with response rate being shown to vary between individual patients (Ellis, 2005). The adverse side effects of ChEIs include diarrhoea, vomiting, cardiac arrhythmia, uncontrolled seizures and therefore limits the use of these drugs (Yiannopoulou & Papageorgiou, 2020).

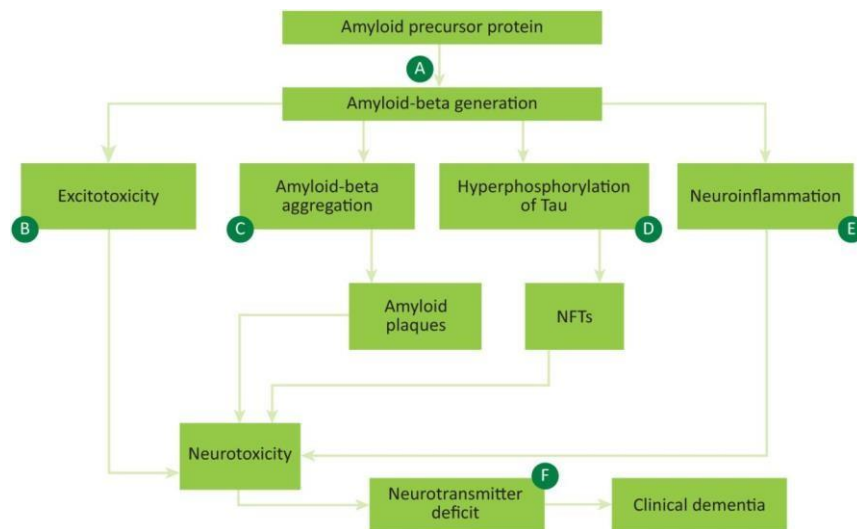


Figure 1.14. The aetiological factors of AD and the therapeutic intervention points. AD treatment strategies include: **A.** secretase enzyme inhibitors. **B.** NMDA receptor antagonists. **C.** monoclonal antibodies. **D.** anti-tau therapy. **E.** NSAIDs i.e. non-steroidal anti-inflammatory drugs. **F.** cholinesterase inhibitors. It should be noted that **B** and **F** are the only FDA approved drugs for AD treatment with **A**, **C**, **D** and **E** being currently explored in clinical trials. Adapted from Briggs et al., (2016).

The other class of AD therapeutics are the NMDA (N-methyl-D-aspartate) receptor antagonists such as memantine. These drugs work by blocking the signalling pathway through the NMDA glutamate receptor to prevent excitotoxicity.

To understand broader use of memantine, a patient study demonstrated that 312,336 patients were dosed with memantine, out of which 60 patients fell out of threshold criteria which confirmed that future benefits can be investigated to explore NMDA antagonists (Kern et al., 2021). Whereas in other study it has been demonstrated in other patients study that NMDA showed adverse effects such as drowsiness, fatigue, constipation, back ache, and hallucination (Jiang & Jiang, 2015).

Currently available therapies only addresses the downstream consequences of AD pathogenesis, such as excitotoxicity and the neurotransmitter deficit that occurs as a consequence of early disease events (as shown in figure 1.14). The next chapter will explore the therapeutic interventions that are currently in clinical trials, which aim to have more upstream effects such as impacting APP processing, A β /tau accumulation and neuroinflammation.

1.2.6.2 Drugs in trial

The major factors which reduces rate of drug development success, are lack of complete understanding of AD mechanisms, lack of accurate early disease diagnostic biomarkers. Currently, there are several drugs or compounds in clinical trials: 33 in phase III, 78 in phase II and 32 in phase I (Plascencia-Villa & Perry, 2020).

There are several studies which were discontinued due to failure to achieve the clinical endpoint such as the BACE inhibitor drug trials did not achieve FDA approval due to the safety and effectiveness concerns. Similarly, the drug trials using γ -secretase inhibitor and modulator failed the FDA approval due to inconsistency in patient's data and clinical trial project was terminated (Huang et al., 2020; Sabbagh, 2020; Weiler et al., 2020). Therefore, alternative treatment approaches and preventative strategies are needed. Newer clinical trials are now focusing on the non-amyloid and anti-tau interventions such as neurotransmitter and neuroinflammation modulators, cognitive enhancers, and neuroprotective agents (Hamelin et al., 2016; Chi et al., 2018). Understanding more about how the brain normally protects itself against damage as well as the molecular basis of risk factors such as obesity, could identify new routes for therapeutic intervention.

1.2.6.3 Risk reduction approaches

A published report described how one third of dementia cases could be prevented through addressing disease modifiable risk factors, therefore there is an urgent need to understand the underlying molecular biology of these risk factors to enable public health strategies to be developed (Livingston et al., 2017).

Studies have already shown that a healthy diet (including vegetables, fruits, nuts with reduced processed food consumption and supplements such as omega-3 and vitamin B12 can reduce dementia risk (Rakesh et al., 2017). Reducing stress in everyday life through incorporation of meditation and yoga practice has shown some preventive and improved effects. Increasing cognitive health through solving puzzles, learning new languages, and engaging with various arts and crafts activities are also proved to be beneficial. Apart from the activities, the overall diet related strategies should be considered instead of individual food or nutrients (Pereira et al., 2007; Lupien, 2009).

Adapting healthy life associated actions are likely to reduce the challenges of cognition. However, the molecular biology for many of these approaches that underpins the associated neuroprotection is still not completely understood.

Type2-diabetes, hypertension and obesity are closely related modifiable risk factors which are known to have a synergistic effect on risk of AD development risk (Edwards et al., 2019). Studies are needed so as to increase the understanding of how conditions such as obesity, influence the nervous system in such a way that makes an individual more susceptible to develop AD. This is not well explored, and it is necessary to understand the factors that could enhance neuroprotection and reduce neuronal damage.

This project will aim to understand how adipocytes secreted adipokines, whose levels are known to vary in obesity, can impact the cellular response to oxidative stress. This will shed light on the underlying mechanisms of obesity associated dementia risk, whilst exploring impact of adipokine associated pathways which might have therapeutic potential.

1.3 OBESITY

Obesity is a complex, reversible physiological state that significantly impacts the physical health and emotional wellbeing of the individual, impacted by the condition (Agha & Agha, 2017). Changes in lifestyle over the last decade have caused a number of individuals classified as being overweight or obese and the number is still increasing significantly (Hruby & Hu, 2015a). Obesity is a multifactorial disease involving interactions between genetic, environmental, and psychosocial factors (Chew et al., 2014). The major risk factors that are estimated to induce obesity includes: unhealthy lifestyle, unusual eating habits, urban development with increased smoking and alcohol consumption habits (Apovian, 2016).

Investigating how obesity influences the biochemistry of the body is important to better understand how this condition increases the risk of developing diseases such as AD and other neurodegenerative diseases.

1.3.1 Classification & epidemiology

Obesity is defined as an abnormal accumulation of fat in body and body mass index of more than 30kg/m² (Apovian, 2016). Obesity occurs due to an imbalance of energy expenditure and food intake that leads to the excessive accumulation of adipose tissue (Hruby & Hu, 2015b). It is a reversible condition which can be addressed with a combination of regular exercise and a long-term low calorie or low-fat diet (Montesi et al., 2016).

In England, the national statistics on obesity in 2021 has confirmed that more than 1 million hospital admissions in 2018-19 were due to obesity as key factor and 10,780 admitted cases were directly attributable to obesity (NHS Digital, 2021). In England, 27% of adults are considered as obese and approximately 36% of adults fall in the overweight category with the prevalence being similar between male and female, however, males are more inclined towards being overweight and females are more prone to categorized into obese condition (Public Health England, 2017). In the UK, the NHS has spent approximately £6 million in 2015 on obesity related disease treatment which is much more than the money spent on the police, fire services and judicial system all together (NHS Digital, 2021).

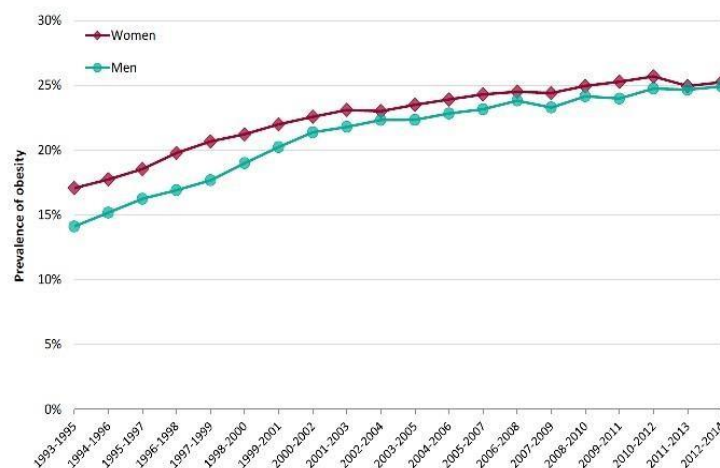


Figure 1.15 Prevalence of obesity. Among adults aged over 16 years, comparing men and women. Adapted from Public Health England, (2017).

In the past 10 years, in European countries obesity prevalence has increased from 10% to 40%, on the other hand in England alone, the prevalence has doubled over the decade (Agha & Agha, 2017). It has been estimated that by 2050, obesity approximately may affect 25% of children, 60% of adult men and 50% of adult women. In addition, if the current situation of lifestyle and dietary intake persists, by 2030 approximately 38% of UK's adult population will become overweight and 20% will be obese (Smith & Smith, 2016). A gender based comparative study between men and women in relation to the prevalence of adult obesity within UK, the figure 1.15 demonstrates that women are at higher risk to develop obesity than men. However, the percentage of prevalence in men has increased faster over the years and the difference between both genders (showed in figure 1.15) decreased over the period of decade (Public Health England, 2017).

1.3.2 Association with dementia

Obesity is a well-documented significant risk factor in association with AD, and obesity prevention or treatment could be an achievable way to reduce risk of AD (Alford et al., 2018). In obesity, lipolysis releases increased amounts of free fatty acid, which in turn, increases the oxidative and endoplasmic reticulum stress resulting in the deteriorating cellular homeostasis and which is also linked to neuroinflammation, disabled cellular functioning and finally death of the neurons (Martin-Jiménez et al., 2017).

Obesity is known to increase the risk of developing type 2 diabetes which is also a major risk factor for AD (Hruby & Hu, 2015a). By some researchers, AD has been nicknamed by some researchers as type 3 diabetes mellitus or brain diabetes (Montesi et al., 2016) due to the pathological similarities between AD and type2 diabetes, specifically with respect to the amyloid dysfunction and increased glycation and lipolysis in both the conditions (Leszek et al., 2017).

Sirtuin-1 (SIRT-1) plays vital role as the interconnected link between type2 diabetes and AD, as shown in figure 1.16. Due to decreased insulin receptor substrate (IRS2) functioning (or increased insulin resistance) and increased neuronal toxicity (due to increased APP processing by β -secretase leading to more $A\beta$ production) the risk of developing type2 diabetes and AD increases. In addition, decreased SIRT-1 expression is proportional to increasing age and inflammation (Lovestone & Smith, 2014).

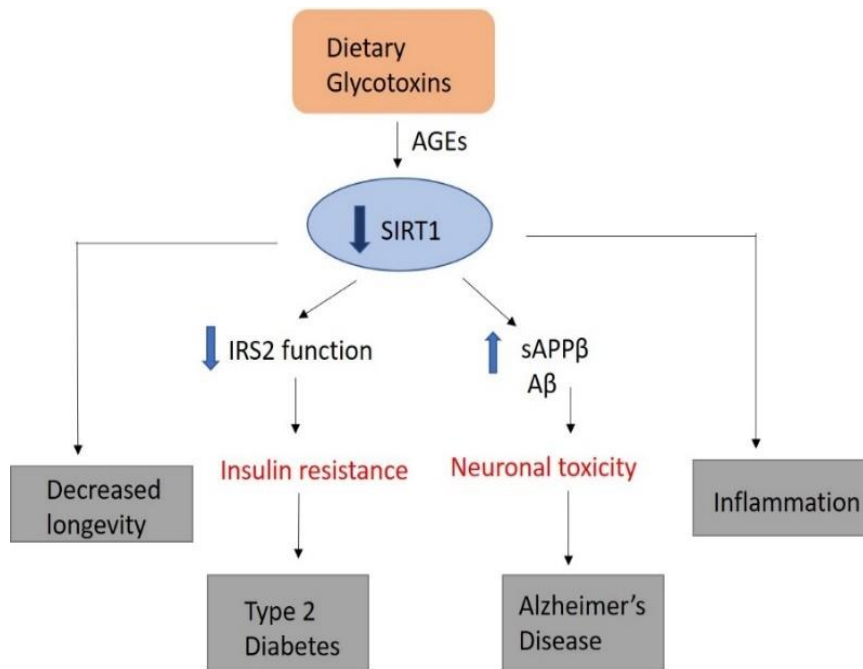


Figure.1.16. Glycotoxins induces hyperproduction of advanced glycation end products (AGEs) that affects pathways involved in aging, inflammation, type2 diabetes and AD. Dietary glycotoxins possesses ability to influence insulin resistance and neuronal toxicity leading to type2 diabetes and AD by reduced sirtuin-1 (SIRT-1) expression, insulin receptor substrate (IRS2) functioning and increased amyloidogenic APP metabolism. Adapted from Cai et al., (2014).

A research study has confirmed the presence of insulin and insulin-like growth factors receptors in the brain including the hippocampus, hypothalamus, cortex and cerebellum to regulate critical metabolic functions as well as neuronal plasticity (Fernandez & Torres-Alemán, 2012).

Interestingly, in an in-vitro study using primary neuronal culture derived from the hippocampus region, A β induced neuronal insulin resistance and interrupted axonal transport was reversed when exposed to exenatide (an anti-diabetic agent) (Bomfim et al., 2012).

The pathological similarities between type2 diabetes and AD are further reinforced by the insulin and glucagon like-peptide-1 (GLP-1) signalling disruption which results in beta cell apoptosis and decreased beta cell regeneration in type2 diabetes which finally leads to increased A β accumulation as demonstrated in a research study (Gejl et al., 2016).

1.4 ADIPOSE TISSUE AND ADIPOKINES

Adipose tissue possesses not only the ability to store energy but also acts as an active endocrine organ with the ability to synthesise a wide range of metabolically active molecules involved in the regulation of body homeostasis (Saely et al., 2012). Adipokines are cytokines secreted from adipose tissues which possess the ability to influence a range of physiological processes and pathways, including those associated with AD (Zorena et al., 2020).

1.4.1 The normal role of adipose tissue

Adipose tissue is a chief source of excess nutrient storage in the form of triacylglycerol. Over last decade understanding of the adipose tissues (AT) role has been changed from a tissue responsible for simply storing triglycerides, to being a complex and metabolically active organ (Ottaviani et al., 2011; Richard et al., 2020).

In addition, as discussed previously, adipocytes produce various secreted proteins called adipokines (Kwon & Pessin, 2013). In adipose tissue, the adipocytes are present in copious amounts. They have the ability to store the excess energy in a reversible manner, i.e., the fat stores can be used in the starvation and pile up during the normal feeding condition. Hence, imbalance in the fat storage or excess storage of fat triggers adipocytes hypertrophy and hyperplasia leading to cellular stress which in turn elicits inflammatory responses and oxidative stress in adipocytes (Fernández-Sánchez et al., 2011b). AT can be subdivided into three subtypes: white, brown and beige adipose tissue. White adipose tissues primarily acts as an energy reservoir and releases the required fatty acids/ lipids required for energy expenditure (Corrêa et al., 2019). Brown adipose tissue helps to accumulate lipids for cold induced adaptive thermogenesis (Rosell et al., 2014). Finally, beige adipose tissue (BeAT), also known as 'browning in white', has a role in thermoregulation in response to cold as well as convert back to white adipocytes in response to thermoneutrality (Cohen & Spiegelman, 2016; Damal Villivalam et al., 2020).

Recent research study has confirmed that the AT acts as secretory organ that regulates secretion of tumor necrosis factor-alpha (TNF- α) which is a critical signalling factor for auto and endocrine function.

The dysregulation of TNF- α release from AT has been shown to result in dysregulation of various metabolic functions (Cawthorn & Sethi, 2008; Choe et al., 2016), and so the important role of AT as an endocrine organ was realised. Various functions of different AT are summarized in Table.1.1.

Table.1.1 Illustrates comparative difference between white, brown and beige adipose tissues (Opatrilova et al., 2018).

White adipose tissue	Brown adipose tissue	Beige adipose tissue
Stores energy in the form of triacylglycerol	Fatty acid oxidation to release heat energy for normal body temperature maintenance	Fatty acid oxidation to release heat energy for normal body temperature maintenance
Subcutaneous fat accumulation or in the abdominal region	Subcutaneous fat accumulation in the interscapular region or in the cervical, axillar, and paravertebral regions	Resides within the white adipose tissue. Uncertain distribution due to the inter-convertible nature of AT
Decreased nerve innervation and vascularization	Highly vascularized and nerve innervated	Densely vascularized.
Possess only unilocular lipid droplets	Possess multilocular lipid droplets	Possess multilocular lipid droplets
Manifest a low oxidative rate	Exhibit higher fatty acid oxidation and glucose uptake	Exhibit maintenance of energy balance similar to brown AT
Few mitochondria are present	High number of mitochondria	High number of mitochondria

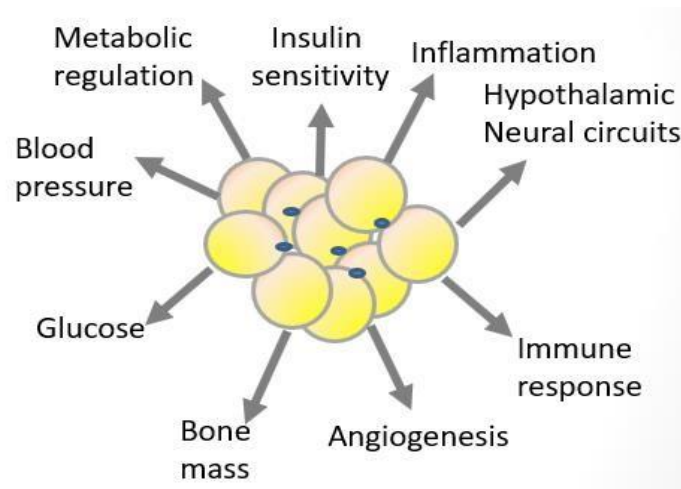


Figure 1.17 AT acts as an endocrine organ and regulate various metabolic pathways such as glucose homeostasis, inflammation, hypothalamic neuronal networking, and others. Adapted from Andrade-Oliveira et al., (2015).

Since the initial discoveries, AT has been shown to release a wide range of growth factors and adipokines (cytokines that are specifically released from adipose tissues) including leptin, adiponectin, visfatin, apelin, vaspin, hepcidin, chemerin and omentin (Andrade-Oliveira et al., 2015). As shown in figure 1.17, the AT secreted adipokines regulates various metabolic pathways such as immune response, insulin sensitivity, inflammation, metabolic regulations and the impact of secreted growth factors and adipokines from AT possess ability to regulate various physiological functions. Dysfunctional AT (or hypertrophy or hyperplasia condition) results in macrophage infiltration, adipocyte necrosis and inflammatory factors release (Ouchi et al., 2011). The role of adipokines will be further explored in section 1.4.2. The understanding of adipokines in relation to obesity and AD could potentially lead to novel therapeutics development.

1.4.2 Adipokines

As described in previous sections, AT secretes and regulates various adipose specific cytokines known as adipokines, which can regulate various metabolic and inflammatory processes (Greenberg & Obin, 2006). In addition, the disturbance in circulating levels of adipokines could lead to dysfunctional biological functions resulting in vascular inflammation, hypertension, cardiovascular diseases, and others (Chen et al., 2020; Corrêa et al., 2019). The physiological role of some of the key adipokines will be explored in more detail in the next section.

1.4.2.1 Leptin

Leptin is 16kDa protein encoded by the *ob* gene and mutation in *ob/ob* gene (leptin) or *db/db* gene (leptin receptor) have been linked to obesity (Wasim et al., 2016). Primarily, leptin regulates appetite and leptin levels are usually proportional to the amount of body fat (Zhang et al., 1994). Leptin regulates body weight and possesses the ability to activate hypothalamic neural circuits (Mazen et al., 2009).

In addition, leptin is also produced by various tissues (other than AT) such as mammary gland, the pituitary gland, skeletal muscle and stomach (Kim & Kim, 2021). Leptin receptors are expressed in hypothalamus, cortex, and hippocampus (McGuire & Ishii, 2016). Leptin can influence various signal transduction pathways (Dardeno et al., 2010), the following highlights a number of pathways influenced by leptin:

- a. JAK/STAT3 pathway = Primary action of site is hypothalamus and regulates appetite, body weight and other neuroendocrine functions.
- b. PI3K pathway = Primary action of site is hypothalamus and regulates appetite, body weight, sympathetic pathway stimulation and insulin regulation.
- c. MAPK pathway = Primary site of action is hypothalamus, liver, pancreas, adipose tissue and myocytes which regulates appetite, body weight, regulation of fatty acid oxidation, cardiomyocytes hypertrophy and sympathetic activity to brown adipose tissue.
- d. AMPK pathway = Primary site of action is hypothalamus, muscles and regulates appetite, body weight, regulates fatty acid oxidation, and insulin stimulation to muscles.
- e. mTOR pathway = Primary site of action is hypothalamus and regulates appetite, and body weight.

1.4.2.2 Resistin

Resistin is another adipokine that was named after its initial research study on insulin resistance, and it acts as a hormone with potential links between obesity, insulin resistance (IR), metabolic syndrome and diabetes (Steppan et al., 2001). Resistin is involved in the regulation and development of IR and is majorly produced by the peripheral blood mononuclear cells (Su et al., 2019).

Research findings involving the mRNA expression have been conflicting with some studies reporting resistin mRNA expression in adipose tissue (Way et al., 2001), whereas other studies have reported either poor or complete absence of resistin expression in the adipose tissue (Sadashiv et al., 2012). Circulating serum resistin has been shown to have a significant effect on insulin regulation through its interaction with toll like receptors (TLRs) and potential to induce expression of various cytokines involved in the regulation of inflammation and signalling pathways (Jamaluddin et al., 2012). Studies showed that resistin could decrease the inflammation induced autophagy in neuronal-like cells (Jie et al., 2018), however, so far, no study has confirmed the role of resistin on neuroprotection under oxidative stress condition.

1.4.2.3 Chemerin

Chemerin is encoded by *Rarres2* gene, which is involved in chemotactic, autocrine/paracrine, adipogenic and reproductive functions (Helfer et al., 2016b). Initially, chemerin was identified as a natural ligand for G-protein coupled receptors (GPCR) and chemerin chemokine like receptors (CMKLR1) also known as Chem23 (Whittamer et al., 2003). CMKLR1 play crucial role in chemerin mediated inflammation, however, the underlying molecular mechanism is still unclear. Chemerin has been recognized as ligand for GPR1, another GPCR and C-C chemokine receptor like 2 (Ccr12), a C-C motif receptor. CMKLR1 is expressed in adipocytes, mainly in white adipose tissue, whereas in brain it is expressed in microglia of hippocampus, ependymal cells, and tanycytes lining the hypothalamus (Helfer et al., 2016a).

A mouse model study has depicted that by participating in various signalling pathways such as Janus kinase2 - signal transducer and activator of transcription3 pathway (JAK2/STAT3) pathway, chemerin induced oxidative stress and autophagy was diminished mediated by the CMKLR1 (Li et al., 2020). Evidence suggests that the inflammation and oxidative stress induced neuronal autophagy has been decreased in the presence of chemerin (An et al., 2021). However, so far, effect of chemerin on the cellular model of neuronal cells in relation to AD under oxidative stress has not been explored.

1.4.3 Adipose tissues and adipokines in obesity

It is estimated that in obesity, hyperinsulinemia condition is partially due to reduced number of adiponectin receptors (Sowers, 2008). As shown in figure 1.18, as obesity increases, the adipose tissues gradually become stressed due to an increased fat deposition and ROS levels. The increased ROS levels influences the release of adipokines, nicotinamide adenine dinucleotide phosphate (NADPH) oxidation and further increases mitochondrial ROS production into the circulation. This eventually results in increased pro-inflammatory mediators and insulin resistance (Lefranc et al., 2018).

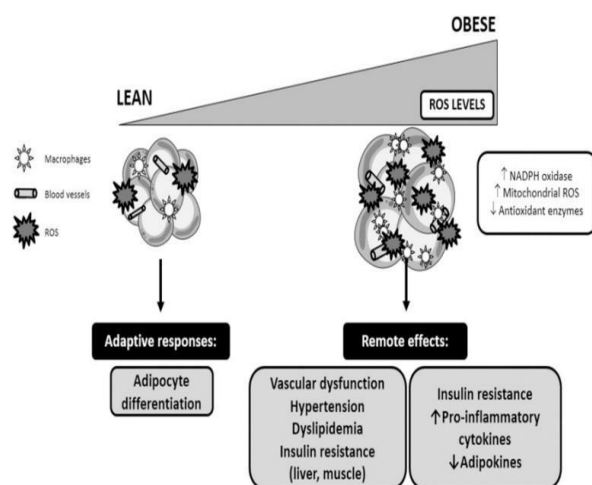


Figure 1.18. Change in adipose tissue in the lean and obese condition with their physiological effects. Adapted from Lefranc et al., (2018).

A research study using mice model demonstrated that release of adipokines from adipose tissues were altered after stroke in lean as well as obese condition, which suggested that any impact on adipose tissues have direct effect on the adipokines secretion (Haley et al., 2017). Resistin is cysteine rich protein, induced during adipogenesis and linked to obesity led insulin resistance and type2 diabetes (Kusminski et al., 2005). The involvement of resistin in the development of obesity and IR has been recorded and resistin is still considered as a biomarker of IR in obesity condition. Increased oxidative stress is related to obesity and activation of NF- κ B and MAPK, contradiction in research studies have been recorded due to inconsistent outcome of studies while understanding the correlation between obesity and resistin circulating levels (Wen et al., 2013).

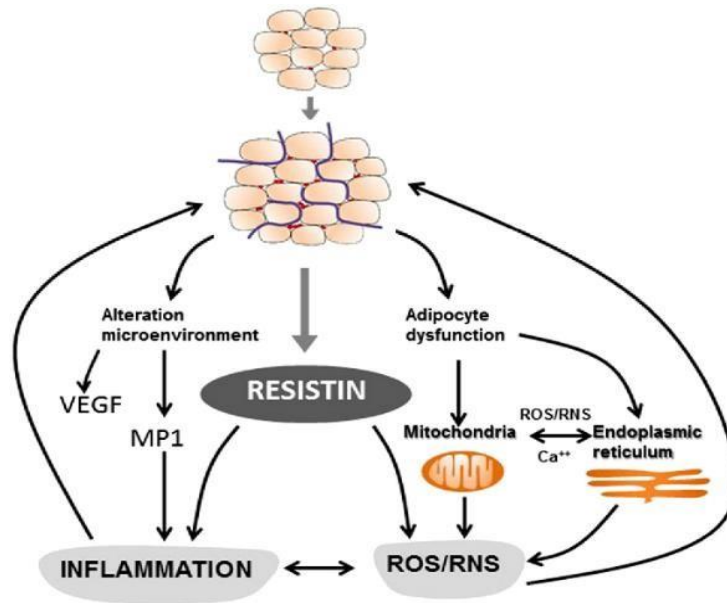


Figure 1.19. Increased resistin levels. Increased adiposity is linked to mitochondrial and endoplasmic reticulum dysfunction that leads to inflammation and oxidative stress which in turn alter the microenvironment and further adipocyte dysfunction completing the feedback loop. Abbreviations used: MP1: metalloproteinase, VEGF: vascular endothelial growth factor, ROS: reactive oxygen species, RNS: reactive nitrogen species. Adapted from Codoñer-Franch & Alonso-Iglesias, (2015).

Clinical and in-vitro studies have confirmed that increased levels of circulating resistin is associated with obesity and obesity led diseases such as cardiovascular disease and malignancy (Codoñer-Franch & Alonso-Iglesias, 2015). In another study, no correlation between serum resistin level and obesity was observed. On the contrary, a molecular study based on mRNA and protein expression in isolated human adipocyte showed very low resistin mRNA levels in obesity led IR condition (Savage et al., 2001; Amirhakimi et al., 2011). As shown in figure 1.19, the initial stages of obesity disrupts the microenvironment of macrophages by shifting the polarization of factors such as vascular endothelial growth factor (VEGF) and metalloproteinase (MP1) which ultimately leads to inflammation. The increased inflammation within the adipocyte further increases the release of pro-inflammatory mediators that induce the robust expression of resistin and its secretion. The dysregulated resistin levels affects mitochondrial and endoplasmic reticulum function which contributes to reactive species generation such as ROS and reactive nitrogen species (RNS). These sequential events complete the circle of obesity-resistin-inflammation mediated by oxidative stress (Nagaev et al., 2006; Lumeng et al., 2007; Lawrence & Natoli, 2011; Coelho et al., 2013).

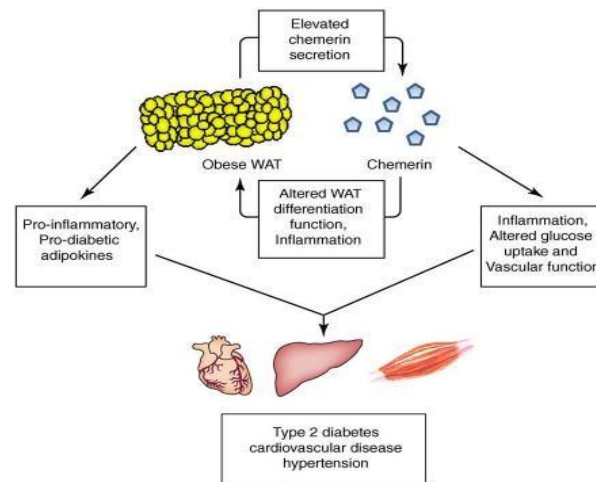


Figure 1.20. Chemerin in obesity condition, chemerin acts as a potential link between chronic inflammation and obesity. Increased level of chemerin increases pro-inflammatory mediators and alter normal physiology affecting various tissues. Adapted from Ernst & Sinal, (2010).

Chemerin expression and release is high in obesity condition. Chemerin is well studied adipokine for the pre-adipocyte differentiation and glucose metabolism, therefore, role of chemerin is crucial link between obesity and chronic inflammation, as shown in figure 1.20. The elevated level of chemerin during obesity can alter the adipogenesis, and its function. In addition, increased inflammatory mediators, dysregulated glucose and adipokines levels further affect organs such as, cardiac, pancreas and muscles. Studies proved that chemerin levels are dysregulated in obesity, hypertension, cardiovascular disease and type 2 diabetes (Sell et al., 2009; Ernst & Sinal, 2010).

Chemerin is multifaceted adipokine linking with food intake, body weight and metabolic disorders. Some contradictory studies dispute that chemerin increases the release of insulin from pancreas, however, still supports chemerin's link with obesity and IR. Chemerin modulation during midlife obesity condition may have useful impact on fat mass distribution (because chemerin is directly proportional to regulation of body fat mass), which makes chemerin a potential candidate as a novel therapeutic factor (Brunetti et al., 2014; Niklowitz et al., 2018; Karczewska-Kupczewska et al., 2020).

Considering the impact obesity has on dementia risk, the role of adipokine dysregulation in AD is still poorly understood. The next section of this thesis will explore what is known about the influence of adipokines in AD, and how their dysregulation might contribute to disease pathogenesis.

1.4.4 Adipose tissue and adipokines in neurodegeneration

As mentioned in previous section, obesity is a major risk factor for AD, and obesity associated adipokine dysregulation may have a role to play in this increased risk. There are several studies which suggested that midlife obesity influences the brain structure and function due to increasing exposure to oxidative stress, inflammation, mitochondrial dysfunction which may contribute to increased A β aggregation (Xu et al., 2011; Dorjgochoo et al., 2011; Ronan et al., 2016). Understanding the role of adipokine dysregulation in exacerbating this disease associated factors, particularly oxidative stress, is one of the aims of this research project. Some adipokines, such as chemerin, leptin, adiponectin has been reported to possess the ability to induce inflammation by influencing the signalling pathways such as JAK2-STAT3, peroxisome proliferator -activated receptors- gamma (PPAR- γ) (Scotece et al., 2017).

Other adipokines have been linked to increased oxidative stress and their role in oxidative stress induced AD, which will be further explored in the discussion chapter. Whilst chemerin and resistin have been reported to contribute towards the pro-inflammatory and oxidative stress environments associated with AD, other adipokines have been reported to have a more protective role. Leptin is known to have neuroprotective effects in AD condition mediated by the leptin receptor (LR)-expressing neurons, present in central nervous system. However, the exact molecular mechanism of this neuroprotective effect remains unclear.

Figure 1.21 represents an overview of leptin and its link to increased risk of AD development in midlife obesity. Leptin has shown neuroprotective effect in AD by inhibiting long-term depression (LTD), glycogen synthase kinase-beta (GSK β) and β -secretase activity by promoting the long-term potentiation (LTP) and A β degradation. Leptin resistance occurs in midlife obesity which may increase the chances of AD development in later life (Lloret et al., 2019; Lizarbe et al., 2018). During obesity, the adipose tissues release inflammatory factors including tumor necrosis factor α (TNF α) and interleukin-6 (IL-6) along with reduced production of adiponectin (an adipokine) that lead to pro-inflammatory and oxidative stress state. Increased level of resistin is observed in inflammation related disease such as rheumatoid arthritis and AD, and it is also known that resistin can influence insulin resistance by acting as chemoattractant for the other chemokines.

Significant increase in resistin have been observed and correlated to inflammatory markers in AD (Demirci et al., 2017; Mauro et al., 2015).

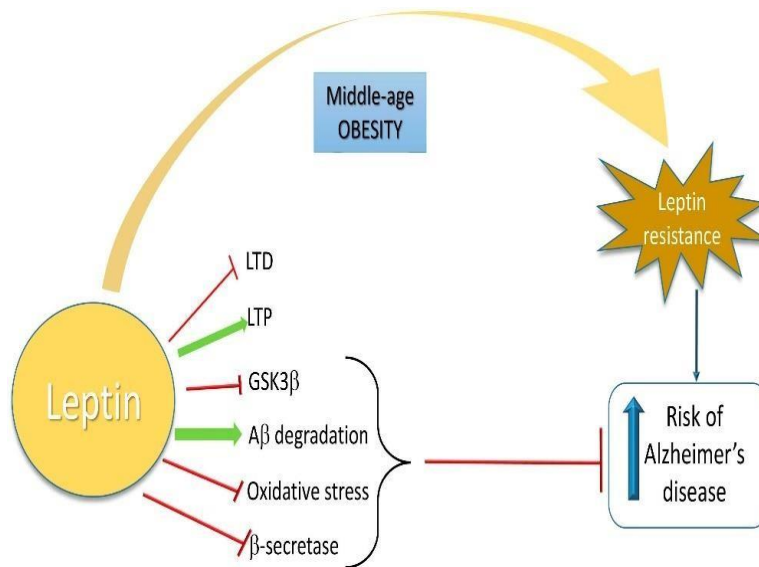


Figure 1.21. Mid-life obesity as risk factor for AD development. During mid-life obesity, increased leptin resistance promotes the risk of AD development in later stage of life. Abbreviations used: LTP: long-term potentiation, LTD: long-term depression, GSK3 β : glycogen synthase kinase-beta. Adapted from Lloret et al., (2019).

Dysregulation of leptin receptor expression and leptin levels worsen the AD pathology or cognition, and AD pathology can further interrupt the leptin signalling by disrupted receptor expression (McGuire & Ishii, 2016; Khemka et al., 2014). Other studies have proposed that leptin attenuates the tau phosphorylation, and its activity can be modulated by A β . Recent study has reported that obesity leads to leptin resistance, which restricts the ability of leptin to cross blood brain barrier and affect the expression of mRNA (Zhang et al., 2016). A study has proved that adiponectin can regulate insulin sensitivity, fatty acid oxidation and inflammatory responses (by acting as an anti-inflammatory mediator). However, the complete mechanism of action is still unclear (Song & Lee, 2013).

Interestingly, chemerin receptors, CMKLR1, have been reported as specific and functional receptors of A β peptides. CMKLR1 has been shown to be activated in the presence of A β 42, which initiates microglial cell migration and clearance of A β 42 deposits which might suggest a potential protective role of chemerin in AD (Peng et al., 2015; Al Hazzouri et al., 2012).

It is clear that there are some inconsistencies in the literature and the impact of adipokines might vary depending on the cellular environment and issues associated with the resistance and receptor sensitivity. Resistance to influence certain adipokines that occurs as a consequence of obesity might explain the loss of neuroprotective effects in AD and underlie the variations in experimental results looking at the role of adipokines in diseased and simple cellular models could be useful in understanding some of the key roles in AD.

The influence of adipokines on AD is therefore likely to be complex and further research is needed, to understand the role of these cytokines in AD pathogenesis, and if targeting adipokine dysregulation could have a therapeutic benefit.

1.5 OXIDATIVE STRESS

Oxidative stress occurs as a consequence of imbalance between reactive oxygen species (free radicals) generation and antioxidant clearance mechanisms, which leads to tissue injury or other metabolic disorders (Betteridge, 2000).

Free radicals are generated during various biochemical reduction- oxidation reactions or redox reactions and are described as being any chemical species with an unpaired electron (Pizzino et al., 2017). ROS play a vital role in the redox reactions of various physiological pathways such as cell signalling, energy metabolism, normal homeostasis, apoptosis, and others (Ristow & Zarse, 2010) but they also have damaging effect on tissues due to generation of free radical species. Oxidative stress therefore interferes with normal mitochondrial function as well as ROS production and has been linked to numerous disorders, as shown in figure.1.22. Increasing age, excess free fatty acids, and glucose levels are the main contributors to increased oxidative stress which occurs due to age associated neuronal functional loss. This initiates further generation of ROS and dysfunctional mitochondrial activity (Chandrasekaran et al., 2017). Oxidative stress is known to increase the risk of age-related disorders such as cardiovascular disease, pulmonary disorders, kidney dysfunctions and neurodegenerative disorders (Liguori et al., 2018). Therefore, therapies that interfere with the production of oxidative stress may influence AD risk development and disease progression.

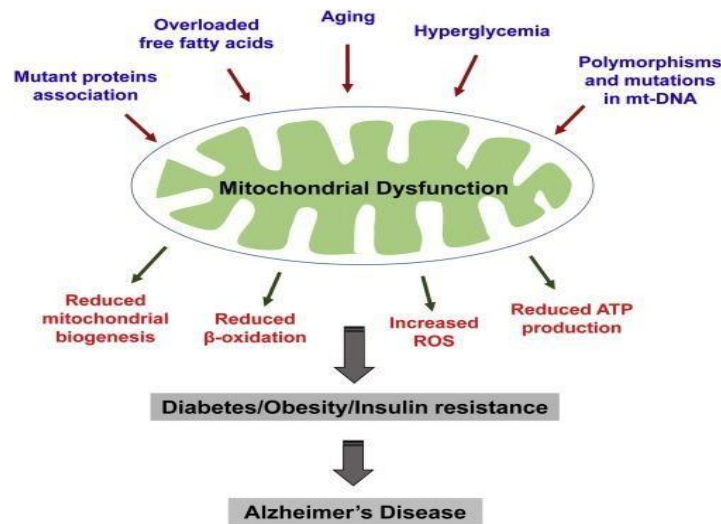


Figure 1.22. Oxidative stress induced mitochondrial dysfunction due to various risk factors lead to metabolic disorders and finally AD. Adapted from Pugazhenthil et al., (2017).

1.5.1 Oxidative stress in obesity

Research studies have confirmed that in obesity, the adipocytes are exposed to oxidative stress, which in turn impacts adipokine release (Marseglia et al., 2014). This increased oxidative stress occurs as a consequence of increased fatty acid oxidation of mitochondria and peroxisome, which increases ROS production (Dulloo et al., 2010). Consumption of a high lipid diet has been shown to contribute towards the over production of free radicals (Waring & Rosenberg, 2008; Fernández-Sánchez et al., 2011a). Another similar study confirmed that oxidative stress can affect adipokine mRNA levels, leading to dysregulated gene expression of adipokines resulting in decreased leptin, adiponectin and resistin mRNA production and increased plasminogen activator inhibitor-1 mRNA expression (Kamigaki et al., 2006).

It is known that obesity initiates change in adipokine secretion (section 1.4.3) and whilst there is not an extensive amount of understanding about the relationship between adipokines and oxidative stress, there are some suggested reports that this is an avenue for research that needs further investigation. The role of chemerin is not well known, however, some research groups have confirmed that the chemerin was positively related to the oxidative stress and inflammatory markers in individuals with increased body weight and leptin levels (Fülöp, 2014).

Studies have confirmed that adipokines are closely related to the immune system and possess ability to recruit the immune cell under oxidative stress conditions (Żółkiewicz et al., 2019). We understand that chemerin and leptin have been linked to oxidative stress, it is unclear if adipokines act to exacerbate or protect cells under oxidative stress conditions, particularly neuronal cells or peripheral cells derived from AD patients.

1.5.2 Oxidative stress in Alzheimer's disease

Oxidative stress has been implicated in AD pathogenesis in numerous research studies (Nunomura & Perry, 2020). Over the years, ROS has emerged as one of the significant factors in dysregulation of neuronal function. With increased age, the oxidative stress in the brain increases, due to an impaired antioxidant system which leads to excessive accumulation of ROS (Huang et al., 2019). It was shown that in AD there are increased markers of ROS, oxidized proteins, lipid peroxidation and decreased antioxidant protective biomarkers in both the brain and peripheral tissues. In addition, these changes were reported early in cognitive disease, which suggests an upstream role for oxidative stress. The evidence supports the importance of ROS regulation and its ability as potential disease modifying agent (Tönnies & Trushina, 2017; Niedzielska et al., 2016).

It has been suggested that in AD, mitochondrial dysfunction leads to ROS accumulation which influences amyloid protein precursor-beta processing which contributes towards the accumulation of A β pathology (Swerdlow et al., 2014). A study has shown that brain contains factors that are oxidizable such as lipids, membrane proteins, nucleic acids, and other molecules, which makes the brain highly sensitive towards the redox reaction. The generation of ROS could lead to damaging the tissues and brain. In addition, the oxidative stress increase with aging in the brain and induce the imbalance in the redox state. Other studies have also reported increased production of ROS via the electron transport chain reaction in neuronal mitochondria during physiological stress and aging which in turn contribute towards AD development (Clarke et al., 2015; Huang et al., 2016).

Hence, understanding of adipokines associated with obesity, such as leptin, adiponectin, chemerin and resistin, with any anti-oxidative or pro-oxidative properties, may shed light on molecular mechanisms associated with the obesity-AD risk.

1.6 CELLULAR MODELS: Exploring AD, obesity & oxidative stress relation

There are numerous cellular models available for the study of AD and obesity, and there are a number of ways to induce and investigate oxidative stress in cell culture. The following sections and chapters will present evidence supporting the use of H₂O₂ induced oxidative stress protocols in SH-SY5Y cells and skin derived fibroblasts in the assessment of adipokine influence over oxidative stress response.

1.6.1 H₂O₂ induced oxidative stress

There are several ways to mimic physiological oxidative stress in cell culture models of disease, most common is the use of H₂O₂ dosing at various concentrations for different incubation periods in relation to the cell line being studied (Upadhyay et al., 2019). H₂O₂ is normal low molecular weight oxygen metabolite or by-product from various metabolic pathways that acts as signalling molecule in insulin signalling cascades and various other growth factor-induced signalling (Sies, 2017). In some disease conditions including AD, high concentration of H₂O₂ metabolites are produced which damages the lipid, DNA and normal cell functioning (Gibson & Huang, 2005). Another method of inducing oxidative stress in cellular models is through use of nitric oxide (NO) (Wei et al., 2000). In some studies, hypoxic conditions have been used to mimic the oxidative stress in a cellular model. Based previous studies and efficiency, H₂O₂ was used to induce oxidative stress in line with other recent research of neurodegenerative disease. The significant link between ROS and neurodegenerative diseases have encouraged researchers towards antioxidants as therapeutic strategies (Coyle et al., 2006; Ismail et al., 2016; Zhang et al., 2020).

Oxidative stress is characterised by the imbalance of the free radical production and degradation such as, to ROS and RNS (García-Sánchez et al., 2020). ROS affects the oxygen regulation by interfering with the electron transport chain. H₂O₂ is considered as potent inducer or central player of redox regulated events and induce oxidative stress. An enzyme superoxide dismutase regulates the redox homeostasis by converting superoxide ions into H₂O₂ and oxygen. Mutation of this enzyme associates the direct pathological link between H₂O₂ lead ROS and neurodegenerative disorders. There are other ways to induce oxidative stress such as using hypoxia chamber which interferes with oxygen supply and increase the free radical release (Garcimartín et al., 2017; Brand, 2010).

There are a number of ways to induce oxidative stress in cell culture model depending on the requirement of the research study, these include:

1. 8-oxo-2'-deoxyguanosine (8-OHdG)- induces DNA base modifications / mutations leading to epigenetic information loss (Nishida et al., 2013).
2. Superoxide radical (O_2^-): generates various free radicals such as hydroxyl radical, hypochlorous acid and peroxy-nitrite that damage the NADPH oxidases which in turn interfere with the normal antioxidant reactions (Wang et al., 2018).
3. Hyperoxia: due to presence of excessive oxygen, the normal partial pressure of oxygen get disturbed leading to the reactive oxygen and nitrogen species (Birben et al., 2012).
4. Hydrogen peroxide (H_2O_2) is a potent cytotoxic agent which damages normal cellular components such as lipid membrane peroxidation, proteins, and DNA hydroxylation (Nirmaladevi et al., 2014). H_2O_2 generates ROS and forms an oxidative stress condition in the cellular models such as in differentiated SHSY5Y cells (Ramalingam & Kim, 2014). In the present study, H_2O_2 was used to induce oxidative stress because of its efficiency, and wide literature support in similar research and accepted by many researchers as an effective oxidizing agent.

1.6.2 SHSY5Y cells

One popular cell line that has been used in the advancement of understanding of AD is the human neuroblastoma, SHSY5Y cell line (Greene et al., 2020). These cells are subclone of the parental neuroblastoma cell line called SK-N-SH, generated in 1970 from a human metastatic bone marrow tumor biopsy which has been shown to carry both neuronal-like and epithelial-like cells (Shipley et al., 2016).

SHSY5Y cells demonstrate the ability to differentiate into mature neuronal-like cells, morphologically as well as functionally (exhibiting specific neuronal markers such neurofilament, neuronal specific enolase and microtubule associated protein with long and interconnected projections) (Kovalevich & Langford, 2013a). Because SHSY5Y cells can exhibit adrenergic, dopaminergic, and cholinergic neuronal subtype characteristics in response to specific culture conditions, they have been commonly used to investigate neuronal-like cell function (Xie et al., 2010).

Various Alzheimer's and Parkinson's disease related research have accepted SHSY5Y cells as a cellular model due to their ability to display neuronal like characteristics such as the presence of neurotransmitter activity upon differentiation (Almathhur et al., 2018; Sang et al., 2018; Xicoy et al., 2017). In addition, adipokine receptor expression has been identified in SHSY5Y cells for example, expression of chemerin receptors including chemerin chemokine like receptor-1 (CMKLR1), G-protein-coupled receptor-1 (GPR1) and chemokine like receptor-2 (CCL2) have been recorded in SHSY5Y cells (Tümmler et al., 2017).

Several factors can be used to promote differentiation of SHSY5Y cells include retinoic acid, phorbol esters and brain-derived neurotrophic factors (BDNF). A comparative study has shown that differentiated SHSY5Y cells do not show tyrosine hydroxylase and dopamine receptor when phorbol esters was used as differentiation factor (Magalingam et al., 2020). Research studies depicted the benefits of BDNF induced differentiation of SHSY5Y cells can be best observed following retinoic acid treatment, but it is time consuming and may increase chances of contamination in comparison to only retinoic acid induced differentiation of SHSY5Y cells (Goldie et al., 2014).

In this research study, the SHSY5Y cell line was considered in both neuronally differentiated and undifferentiated forms since the oxidative stress response of both dividing and senescent cells was of interest. The neuronally differentiated cells were produced using the common retinoic acid treatment method (Shiple et al., 2016; Agholme et al., 2010).

Retinoic acid is a vitamins A derivative which promotes the SHSY5Y cell survival, differentiation and inhibits the proliferation by activating the phosphatidylinositol 3- kinase/Akt signalling pathway and upregulating the B-cell lymphoma (Bcl-2) protein which is anti-apoptotic protein (Lopez-Carballo et al., 2002). Successful differentiation can be detected visually by observation of morphological changes and staining of specific neuronal markers such as neurofilament, microtubule associated protein and neuron specific enolase (Shiple et al., 2017; Cheung et al., 2008; Yoon et al., 2020; Bell et al., 2020).

1.6.3 3T3-L1 cells

3T3-L1, human embryonic fibroblast cell line is a well-documented pre-adipocyte cell line and used as an in-vitro model for adipogenesis (Banjare et al., 2018). Previous studies have confirmed that differentiated 3T3-L1 cells release a wide range of adipokines or cytokines such as leptin, adiponectin, TNF- α , IL-6 (Tsubai et al., 2017) which is a useful tool for the understanding the adipocyte-like and adipokines behaviour for the research. For our research study, the 3T3-L1 cell line was used and differentiated from fibroblast state (pre-adipocytes) to adipocyte-like phenotype using commercially available inducing factors including insulin, dexamethasone, and 3-isobutyl-1- methylxanthine. A study has shown that these inducing factors, inhibit the proliferation of fibroblast and dedicate the cells towards irreversible differentiation to mature adipocyte-like during the incubation period (Zebisch et al., 2012). The adipocyte-like culture releases adipokines or growth factors from the differentiated adipose tissues into the surrounding/ incubated culture media, this media was further used as conditioned media to explore the influence of the extracted culture media or conditioned media in relation to the stress response in SHSY5Y cells.

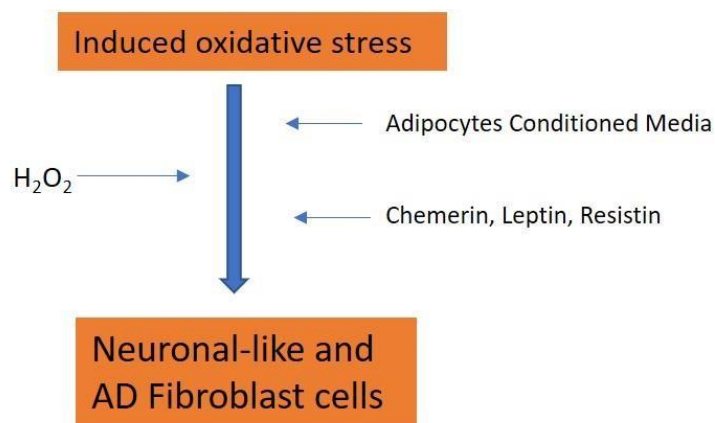
1.6.4 Skin-derived fibroblasts cells

Patient derived fibroblast cells are proving to be a useful tool in the investigation of AD. These cells have been shown to demonstrate many of the phenotypic features of AD neuronal-like cells such as altered mitochondrial function, calcium signalling dysregulation. In addition, they have the advantage of being more accessible than human brain tissue (Sarasija et al., 2018).

The advantage of skin derived fibroblast cells from AD donors is that these cells already possess biochemical characteristics similar to actual AD conditions such as an increased A β _{42/40} ratio and an individual levels of each A β peptide, however, the dominant feature will be the *PSEN* or *APP* mutation (Yagi et al., 2011; Kondo et al., 2013; Duan et al., 2014). In a recent study, it was confirmed that AD patient derived fibroblasts express oxidative stress phenotype (Hu et al., 2019) which validates their potential in shedding light on the relationship between obesity, oxidative stress, and AD. So far, no study has confirmed the co-relation between the obesity and AD using skin-derived fibroblast cells under oxidative stress.

AIM OF THE STUDY

The aim of this project is to explore the influence of adipocytes on neuronal function under oxidative stress in relation to Alzheimer's disease. We hypothesize that the adipocyte-like secreted adipokines or other growth factors and individual adipokines (chemerin, leptin and resistin) possess the ability to restore the neuronal-like cell proliferation under oxidative stress. In addition, we hypothesize that the chemerin may have rescue effect in AD cellular model under oxidative stress.



OBJECTIVES

1. Confirmation of the differentiated neuronal-like and adipocytes-like cells using ICC and Oil-Red-O staining, respectively.
2. Investigate the impact of CM from 3T3-L1 cells on neuronal-like and non-neuronal cells in relation to H₂O₂ induced oxidative stress.
3. Explore the impact of individual adipokines (chemerin, leptin and resistin) exposure on neuronal-like and non-neuronal cell viability with H₂O₂ induced oxidative stress.
4. Evaluate the effect of chemerin on AD and non-AD donors derived fibroblast cell viability under H₂O₂ induced oxidative stress.

Chapter 2. Materials and Methods

2.1 Materials

Cell culture associated drug studies, immunocytochemistry (ICC) and 3-(4,5-dimethylthiazol-2-yl)-2,5-diphenyltetrazolium bromide (MTT) assay were used to attain an understanding of how adipokines influence cellular responses to H₂O₂ induced oxidative stress. To achieve the aim of the research, as given in table.2.1, various reagents or experimental materials were used for the maximum benefit of the reagents used and optimum storage conditions were maintained.

Table.2.1 The table below enlists the experimental materials used in this research to address the product code, suppliers, and the utilisation of the reagents.

Materials	Supplier	Catalogue/ Product code	Remarks
Cell culture			
Fetal calf serum (FCS)	Labtech, Sussex, UK	115/500	For SHSY5Y and 3T3-L1 cells normal growth. Stored at 2-8°C.
Penicillin/streptomycin (P/S)	Labtech, Sussex, UK	84122-100	For SHSY5Y and 3T3-L1 cells normal growth. Aliquots stored at -20°C.
L-glutamine	TM lab consumable	---	For SHSY5Y and 3T3-L1 cells normal growth. Aliquots stored at -20°C.
Fetal bovine serum (FBS)	TM lab consumable	---	For 3T3-L1 cell differentiation Aliquots stored at -20°C.

Materials	Supplier	Catalogue/ Product code	Remarks
SHSY5Y cell culture			
SH-SY-5Y cells	European collection of cell cultures (ECACC) and UoM	94030304	For neuronal-like cell culture. Stored at -80 °C for short term and in liquid nitrogen for long storage.
Dulbecco's modified eagle's medium (DMEM)-high glucose	Fisher Scientific, Loughborough, UK	11590366	For SHSY5Y, 3T3-L1 cells cell culture. Stored at 2-8°C.
N2- Supplement	Fisher Scientific, Loughborough, UK	17502-001	For SHSY5Y cell differentiation. Aliquots stored at -20 °C.
Laminin	Sigma-Aldrich, Dorset, UK	L2020-1MG	For SHSY5Y cells differentiation. Solvent: PBS w/o Mg, Ca. Dilution :1:20. Aliquots stored at -20 °C.
Retinoic acid (RA)	Sigma-Aldrich, Dorset, UK	R2625	For SHSY5Y cell differentiation. Solvent: dimethyl sulfoxide (DMSO), Ethanol. Concentration :10µM,1 µM. Storage: -20 °C.
Ethanol	TM lab consumable	----	Light protected. For SHSY5Y cell differentiation. Storage: room temperature.
3T3-L1 cell culture			
3T3-L1 cells	American Type Culture Collection (ATCC), Middlesex, UK	CL-173 3T3-L1	For adipocyte-like cell culture. Stored at -80 °C for short term and in liquid nitrogen for long storage.

Materials	Supplier	Catalogue/ Product code	Remarks
Dulbecco's modified Eagle's medium (DMEM)	American Type Culture Collection (ATCC), Middlesex UK	ATCC® 30-2002™	For 3T3-L1 cell culturing.
Dexamethasone (DEX)	Labtech, Sussex, UK	23548	For 3T3-L1 cell differentiation Solvent: DMSO Aliquots stored at -20°C.
Methyl-isobutyl-xanthine (IBMX)	Sigma-Aldrich, Dorset, UK	15879	For 3T3-L1 cell differentiation Solvent: DMSO Aliquots stored at -20°C.
Insulin	Sigma-Aldrich, Dorset, UK	10516	For 3T3-L1 cells differentiation. Stored at 2-8°C.

Fibroblast cell Culture

Minimum essential media (MEM)	Fisher Scientific, Loughborough, UK	31095	For fibroblast cell culture. Stored at 2-8°C.
Non-essential amino acid (NEAA)	Fisher Scientific, Loughborough, UK	11140050	For fibroblast cell culture. Stored at 2-8°C.

ICC (For SHSY5Y cells)

Anti- neurofilament, monoclonal antibody	Millipore, Hertfordshire, UK	MAB1592	Mouse primary antibody. Solvent: 1% BSA. Aliquoted and stored at -20°C.
Monoclonal-anti-microtubule associated protein (2a+2b)	Sigma-Aldrich, Dorset, UK	M1406-100UL	Mouse primary antibody. Solvent: 1% BSA. Aliquots stored at -20 °C.

Materials	Supplier	Catalogue/ Product code	Remarks
Neuron specific enolase	Proteintech, Nottingham, UK	66150-1-Ig	Mouse primary antibody. Solvent: 1% BSA. Aliquots stored at -20°C.
Polyclonal goat anti-mouse	DAKO, Cheshire, UK	P0447	IgG - used as negative control Solvent: 1% BSA. Dilution used: 1:200. Aliquots stored at -20°C.
Goat anti-mouse IgG H&L PE conjugated	Abcam, Cambridge, UK	ab97024	Polyclonal secondary antibody Solvent: 1% BSA. Dilution used: 1:200 Stored at 2-8°C.
Ammonium chloride	Fisher Scientific, Loughborough, UK	10785701	ICC of SHSY5Y cells. Solvent: PBS. Concentration: 50mM. Stored at room temperature.
TritonX-100	Sigma-Aldrich	T8787-100ml	For ICC.
Bovine serum albumins (BSA)	Fisher Scientific, Loughborough, UK	BP 9701-100	For ICC. Solvent: PBS Freshly prepared.
Vectashield mounting medium with DAPI	Vectolaboratories, CA, USA	H-1200	For ICC.
Oil-Red-O staining (For 3T3-L1 cells)			
Oil-Red-O stain	Sigma-Aldrich, Dorset, UK	O1391-500ml	For the 3T3-L1 cells staining Stored at room temperature.

Materials	Supplier	Catalogue/ Product code	Remarks
Paraformaldehyde	Sigma-Aldrich, Dorset, UK	P6148- 500G	For the 3T3-L1 cells staining Stored at room temperature

MTT assay

3-(4,5-dimethylthiazol- 2-yl)-2,5- diphenyltetrazolium bromide (MTT)	TM Lab consumable	--	For cytotoxicity assay (MTT assay). Solvent: PBS. Concentration: 3mg/ml Stored at 20 °C.
Recombinant human chemerin	Peprtech	300-66	Cell culture assay.
Recombinant human resistin	Peprtech	450-16	Cell culture assay.
Leptin human	Sigma	L4146	Cell culture assay.

2.2. Methods

2.2.1. Cell culture

Three different cell lines were used in the present study. The commercially available cell lines were thawed, cultured, and maintained using cell culture technique as described below in section 2.2.2. Cultured cells were cryopreserved in liquid nitrogen for future use. The cell lines used were:

1. **3T3-L1 cells, pre-adipocytes:** The cell line was purchased from ATCC using catalogue number 3T3-L1 (ATCC® CL-173™) and delivered as frozen vial. These *mus musculus*/mouse derived embryonic cells exhibited fibroblast like morphology and adherent characteristics were deposited in 1974 without passage number by the depositor (ATCC, 2014). 3T3-L1 cells are generally used as in-vitro adipocytes model which displays characteristics of adipocyte-like cells including the lipid load (Morrison & McGee, 2015). The cell lines were maintained and differentiated into adipocytes-like by following differentiation cell culture method which will be discussed in detail in section 2.2.3.
2. **SHSY5Y cells, neuroblastoma cells:** The SHSY5Y cells were supplied as frozen vial, passage 6 by ECACC, general collection of catalogue number- 94030304. The SHSY5Y cells were subcloned from SK-N-SH cell line which was sub-lined three times from bone marrow biopsy of metastatic neuroblastoma of 4-year-old female and established as culture in 1970. The SHSY5Y cells were cultured and differentiated using commercially available reagents among which all-trans-RA played vital role for differentiation (Korecka et al., 2013). The use of SHSY5Y cells have been documented widely in numerous neurodegenerative studies including AD (Xicoy et al., 2017; Greene et al., 2020; Guo et al., 2021).
3. **Skin derived fibroblast cells:** The human skin derived cells used in the present study showed fibroblast like characteristics and were purchased from the Coriell Institute within the National Institute of Aging (NIA) cell culture repository. The fibroblast cells were obtained from patients with sporadic AD and non-AD donors. The disease characteristics and age of the cell lines used are listed in table.2.2 The skin derived fibroblast cells have been popularly used for various neurodegenerative research studies including AD (Auburger et al., 2012).

Table.2.2. Donor details and disease characteristics of the skin-derived fibroblast cells used in this study are given in the table.

Donor	Catalogue No.	Passage received	Age/Gender	Disease Characteristics
Sporadic AD patients	AG05809	3	63yrs/Female	Moderate dementia with insidious onset
	AG07872	3	53yrs/Male	Affected with AD
	AG06869	3	60yrs/Female	Moderate dementia with impaired memory
Non-AD patients	AG08509	3	73yrs/Male	Unaffected donor
	AG08125	3	64yrs/Male	Unaffected donor
	AG08517	3	66yrs/Female	Unaffected donor

2.2.1.1 Image Analysis:

To observe the morphological changes and estimate the confluency of the cell culture, images were captured using an inverted bright field microscope TJ002/Nikon2000i (Nikon, Germany), at different magnifications (mentioned in respective result section). The images presented were taken once to confirm the effective progression of cell culture. The images of 3T3-L1 cells after Oil-Red-O staining, were captured using an inverted bright field microscope and BioTek Cytation3 (BioTek Instruments Inc., USA), a cell imaging multi-mode reader (section 3.2.1.1). The immunofluorescent images of SHSY5Y cells after ICC, were captured using Carl Zeiss Vert.A1 (Zeiss, Germany), a confocal microscope with DAPI and Cy3 filter (section 3.2.2.2) and BioTek Cytation3 with DAPI and Cy3 filter (section 3.2.2.3.1/3.2.2.4.1) was used. The Oil-Red-O staining and ICC experiments were performed once, to approve the existence of markers present specifically in differentiated 3T3-L1 and SHSY5Y cells and confirm the cellular models were established (adipocyte-like and neuronal-like, respectively). Therefore, no statistical images analysis was performed.

2.2.2. Cell culture maintenance

2.2.2.1. Thawing of frozen cells

Cell lines were frozen in DMSO, a cryoprotectant, until required as described in section 2.2.2.3. This ensured appropriate passage of cells were used for the future experiments. Rapid thawing of the frozen cell cultures is important to optimise the number of viable cells because DMSO is toxic above 4°C.

DMSO prevents the formation of intracellular and extracellular ice crystals which compromise cell viability (Wang et al., 2007). The frozen cell vial was retrieved from liquid nitrogen and transferred to water-bath, 37°C. As soon as the frozen vial started to thaw, the cells were transferred to 5ml pre-warmed media (relevant to the individual cell line) in a falcon tube. After a uniform mixing, the falcon tube was centrifuged (VWR®, MegaStar 1.6) at speed 400xg for 4 mins used for SHSY5Y cells as well as fibroblast cells and 200xg for 5 mins used for the 3T3-L1 cells. The collected pellet at the falcon bottom was mixed with fresh pre-warmed media and the cell suspension was transferred to a T25 flask and placed in a humidified incubator, 5% CO₂ and 37°C.

2.2.2.2. Sub-culturing

The process of sub-culturing, generally known as splitting or passaging includes detaching the growing cells, centrifuging, and transferring to a fresh media to facilitate a continuous growth and maintain cell population increase (Mustafa et al., 2011). Similar splitting method was used for all the cell lines with different centrifugation speed. The cell lines used in this study were adherent cell cultures. The cell cultures were allowed to attain the 70-80% confluency with 50% pre-warmed fresh media change every alternate day to ensure continuous nutrient supply and healthy cell growth. For splitting, the growing culture flask was kept in the sterile class II biosafety cabinet and the old media was removed. The culture flask with attached cells was washed with sterile phosphate buffer saline (PBS). When extra trace of media was removed by PBS washing, the cell monolayer was trypsinized by adding EDTA-trypsin and incubated in humidified condition for 1 minute, 37°C and 5% CO₂. The detached cells were collected in a falcon tube and centrifuged (400xg for 4 mins used for SHSY5Y cells as well as fibroblast cells and 200xg for 5 mins used for 3T3-L1 cells).

The cells collected at bottom after centrifugation as pellet, were mixed evenly and transferred to the new T75 flask with fresh pre-warmed media, after a uniform mix, the flask was maintained in humidified condition, 37°C and 5% CO₂.

2.2.2.3. Cryopreservation

The cryopreservation technique, also called as freezing method, is process of reducing the cell viability slowly by decreasing the temperature 1°C per minute and finally to a dormant state in specialized container (Nalgene™ freezing container). In this study, the freezing media was prepared freshly using 90% FBS with 10% DMSO as a cryoprotectant. To freeze the cells for future use, the growing cell culture was detached and collected after trypsinization and centrifuged (as explained in the section 2.2.2.2). The cell pellet was resuspended, pipetted to a labelled cryovials, and then transferred to Nalgene™ freezing container (stored at -80°C). After 24 hrs, cryovials were transferred and stored in liquid nitrogen (below -190°C). Frozen vials were used within the experiments detailed here, to ensure that comparable passage numbers were used and increase consistency.

2.2.3. Establishing an adipocyte-like cell culture model

3T3-L1 cells were used as pre-adipocytes for this study and were cultured and maintained to establish an adipocyte-like cellular model. The mouse derived embryonic fibroblasts; 3T3-L1 cells were purchased from ATCC as a frozen cell sample. Frozen vials were thawed and cultured in T25 flasks using normal growth media as described in section 2.2.2. Once the cell culture reached 70%-80% of confluency in T25, the cells were sub-cultured and transferred to T75 flask for further cell culture and frozen stock preparation. Studies on differentiation of 3T3-L1 cells have shown that passages between 6-10 have low differentiation (Kassotis et al., 2017) potential. In this study, the cell culture between passage 10-15 were used which showed optimal cell viability and differentiation. The pre-adipocytes expansion media was prepared using 90% DMEM +10% FCS +1% P/S. For the future use, the 3T3-L1 cells were frozen down using 90% pre-adipocytes expansion media and 10% (v/v) DMSO, as described in section 2.2.2.3.

2.2.3.1. Maintenance and expansion of 3T3-L1

Pre-adipocyte expansion media comprised of 90% DMEM media supplemented with 10% FCS and 1% P/S was used for the maintenance of 3T3-L1 cells. The 3T3-L1 cells were cultured and sub-cultured in T75 flask with 1:10 ratio and the media was replaced with fresh pre-warmed pre-adipocyte expansion media in every 72 hrs. Once cells reached 70-80% confluency, cells were harvested via trypsinization and incubated with EDTA-trypsin for one minute in incubator (37°C, 5% CO₂) and collected cells were centrifuged at 200xg for 5 mins. The cell pellet was resuspended in complete media and transferred to T75 flask with fresh media, similar culture process was repeated to maintain and increase the cell population.

2.2.3.2. Differentiation of 3T3-L1 to adipocyte-like cells

For the differentiation, 3T3-L1 cells were detached and collected by trypsinization and centrifugation (section 2.2.2). The obtained pellet was resuspended in 1ml of fresh pre-warmed preadipocyte expansion media and cell count was performed using a haemocytometer to calculate the volume of cell suspension needed to achieve the appropriate cell density for seeding.

The cells were seeded in the 24 well plates at a cell density of 2×10^4 cells per ml. The desired volume of cells was resuspended in the final volume of pre-adipocyte expansion media. The seeded cells were allowed to grow for 48 hrs in humidified condition and 5% CO₂. After 48 hrs, the cells were fed with the pre-adipocyte expansion media and incubated as a confluent culture (100%) for another 48 hrs. After 48 hrs, the pre-adipocyte expansion media was replaced with the differentiation media and incubated at 37°C and 5% CO₂. The differentiation media was prepared by adding 90% DMEM with 10% FBS, 1 μ M dexamethasone, 0.5mM isobutyl methylxanthine (IBMX) and 1 μ g/ml insulin and the cells were incubated for another 48 hrs. Dexamethasone is an adipogenic inducer in murine derived in-vitro models (Peshdary & Atlas, 2018). IBMX is a phosphodiesterase inhibitor which acts as initiator of adipocytes maturation related transcriptional cascade (Pantoja et al., 2008).

In the presence of insulin, increase in the glucose uptake into adipocytes was observed by translocation of glucose transporter type 4 (GLUT4) receptor (Vishwanath et al., 2013). After 48 hrs, the differentiation media was replaced with the maintenance media (90% of DMEM with 10% FBS and 1µg/ml insulin) for another 72 hrs. After this point, extra care was exercised due to low cell adhesion and high risk of contamination. The maintenance media was replaced every 72 hrs of incubation for further 15 days until the cells became fully differentiated. This was evidenced by the presence of excess lipid droplets over the confluent 3T3-L1 cell culture and very thick media with a pale-yellow appearance. Any sign of cloudy/ orange appearance of media indicated contamination and unsuccessful differentiation.

2.2.3.3. Confirmation of 3T3-L1 differentiation

In order to confirm the differentiation of 3T3-L1 cells, Oil Red-O staining was performed (Kraus et al., 2016). Oil Red-O working solution was prepared fresh using 60: 40 ratios of Oil Red-O stain and distilled water (dH₂O), i.e., 6 ml of Oil Red-O stain and 4ml dH₂O. Once the cells were fully differentiated (week 3 or 21st day of seeded cells), the media was completely removed from each well and the cells were washed with PBS. After removing PBS, the cells were incubated with 200 µl of 8% paraformaldehyde for 30 mins at room temperature to fix the cells. The fixed cells were washed twice with PBS. The PBS was completely removed, and freshly prepared Oil Red-O stain was added and incubated for 1 hr at room temperature. After an hr, the stain was removed, and cells were washed with PBS three times. The stained cells were submerged in PBS to avoid drying of stained cells and stored at 4°C, overnight. Images were taken the next day using BioTek Cytation3 (discussed in 2.2.1.1).

2.2.4. Establishing neuronal-like cell culture model

The human neuroblastoma, SHSY5Y cell line was used to generate neuronal-like cell model to investigate cellular changes relevant in AD (de Medeiros et al., 2019). Differentiated SHSY5Y cells are well characterised and resemble closely with human neuronal-like phenotype (Korecka et al., 2013). Cells were maintained and sub-cultured between passage 6 and 15 because cell survival decreases and differentiation become more difficult (Shipley et al., 2016).

The SHSY5Y cells were differentiated into mature neuronal-like cells by following two protocols which will be discussed in detail in section 2.2.4.2. Briefly, these two incubation periods were optimized to confirm that by following both differentiation protocols, similar neuronal-like cells were obtained (Armstrong et al., 2005).

2.2.4.1 Maintenance and expansion of SHSY5Y cells

SHSY5Y cells were cultured and maintained using 90% DMEM- high glucose media supplemented with 10% FCS as a source of growth factors, 1% L-glutamine (an essential amino acid), and 1% P/S in T75 flasks with the 50% fresh pre-warmed media being replaced every 48 hrs. The growing cell culture was allowed to expand until 70-80% confluent. Cells were passaged after this, trypsinized and incubated with EDTA-trypsin for 1 min in incubator (37°C, 5% CO₂) and detached cells were centrifuged at 400xg for 4 mins. The cell pellet collected was resuspended in complete media and transferred to T75 flask with fresh pre-warmed media. Regularly half volume of media was replaced and sub-cultured to maintain, increase, and facilitate freezing of cell stocks.

2.2.4.2 Differentiation of SHSY5Y cells into neuronal-like cells

The human neuroblastoma, SHSY5Y cells were differentiated into mature neuronal like cells by following two protocols: 10-days (using 10µM RA) and 21-days (using 1µM RA) protocols. These protocols aim to induce homogeneous and mature neuronal behaviour by decreasing proliferation, extending the axonal projections allowing communication with neighbouring cells and expressing specific neuronal markers. The neuronal markers used for the confirmation of differentiated SHSY5Y cells were neuronal specific enolase (NSE), microtubule associated protein 2 (MAP2) (Kovalevich & Langford, 2013a) and neurofilament (NF) (Forster et al., 2016). These specific neuronal markers were used to confirm differentiation of SHSY5Y cells into neuronal-like phenotype. The RA stock of 10 mM was prepared, aliquoted, and stored at -20°C, wrapped in foil to protect from light (RA is light sensitive reagent).

For working stock, a 10 μ M or 1 μ M stock was made in 99.9% filtered ethanol. RA is required to regulate the signalling pathways involved in the transitioning and post-mitotic differentiation of SHSY5Y cells (Lopes et al., 2010).

Cells were seeded onto laminin-coated coverslips to facilitate SHSY5Y cell differentiation by enabling homogeneous attachment (Teppola et al., 2018). Laminin (aliquoted and stored at -20°C) was thawed and dilution of 1:20 in PBS without Mg⁺ and Ca⁺ was freshly prepared. This was used to coat the glass coverslips prior to cell seeding. In each well, 500 μ l of laminin was added and incubated (at 37°C, 5% CO₂) for 30 mins. After the incubation, the laminin was removed.

The SHSY5Y cells were detached, once attained 70% confluency, and seeded in 6 well plates for differentiation. The cells were harvested by trypsinization and cells were collected and centrifuged at 400 x g for 4 mins. After collecting the pellet, cells were resuspended in 1ml of complete media and the cell counting was performed using haemocytometer. A cell density of 5 x 10⁴ cells per well was used for seeding in 6 well plate with pre-warmed media. The plate was uniformly swirled to evenly distribute cells in each well and incubated to grow for 48 hrs. Complete media was replaced with serum-free differentiation media (47ml of DMEM: F12 + 1ml of N2-supplement + 1ml of L-glutamine + 1ml of P/S and 1 μ M/ml or 10 μ M/ml of RA depending on the 10/21-days protocol being followed) to allow genomic transformation of cells from immortal neuroblastoma to the neuron-like cells (Forsby, 2011).

The plates were covered in foil to avoid light exposure to the cells for rest of the differentiation period because the RA in differentiation media is extremely sensitive to light and undergoes structural change by photoisomerization which can affect the nuclear receptors and differentiation (Kunchala et al., 2000). After every 48 hrs, half media was replaced with fresh pre-warmed differentiation media until day 10 or 21. Microscopic images of undifferentiated and differentiated SHSY5Y cells were captured from respective wells on day 0,3,5,7,10,13,15,19 and 21 (discussed in 2.2.1.1).

2.2.4.3. Optimization: Differentiation protocols

Differentiation of SHSY5Y cells required optimization. The following optimization steps were carried out to obtain an effective differentiation protocol:

Cell density: In order to achieve 60% confluency before differentiation, different cell densities were explored. After cell counting the cells were seeded using cell density of 3×10^4 , 4×10^4 and 5×10^4 per well (Jantas et al., 2020; Murillo et al., 2017).

RA: Differentiation of SHSY5Y cells can be impacted by degradation of RA (Veal et al., 2002). Optimization of RA use within the cell culture system was required. The RA was initially used by dissolving directly in the media without taking light protective measures, then the media with added RA was covered during storage. Finally, the media was prepared fresh every time for the half media change.

Ethanol: Ethanol was used as solvent for dissolving RA to oxidise the alcohol of RA into all-trans-RA structural form. Two different concentrations, 95% and 100% concentration of ethanol were used for RA stock and working stock preparation (Serio et al., 2019) (Sigma product sheet for RA-R2625). 99.9% of ethanol was used instead of 100% because of the availability at university and upon optimization, the 99.9% ethanol solution worked.

2.2.4.4. Confirmation of neuronal-like phenotype

For the confirmation of the differentiation of SHSY5Y cells, ICC was performed to detect the presence of neuronal markers including NSE, MAP2 and NF in differentiated cells in comparison to undifferentiated SHSY5Y cells. For the ICC experiment, cells from both differentiation methods were used (i.e., 10 or 21-day differentiation method). The delicate axonal outgrowth between the cells, required careful handling during the ICC experiment. The ICC experiment was performed once to confirm the successful differentiation of SHSY5Y cells.

The SHSY5Y cells were seeded on coverslips for differentiation and the coverslips with cells were removed from each well after ICC for the imaging. The media was removed completely from each well and washed with PBS three times. The cells were fixed with 4% paraformaldehyde for 10 mins. After removing the paraformaldehyde, the cells were quenched to reduce background fluorescence by washing once with 50mM of ammonium chloride in PBS (Nybo, 2012). Excess of ammonium chloride was removed by washing with PBS twice for 5 mins. To allow antibodies access into the cells were permeabilized with 0.5% TritonX-100 for 5 mins. After the permeabilization, the cells were washed with PBS three times for 5 mins. To prevent nonspecific binding of antibodies, cells were incubated for 1 hr in 5% bovine serum albumin (BSA) in PBS at room temperature. After the blocking step, the cells were washed 3 times with PBS. After washing, the cells were incubated with primary antibodies (Ab) or immunoglobulin (IgG) Ab as negative control for 1 hr. IgG was incubated as same concentration as the primary Ab detailed below. The negative control was included to demonstrate the specificity of staining of the target antigen. Listed below are primary Ab and negative Ab:

- Anti- NF, mouse- monoclonal Ab (1 μ g/1ml) in 1% BSA in PBS.
- Mouse-MAP2, mouse-monoclonal Ab (1 μ g/1ml) in 1% BSA in PBS.
- Mouse-NSE, monoclonal Ab (mouse- monoclonal antibody (5 μ g/ml) in 1% BSA in PBS.
- Polyclonal goat anti-mouse IgG/horseradish peroxidase (HRP) (as negative Ab) in 1% BSA in PBS.

After completion of the 1hr incubation, the cells were washed 3 times with PBS. Cells were incubated with a secondary antibody i.e., goat anti-mouse IgG, heavy and light chain (H&L) phycoerythrin (PE) conjugated (mouse- monoclonal antibody (150 μ g/150ml), 1:200 dilution with 1% BSA in PBS for 1 hr in dark. After 1 hr, the excess secondary Ab was removed by washing 3 times with PBS, excess PBS was removed, and coverslips were mounted using a vectashield, 4',6-diamidino-2-phenylindole (DAPI) to preserve fluorescence and stain the nuclei. Excess of DAPI was soaked from the edges of the coverslip using tissue paper and sealed with the nail polish. Literature or research studies was referred to confirm the consideration of mouse antibodies for ICC experiment on human derived SHSY5Y cells and upon optimization, the

neuronal markers showed expected results (will be discussed in section 3.2.2.2). The slides were stored at 4-8°C in dark and images of differentiated, undifferentiated, and negative control SHSY5Y cells were captured next day using confocal microscope (discussed in 2.2.1.1).

2.2.4.5 Optimization: primary/secondary Ab ratio

Primary/secondary Ab ratio: various combination of primary to secondary Ab ratios were used to optimize the ICC protocol for differentiated cells. After the optimization, the final Ab ratios used for the ICC will be discussed in the table 3.1. The dilutions used are shown in table.2.3.

Table.2.3. Optimization of primary and secondary Ab using different dilutions or ratios were performed to obtain the accurate combination for ICC protocol. In the table given below are Ab dilutions (in ratio form), type of Ab, and incubation duration are listed.

Antibody Used	Type of Ab	Dilution used
NF Ab	Primary	1:50, 1:100, 1:200
MAP2 Ab	Primary	1:100, 1:150
NSE Ab	Primary	1:50, 1:100
PE-Conjugated	Secondary	1:100,1:150, 1:200
IgG monoclonal	Negative control	Same as primary Ab for each marker

2.2.5 Establishing fibroblast cell culture

Human skin derived fibroblast cells from three AD patient and three non-AD donors of different age groups were obtained from Coriell Institute, NIA. Cell line details are given in table.2.2. The fibroblast cells obtained from Alzheimer’s patients possess reduced cell growth as they were diseased. The fibroblast cell cultures were maintained and sub-cultured (detailed in following section 2.2.5.1) up to passage 15 (Unger et al., 2009).

2.2.5.1 Maintenance and expansion of fibroblast cells

The fibroblast cells were cultured and maintained using normal complete media comprised of 85% DMEM-high glucose media supplemented with 15% FBS, 1% L-glutamine, 1% P/S, 1% non-essential amino acid (NEAA) in T75 flask. The cell culture growth was maintained with half pre-warmed fresh complete media change every alternate day. The growing cell culture was allowed to reach 70-80% confluency in a T75 flask, then the cells were passaged by trypsinization using EDTA-trypsin for 1 minute in incubator (at 37°C and 5% CO₂) and detached cells were centrifuged at 400xg for 4 mins. The cell pellet collected was resuspended in complete media and transferred to T75 flask with fresh pre-warmed media. The fibroblast cell culture was maintained and cryopreserved using 90% normal complete media + 10% DMSO and stored in liquid nitrogen for future use.

2.2.6 Measuring cell viability of cultured cells

MTT is colorimetry assay which involves the conversion of soluble MTT dye, a yellow powder, into insoluble purple coloured formazan. The MTT assay is a well-documented method for determining cell viability; NADPH dependent cellular oxidoreductase enzymes present reduce the tetrazolium dye, MTT, into insoluble formazan (Kumar et al., 2018). DMSO is needed to dissolve the insoluble formazan and facilitates the quantification of colorimetric changes using plate reader at 540-690 nm optical density (Van Meerloo et al., 2011). MTT assay is sensitive and show linearity up to approximately 10⁶ cells per well, and thus it is the most popular and adapted assay in research labs (Kumar et al., 2018).

2.2.6.1 General MTT assay protocol

The MTT dye was prepared using 3mg/ml in sterile PBS. Once the cells were ready for MTT assay, the plates were kept in sterile hood and 250 µl MTT per ml was added to each well and incubated for 3 hrs. Media containing the MTT solution was removed and 1ml DMSO was added to the dissolve the crystals of formazan, after incubation and the plate was read using plate reader (Omega software Version5, BMG Labtech, Germany) at 540nm/690nm wavelength.

2.2.6.2 Dose dependent assay on SHSY5Y cells using H₂O₂

A study in which the responses are recorded, based on cellular activity in exposure to any toxic agent, drug, fluorescent dye and others is called as dose dependent assay (Efeoglu et al., 2016). In this study, the cell viability was recorded in the presence and absence of different doses of H₂O₂, and EC₅₀ was calculated after incubation with different H₂O₂ concentrations in order to estimate the dose dependency required to get appropriate concentration for further studies. Oxidative stress is one of the major key factors to manifest neuropathologies in AD and it possesses ability to damage cellular and molecular pathways (Ton et al., 2020).

2.2.6.2.1 H₂O₂ dose dependent assay on undifferentiated SHSY5Y cells

To determine a specific dose concentration to achieve EC₅₀, different doses of H₂O₂ were used ranging between 50-500µM. The cells were plated with each dose and incubated for 24 hrs. From stock 8.8M concentration (concⁿ) of H₂O₂, a 100mM working stock was prepared in sterile PBS using 56µl volume (V) of H₂O₂. Working stock was stored at 2-8°C until 1 week. To prepare 100mM (0.1M) of H₂O₂ in PBS from 8.8M of H₂O₂ stock:

$$= \text{conc}^n (\text{required}) \times V (\text{required}) = \text{conc}^n (\text{final}) \times V (\text{final})$$

$$= 8.8\text{M} \times V (\text{required}) = 0.1\text{M} \times 5\text{ml}$$

$$= V (\text{required}) = \frac{0.1\text{M} \times 5\text{ml}}{8.8\text{M}} = 0.056\text{ml} = 56\mu\text{l} \text{ (hence, } 56\mu\text{l of H}_2\text{O}_2 \text{ stock} + 4.94\text{ ml PBS)}$$

To obtain EC₅₀ dose concⁿ of H₂O₂ for undifferentiated SHSY5Y cells, MTT method was followed. The undifferentiated SHSY5Y cells were seeded from growing T75 flask after 70-80% confluency was attained. The SHSY5Y cells were harvested by trypsinization, resuspended, and seeded with cell density of 4 x 10⁴ cells per well in 24 well plate. The plates were seeded in triplicate (n=3).

After seeding, the cells were incubated in the humid incubator, 37°C and 5% CO₂ for 24 hrs to allow the cells adhere and adjust in each well. After 24 hrs, the seeded SHSY5Y cells were treated with 50, 100, 150, 250 and 500µM of H₂O₂. The dosed plates were placed in the incubator, maintained at 37 °C and 5% CO₂ for 12 and 24 hrs. After the completion of respective experiment dosing time, MTT reagent was added to a final concⁿ of 3mg/ml and incubated for 3 hrs (37°C and 5% CO₂) (Datki et al., 2003). An equal volume of DMSO was added to each well to dissolve the insoluble formazan and read in the spectrophotometer at optical density (OD) 540nm and 690nm. Each experiment was performed in 3 technical and 3 biological repeats (as n=3). The statistical analysis to obtain EC50 using GraphPad Prism5 (detailed in section 2.3). Data obtained was normalised by following formula:

$$OD(\text{control}) - OD(\text{Test}) \div OD(\text{Test}) \times 100$$

2.2.6.2.2 H₂O₂ dose dependent assay on differentiated SHSY5Y cells

To estimate the EC50 value of H₂O₂ induced oxidative stress in mature neuronal-like cells (differentiated SHSY5Y cells), different doses of H₂O₂ were used ranging between 50-500µM. From stock H₂O₂ of 8.8M concⁿ, a 150 mM working stock was prepared in sterile PBS.

Working stock was stored at 2-8°C for until 1 week:

$$= \text{conc}^n (\text{required}) \times V (\text{required}) = \text{conc}^n (\text{final}) \times V (\text{final})$$

$$= 8.8\text{M} \times V (\text{required}) = 0.15\text{M} \times 5\text{ml}$$

$$= V (\text{required}) = \frac{0.15\text{M} \times 5\text{ml}}{8.8\text{M}} = 0.085\text{ml} = 85 \mu\text{l} \text{ (hence, } 85 \mu\text{l of H}_2\text{O}_2 \text{ stock + 4.91 ml PBS)}$$

SHSY5Y cells differentiated into neuronal-like cells using the 10-day protocol were treated with 50, 100, 150, 250 and 500 μ M H₂O₂ for 12 and 24 hrs followed by MTT assay for EC50 dose value estimation was performed (detailed in 2.2.6.2.1 and 2.3).

2.2.6.2.3 H₂O₂ dose dependent assay on skin derived fibroblast cells

To determine a specific H₂O₂ concⁿ to achieve EC50, different doses of H₂O₂ were used ranging between 0.5-1.5 mM from stock H₂O₂ (Ramamoorthy et al., 2012). Stock H₂O₂ of 8.8M concⁿ was used and working stock was prepared (section 2.2.6.2.2, used for calculation) in sterile PBS.

Fibroblast cells (from AD and non-AD donors) were harvested from growing/continuous cell culture in T75 flask (80% confluent). The cells were trypsinized using EDTA-trypsin. The detached cells were transferred to falcon tube and centrifuged at 400xg for 4 mins, the collected pellet was resuspended in complete media and seeded with 5x10⁴ cell density per well in 6 well plate (Richards et al., 2011). The plates were seeded in triplicate. The cells were placed in the humid incubator, 37 °C and 5% CO₂ for 24 hrs to allow the cells to adhere and adjust in each well. After 24 hrs, the seeded fibroblast plates were taken out from the incubator and placed in the sterile hood. Different doses of H₂O₂ i.e., 0.5-1.5mM were added in each well and incubated for another 24 hrs in the incubator, 37°C and 5% CO₂. After 24 hrs, MTT assay was performed, and data was obtained for the statistical analysis (will be discussed in section 2.3).

2.2.6.3 Investigating the effect of co-treatment using CM from 3T3-L1 cells on SHSY5Y cell viability

Conditioned media (CM) is media harvested from cultured cells and consists of metabolites, different growth factors, cytokines, and secreted proteins (ATCC, 2019). Differentiated 3T3-L1 cells acts like adipocytes and actively secrete many adipokines as well as other growth factors. It would be useful to understand the importance of these secreted adipokines in relation to neuronal like cells which makes 3T3-L1 cells very useful tool of investigation (Takahashi et al., 2008).

Our peer research group, Dewhurst et al., unpublished, have confirmed that the CM obtained from the differentiated 3T3-L1 cells contains adipokines such as adiponectin, chemerin, resistin, interleukins and other growth factors.

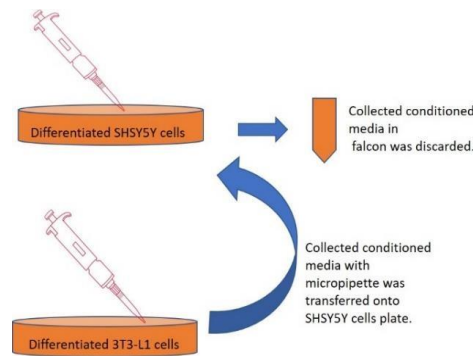


Figure 2.1 Schematic diagram represents the general steps involved in the CM technique. Firstly, the culture media was removed from the differentiated SHSY5Y cells in falcon tube to be discarded, then the CM collected from 3T3-L1 cells was transferred on to the differentiated SHSY5Y cells for further studies.

As shown in figure.2.1, the growing culture media from the differentiated SHSY5Y cells was collected using micropipette in the falcon tube and discarded. The media was harvested from the differentiated 3T3-L1 cells and transferred on to differentiated SHSY5Y cells for 24 hrs incubation as CM and placed in humidified incubator maintained at 37 °C, 5% CO₂. Similar, experimental method was performed using undifferentiated SHSY5Y cells.

2.2.6.4 Effect of co-treatment using adipocyte-like and pre-adipocyte (3T3-L1) derived CM on oxidative stress induced cytotoxicity in differentiated and undifferentiated SHSY5Y cells

To understand the role of adipokines present in the CM on SHSY5Y cells, the CM from differentiated 3T3-L1 (adipocyte-like) and undifferentiated 3T3-L1 (pre-adipocytes) cell culture was incubated with differentiated and undifferentiated SHSY5Y cells. Similar, three co-treatment methods for CM were performed using CM from adipocytes and pre-adipocytes (as shown in figure 2.2) on SHSY5Y cells (differentiated and undifferentiated).

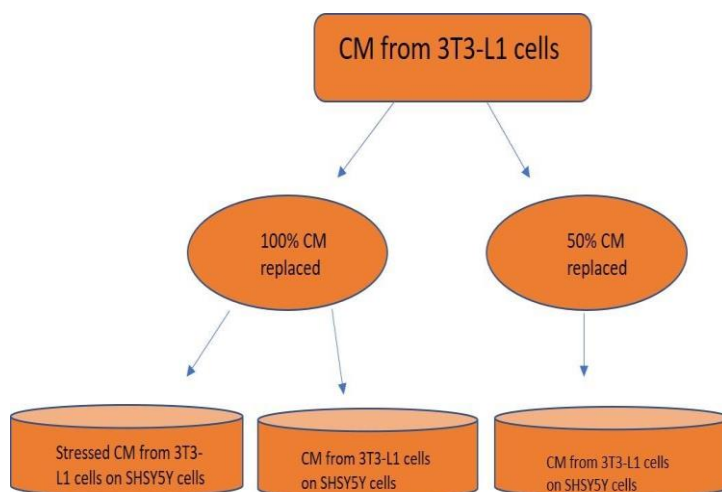


Figure 2.2. Three different co-treatment conditions were used with CM from 3T3-L1 cells on the SHSY5Y cells (differentiated and undifferentiated). Stressed CM referred to the CM derived from 3T3-L1 cells which was pre-treated with 150 μ M dose of H₂O₂ (24hrs prior to experiment).

SHSY5Y cells were plated with cell density of 5×10^4 cells per well and differentiated, as discussed in section 2.2.4.2. Three conditions were investigated: stressed CM treatment with complete or 100% media replacement, 3T3-L1 CM treatment with complete or 100% media replacement and lastly, 3T3-L1 CM treatment with complete or 50% media replacement. For the H₂O₂ stressed CM treatment condition, the adipocytes were incubated with H₂O₂ for 24 hrs. After 24 hrs, the plates were placed in sterile hood and the media from the adipocytes was used as CM and incubated on the SHSY5Y cells after removal of growing culture media (of SHSY5Y cells) and then the plates were incubated in the humidified incubator for another 24 hrs. After completion of incubation time, the MTT assay was performed, and data was obtained. For 3T3-L1 CM treatment with complete or 100% media replacement experiment, the media was completely removed from the SHSY5Y cells (differentiated and undifferentiated) and replaced with the CM from differentiated 3T3-L1 cells. For the 3T3-L1 CM treatment with complete or 50% media replacement experiment, 1ml of continuous growing media was removed from the SHSY5Y cells (differentiated and undifferentiated) and replaced with 1ml of differentiated 3T3-L1 CM to ensure cellular exposure to equal amounts of each media type. Cells were returned to a humidified incubator for 24 hrs. After completion of incubation time, the MTT assay was performed, and data was obtained, and statistical analysis was performed to understand the effect of CM on neuronal-like cell viability under oxidative stress (will be discussed in section 2.3).

2.2.6.5 Investigating the co-treatment effect of commercial adipokines under oxidative stress on SHSY5Y cells response

Assessing the effect of CM from 3T3-L1 cells allowed us to explore the impact of an adipokine rich environment on cellular function, however, it did not allow us to examine the importance of individual adipokines in response to oxidative stress. To estimate the effect of chemerin, leptin and resistin on the SHSY5Y cells, commercially available chemerin, leptin and resistin were added individually to the differentiated and undifferentiated SHSY5Y cells, in the presence and absence of H₂O₂. Adipokines were investigated individually as follows; chemerin and resistin were added at a final concentration of 5,10 and 20nM (Rodríguez-Penas et al., 2015; Sarmiento-Cabral et al., 2017) and leptin at concentration of 50, 100 and 200nM (Kaeidi et al., 2019). Studies have shown that there was a positive co-relation between chemerin, resistin and leptin (Ernst et al., 2010). The differentiated and undifferentiated SHSY5Y cells were incubated in the presence of adipokines with and without H₂O₂ for 24 hrs. The undifferentiated SHSY5Y cells were seeded at 5 x 10⁴ cells per well in 24 well plate and placed in the humid incubator, 37°C and 5% CO₂ for 24 hrs. After 24 hrs, the plates were kept in the sterile hood and chemerin, resistin and leptin doses were added to wells in triplicate (n=3) with and without H₂O₂ (1µl/ml or final H₂O₂ concentration of 100µM). After the dosing, the plates were placed in the incubator for 24 hrs. Similar dosing was performed with differentiated SHSY5Y cells with and without H₂O₂ (1µl/ml for final H₂O₂ concentration of 150 µM) and MTT assay was performed for cell viability. The data obtained was tested for statistical significance to compare the effect of individual adipokines on neuronal-like cell viability under oxidative stress condition (will be discussed in section 2.3).

2.2.6.6 Investigating the effect of commercial chemerin response on fibroblast cells

To estimate the effect of chemerin on the skin derived fibroblast cells derived from non-AD and AD donors, these cells were exposed to chemerin in the presence and absence of H₂O₂. The chemerin doses used were same as in section 2.2.6.5. The fibroblast cells were harvested from growing/continuous cell culture in T75 flask (80% confluent). The cells were trypsinized using EDTA-trypsin.

The detached cells were transferred to falcon tube and centrifuged at 400xg for 4 mins. The collected pellet was resuspended in complete media and seeded with 5×10^4 cell density well in 6 well plate (Richards et al., 2011), in triplicate (n=3). After seeding, cells were placed in the humid incubator, 37 °C and 5% CO₂ for 24 hrs to allow the cells to adhere and adjust in each well. After 24 hrs, the seeded fibroblast plates were taken out from the incubator and placed in the sterile hood. The chemerin doses of 10nM and 20nM were used with and without H₂O₂ (1mM dose) and incubated for 24 hrs in the incubator, 37°C and 5% CO₂. After 24 hrs, the MTT assay was performed. The data obtained and statistically analysed, as discussed in following section 2.3.

2.3 STATISTICAL ANALYSIS

Each MTT experiment was performed in three triplicate and three biological repeats (n=3). The data was normalised using excel (by equation given in section 2.2.6.2.1) and then averaged as final n1, n2 and n3, thereafter, these 'n' values were used in GraphPad Prism5 (Software, CA, USA) for the statistical analysis and graph presentation (discussed in respective results chapter). Data are provided as mean \pm SEM, (n=3), n represents the number of independent experiments. The data was considered as statistically significant with $p < 0.05$. To obtain EC50 dose of H₂O₂, data was normalised and tested using non-linear regression and best fit EC50 value was obtained. The data was obtained from SHSY5Y cells and distribution for normality was tested using Kolmogorov-Smirnov test. The data was analysed using Kruskal Wallis test for non-parametric test (because the data was not normally distributed) followed by the post-hoc test by Dunns multiple comparison for difference between the treatments. The data from skin derived fibroblast cells was obtained and distribution for normality was tested using Kolmogorov-Smirnov test. The data was analysed using two-way ANOVA for parametric test followed by post hoc Bonferroni multiple comparison between different groups.

Chapter 3. RESULTS

3.1 Cell culture

To address our hypothesis, in-vitro cell culture work was chosen to allow a targeted investigation of the influence of adipokines on cellular response to H₂O₂ oxidative stress since this method allows environmental manipulation with cost effectiveness. For the present study, three different cell lines were used: 3T3-L1 cells, SHSY5Y cells and human skin derived fibroblasts cells. As discussed in the methods section (2.2.1), each of the cell lines were cultured using similar culturing techniques. 3T3-L1 and SHSY5Y cells were differentiated into more mature adipocyte-like and neuronal-like cells, respectively in order to investigate cell viability under oxidative stress condition in the absence and presence of adipokines. Commercially available skin derived fibroblasts from AD and non-AD donors were used for this study and these cells did not require differentiation before the experiments.

3.1.1 3T3-L1 cell culture

3T3-L1 pre-adipocytes are mouse embryo derived adherent type-fibroblast cells (ATCC, 2014), and were purchased from ATCC as a frozen culture with unknown passage number. The frozen 3T3-L1 cells were thawed in T25 flask to be grown as a viable adherent cell culture. The continuous growth of the culture was monitored by observing and taking images using light microscopy every 48 hrs.

3T3-L1 pre-adipocytes reached approximately 40% confluency on day2 and 80% confluency by day4 (as shown in figure 3.1.A and 3.1. B respectively). The presence of visible nuclei within the elongated cell body and adherent flat features of the cells were observed confirming that the cells were healthy and valid for further experimental use, as well as cryopreservation. On day4 (figure 3.1. B), the cells looked morphologically slightly bigger in comparison to day2 (figure 3.1.A), may be with the increased incubation time in culture the cells adjusted and extended the cellular ends as adherent cells.

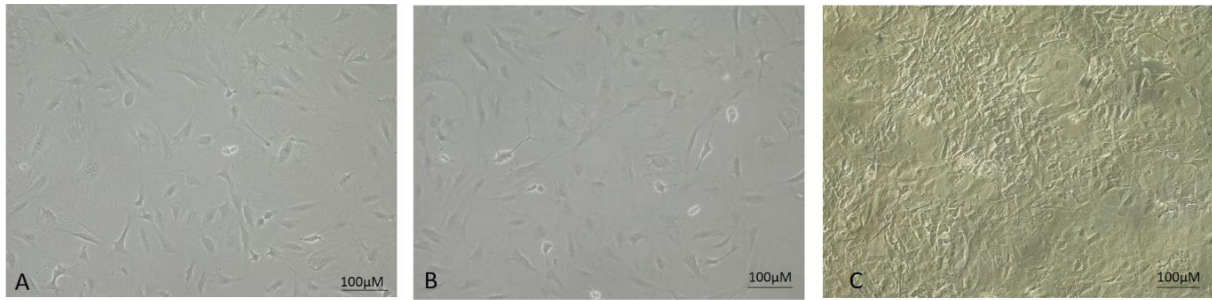


Figure 3.1. Observation of 3T3-L1, pre-adipocytes cell culture: 3T3-L1 cell culture confluency was visually estimated. While maintenance of cell culture, the media was replaced every 48 hrs and the cells looked intact. **A.** attained 40% confluency after day2 of thawing. **B.** reached 80% confluency on day4. **C.** obtained 100% confluency on day 6 of thawing. Morphological changes were captured at 200-fold magnification.

Culturing beyond day6 resulted in an over confluent or 100% confluent culture (as shown in figure 3.1.C) and was not acceptable to use for further experiments. In addition, these cells were visually observed to be overgrown on each other and did not present as isolated individual cells with associated elongated cell body features. Tiny droplets of lipids were observed in overconfluent cultures, which is not a pre-adipocyte characteristic.

3.1.2 SHSY5Y cell culture

The SHSY5Y cells, are neuroblastoma cells with adherent culturing characteristics, purchased from ECACC with passage number 6 as a frozen ampule of cryovial. The growth progression of the culture was monitored by visual observation each day and taking images using light microscopy.



Figure 3.2. Progression of SHSY5Y cell culture confluency: SHSY5Y cell culture progression was visually observed. The cells appeared as intact and healthy with no sign of contamination. The SHSY5Y cell culture: **A.** reached 40% confluency on day2 after of thawing. **B.** attained 70% confluency on day4 of culturing. **C.** achieved 100% confluency on day6 after thawing. The images presented were captured using and 100-fold magnification.

On day2, the SHSY5Y cells appeared to be 40% confluent (figure 3.2.A). The SHSY5Y cells reached confluency of 70% by day4 (figure 3.2.B). Cells were observed as having a short, sharp/spiny cell body with stretched out ends. The SHSY5Y cell culture reached 90% confluency on day6, (figure 3.2.C) this was noted as an overgrown culture and was not used for further splitting and differentiation or cryopreservation for future use.

3.1.3 Fibroblasts cell culture

Human skin derived cells were purchased from Coriell Institute in the form of frozen ampule. The cell morphology of these human skin derived cells was fibroblast-like and they grew slowly as cell culture evident by decelerated confluency progression day by day. Six different skin derived fibroblast cell lines were used in this study: three non-AD donors cell lines and three AD patient derived cell lines. All six cell lines were extracted from different donors with different age group and gender, though the non-AD and diseased groups were age and gender matched as much as commercial availability would allow.

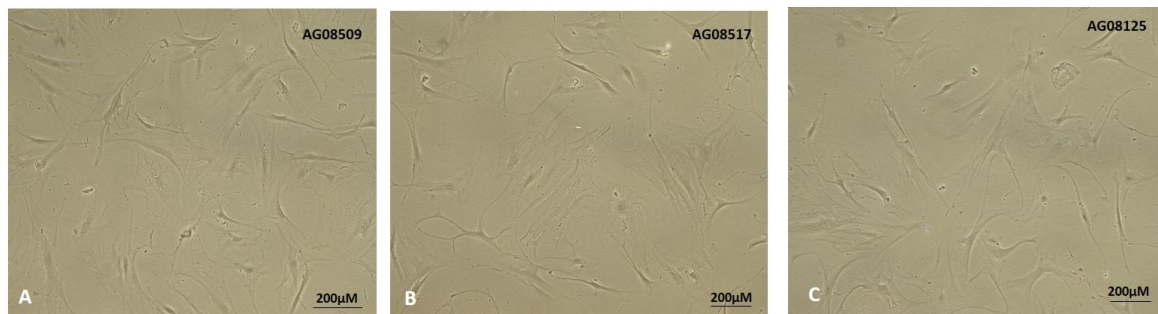


Figure 3.3. Cell morphology of skin derived fibroblasts from non-AD donors after 48hrs of culture. **A.** the cell line, AG08509 was cultured and observed to be 40% confluent. The cells appeared to be elongated towards the end. **B.** the cell line, AG08517 was cultured and reached approximately 50% confluency. The cells displayed stretched out ends and flattened cell body. **C.** the cell line, AG08125 was cultured and recorded with 50% confluency and individual cells showed thin and extended ends. The images were taken using 200-fold magnification.

Three cell lines from the non-AD donors, skin derived fibroblast cells demonstrated slow growth and proliferation. The cell line, AG08509 (derived from an unaffected 73-year-old male) demonstrated fibroblast like characteristics; cells appeared elongated and grew as a monolayer with 40% confluency after 48 hrs (figure 3.3.A).

Furthermore, few cells showed flattened cell bodies. The cell line, AG08517 (obtained from an unaffected 66-year-old female) appeared to be 50% confluent after 48 hrs and morphologically exhibited flat and spiked cell bodies with extended ends (figure 3.3.B). The cell line, AG08125 (obtained from an unaffected 64-year-old male) displayed elongated end morphology and few cells were flat in appearance with 50% confluency after 48 hrs of culturing (figure 3.3.C).

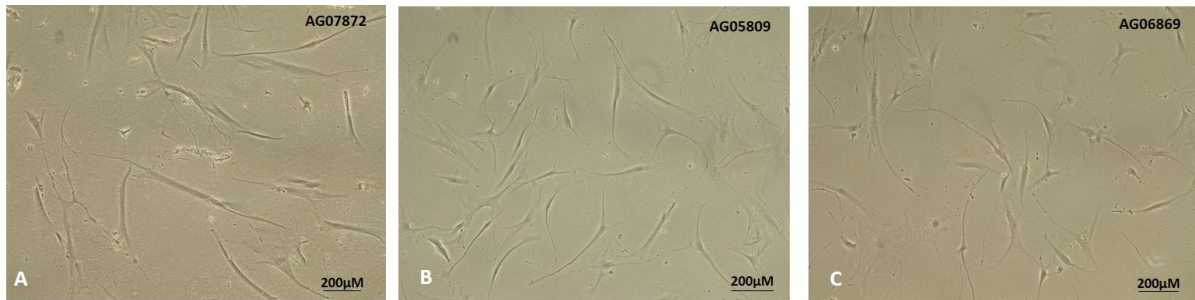


Figure 3.4. Cell morphology of skin derived fibroblast from AD donors after 48 hrs of cell culture. **A.** the cell line, AG07872 was cultured and visually observed to be 30% confluent. The cells showed elongated and spiked cell body. **B.** the cell line, AG05809 looked 40% confluent. The cells demonstrated stretched out, extended and spiked cell body. **C.** the cell line, AG06869 was cultured and recorded with 40% confluency and individual cells showed thin, extended, and flattened cell body. The images were taken at 200-fold magnification.

Three cell lines from different AD donors skin derived fibroblast were used. In general, the culture growth was observed as slow. The cell line, AG07872 was derived from a clinically AD affected patient of 53 years old male. After 48 hrs, cells were approximately 30% confluent and had fibroblast-like characteristics; individual cells showed elongated ends with thin cell bodies. Few cells showed webbed like cell bodies (figure 3.4.A). The cell line, AG05809 was obtained from a clinically affected with moderate dementia patient of 66 years old female. The cell culture appeared to be 40% confluent and showed thin and segmented cell body with stretched out end in cellular morphology after 48 hrs (figure.3.4. B). The cell line, AG6869 was derived from a clinically affected moderate dementia patient of 60 years old female. After 48 hrs, the cells demonstrated morphological feature of extended ends with slender cell bodies and a few cells had flattened cell bodies with 40% confluency (figure 3.4.C).

As expected, the fibroblast cells derived from non-AD donors demonstrated faster proliferation in comparison to the AD donors derived fibroblast cells.

3.2 Differentiation of cell lines

To understand the adipocytes and neuronal cellular activity, the commercially available immature pre-adipocytes and neuroblastoma (3T3-L1 and SHSY5Y, respectively) cells were differentiated into mature adipocyte-like and neuronal-like cells, respectively, using commercially available chemicals for differentiation as described in section 2.2.3.2 and 2.2.4.2.

Differentiated 3T3-L1 cells function as mature adipokine secreting adipocytes such as resistin, leptin, chemerin, adiponectin, interleukins, and other growth factors (peer group Dewhurst et al., unpublished). Conditioned media harvested from the differentiated 3T3-L1 cells was used to investigate its effect on the viability of differentiated SHSY5Y (neuronal-like) cells under H₂O₂ induced oxidative stress. The viability of neuronal-like cells under oxidative stress was also investigated in the presence of commercially available adipokines (chemerin, resistin and leptin). In addition, experiments were performed using skin-derived fibroblast cells to estimate the commercially available chemerin on fibroblast cells under H₂O₂ induced oxidative stress.

3.2.1. 3T3-L1 differentiation: pre-adipocytes into adipocyte-like cells

The 3T3-L1 cells were chemically modulated and differentiated from pre-adipocyte fibroblast cells into mature adipocyte-like cells using a 3-week differentiation protocol, when cells were exposed to mixture of human insulin, dexamethasone and IBMX (Zebisch, 2012). The morphological changes during the differentiation process were observed microscopically and images were captured during differentiation progression, as shown in figure 3.5 (A-H).

Cells were cultured as two groups: undifferentiated and differentiated 3T3-L1 cells (as shown in figure 3.5). The undifferentiated cells were cultured in the growth culture media and the differentiated cells were grown in differentiation and maintenance media in order to acquire mature adipocyte-like characteristics during the incubation period. On day2, 3T3-L1 cells under both conditions reached 100% confluency and were allowed to grow in growth culture media as confluent cultures.

The undifferentiated 3T3-L1 cells were maintained in growth culture media, whereas differentiated cells were incubated in expansion media and both conditions were morphologically similar at this point of incubation (figure 3.5. A and B).

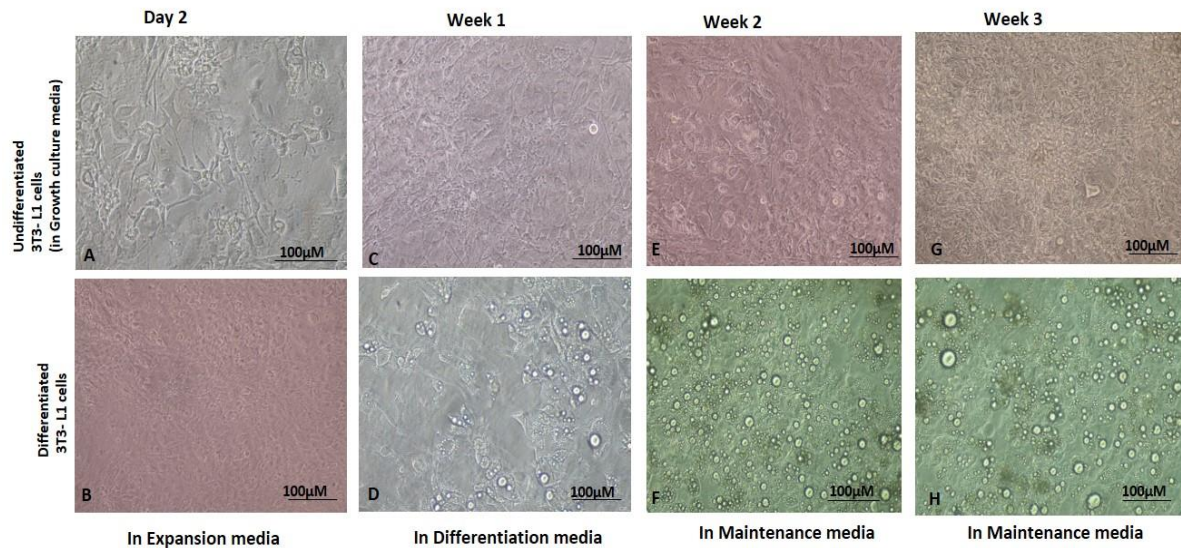


Figure 3.5. Microscopic overview of 3T3-L1 cell culture progressive differentiation from pre-adipocytes to mature adipocytes-like over 3 weeks. On day2, **A-B**. the 3T3-L1 cells, were allowed to grow as confluent 3T3-L1 culture in expansion media. **C**. on week 1, the cells continued to grow as confluent culture in growth culture media as control. **D**. the cells continued to grow as confluent culture in differentiation medium. **E**. during week 2 incubation period, the cells were incubated with maintenance media, **F**, stable lipid droplets were observed as an indication of successful differentiation progression in comparison to the control **E**. In week 3, the confluent culture continued to grow in maintenance media and displayed solid lipid droplets confirms differentiation of 3T3-L1 cells, **H**, in comparison to control **G**. Images were taken at 200-fold magnification.

Lipid droplets were observed in 3T3-L1 cells, during incubation with differentiation media but not in the undifferentiated control cells on week 1 (figure 3.5. C and D). The number of lipid droplets increased (confirmed by visual observation during differentiation progression, no quantitative values were recorded) by end of week 2, whilst the undifferentiated cells maintained a fibroblast like morphology (figure 3.5. E and F). On last day of 3rd week, visibly large number of lipid droplets were observed, and the culture media was viscous and pale yellow, suggestive of triglycerides present in the media of differentiated 3T3-L1 cells (Kong et al., 2017). Oil Red-O staining of 3T3-L1 cells on last day of 3rd week was performed which confirmed successful differentiation (result will be discussed in section 3.2.1.1, figure 3.7).

3.2.1.1 Determination of differentiated 3T3-L1 by Oil-Red-O staining

To confirm the differentiation of 3T3-L1 cells into adipocytes-like, diazo dye was used to confirm the presence of lipids (Kraus et al., 2016). Optimization was performed to establish a standard protocol for the qualitative Oil Red-O staining of cultured adipocytes to confirm successful differentiation. Determination of differentiated SHSY5Y by ICC: 21-day protocol

3.2.1.1.1. PBS wash

Cells were stained using protocol outlined in 2.2.3.3. The optimization of PBS wash step was performed to ensure no unspecific binding by the Oil-Red-O stain, as shown in figure 3.6.

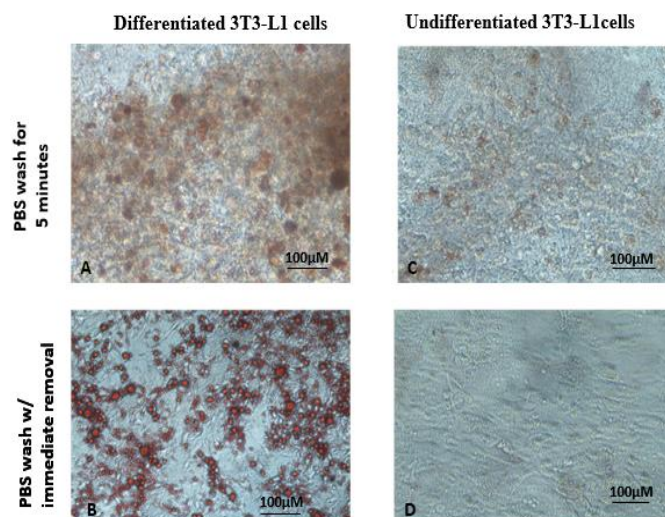


Figure 3.6 Optimization of Oil Red-O staining: comparison of PBS wash with 5 mins wait and immediate removal: **A+B**. PBS washed 3T3-L1 cells for 5 mins, the differentiated cells did not show any strong and clear individual cells in comparison to the undifferentiated cells demonstrated weak red stained cells. **C+D**. when the PBS buffer was removed immediately from 3T3-L1 cells, the differentiated cells showed strong and clear red stained cells in comparison to the control cells with negligible presence of red stained cells. Images were taken at 200-fold magnification.

5 mins PBS incubation was used to remove excess fixative and Oil Red-O solution, which resulted in weak and ambiguous staining. Individual cells were impossible to distinguish, and the intensity of the stain was hazy (figure 3.6.A-B).

Although, when the cells were washed with PBS solution and immediately removed, the visual difference between differentiated and undifferentiated stained cells was more distinguishable (figure 3.6.C-D), the differentiated adipocyte-like cells could be identified by intensely stained red lipid droplets. However, unexpectedly the undifferentiated cells showed little or weak traces of red coloured Oil Red-O stain, maybe due to the unspecific binding of Oil Red-O dye and presence of some lipid droplets (because of 3 weeks long incubation) secreted by pre-adipocytes. Therefore, immediate removal of PBS step was used for subsequent confirmation of 3T3-L1 differentiation protocol. The optimization of Oil Red-O staining experiment was performed once to confirm the optimum PBS wash needed/required for 3T3-L1 cells differentiation (discussed in section 2.2.1.1).

3.2.1.1.2 Fixative solution

Oil Red-O staining often requires optimization to reflect the differences in sensitivities between tissues (Kraus et al., 2016). Different fixative strengths were investigated in attempt to enhance the efficacy of Oil Red-O staining of differentiated 3T3-L1 cells. The 8% paraformaldehyde as fixative was used to reduce unspecific binding.

Fixing the cells with 8% paraformaldehyde resulted in clearly visible individual cells with dominant red stained 3T3-L1 cells and less non-specific background staining, whereas cells fixed with 10% paraformaldehyde gave increased background intensity and cloudy red stained appearance (figure 3.7.A and C, respectively). Similarly, the undifferentiated cells using 10% paraformaldehyde showed unspecific binding resulted in higher number of red stained cells in comparison to cells fixed with 8% paraformaldehyde (figure 3.7. B and D, respectively). Due to the presence of unspecific binding obtained after 10% paraformaldehyde, the images obtained in, figure 3.7. A and B showed traces of Oil Red-O in both the conditions. No stained cells were observed in the negative control condition (no Oil Red-O stain was added to the respective wells) (figure 3.7.E-F). The use of 8% paraformaldehyde for fixation was therefore incorporated in further Oil Red-O staining protocols which was used for the confirmation of 3T3-L1 pre-adipocytes into lipid secreting adipocyte-like cells.

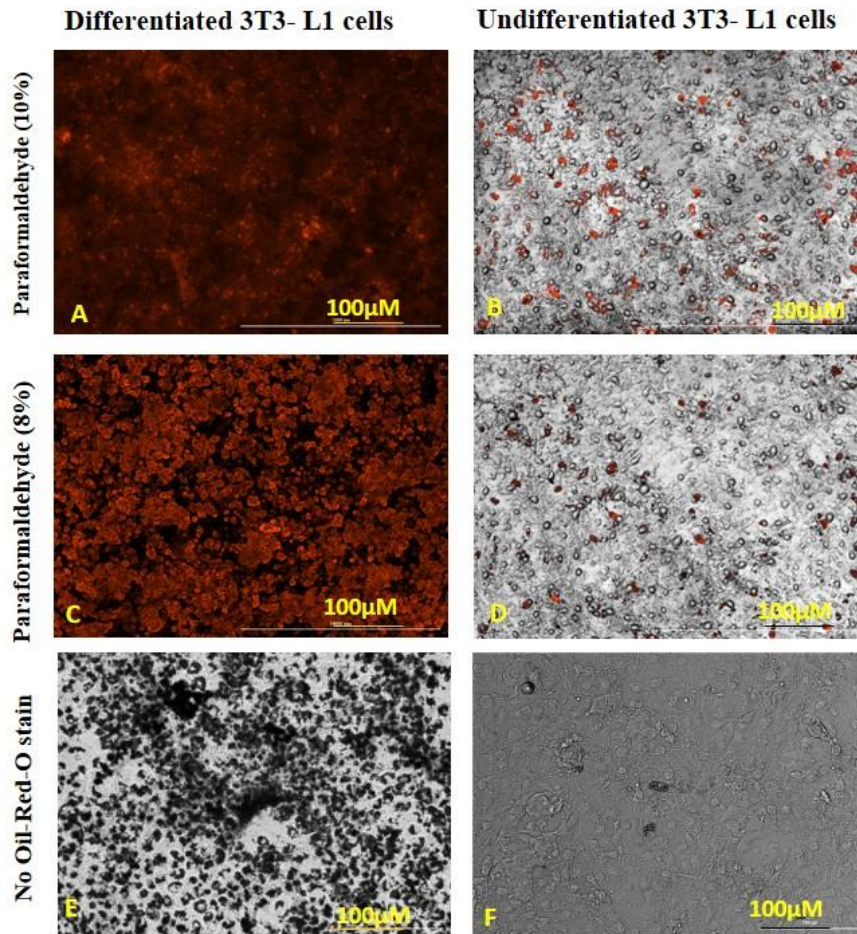


Figure 3.7 Optimization of Oil Red-O staining: comparison of paraformaldehyde 10% and 8%. After 21-day differentiation protocol, the lipid-containing cells was achieved and confirmed by using Oil Red-O. Two different concentrations of paraformaldehyde were used as a fixative and the clarity of stained cells was compared. This informed the concentration of paraformaldehyde used in further experimental protocols. **A.** the Oil Red-O-stained cells with 10% paraformaldehyde showed clear presence of lipid accumulated on 3T3-L1 cells in comparison to the undifferentiated cells, **B.** with few traces of weak stained cells. **C.** stained differentiated cells with 8% paraformaldehyde, demonstrated the sharpest red stain in comparison to undifferentiated stained cells, **D.** with few traces of red stained cells. **E** and **F**, the differentiated and undifferentiated cells did not showed presence of red stained cells without Oil Red-O stain after the fixative step using paraformaldehyde. The images were captured at 200-fold magnification.

The optimization of Oil Red-O staining experiment was performed once to confirm the optimum percentage of paraformaldehyde as fixative required to obtain differentiated 3T3-L1 cells (discussed in section 2.2.1.1). This protocol was used as final protocol for the differentiation and Oil-Red-O staining (with immediate PBS wash and 8% paraformaldehyde), as shown in figure 3.7.

3.2.2 SHSY5Y differentiation:

The development of a reliable method to differentiate SHSY5Y cultures is vital to facilitate translational experiments that are reproducible and accurately mimic the human nervous system (Presgraves, 2003). SHSY5Y cells used in this study were differentiated from neuroblastoma cells into neuronal-like cells using a RA-induced differentiation protocol.

Two different protocols were followed and compared based on the selected RA concentration and the incubation time: 10-day protocol with 10 μ M of RA (Armstrong et al., 2005) and 21-day protocol with 1 μ M of RA (Korecka et al., 2013). In the first instance, we aimed to compare the two published neuronal differentiation methods and consider the advantages and limitations of each method. After the establishment of successful differentiation, the study aimed to compare the responses of neuronal-like and non-neuronal-like cell types to H₂O₂ induced oxidative stress and the influence of adipokine treatment on these different cell types.

3.2.2.1 Optimization of SHSY5Y cells differentiation protocol

Differentiation protocols of SHSY5Y cells shows a wide range of variables within the literature (Dwane et al., 2013; Zhang et al., 2020; Getachew et al., 2020). To ensure the optimum differentiation within our lab setting, investigation on incubation time, cell density, RA concentration and ethanol concentration was carried out (for the RA working solution preparation), as described in section 2.2.4.3. While optimizing, single parameter was changed in each trial in order to establish the final standard operating procedure (SOP) for successful differentiation, by confirming the morphological changes such as neuritic extensions, elongated cell bodies and enhanced networking to resemble mature/differentiated neuronal-like cells.

3.2.2.1.1 Cell density

Optimizing the initial seeding density is a very basic and crucial step in the differentiation process since the success of the differentiation is dependent on confluency at the start of the process (Encinas, 2000).

The initial cell densities compared were 3×10^4 , 4×10^4 and 5×10^4 cells per well in a 6 well plate. Visual observation of seeded cells showed that the desired uniformity and cell density of 50-60% confluency after 48 hrs was achieved with 5×10^4 per well (figure 3.8.C), in comparison to 30% confluency with 3×10^4 cells per well seeded cell density and 40% confluency with 4×10^4 cells per well seeded cell density (as shown in figure 3.8. A and B, respectively).

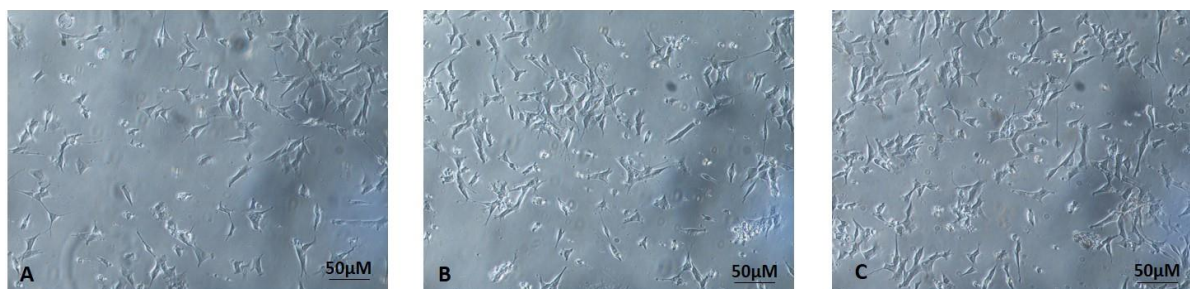


Figure 3.8 Optimizing the initial cell density required for SHSY5Y differentiation after 48 hrs. The SHSY5Y cells were seeded with given cell densities and showed following confluency after 48 hrs of incubation: **A.** attained 30% confluency using 3×10^4 after 48 hrs of thawing. **B.** achieved 40% confluency using 4×10^4 . **C.** with seeded 5×10^4 cell density, 50-60% confluency was obtained after 48 hrs of thawing. Images presented were taken at 100-fold magnification.

3.2.2.1.2 Ethanol concentration

Differentiation of SHSY5Y cells required lyophilized RA to be dissolved in DMSO (to be used as stock solution) and then in ethanol (to be used as working solution). Two strengths of ethanol were investigated in this study; 95% and 99.9% ethanol and the impact of 2-8°C storage of the dilutions prior to use. When the RA was pre-prepared as working solution and stored at 4° C to be used for the differentiation media change, the results showed increased cell death using 99.9% and 95% ethanol (figure 3.9.A and C). Although, when RA was freshly prepared before the differentiation media change using 99.9% ethanol to dissolve RA (figure 3.9.D), there was no adverse effect on cell viability and normal cell proliferation at the initial differentiation stage continued in comparison to RA when dissolved in 95% ethanol (figure 3.9.B).

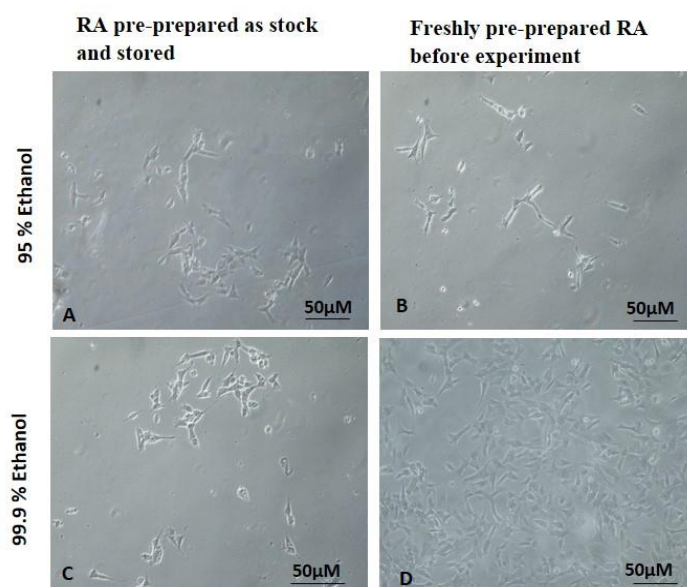


Figure 3.9 Microscopic images of SHSY5Y cells displayed the impact of prepared RA on the viability of SHSY5Y cells. **A.** RA was dissolved in 95% ethanol and added to the media prepared in bulk for further use. **B.** RA was added to the media freshly before treating the SHSY5Y cell using 95% ethanol. **C.** 99.9% ethanol was used as solvent for RA to prepare bulk media to be used for SHSY5Y cells differentiation. **D.** RA was dissolved in 99.9% ethanol and added freshly to the media before treating the SHSY5Y cells. The images were captured at 100-fold magnification.

Morphological changes were observed during the incubation for differentiation, for example, in figure 3.9.B, with freshly pre-prepared RA-95% ethanol, the cells appeared to have thinner cell body in comparison to the cells incubated with rest of the treated cells, figure 3.9. A, C and D. Highest cell viability was associated with RA diluted with 99.9% ethanol and used as freshly prepared and this was subsequently used for further experiments. The optimization of ethanol concentration experiment was performed once to confirm the optimum percentage of ethanol concentration as solvent required to obtain differentiated SHSY5Y cells (discussed in section 2.2.1.1).

3.2.2.1.3 Assessment of RA stability

RA is light sensitive even when it is dissolved in the media, therefore, assessment of differentiation media storage was required to ensure differentiation inducing properties were not lost during the procedure (Tolleson et al., 2005).

This was accomplished by comparing SHSY5Y cells viability during differentiation with and without direct light exposure to the prepared differentiation media. As shown in figure 3.10.A, the cells were treated with the differentiation media with no protection from direct light and on day4 of differentiation, the cells demonstrated no outgrowth of neurites with substantial cells loss which indicated unsuccessful differentiation.

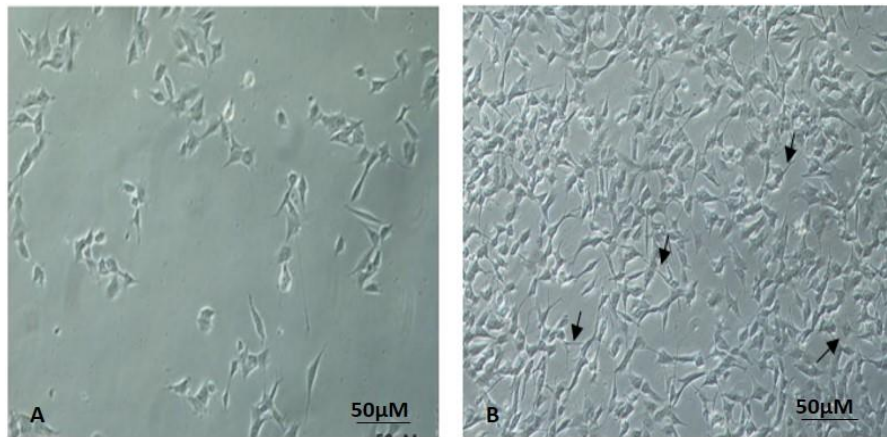


Figure 3.10 Microscopic images of SHSY5Y showing the impact of exposure of differentiation media to direct light on SHSY5Y cells on day4. **A.** The differentiation media was not protected from direct light. **B.** The differentiation media was protected from direct light by foil wrapping. The black arrows are pointed on the initial neuritic projections between adjacent neuronal cells after 4 days of incubation. Images were captured using 200-fold magnification.

However, when RA was added in the differentiation media and the media was protected from direct light by covering in aluminium foil, on day4 the cells were observed and demonstrated initial neurites projections or outgrowth as early signs of differentiation, indicated by arrows in figure 3.10. B. Morphologically, the cells in light exposed RA, figure 3.10.A, looked slightly flattened and irregular shapes in comparison to the cells with RA protected from light, which appeared to have sharp ends and uniformed cell bodies in the cell culture (figure 3.10.B). Based on the RA stability optimization, all future experiments involved were followed by this step where the differentiation media was protected from direct light to prevent RA inactivation. The optimization of RA stability in media experiment was performed once to confirm the importance of RA in media exposure to direct light required to obtain differentiated SHSY5Y cells (discussed in section 2.2.1.1).

3.2.2.2 Optimization of ICC to confirm SHSY5Y differentiation

RA induced differentiation of SHSY5Y cells into neuronal-like cells was confirmed by ICC to detect recognized neuronal markers which mark a shift in phenotype after the differentiation process. Fully differentiated SHSY5Y cells have been previously mentioned to express a variety of neuronal specific markers.

The neuronal markers used to determine the differentiation of SHSY5Y cells by following the 10-day and 21-day protocol in this study were: NSE (Forster et al., 2016), NF and MAP2 (Kovalevich & Langford, 2013). These neuronal markers were found to be associated with the neuronal-like differentiated cells in comparison to the undifferentiated cells. Visualisation of the specific markers present in the differentiated SHSY5Y cells were recorded using polyclonal PE-conjugated secondary antibody as described in section 2.2.4.4.

Neuronal markers (NSE, MAP2 and NF) have been used by researchers to demonstrate efficiency of neuronal differentiation but there are some variations in the antibody conditions or ratio used to demonstrate the neuronal phenotype (Abdulwanis Mohamed et al., 2020). Various primary and secondary antibody dilutions or ratios were initially assessed in SHSY5Y cells, which were differentiated by using the 10-day protocol.

After optimization, the final primary and secondary antibody conditions achieved from 10-day protocol SHSY5Y cells (differentiated) were used in 21-day protocol differentiated SHSY5Y cells. Therefore, ICC confirmation remained consistent between the 10 and 21-day protocols. The optimization of the ICC experiment was performed once to confirm the optimum ratio of primary and secondary antibodies required for confirmation of differentiated SHSY5Y cells (discussed in section 2.2.1.1).

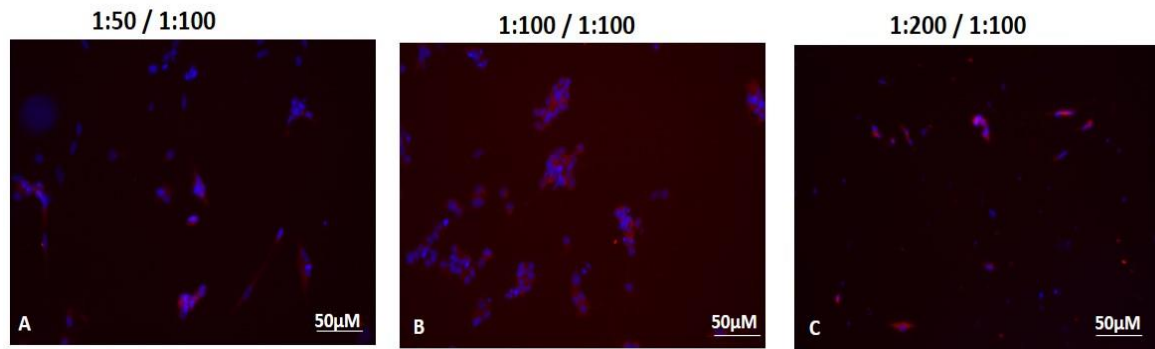


Figure 3.11. Immunofluorescence images of differentiated SHSY5Y cells are presented: different ratios of NF and PE-conjugate Ab was used, however, ratios used were unable to locate the NF fluorescence. **A.** 1:50 for NF Ab and 1:100 for PE-conjugate Ab was used. **B.** 1:100 for NF Ab and 1:100 for PE-conjugate Ab was used. **C.** 1:200 for NF Ab and 1:100 for PE-conjugate Ab was used. Images were taken using 100-fold magnification.

The neurofilaments are the intermediate filaments present in the cytoplasm of the neuron, essential for the axonal development (Yuan et al., 2017). The NF marker was used as primary antibody Ab, to detect the presence of neuronal filaments in the differentiated neuronal-like SHSY5Y cells. PE-conjugated secondary Ab was used as a secondary antibody. Slight NF fluorescence within the neurite projection between distant neuronal-like cells was present and detected when primary/secondary Ab (NF/PE-conjugate) ratio of 1:50/1:100 and 1:200/1:100 were used (figure 3.11.A and C, respectively). In addition, the NF/PE-conjugate Ab ratio of 1:100/1:100, demonstrated NF fluorescence in close vicinity with the nuclei stained DAPI. However, it is likely that non-specific binding of the secondary antibody resulted in the higher background fluorescence, therefore making the location of extended neurites projection more difficult to detect (figure 3.11.B). The blue fluorescence detected, figure 3.11.A, B and C, was DAPI stained nuclei of cells, which confirmed the presence of intact SHSY5Y. Therefore, the ratios of primary and secondary Ab used was not optimum to locate the presence of neurofilament in the cytoplasm of the differentiated SHSY5Y cells.

Another neuronal marker verified was MAP2. MAP2 is an isoform of MAPs family, which stabilizes the cytoskeleton and localized in the dendrites of the differentiated neurons. The MAP2 marker with concentration 1µg/1ml, was used to determine the presence of neuron specific MAP2 to confirm the differentiation in line with recommendations of another research (Soltani et al., 2005).

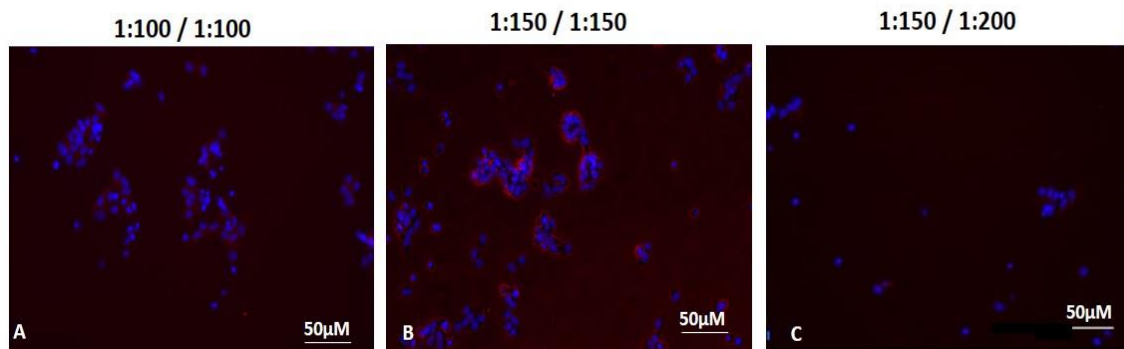


Figure 3.12. Immunofluorescence images of differentiated SHSY5Y cells are presented: different ratios of MAP2 and PE-conjugate Ab was used, however, ratios used were unable to locate the MAP2 evidently: **A.** 1:100 for MAP2 Ab and 1:100 for PE-conjugate Ab was used. **B.** 1:150 for MAP2 Ab and 1:150 for PE-conjugate Ab was used. **C.** 1:150 for MAP2 Ab and 1:200 for PE-conjugate Ab was used. Images were taken using 100-fold magnification.

PE-conjugated secondary Ab was used as a secondary antibody. Negligible MAP2 fluorescence was detected when primary/secondary Ab (MAP2/PE-conjugate) ratio of 1:100/1:100 was used (figure 3.12.A). No MAP2 fluorescence within the neurite projections between distant neuronal-like cells was present with 1:150/1:200 (MAP2/PE-conjugate), only the presence of DAPI stained nuclei of SHSY5Y cells was observed (figure 3.12.C). In addition, the MAP2 /PE-conjugate Ab ratio of 1:150/1:150, the MAP2 fluorescence was detected, but only near the clustered SHSY5Y cells with blue fluorescence by DAPI stained nuclei. Maybe non-specific binding by the secondary antibody, resulted in presence of higher background fluorescence and the location of extended neurites projection was difficult to detect. Therefore, the ratios of primary and secondary Ab used was not optimum to locate the presence of microtubule associated protein in the cytoplasm of the differentiated SHSY5Y cells.

Third neuronal marker used for the ICC was NSE. NSE is an isozyme of glycolytic enzyme enolase which is highly specific to the late events of differentiating neurons progressing towards neuronal maturation (Isgrò et al., 2015). NSE marker with concentration 5µg/ml, was used as primary Ab to verify the presence of specific enolase enzyme in the cytoplasm of the neuronal like SHSY5Y cells.

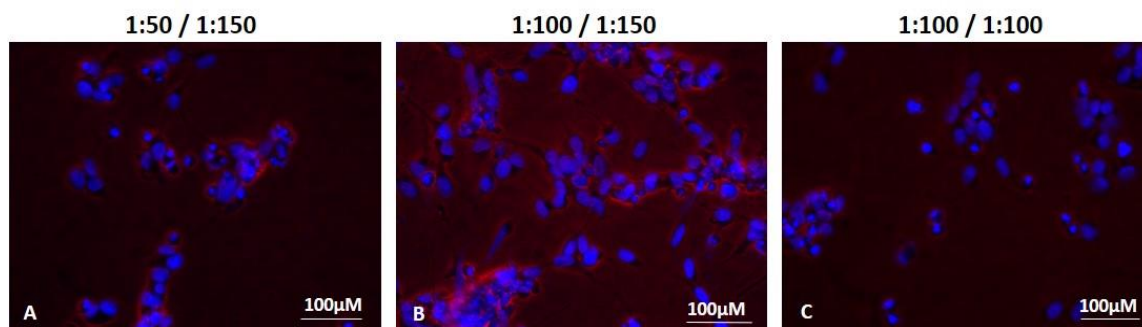


Figure 3.13. Immunofluorescence images of differentiated SHSY5Y cells are presented: different ratios of NSE and PE-conjugate Ab was used, however, ratios used were unable to locate the NSE clearly: **A.** 1:50 for NSE Ab and 1:150 for PE-conjugate Ab was used. **B.** 1:100 for NSE Ab and 1:150 for PE-conjugate Ab was used. **C.** 1:100 for NSE Ab and 1:100 for PE-conjugate Ab was used. Images were taken using 200-fold magnification.

PE-conjugated secondary Ab was used as a secondary antibody. The NSE /PE-conjugate Ab ratio of 1:50/1:150 used, was unable to detect the presence of NSE clearly due to weak fluorescence was observed in outer area of clustered cells with the nuclei stained with DAPI (figure 3.13.A). The incubated, 1:100/1:150 Ab ratio (NSE /PE-conjugate) showed presence of increased background fluorescence, maybe due to non-specific binding of the secondary antibody which resulted in difficult detection of enolase specifically present in cytoplasm of neuronal-like cells (figure 3.13.B). In addition, very weak NSE fluorescence was detected when primary/secondary Ab (NSE /PE-conjugate) ratio of 1:100/1:100 was used, only the presence of DAPI stained nuclei of SHSY5Y cells was observed clearly (figure 3.13.C). Therefore, the ratios of primary and secondary Ab used was not optimum to locate the presence of neuron specific enolase in the cytoplasm of the differentiated SHSY5Y cells. The ICC optimization was performed once to confirm the presence of neuronal specific markers so the success of the differentiation can be confirmed (discussed in section 2.2.1.1). Based on the detection of the markers i.e., NF, MAP2 and NSE, none of the dilutions were optimum for the ICC to detect the presence of neuronal markers and successful differentiation followed by this optimization protocol could not be concluded.

After the series of optimization attempted, the finalized primary Ab/secondary Ab ratio used as definitive ratio in combination to confirm the differentiation of all-trans-RA mediated differentiation protocol was obtained and the final Ab ratio for ICC are listed in table 3.1. The final fluorescence images obtained will be discussed in section 3.2.2.3.1 and 3.2.2.4.1.

Table.3.1. Final antibody ratios used for the concluding ICC SOP followed by SHSY5Y differentiation are shown in the table below. The table below includes types of Ab and ratio, manufacturer and incubation time used.

Antibody Used	Type of Ab	Dilution used
NF Ab	Primary	1:500
MAP2 Ab	Primary	1:500
NSE Ab	Primary	1:200
PE-Conjugated	Secondary	1:200
IgG monoclonal	Negative control	Same as primary Ab for each marker

3.2.2.3. SHSY5Y differentiation: 10-days protocol

During neuronal differentiation, a number of morphological changes have been reported such as the extension of neuritic ends, halted cell division and clustering of neuronal cells (Agholme et al., 2010). These progression of SHSY5Y cells differentiation was visually observed every 48 hrs and images were captured and presented in figure 3.14. The RA mediated SHSY5Y cells were differentiated using 10 μ M concentration for 10-days, as discussed in 2.2.4.2. Upon differentiation, SHSY5Y cells exhibited morphological and confluency change including discontinued cell division, extensive neurite outgrowth, clustered cells with neurite extensions connected to the other grouped cells as well as individual cells for stronger networking with other cells (the progression of differentiation is shown in figure 3.14). Undifferentiated SHSY5Y cells (figure 3.14.E) showed no sign of neurite elongation in comparison with differentiated cells (figure 3.14.F). Confluency played a vital role to initiate differentiation in SHSY5Y cells. After 24 hrs of cell seeding, approximately 50-60% confluency was achieved in each well as shown in figure 3.14. A-day0.

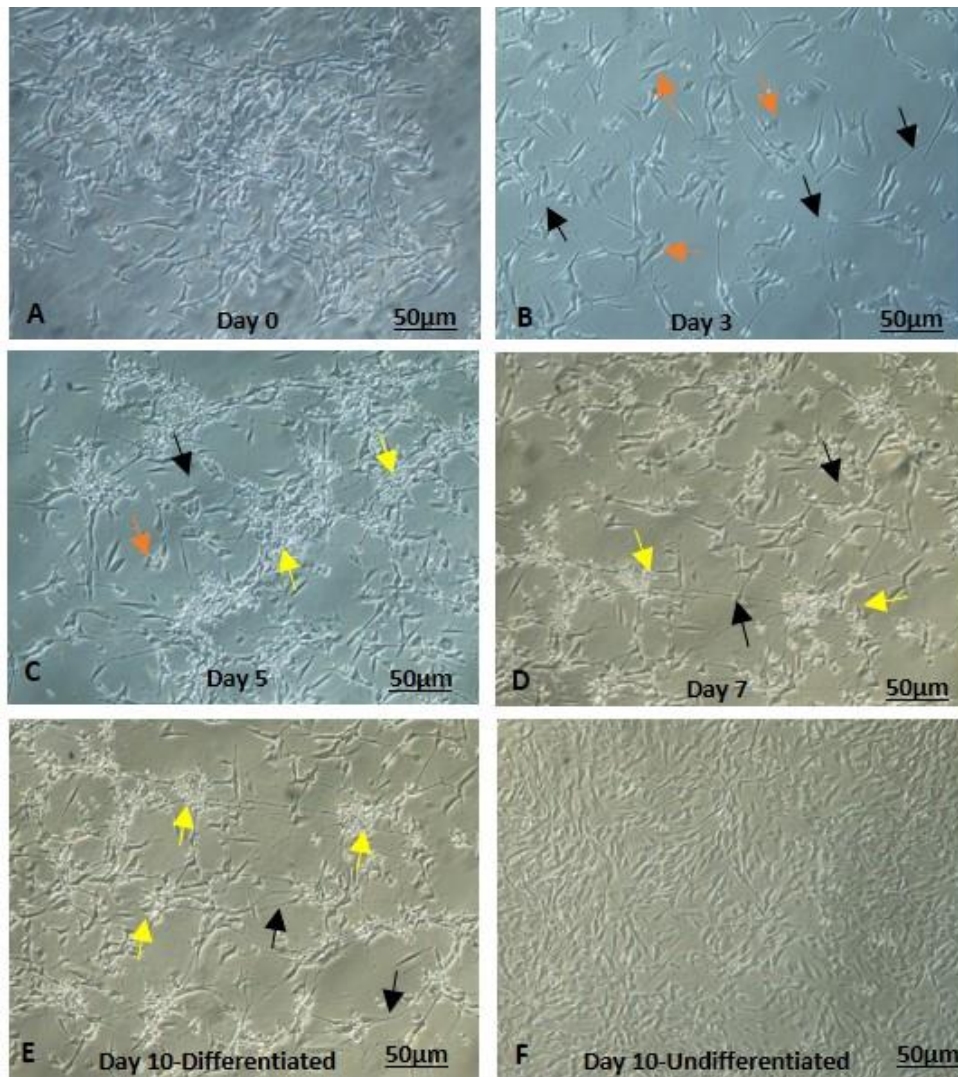


Figure 3.14. Morphological changes in SHSY5Y cells during the neuronal differentiation progression when 10-day protocol was followed, in presence of RA ($10\mu\text{M}$). **A.** day 0, after 24 hrs of cell seeding the cells appeared as sparse in monolayer. **B.** day3, the initial presence of neurite extensions and axonal outgrowth were observed (follow black arrows). Epithelia-like cells which did not differentiate as neuronal-like or S-type cells were also captured (see orange arrows). **C.** day 5, the cells continued to differentiate with visible stronger neurites extension (follow black arrows), and initial small, clustered cells as grouped neuron cells were noted (follow yellow arrows). Fewer S-type cells were seen (follow orange arrows). **D.** day7, the cells demonstrated stable and solid neurites projections with nearby cells (follow black arrows) and outreaching the distant placed grouped cells (follow yellow arrows). No S-type cells were observed. **E.** day10, cells showed very well organized and strong neurite outgrowths interconnection between differentiating cells (follow black arrows) and as well as with stable clustered grouped neuronal like cells (follow yellow arrows). **F.** day10, undifferentiated cells were observed to be 100% confluent neuroblastoma cells. The images were captured using 200-fold magnification.

It is well documented in literature that SHSY5Y cells are heterogenous culture type and comprised of S and N type of cells inherited from the parental cell line, SK-N-SH (Yusuf, 2013).

S-type cells retain epithelial-like properties and appear large and flatter, whereas N-type cells possess neuronal characteristics such as small and slightly elongated cell bodies with sharp ends with potential to differentiate into mature neuronal-like cells (Bell et al., 2020). We therefore expected to observe higher number of N-type over S-type as differentiation progressed towards end day and the results obtained were as expected. The first sign of SHSY5Y differentiation was observed on day 3, presence of short extensions from neurite ends to outreach the neighbouring cells for cellular networking (shown by black arrows). Moreover, an increased number of S-type cell population was observed (figure 3.14. B, shown by orange arrows). On day 5, small clusters of cells were present (figure 3.14.C, shown by yellow arrows) and more interconnected cells, with both distant and neighbouring cells were observed (figure 3.14.C, shown by black arrows) as well as the presence of stable and mixed neuritic extensions were present (short and elongated, respectively). The number of S-type population was reduced in comparison to day 3 (figure 3.14.C, shown by yellow arrows). On day 7, the cells showed an increased number of interconnected cells, an increased number of elongated neurites extension to communicate with distant adhered differentiating or clustered group (figure 3.14.D, shown by black arrows), the presence of more interconnected clustered cell groups (figure 3.14.D shown by yellow arrows), and S-type cells were absent. On day 10, a well-established network of homogeneous neuronal-like cells was observed. The neuritic connections appeared to be strong, stable and elongated with complete absence of S-type cell population (figure 3.14.E). Increased number of clustered cell groups were present (figure 3.14.E, shown by yellow arrows) with excellent neurite extensions between differentiating cells (figure 3.14.E, shown by black arrows). On day 10, the undifferentiated cells (which were cultured parallelly to the differentiating cells) were observed as confluent, heterogenous mixture of cells (figure 3.14.F), with no signs of differentiation in comparison to the day 10 (figure 3.14.E) differentiated SHSY5Y cells. Using neuritic outgrowth and increased N- type population over S-type as an indicator of neuronal differentiation, it was confirmed that by day 10, differentiation had been achieved only when SHSY5Y cells were exposed to RA and but not in cells in the absence of RA. This was further confirmed using ICC method for detection of neuronal markers (will be discussed in following, section 3.2.2.3.1 and for the independent experiment refer section 2.2.1.1).

3.2.2.3.1 Determination of differentiated SHSY5Y by ICC: 10-day protocol

Expression of neuron specific markers was determined by ICC, using NF (with ratio 1:500), MAP2 (with ratio 1:500) and NSE (with ratio 1:200) markers as the primary Ab and DAPI for nuclei of neuronal-like cells. A PE-conjugated secondary antibody (with ratio 1:200) was used to give fluorescence with specific combination of primary Ab. An IgG Ab was used as negative control to ensure any unspecific binding and visual confirmation of specific marker present (discussed in detail in section 2.2.4.4).

ICC was performed on differentiated and undifferentiated SHSY5Y cells on day 10 (on the final day of differentiation). Upon incubation of differentiated cells with primary/secondary Ab (NF/PE-conjugated) ratio of 1:500/1:200, neuronal filaments specific to neuronal-like cells showed green fluorescence (figure 3.15. A). Due to differentiation, a higher number of neurite extensions were present which made it difficult to identify individual DAPI stained nuclei. In addition, cells were present behind or on the neurites projection due which few extended neurites and clustered cell groups were stained, and identification of individual nuclei was difficult. As expected, the DAPI stained neuronal-like cells showed blue fluorescence and confirmed the presence of nuclei (figure 3.15.B) with no green fluorescence. Green and blue fluorescence obtained from the NF marker with DAPI (figure 3.15.C) confirmed the existence of intermediate filament in the cytoplasm of differentiated SHSY5Y cells and successful neuronal-like differentiation was achieved. In addition, the differentiated SHSY5Y cells were incubated with primary/secondary Ab (MAP2/PE-conjugated) ratio of 1:500/1:200 and microtubule related protein specific to neuronal-like cells showed green fluorescence (figure 3.15. D). Higher number of neurite extensions were present which made detection of individual DAPI stained nuclei difficult to detect. In addition, maybe presence of clustered cell groups appeared to be stained and identification of individual nuclei was difficult. The presence of blue fluorescence obtained after DAPI stained neuronal-like cells determined the presence of nuclei of differentiated cells (figure 3.15.E) without green fluorescence. The fluorescence obtained from the MAP2 marker + DAPI combined (figure 3.15.F), confirmed the presence of proteins correlated to microtubules in the cytoplasm of differentiated SHSY5Y cells and successful neuronal-like differentiation was attained.

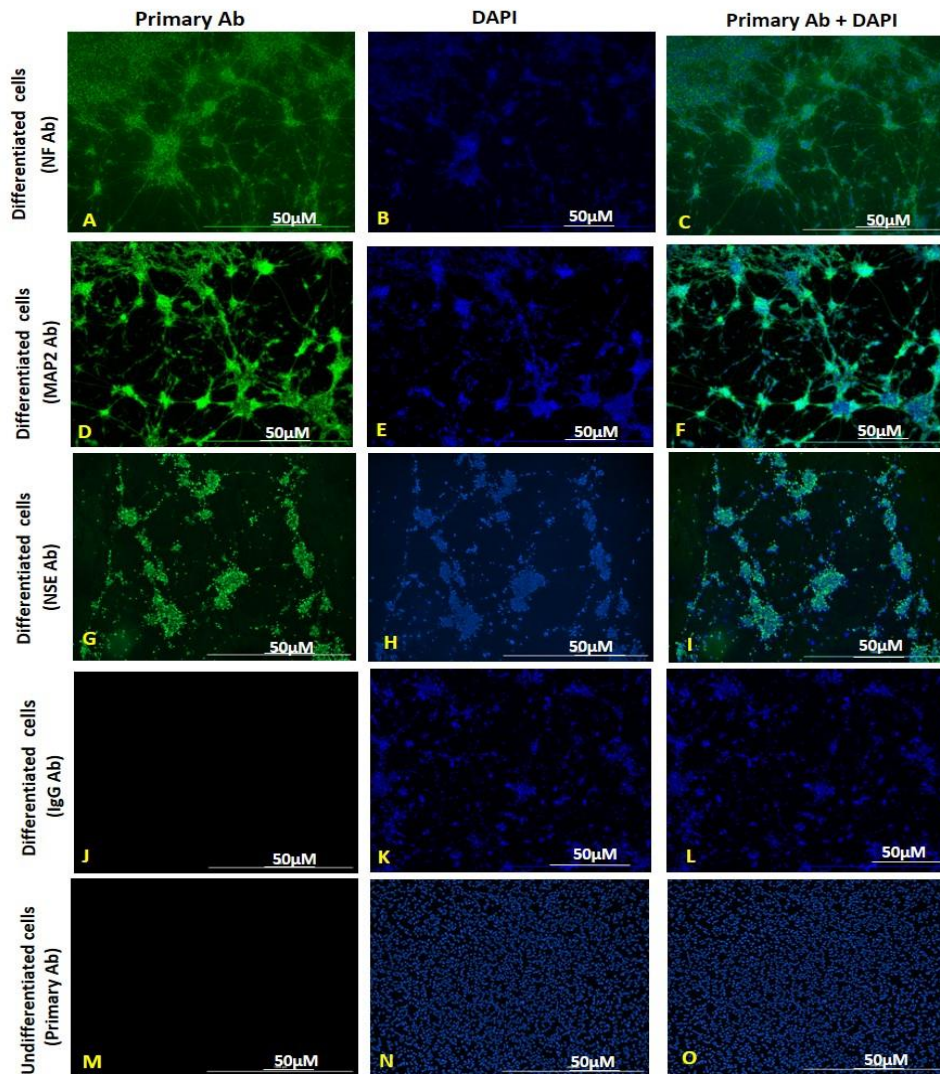


Figure 3.15. Immunofluorescence images representation after RA- mediated differentiation to detect the expression of neuron specific markers (NF, MAP2 and NSE) in differentiated in comparison to undifferentiated cells. NF, MAP2 and NSE were used as primary Ab, PE- conjugated secondary Ab and IgG Ab was used as negative control (incubated alongside with each primary Ab, but only one of the images is shown for reference). In addition, each neuronal marker was incubated with undifferentiated cells, but only one condition was showed as reference. **A.** green fluorescence was detected in the presence of NF marker. **B.** blue fluorescence was detected due to specific binding of DAPI to the nuclei in neuronal-like cells. **C.** the localization of intact differentiated cells was observed in the presence of NF + DAPI. **D.** microtubule associated proteins in the cytoplasm in differentiated cells was recorded in the presence of MAP2 marker. **E.** differentiated cells incubated with DAPI showed blue fluorescence. **F.** in the presence of MAP2 + DAPI as marker, the microtubule associated proteins in neuronal-like cells and associated nuclei was detected. **G.** green fluorescence was observed upon incubation of differentiated cells with NSE marker. **H.** blue fluorescence shown by the DAPI stained differentiated cells, confirmed the presence or location of nuclei of neuronal-like cell. **I.** in the presence of NSE marker + DAPI, the differentiated cells were precisely localized. **J.** the differentiated cells did not show any sign of fluorescence, in the presence of IgG Ab. **K+L.** the differentiated cells did not show any fluorescence in the presence of only DAPI and IgG Ab with DAPI, respectively. **M.** the undifferentiated cells did not showed any fluorescence in presence of the neuronal markers. **N+O.** the undifferentiated cells showed presence of DAPI stained nuclei, but no fluorescence was detected when incubated with neuronal markers and DAPI, respectively. Images were taken with 100-fold magnification.

Furthermore, the differentiated SHSY5Y cells were incubated with primary/secondary Ab (NSE/PE-conjugated) ratio of 1:200/1:200 and enolase enzyme specific to neuronal-like cells showed green fluorescence (figure 3.15. G). Blue fluorescence was obtained upon DAPI stained neuronal-like cells and confirmed the presence of nuclei of differentiated cells (figure 3.15.H) with no green fluorescence. Because higher number of neurite extensions were present, detection of individual DAPI stained nuclei was difficult but still few nuclei were visibly detected. The fluorescence obtained from NSE marker with DAPI combined (figure 3.15.I), determined the existence of enolase enzyme in the cytoplasm of differentiated SHSY5Y cells and successful neuronal-like differentiation was accomplished.

Moreover, the differentiated SHSY5Y cells were incubated with IgG/secondary Ab (NF or MAP2 or NSE /PE-conjugated) with ratio similar to then primary Ab used (only one of the ICC images is presented as shown in figure 3.17 (J-L), as reference of ICC results obtained) and no green fluorescence was detected specific to neuronal-like cells (figure 3.15. J) which suggested no non-specific binding. The presence of blue fluorescence obtained after DAPI stained neuronal-like cells determined the presence of nuclei of differentiated cells (figure 3.15.K) and confirmed the presence of cells. No green fluorescence obtained from the IgG marker with DAPI combined, confirmed the presence of differentiated SHSY5Y cells and successful neuronal-like differentiation was attained with no unspecific binding (figure 3.15.L).Likewise, the undifferentiated SHSY5Y cells were incubated with primary/secondary Ab (NF or MAP2 or NSE /PE-conjugated) with ratio similar to then primary Ab used (only one of the ICC images is shown as reference of results obtained) and no green fluorescence was detected specific to neuronal-like cells (figure 3.15.M-O) which suggested that the cells were not differentiated. The presence of blue fluorescence obtained after DAPI stained nuclei of undifferentiated cells (figure 3.15.N) and confirmed the presence of cells. No green fluorescence obtained from the primary Ab + DAPI combined, confirmed the presence of undifferentiated SHSY5Y cells and no differentiation was attained in these set of cells (figure 3.15. O). The NF, MAP2 and NSE markers were detected in the differentiated SHSH5Y cells but not in the non-differentiated cells and negative controls, thus confirmed that after following 10-day protocol was successfully achieved neuronal differentiation. The experiment was performed once to confirm successful differentiation (discussed in 2.2.1.1).

3.2.2.4 SHSY5Y differentiation: 21-day protocol

The 21-day neuronal differentiation protocol was trialled, and results were compared to the previously described 10-day differentiation protocol (section 3.2.2.3) to assess if there was any perceived value in using the more time consuming 21-day method.

Differentiation in SHSY5Y cells was performed mediated by RA (1 μ M). On day 0, the cells were 60% confluent (figure 3.16. A). On day 3, the first neuritic extensions were noted (pointed by black arrows). The neurite extensions were low in number and the majority of cell population looked heterogeneous and intact in morphology with no sign of axonal outgrowth (figure 3.16. B). On day 5, the heterogeneous culture was observed with epithelial-like or S-type (shown by orange arrows) and N-type (indicated by black arrows) cells (figure 3.16.C). In addition (on day 5), increased number of S-type cells were present along with N-type cells (neuronal-like), short neuritic projections were observed as well as decreased cell density in comparison to day 0 was observed. On day 7, the cells continued to differentiate and the presence of short and long neuritic extensions were recorded. The neighbouring cell started to interconnect, as well as with distantly adhered cells. The S-type cells were observed with no sign of axonal outgrowth (shown by orange arrows) (figure 3.16. D). On day 10, an increased number of S-type of cells were observed (indicated by orange arrows) along with increased number of elongated neuritic outgrowths. The projections seemed to be very stable and thick (indicated by black arrows) (figure 3.16. E). On day 13, an initial clustered group of cells were noted (indicated by yellow arrows) in the differentiating cells. The clustered cells at this point did not look like an intact group. Increased number of interconnected neuritic outgrowths were observed (indicated by black arrows). The differentiating culture seemed homogeneous with no sign of S-type of cells at this point (figure 3.16. F). On day 15 and 17, the cultured cells continued to differentiate into neuronal-like cells. An increased number of rigid clustered cells was observed and captured (figure 3.16. G + H) and were interconnected with the other cultured groups as well as differentiated cells by axonal outgrowths. More neuritic extensions were observed and reduction in cell density was recorded. On day 21, a well-organized and significant group of cells were observed with excellent interconnection with other differentiating cells by extending out the neuritic projections (figure 3.16.I).

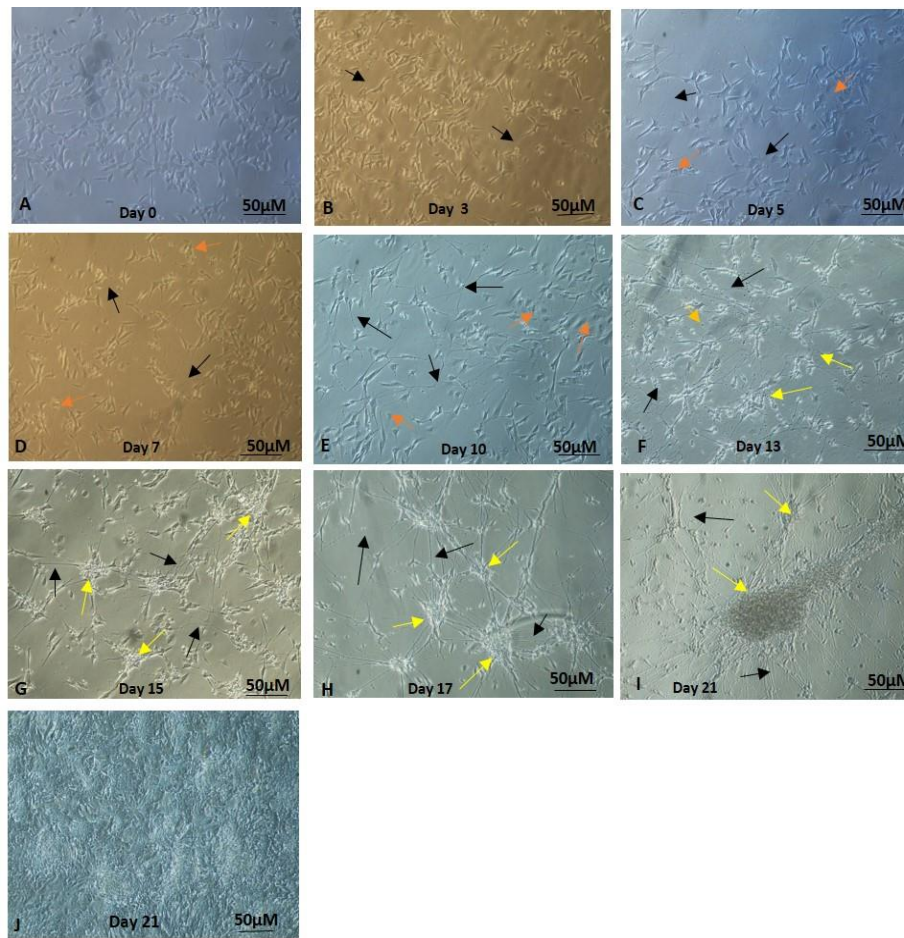


Figure 3.16. Morphological changes in SHSY5Y cells during the RA mediated neuronal differentiation (21-day protocol). **A.** the SHSY5Y cells were seeded, day 0, after 24 hrs of the cells appeared as monolayered and sparsely distributed. **B.** day3, first neurite extensions and axonal outgrowths were observed (pointed by black arrow). **C.** day 5, epithelial-like cells which do not differentiate into neuronal-like, or S-type cell population was visible (pointed by orange arrows) and short neurite extension between adjacent cells (pointed by black arrows). Also, reduced cell density was observed. **D.** day7, differentiating cells showed short and long neurite projections to outreach with each other (pointed by black arrows), S-type cells were observed with no axonal outgrowth (pointed by orange arrows). **E.** day10, cells showed strong neurite outgrowth between differentiating cells, also, outreaching distant adherent grouped cells (pointed by black arrows). More S-type cells were observed (pointed by orange arrows). **F.** day13, first loosely fitted clustered group of neuronal-like cells were observed (pointed by yellow arrows). Increased number of extended axonal outgrowth was observed (pointed by black arrows) with no S-type cells present. **G+H.** day15+17, increased number of clustered group of cells (pointed by yellow arrows) and more elongated neuritic projections (pointed by black arrows) were visible with reduced cell confluency. **I.** well established network of neuronal-like cells was attained on day 21 with thick and extended neurite projections. **J.** undifferentiated cells were observed to be 100% confluent neuroblastoma cells. The images were captured using 200-fold magnification. Over the period of incubation variation in thickness of cell body was observe

The undifferentiated cells (cultured in parallel to the differentiated cells) on day 21 appeared to be over confluent and heterogenous population of cells with no sign of neuronal-like morphological characteristics such as neuritic projections between cells (figure 3.16. J).

3.2.2.4.1 Determination of differentiated SHSY5Y by ICC: 21-day protocol

Neuron specific markers association with differentiated cells in comparison to the undifferentiated cells was determined by ICC. NF (using ratio 1:500), MAP2 (using ratio 1:500) and NSE (using ratio 1:200) markers were used as primary Ab. PE-conjugated secondary Ab (using ratio 1:200) was used to investigate the presence of fluorescence as a result of incubation with primary/secondary Ab to confirm the success of differentiated SHSY5Y cells using 21-day protocol. IgG Ab was used as negative control (discussed in section 2.2.4.4) in relation to detected fluorescence from specific markers. DAPI was used to stain individual cell nuclei. Differentiated and undifferentiated cells were used for ICC on day 21 (end day of differentiation protocol).

In addition to the morphological changes observed (as shown in previous section, 3.2.2.3.1), ICC was carried out on the differentiated and undifferentiated SHSY5Y cells on day 21 (the final day of differentiation). After differentiated cells were incubated with primary/secondary Ab (NF/PE-conjugated) ratio of 1:500/1:200, neuronal filaments specific to neuronal-like cells showed green fluorescence (figure 3.17. A) and the DAPI stained neuronal-like cells showed blue fluorescence which confirmed the presence of nuclei (figure 3.17.B) with no green fluorescence. The fluorescence obtained from the NF marker with DAPI together (figure 3.17.C) confirmed the existence of intermediate filament in the cytoplasm of differentiated SHSY5Y cells and successful neuronal-like differentiation was achieved after 21-days.

Furthermore, the differentiated SHSY5Y cells were incubated with primary/secondary Ab (MAP2/PE-conjugated) ratio of 1:500/1:200 and green fluorescence confirmed specific binding to the microtubule related protein specific to neuronal-like cells (figure 3.17. D). The presence of blue fluorescence obtained after DAPI was incubated with neuronal-like cells, confirmed the presence of nuclei of differentiated cells (figure 3.17.E) with no fluorescence. The fluorescence obtained from the MAP2 marker with DAPI combined (figure 3.17.F), confirmed the presence of proteins associated with microtubules in the cytoplasm of differentiated SHSY5Y cells and successful neuronal-like differentiation was attained.

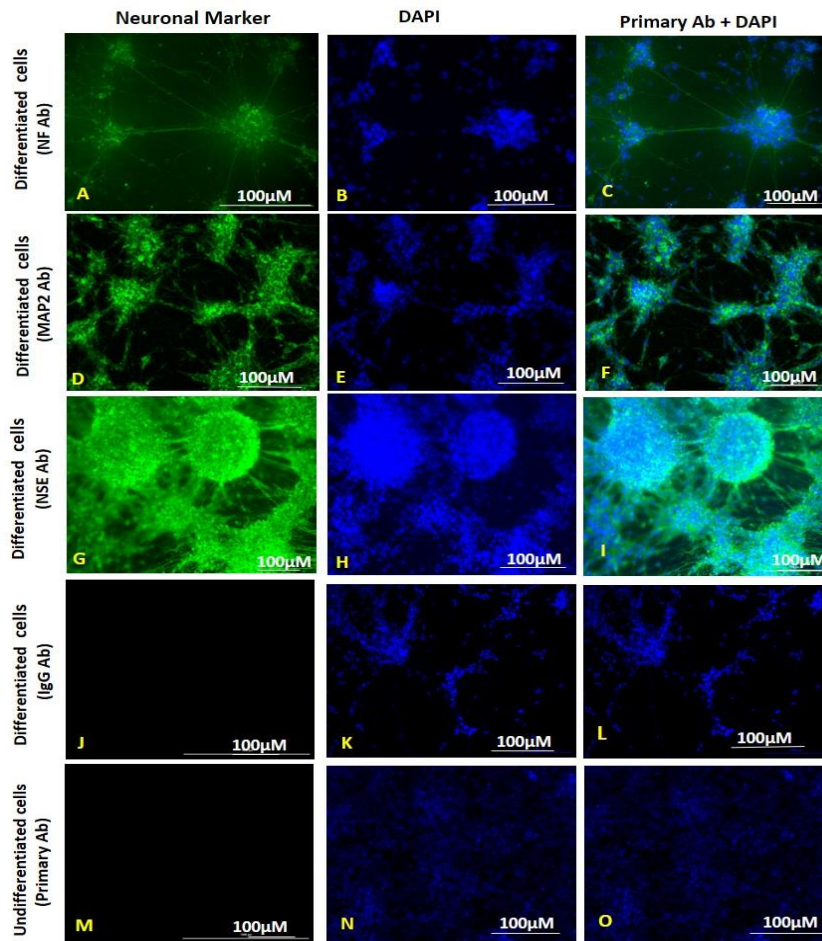


Figure 3.17. Immunofluorescence images to assess neuron specific markers (NF, MAP2 and NSE) in differentiated in comparison to undifferentiated cells after RA- mediated differentiation. NF, MAP2 and NSE were used as primary Ab and PE- conjugated secondary Ab and IgG Ab was used as negative control (incubated alongside with each primary Ab, but only one of the images is shown for reference). In addition, each neuronal marker was incubated with undifferentiated cells, but only one condition was showed as reference. **A.** green fluorescence was detected in the presence of NF marker. **B.** blue fluorescence was detected in DAPI stained neuronal-like cells to locate the nuclei. **C.** the localization of intact differentiated cells was observed in the presence of NF + DAPI. **D.** microtubule associated proteins in the cytoplasm of the differentiated cells was detected in the presence of MAP2 marker. **E.** differentiated cells stained with DAPI showed blue fluorescence. **F.** in the presence of MAP2 + DAPI as combined marker, the microtubule associated proteins in neuronal-like cells and associated nuclei were detected. **G.** green fluorescence was observed upon incubation of differentiated cells with NSE marker. **H.** blue fluorescence obtained by the DAPI stained differentiated cells, confirmed the presence or location of nuclei of neuronal-like cells. **I.** in the presence of NSE + DAPI, the differentiated cells were precisely localized. **J.** the differentiated cells did not show any sign of fluorescence, in the presence of IgG Ab. **K+L.** the differentiated cells did not show any fluorescence in the presence of only DAPI and IgG Ab with DAPI, respectively. **M.** the undifferentiated cells did not showed any fluorescence in presence of the neuronal markers. **N+O.** the undifferentiated cells showed presence of DAPI stained nuclei, but no fluorescence was detected when incubated with neuronal markers + DAPI, respectively.

Moreover, the differentiated SHSY5Y cells were incubated with primary/secondary Ab (NSE/PE-conjugated) ratio of 1:200/1:200 and enolase enzyme specific to neuronal-like cells

showed green fluorescence and confirmed the SHSY5Y cells were effectively differentiated (figure 3.17. G). Blue fluorescence was detected in neuronal-like cells when stained with DAPI and confirmed the presence of nuclei of differentiated cells (figure 3.17.H) with no green fluorescence. The fluorescence obtained from NSE marker + DAPI together (figure 3.17.I), determined the presence of enolase enzyme in the cytoplasm of differentiated SHSY5Y cells and successful neuronal-like differentiation was accomplished. It was interesting to observe the increased activity of enolase enzyme due to which very bright and dominant green fluorescence was measured. In addition, the differentiated SHSY5Y cells were incubated with IgG/secondary Ab (NF or MAP2 or NSE /PE-conjugated) with ratio similar to the primary Ab used (only one of the ICC images is presented in figure 3.17 (J-L), as reference of ICC results obtained) and no green fluorescence was detected specific to neuronal-like cells (figure 3.17. J) which suggested that no non-specific binding was present. The presence of blue fluorescence obtained after DAPI stained neuronal-like cells determined the nuclei of differentiated cells located (figure 3.17.K) and confirmed the presence of cells. No green fluorescence obtained from the IgG marker + DAPI combined staining and confirmed the presence of differentiated SHSY5Y cells and successful neuronal-like differentiation was attained with no unspecific binding (figure 3.17.L). Similarly, the undifferentiated SHSY5Y cells were incubated with primary/secondary Ab (NF or MAP2 or NSE /PE-conjugated) with ratio similar to then primary Ab used (only one of the ICC images is showed for reference of ICC results obtained, as shown in figure 3.17 (M-O) and no green fluorescence was detected specific to neuronal-like cells (figure 3.17.M) which suggested that the cells were not differentiated. The presence of blue fluorescence obtained with DAPI stained nuclei of undifferentiated cells (figure 3.17.N) and confirmed the presence of cells. No green fluorescence obtained from the primary Ab + DAPI combined and confirmed the presence of undifferentiated SHSY5Y cells, and no differentiation was attained in this group of cells (figure 3.17.O).

The NF, MAP2 and NSE markers were detected in the differentiated SHSH5Y cells in comparison to the undifferentiated cells and negative controls, thus confirmed that the neuronal differentiation was successfully achieved using 21-day protocol. The ICC was performed once to confirm the successful differentiation of SHSY5Y cells (discussed in section 2.2.1.1).

3.2.2.5 Comparing 10-day and 21-day protocol for differentiation

As discussed in detail in the above sections, neuronal differentiation of SHSY5Y cells was achieved by following both the 10-day and 21-day protocols, in table.3.2. The table given above was constructed to compare different criteria of both protocols to see if there was an advantage to either of the two methods. Therefore, in order to utilize time efficiently, the 10-day protocol was adopted as the final protocol for further experiments in this study.

Table.3.2. The table below compares the features and results obtained from RA-mediated 10- and 21-day protocols in the efficacy to achieve neuronal differentiation.

Criteria of comparison	Differentiated SHSY5Y cells (10-days protocol)	Differentiated SHSY5Y cells (21-days protocol)	Undifferentiated SHSY5Y cells (10+21days protocol)
RA concentration	10 μ M	1 μ M	No RA added
Differentiation rate	Neurite outgrowth visible after day5	Neurite outgrowth visible after day10	Neurite outgrowth absent
NSE marker	Present	Present	Absent
MAP2 marker	Present	Present	Absent
NF marker	Present	Present	Absent
Morphology	Stable neurite with outgrowth, networking with neighbouring group of cells, on day10	Stable neurite outgrowth, networking with neighbouring group of cells, on day21	Overconfluent culture with no neurite outgrowth.

3.3 Estimation of cell viability in oxidative stress

Oxidative stress is a common feature of both AD and obesity. It affects the mitochondrial function resulting in A β accumulation and finally AD pathogenesis (Fracassi et al., 2021). H₂O₂ is well known oxidative stress inducer in SHSY5Y cell culture within 24 hrs incubation (Huang et al., 2020). In the present study, established cell culture models were used to investigate the interaction of neuronal- and adipocyte-like cells when exposed to oxidative stress.

It has been established within our lab that 3T3-L1 cells can be differentiated into adipocyte-like cells (section 2.2.3.2) and it was confirmed that the profile of adipokines or growth factors secreted by these cells were comparable to differentiated or mature adipocyte-like including resistin, leptin, chemerin, adiponectin, interleukins, and others (Dewhurst et al., unpublished). We investigated whether these adipokines or growth factors secreted had any impact on SHSY5Y cell viability, when exposed to oxidative stress. Furthermore, to recapitulate the obese adipocyte state, we examined whether adipokines secreted from differentiated 3T3-L1 had a different impact on SHSY5Y cell viability.

3.3.1. Optimization of H₂O₂ dose on SHSY5Y cells

Firstly, the experiments were aimed to identify the optimum concentration of H₂O₂, and incubation times required to induce cell death in approximately 50% of the cell population. In the literature, a range of H₂O₂ concentrations between 50-500 μ M and incubation periods of 12 hrs and 24 hrs have been used to obtain oxidative stress induced cell death. Therefore, these parameters (H₂O₂ concentrations and incubation time) were investigated in differentiated and undifferentiated SHSY5Y cells (Garcimartín et al., 2017; Hanafy et al., 2020).

3.3.1.1. Effect of variable H₂O₂ concentration on differentiated SHSY5Y cell viability at 12 hrs and 24 hrs

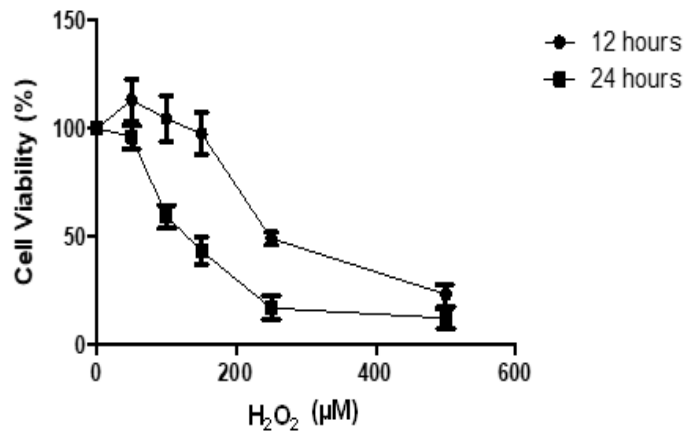


Figure 3.18. Impact of H₂O₂ dose on cell viability in differentiated SHSY5Y cells (12 hrs and 24 hrs incubation) was explored. The differentiated cells were treated with H₂O₂ doses between 50-500µM for 12 hrs and showed a small increase in cell viability at dose 50µM but decline in cell viability was observed using H₂O₂ doses between 100 - 500µM. The EC₅₀ obtained for 12 hrs was 250µM. Similarly, differentiated cells were treated with H₂O₂ dose range between 50-500µM for 24 hrs. 50µM dose showed minor reduction in cell viability and H₂O₂ dose range 100 -500µM showed continued cell viability reduction. The EC₅₀ obtained for 24 hrs was 150µM. Data was analysed by GraphPad- Prism5. Each point of dose are in triplicate (n=3) and presented as mean ± SEM.

Cell viability of differentiated SHSY5Y cells was assessed after 12 hrs incubation with H₂O₂ dose range of 50, 100, 150, 250 and 500µM. Although there was small increase in cell viability at 50µM and 100µM (128.3 ± 13.8 and 116.1 ± 15.2, respectively) but there was an overall decrease in cell viability with increasing H₂O₂ concentration, 150µM and 500µM (102.1 ± 11.2 and 26.4 ± 4.28, respectively). The EC₅₀ dose obtained was 250µM with half (52.9 ± 2.4) for differentiated SHSY5Y after 12 hrs incubation with H₂O₂ dose (figure 3.18, 12 hrs). Similarly, results obtained after the differentiated SHSY5Y cells were incubated with H₂O₂ for 24 hrs, an overall decrease in cell viability was observed. Slight reduction in viability was found with 50 µM with (92.9 ± 5.4). Further decreased cell viability was obtained with increased dose of H₂O₂ i.e., 100µM, 250µM and 500µM with (63.9 ± 5.4, 29.3 ± 5.2, 23.5 ± 4.02, respectively). The EC₅₀ dose obtained was 150 µM with (43.6 ± 7.2) for neuronal-like cells after 12 hrs incubation with H₂O₂ dose (figure 3.18, 24 hrs). On the basis of results obtained from 12- and 24 hrs with H₂O₂, the concentration of 150 µM for 24 hrs was considered as the final dose to induce oxidative stress in differentiated SHY5Y cells in further experiments.

Results are stated as mean \pm SEM (% viability). To obtain the EC50, the experiments were repeated in triplicate (n=3) and data was analysed using GraphPad Prism 5 (detailed in section 2.3).

3.3.1.2 Effect of variable H₂O₂ concentration on undifferentiated SHSY5Y cell viability at 12 hrs and 24 hrs

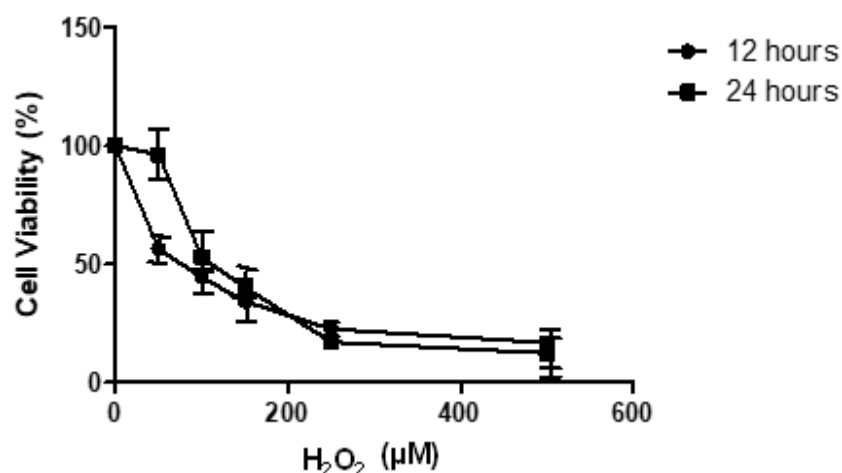


Figure 3.19. The impact of H₂O₂ dose on cell viability of undifferentiated SHSY5Y cells (12hrs and 24hrs incubation). The undifferentiated cells were treated with H₂O₂ dose range between 50-500 μ M for 12hrs. The H₂O₂ doses between 50-500 μ M showed gradual decrease in cell viability and 50 μ M was obtained as EC50 for H₂O₂ doses. Undifferentiated cells were also treated with H₂O₂ dose range between 50-500 μ M for 24hrs. 50 μ M dose showed minor reduction in cell viability and H₂O₂ dose range 100-500 μ M showed gradually decreased cell viability and EC50 attained was 100 μ M. Data was analysed by GraphPad Prism5. Each point of dose were repeated in triplicate (n=3) and presented as mean \pm SEM.

Cell viability of undifferentiated (non-neuronal cells) SHSY5Y cells was evaluated after 12 hrs of incubation with H₂O₂ dose range between 50 – 500 μ M (figure 3.19, 12 hrs). A minor reduction in cell viability was recorded using 50 μ M H₂O₂ dose with (91.3 \pm 18.2) and an overall decrease in cell viability with increasing H₂O₂ concentration i.e., 100, 150, 250 and 500 μ M with (46.4 \pm 9.28, 39.29 \pm 11.2, 28.8 \pm 1.5 and 22.3 \pm 12.28, respectively). The EC50 dose calculated was 50 μ M with (52.9 \pm 2.4) for undifferentiated cells after 12 hrs incubation with H₂O₂ dose. In addition, the results obtained after the undifferentiated cells were incubated with H₂O₂ for 24 hrs, an overall decrease in cell viability was observed. Slight reduction in viability was found with 50 μ M with (93.2 \pm 15.4). Further decreased cell viability was obtained with increased dose of H₂O₂ i.e., 150, 250 and 500 μ M (41.3 \pm 9.4, 27.8 \pm 1.2, 20.5 \pm 8.02, respectively).

The EC50 dose obtained was 100 μ M with (52.6 \pm 8.2) for undifferentiated cells after 24 hrs incubation with H₂O₂ dose (figure 3.19, 24hrs). Based on results obtained from 12- and 24hrs with H₂O₂, the concentration of 100 μ M for 24 hrs was considered as the final dose to induce oxidative stress in undifferentiated SHY5Y cells in further experiments. Results are stated as mean \pm SEM (% viability). The EC50 was calculated, and experiments were repeated in triplicate (n=3) analysed using GraphPad Prism 5 (detailed in section 2.3).

3.3.2 Exploring the effect of co-treatment using differentiated and undifferentiated (3T3-L1) derived conditioned media on oxidative stress induced cytotoxicity in differentiated and undifferentiated SHSY5Y cells

Adipokines have a recognized role on cell viability. Adipokines are secreted from adipocytes into their environment (cultured media in case of this study) (Little & Safdar, 2015; El-Hattab et al., 2020). To understand the effect of adipokines on the viability of neuronal cells under oxidative stress, conditioned media (CM) was taken from cultured differentiated, as well as undifferentiated (3T3-L1), and incubated with undifferentiated (non-neuronal) and differentiated (neuronal-like) SHSY5Y cells for 24 hrs with and without H₂O₂ (figure 3.20. A-B). Overall, the CM from differentiated 3T3-L1 showed neuroprotective effect evident by increased cell viability of SHSY5Y cells under oxidative stress.

The effect of 3T3-L1 CM on the viability of undifferentiated cells under oxidative stress was investigated (figure. 3.20.A). 100 μ M of H₂O₂ as well as CM from differentiated 3T3-L1 and undifferentiated 3T3-L1 were used as co-treatment condition and were incubated with undifferentiated cells for 24 hrs. CM from differentiated and undifferentiated 3T3-L1 caused a significant decrease (***p<0.001) in the overall cell viability of undifferentiated SHSY5Y cells with and without H₂O₂ in comparison to the untreated cells (CM from differentiated 3T3-L1 without H₂O₂ = 48 \pm 8.09; CM from differentiated 3T3-L1 with H₂O₂ = 29 \pm 1.7; CM from undifferentiated 3T3-L1 without H₂O₂ = 43 \pm 6.7; CM from undifferentiated 3T3-L1 with H₂O₂ = 38 \pm 11.9).

In addition, significantly reduced cell viability ($*p < 0.05$) was noted in CM from differentiated 3T3-L1 without $H_2O_2 = 43 \pm 6.7$ in comparison to CM from differentiated 3T3-L1 with $H_2O_2 = 23 \pm 0.7$. The reduced cell viability indicated that the undifferentiated SHSY5Y cells were not able to adjust and continue the normal growth in the presence of CM.

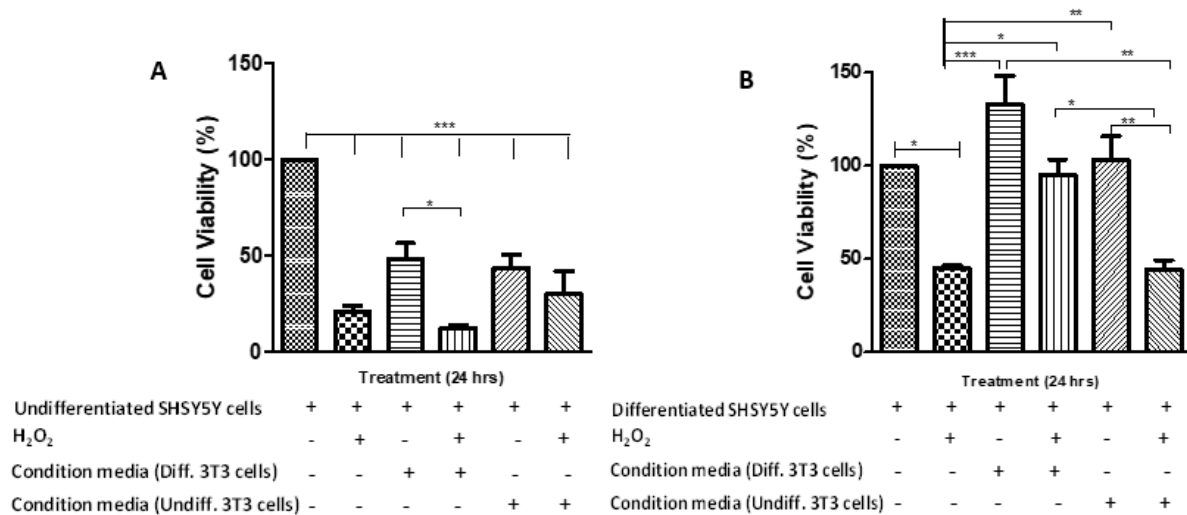


Figure 3.20. To explore the impact of co-treatment using differentiated and undifferentiated 3T3-L1 derived CM on oxidative stress induced cytotoxicity in differentiated and undifferentiated SHSY5Y cells. **A.** undifferentiated SHSY5Y cells were treated with $100\mu M H_2O_2$ for 24 hrs, associated with a decrease in cell viability. CM from differentiated and undifferentiated 3T3-L1 elicited a decrease in cell viability in comparison to untreated controls. Co-incubation of CM from undifferentiated 3T3-L1 had restorative effect on the response of the undifferentiated SHSY5Y cells treated with H_2O_2 . **B.** The differentiated SHSY5Y cells were treated with $150\mu M H_2O_2$ for 24 hrs which was related to decrease in cell viability. Overall variation in the cell viability of differentiated SHSY5Y cells was observed when incubated with different treatments in comparison to the untreated cells. Significant increase in the viability of differentiated SHSY5Y cells was observed when incubated in CM from differentiated 3T3-L1 with and without H_2O_2 and CM of undifferentiated in comparison to the H_2O_2 treated. The data obtained are presented as mean \pm SEM (each experiment was repeated in triplicate, $n=3$). Data was analysed by using GraphPad Prism5 and statistical significance was considered at $*p < 0.05$, $**p < 0.01$, $***p < 0.001$.

The MTT assay results obtained showed overall inconsistent cell viability of differentiated SHSY5Y in the presence and absence of H_2O_2 co-treated with CM from differentiated and undifferentiated 3T3-L1, as shown in figure 3.20.B. $150\mu M$ of H_2O_2 was used in this experimental study to induce oxidative stress for 24 hrs. The H_2O_2 only treated cell showed significant reduced cell viability in comparison to the untreated cells ($*p < 0.05$).

Moreover, the CM from differentiated 3T3-L1 with and without H₂O₂ as well as undifferentiated 3T3-L1 supported a significant increase (*p<0.05), ***p<0.001, **p<0.01, respectively) in cell viability of in comparison to the H₂O₂ only treated cells (CM from differentiated 3T3-L1 without H₂O₂ = 132.6 ± 9.01; CM from differentiated 3T3-L1 with H₂O₂ = 95.1 ± 4.3; CM from undifferentiated 3T3-L1 without H₂O₂ = 102.6 ± 7.8; CM from undifferentiated 3T3-L1 with H₂O₂ = 44 ± 3.9). In addition, significant increase in cell viability was measured in CM from differentiated 3T3-L1 with H₂O₂ and CM from undifferentiated 3T3-L1 without H₂O₂ (*p<0.05, **p<0.01, respectively) in comparison to CM from undifferentiated 3T3-L1 with H₂O₂.

The data was analysed using GraphPad Prism 5. The data are presented as mean ± SEM (% viability) and each experiment was repeated in triplicate, n=3. Statistical significance was considered with *p<0.05, **p<0.01, ***p<0.001, when the incubated treatments were compared to untreated and H₂O₂- only treated cells (statistical analysis detail given in section 2.3).

The cell viability experimental results suggested that the adipokines/other growth factors secreted by the differentiated 3T3-L1 cells or adipocyte-like had a neuroprotective effect during H₂O₂ induced oxidative stress. No effective neuroprotective effect was observed in the undifferentiated SHSY5Y cells or non-neuronal cells. Therefore, the following experiments were performed to better understand the effect of these released adipokines or growth factors in the conditioned media in relation to the cell viability under oxidative stress.

3.3.3. Exploring the effect of co-treatment using stressed adipocyte and pre-adipocyte (3T3-L1) derived CM on oxidative stress induced cytotoxicity in differentiated and undifferentiated SHSY5Y cells

Obesity is characterised by chronic low-level inflammation and persistent oxidative stress. The adipocytes secreted adipokines and oxidative stress are co-related which could influence the adipokine level and effectiveness (Li et al., 2019; Sakurai et al., 2009). Cultured media was therefore derived from adipocytes (differentiated 3T3-L1 cells) that had been ‘stressed’ by exposure to H₂O₂ to investigate whether the resultant conditioned media had a different influence on the viability of neuronally differentiated and undifferentiated SHSY5Y cells. Because the

H₂O₂ was added or mixed to/with the cultured media of adipocyte-like cells, it was not possible to separate the added H₂O₂ from cultured media, so we had to consider the possibility that neuronal-like cells damage was not solely because of CM.

The cytotoxic assay results showed for the undifferentiated SHSY5Y cells under oxidative stress (figure 3.21.A), 100µM of H₂O₂ was used to stress the differentiated 3T3-L1 and CM from differentiated 3T3-L1 and undifferentiated 3T3-L1 were used as co-treatment condition to be incubated with undifferentiated SHSY5Y cells for 24 hrs. CM from both differentiated and undifferentiated 3T3-L1 caused a significant decrease (**p<0.001) which was observed as the overall cell viability of undifferentiated SHSY5Y cells with and without H₂O₂ in comparison to the untreated SHSY5Y cells (CM from differentiated 3T3-L1 without H₂O₂ = 48 ± 0.09; CM from differentiated 3T3-L1 with H₂O₂ = 37.1 ± 1.7; CM from undifferentiated 3T3-L1 without H₂O₂ = 74 ± 0.07; CM from undifferentiated 3T3-L1 with H₂O₂ = 68 ± 1.09).

In addition, significant increase in cell viability was recorded in CM from differentiated 3T3-L1 without H₂O₂, CM (pre-stressed with H₂O₂) from differentiated 3T3-L1 without H₂O₂ (43.3 ± 0.7), and CM from undifferentiated 3T3-L1 with and without H₂O₂ in comparison to the H₂O₂ only treated cells (**p< 0.01, ***p<0.001). Moreover, significantly reduced cell viability was obtained in CM from undifferentiated 3T3-L1 with and without H₂O₂ in comparison to the CM from differentiated 3T3-L1 with and without H₂O₂ (***p<0.001).

The results obtained suggested that the undifferentiated SHSY5Y cells were not able to adjust and continue the normal growth in the presence of CM whereas slightly increased cell viability in undifferentiated SHSY5Y (non-neural) with undifferentiated 3T3-L1(pre-adipocytes) CM indicated the possibility of presence of growth factors that supports the cellular proliferation even under oxidative stress.

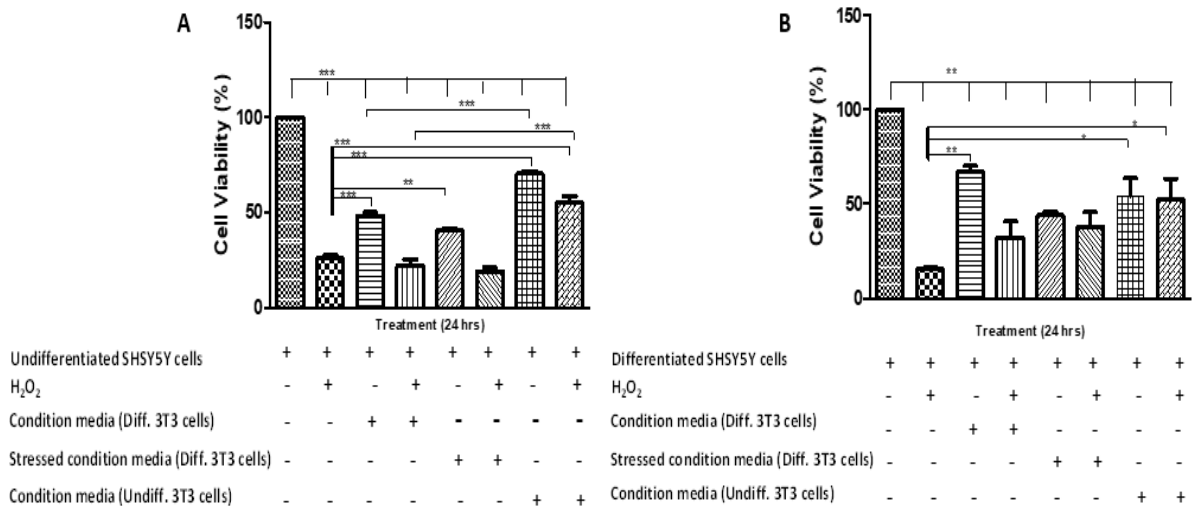


Figure 3.21. To explore the impact co-treatment using differentiated 3T3-L1 (or non-stressed in this study), stressed differentiated 3T3-L1 and undifferentiated 3T3-L1 derived CM on oxidative stress induced cytotoxicity in differentiated (neuronal-like) and undifferentiated (non-neuronal) SHSY5Y cells. **A.** non-neuronal SHSY5Y cells were treated with 100 μ M H₂O₂ for 24 hrs to achieve induced oxidative stress. An overall, significant decreased cell viability was measured when SHSY5Y cells were treated with CM from differentiated and undifferentiated 3T3-L1 with and without H₂O₂ in comparison to the untreated SHSY5Y cells. Significant increase in cell viability was observed in differentiated (stressed and non-stressed) CM without H₂O₂, CM from undifferentiated 3T3-L1 with and without H₂O₂ in comparison to the cells with H₂O₂ only treated cells. **B.** The undifferentiated SHSY5Y cells were treated with 150 μ M H₂O₂ for 24 hrs to attain induced oxidative stress. A significant increase in differentiated SHSY5Y cell viability was measured with CM from differentiated 3T3-L1 without H₂O₂ and CM of undifferentiated 3T3-L1 with and without H₂O₂ in comparison to the H₂O₂ only treated cells. The data are presented as mean \pm SEM and each experiment was repeated in triplicate (n=3). The data was analysed using GraphPad Prism5. Statistical significance was considered at *p<0.05, **p<0.01, ***p<0.001.

The effect of pre-oxidized or stressed CM from differentiated and differentiated 3T3-L1 on the differentiated SHSY5Y (neuronal-like) cell viability under oxidative stress was further explored following the co-treatment experiment (figure 3.20). In section 3.3.2, the SHSY5Y cells were examined for neuroprotection against oxidative stress, however, in this section, the obesity-like condition was attempted to be mimicked.

150 μ M of H₂O₂ was used to induce oxidative stress prior to the experiment and thereafter, CM from differentiated-undifferentiated 3T3-L1 were used as co-treatment condition for 24 hrs (figure 3.21.B). An overall, significant reduction in cell viability of differentiated SHSY5Y cells was observed in different treatment conditions (**p<0.01) in comparison to the untreated SHSY5Y cells.

Decreased cell viability indicated that neuronal-like cells were unable to proliferate to full potential in the presence of the CM from differentiated and undifferentiated 3T3-L1 under oxidative stress, especially when the CM from the differentiated were already stressed. When the differentiated SHSY5Y cells were incubated with the CM from differentiated 3T3-L1 without H₂O₂ and CM from undifferentiated 3T3-L1 with and without H₂O₂, a significant increase in cell viability was attained (differentiated 3T3-L1-CM without H₂O₂= 66.29 ±1.02, undifferentiated 3T3-L1-CM without H₂O₂ = 50.66 ±10.06, preadipocyte CM with H₂O₂ =52 ± 11.06) in comparison to the H₂O₂ only treated cells.

The data was analysed using GraphPad Prism 5, detailed in method section 2.3. The data are presented as mean ± SEM (% viability) and each experiment was repeated in triplicate, n=3. Statistical significance was considered at *p<0.05, **p<0.01, ***p<0.001. The data obtained suggested that under H₂O₂ induced oxidative stress condition, the differentiated SHSY5Y (neuronal-like) cells with stressed growth factors or adipokines did not show distinguished cell proliferation in compare to the untreated SHSY5Y cells.

3.3.4. Exploring the effect of co-treatment using stressed adipocyte and pre-adipocyte (3T3-L1) derived half CM change on oxidative stress induced cytotoxicity in differentiated and undifferentiated SHSY5Y cells

Half media change has been used successfully and allowed adipokine exposure with a reduced impact of complete removal of normal growth media. To eliminate the possibility that in previous experiments (section 3.3.3, figure 3.21), the complete replacement of cultured media from SHSY5Y cells with CM from 3T3-L1 cells may had removed essential growth factors in SHSY5Y cell culture. Therefore, this experiment was performed to understand the neuroprotection using SHSY5Y cells under oxidative stress, and instead of complete removal of normal growth media, only half volume of media was replaced on SHSY5Y cells so that the cells could be exposed to both normal growth media as well as CM.

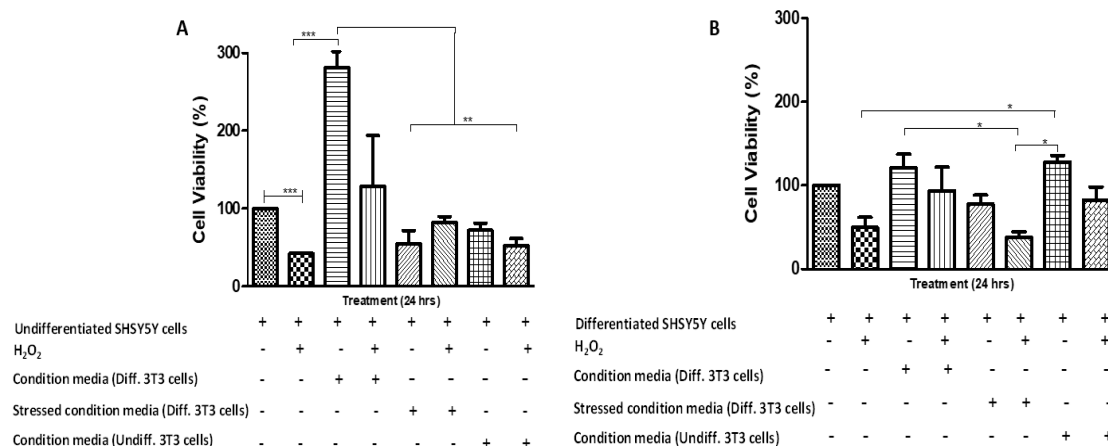


Figure 3.22. To investigate the effect of co-treatment using half media change condition derived from differentiated 3T3-L1 (or non-stressed in this study), stressed differentiated 3T3-L1 and undifferentiated 3T3-L1 on oxidative stress induced cytotoxicity in differentiated and undifferentiated SHSY5Y cells. **A.** non-neuronal SHSY5Y cells were treated with 100µM H₂O₂ for 24 hrs to induce oxidative stress. Significant decrease in cell viability was observed with H₂O₂ only treated SHSY5Y cells in comparison to the untreated SHSY5Y cells. Significantly increased cell viability was measured in undifferentiated SHSY5Y cells when incubated with differentiated 3T3-L1- CM without H₂O₂ with in comparison with H₂O₂ only treated SHSY5Y cells. In addition, significant reduction in cell viability was recorded in stressed differentiated 3T3-L1 and undifferentiated 3T3-L1 with and without H₂O₂ in comparison to the differentiated 3T3-L1- CM without H₂O₂. **B.** The differentiated SHSY5Y cells were treated with 150µM H₂O₂ for 24 hrs to obtained induced oxidative stress. Significant increase in differentiated SHSY5Y cell viability was measured with CM from undifferentiated 3T3-L1 without H₂O₂ in comparison to H₂O₂ only treated SHSY5Y cells. Significant decrease in cell viability was measured with stressed differentiated 3T3-L1-CM with H₂O₂ in comparison to differentiated 3T3-L1-CM without H₂O₂ and significant increased cell viability was observed in undifferentiated 3T3-L1 without H₂O₂ in comparison to stressed differentiated 3T3-L1-CM with H₂O₂. The data are presented as mean ± SEM and each experiment was repeated in triplicate, (n=3). The data was analysed using GraphPad Prism5. Statistical significance was considered at *p<0.05, **p<0.01, ***p<0.001.

The MTT assay results were obtained using undifferentiated SHSY5Y cells under oxidative stress, showed in figure 3.22.A. 100µM of H₂O₂ dose was used to stress the differentiated 3T3-L1 and CM from differentiated 3T3-L1 and undifferentiated 3T3-L1 were used as co-treatment condition to be incubated with undifferentiated SHSY5Y cells for 24 hrs. Significant decrease in cell viability was observed in H₂O₂ only treated SHSY5Y cells in comparison to the untreated SHSY5Y cells. In addition, significant increase in cell viability was measured in CM from differentiated 3T3-L1 without H₂O₂ (280.6 ± 17.9) in comparison to the H₂O₂ only treated SHSY5Y cells. Moreover, significantly reduced cell viability was measured in undifferentiated and stressed differentiated 3T3-L1-CM with and without H₂O₂, with (undifferentiated 3T3-L1-CM without H₂O₂ = 80.3 ± 2.07, undifferentiated 3T3-L1-CM with H₂O₂ = 51.6 ± 2.67, stressed differentiated 3T3-L1-CM without H₂O₂ = 81.6 ± 7.5, stressed differentiated 3T3-L1-CM with H₂O₂ = 54.6 ± 9.03) in comparison to the CM from differentiated 3T3-L1 without H₂O₂.

Differentiated SHSY5Y cells were incubated with differentiated 3T3-L1-CM and undifferentiated 3T3-L1-CM with and without H₂O₂. Significantly increased cell viability was measured in SHSY5Y cells in undifferentiated 3T3-L1-CM without H₂O₂ (128 ± 7.5) in comparison to the H₂O₂ only treated SHSY5Y cells. Similarly, significant increase in cell viability was measured in SHSY5Y cells in undifferentiated 3T3-L1-CM without H₂O₂ in comparison to the stressed differentiated-3T3-L1-CM with H₂O₂ (38.1 ± 6.1). Reduced cell viability was measured in stressed differentiated-3T3-L1-CM with H₂O₂ in comparison to the undifferentiated 3T3-L1-CM without H₂O₂. The data was analysed using GraphPad Prism 5, detailed in method section 2.3. Data are presented as mean \pm SEM (% viability) and each experiment was repeated in triplicate, n=3. Statistical significance was considered at *p<0.05, **p<0.01, ***p<0.001.

3.3.5. Understanding the effect of commercial adipokines on SHSY5Y cell viability

Considering the ability of adipocyte derived CM to influence differentiated (neuronal-like) and undifferentiated (non-neuronal) SHSY5Y cells under oxidative stress, the next step was to study the influence of key individual adipokines. Previous studies have identified that adipokines may have neuroprotective effects as antioxidant and anti-inflammatory agents (Haidari et al., 2019). The next phase of this study therefore used commercially available adipokines to determine their individual role on the cell viability of differentiated and undifferentiated SHSY5Y cells. The adipokines used were chemerin, leptin and resistin. Chemerin and leptin were selected because studies have confirmed the expression of their respective receptors in SHSY5Y cells (Tümmler et al., 2017; Lu et al., 2006). Furthermore, resistin has been strongly inter-linked with IR and obesity (Tripathi et al., 2020), however no study so far has confirmed their direct involvement in relation to AD and obesity under oxidative stress (detailed in chapter 4, discussion).

3.3.5.1 Effect of chemerin on differentiated and undifferentiated SHSY5Y cell viability in the presence and absence of H₂O₂ induced oxidative stress

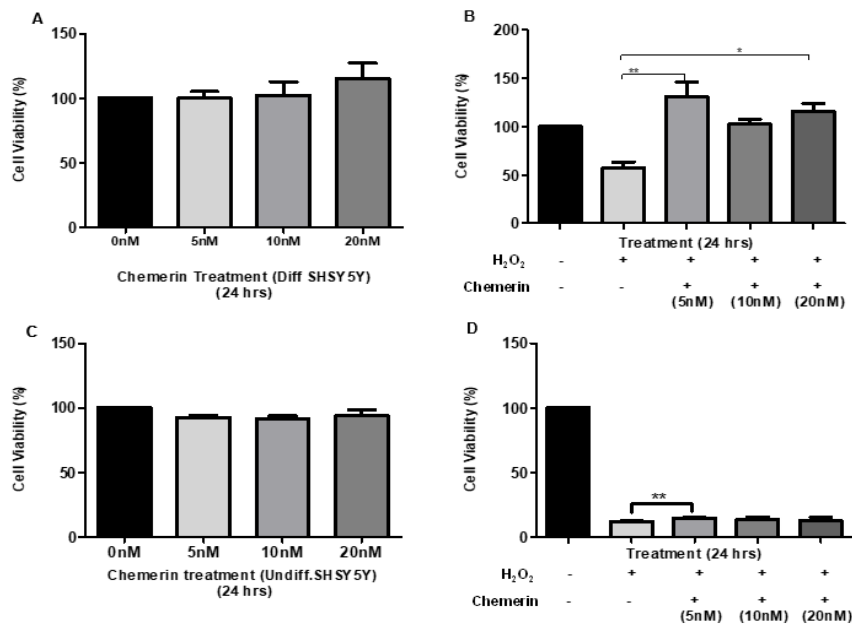


Fig.3.23. Exploring the impact of commercially available chemerin on differentiated SHSY5Y cell viability. **A.** The differentiated SHSY5Y cells were treated with increasing doses of chemerin (5nM, 10nM and 20nM) for 24hrs without H₂O₂. **B.** differentiated SHSY5Y cells were co-treated with 150μM of H₂O₂ and chemerin for 24 hrs. A significant increase in cell viability was observed in differentiated SHSY5Y cells co-treated with H₂O₂ and 5 and 20nM doses of chemerin in comparison to H₂O₂ only treated differentiated SHSY5Y cells. **C.** the undifferentiated SHSY5Y cells were treated with three doses of chemerin- 5nM,10nM and 20nM for 24 hrs incubation without H₂O₂ and no significant change in cell viability using different doses of chemerin was observed. **D.** undifferentiated SHSY5Y cells were co-incubated with 100μM of H₂O₂ with chemerin for 24 hrs. There was statistically significant increase in cell viability cells was obtained with in chemerin (5nM) +H₂O₂ in comparison to cells H₂O₂ only treated undifferentiated SHSY5Y cells. The data are presented as mean ± SEM and was analysed using GraphPad Prism5. Statistical significance was considered at *p<0.05, **p<0.01. Each experiment was performed in triplicate, (n=3).

Three doses of chemerin (5,10 and 20nM) without and with 150μM of H₂O₂ were used and co-treated with differentiated SHSY5Y cells (figure 3.23.A and B, respectively) for 24 hrs.

In the absence of H₂O₂ treatment, the incubated three doses of chemerin did not show any statistical difference in cell viability (figure 3.23.A) in comparison to the untreated cells. Whereas significantly increased cell viability was measured in differentiated SHSY5Y cells co-treated with H₂O₂ + 5nM (130.3 ± 6.1) and 20nM (115 ± 4.4) doses of chemerin in comparison to the H₂O₂ only treated differentiated SHSY5Y cells, *p<0.05, **p<0.01.

Similarly, undifferentiated SHSY5Y cells were incubated with three doses of chemerin and co-incubated without and with 100 μ M of H₂O₂ for 24 hrs (figure 23.C and D, respectively). Different doses of chemerin showed no change in cell viability in undifferentiated SHSY5Y cells in the absence of H₂O₂. However, co-treated condition of chemerin of 5nM (12.3 ± 0.79) and H₂O₂ with an undifferentiated SHSY5Y cells showed significant increased cell viability under oxidative in comparison to the H₂O₂ only treated undifferentiated SHSY5Y cells, **p<0.01.

The data was analysed using GraphPad Prism 5, detailed in section 2.3. The data are presented as mean \pm SEM (% viability) and each experiment was repeated in triplicate, n=3. Statistical significance was considered at *p<0.05, **p<0.01. Overall, the results suggested neuroprotective effects of chemerin against H₂O₂ induced cell death are specific to the differentiated SHSY5Y (neuronal-like) cells. The increasing concentration of chemerin effectively improved the cell viability of neuron-like cells under H₂O₂ induced oxidative stress condition with statistically significant difference, but in undifferentiated SHSY5Y (non-neuronal) cells, chemerin failed to show effective protection towards cell survival.

3.3.5.2 Effect of leptin on differentiated and undifferentiated SHSY5Y cell viability in the presence and absence of H₂O₂ induced oxidative stress

To determine the neuroprotective effect of commercially available leptin on differentiated SHSY5Y cells (neuronal-like) and undifferentiated SHSY5Y cells (non-neuronal), three doses of leptin (50,100 and 200nM) were co-treated without and with H₂O₂ for 24 hrs (figure 3.24).

Leptin had no effect on the viability of differentiated SHSY5Y cells in comparison to the untreated SHSY5Y cells (absence of H₂O₂) (figure 3.21.A). However, H₂O₂ induced decrease in cell viability was significantly inhibited by leptin (50, 100 and 200nM) in differentiated SHSY5Y cells (leptin (50nM) + H₂O₂ = 109.6 ± 5.3 , leptin (100nM) + H₂O₂ = 106.6 ± 1.3 and leptin (200nM) + H₂O₂ = 100.3 ± 1.9) in comparison to the differentiated SHSY5Y (neuronal-like) cells with H₂O₂ treatment (figure 3.21.B), *p<0.05, **p<0.01.

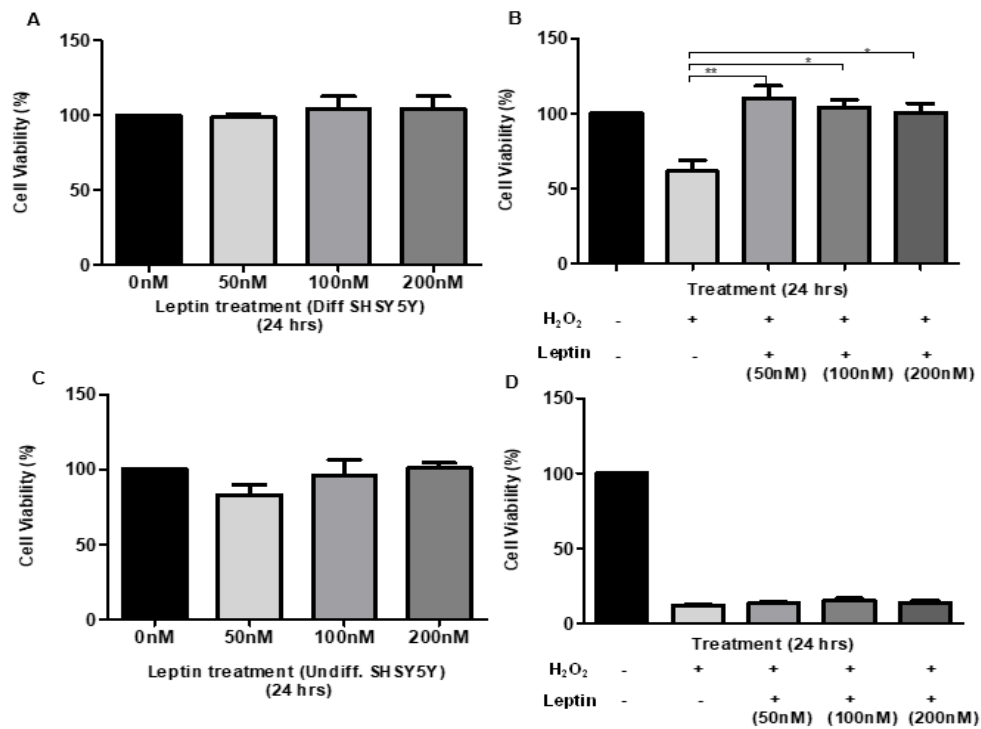


Figure 3.24. Exploring the impact of commercially available leptin on H₂O₂ induced oxidative stress in differentiated (neuronal-like) and undifferentiated (non-neuronal) SHSY5Y cells. Leptin was used with 3 doses (50,100 and 200nM) for 24hrs with and without H₂O₂. **A.** No change in the cell viability of differentiated SHSY5Y cells was recorded with 50nM,100nM and 200nM doses of chemerin without H₂O₂. **B.** H₂O₂ dose of 150μM was co-treated with leptin on differentiated SHSY5Y cells. Significantly increased cell viability was measured using 50, 100 and 200nM doses of leptin in comparison to H₂O₂ only treated differentiated SHSY5Y cells. **C.** 3 doses of leptin was used on undifferentiated SHSY5Y cells for 24 hrs incubation without H₂O₂. No significant change in undifferentiated SHSY5Y cell viability was measured using 50,100 and 200nM doses of chemerin. **D.** The H₂O₂ induced oxidative dose on undifferentiated SHSY5Y cells used was 100μM co-treated with leptin. No significant change in cell viability was measured using 50, 100 and 200nM dose in comparison to the H₂O₂ only treated undifferentiated SHSY5Y cells. The data are presented as mean ± SEM. The data was analysed using GraphPrism5, and statistical significance was considered at *p<0.05, **p<0.01. Each experiment performed was in triplicate, n=3.

Similar to differentiated SHSY5Y cells, three doses of leptin were used on undifferentiated SHSY5Y cells for 24 hrs with and without H₂O₂, as shown in figure 3.24. C and D. The results obtained demonstrated no impact of leptin doses (all 3 doses) on the undifferentiated SHSY5Y cell viability in absence as well as presence of H₂O₂ induced oxidative stress and no statistical difference was measured. Whereas the differentiated SHSY5Y (neuronal-like) cells showed neuroprotection with all doses under oxidative stress with statistical difference in comparison to only H₂O₂ treated cells. The data was analysed using GraphPad Prism 5, detailed in method section 2.3. The data are presented as mean ± SEM (% viability) and each experiment was repeated in triplicate, n=3. Statistical significance was considered at *p<0.05, **p<0.01.

3.3.5.3 Effect of resistin on differentiated and undifferentiated SHSY5Y cell viability in the presence and absence of H₂O₂ induced oxidative stress

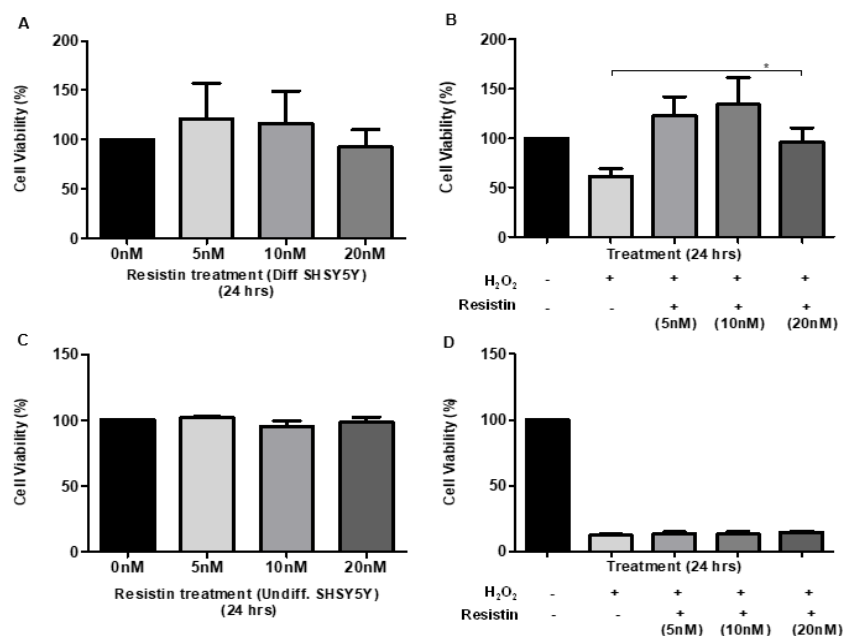


Figure 3.25. Exploring the impact of commercially available resistin on differentiated (neuronal-like) and undifferentiated (non-neuronal) SHSY5Y cells with and without H₂O₂ induced oxidative stress. 3 different doses of resistin were used i.e., 5,10 and 20nM for 24hrs. **A.** the treatment of resistin only with different doses had no significant effect on the differentiated SHSY5Y cell viability in comparison to the untreated differentiated SHSY5Y cells. **B.** resistin prevented decrease in SHSY5Y cell viability in presence of H₂O₂ co-treated with 10nM dose of resistin with statistically significant difference in comparison to H₂O₂ only treated differentiated SHSY5Y cells. **C and D.** The treatment of undifferentiated SHSY5Y cells without and with H₂O₂ (100μM), respectively in presence of resistin had no impact on the viability with either of doses used. The data are presented as mean ± SEM. The data was statistically analysed using GraphPad Prism5. Statistical significance was considered at *p<0.05, **p<0.01. Each experiment performed was in triplicate, n=3.

The neuroprotective effect of commercially available resistin was assessed by incubating dose range of 5,10 and 20nM for 24 hrs on differentiated (neuronal-like) and undifferentiated (non-neuronal) SHSY5Y cells with and without H₂O₂ induced oxidative stress (figure 3.25). Although the incubation of increasing doses of resistin (5-20nM) with differentiated SHSY5Y cells without H₂O₂ (figure 3.25.A), showed effective increase in cell viability, there was no statistically significant difference in comparison to the differentiated SHSY5Y cells with no H₂O₂ treatment.

Results obtained from the co-treatment of differentiated SHSY5Y cells (figure 3.22.B) with 150 μ M H₂O₂ + 10nM resistin showed significant increase in cell viability in comparison to H₂O₂ only treated differentiated SHSY5Y cells (resistin+ H₂O₂ =133.6 \pm 17.3). The highest rescue effect in relation to cell viability under oxidative stress was measured in 10nM dose in comparison to the neuronal-like cells with H₂O₂ only treatment.

The undifferentiated SHSY5Y cells were incubated with three different doses of resistin for 24 hrs without H₂O₂ (figure 3.22.C). Using 5,10 and 20nM doses of resistin, no significant change in cell viability ($p>0.05$) was measured in undifferentiated SHSY5Y cells with resistin treatment in comparison to the untreated cells. The results suggested that the resistin did not have any active impact on the cell proliferation without oxidative stress condition. For H₂O₂ induced oxidative stress in undifferentiated SHSY5Y cells, 100 μ M dose of H₂O₂ was used for the co-treatment with resistin (figure 3.22.D), no significant rescue effect in relation to cell viability ($p>0.05$) were measured with all three doses in comparison to the H₂O₂ only treated undifferentiated SHSY5Y cells. Overall, the neuroprotective effect of resistin on neuronal-like cells was only observed with 10nM dose of resistin under oxidative stress condition. The data was analysed using GraphPad Prism 5, detailed in method section 2.3. The data are presented as mean \pm SEM (% viability) and each experiment was repeated in triplicate, $n=3$. Statistical significance of data was considered at $*p<0.05$.

3.3.6 Understanding the effect of commercial chemerin on human skin derived fibroblast cell viability

Considering the impact of individual adipokines effect on the neuroprotection, it would be interesting to investigate the effect of adipokines on AD patient derived skin fibroblast cells as these cells possess characteristics associated with AD. For example, increased activity of bradykinin (neuropeptide mediator) signal transduction cascade leads to tau phosphorylation and significant oxidative stress in AD skin fibroblast could be predictive of AD development (Jong et al., 2003). Commercially available adipokines were used to establish their individual impact on the cell viability of human skin- derived fibroblast cells. The impact of chemerin, leptin and resistin on cell lines from AD and non-AD donors were investigated.

The concentration dose of H₂O₂ used was optimised and 1mM for 15 mins H₂O₂ incubation was used as finalised dose to induce oxidative stress in fibroblast cells. MTT, a cytotoxicity assay was performed to obtain the data (Uberti et al., 2002; Hahn et al., 2017). Very short exposure of H₂O₂ was given to the fibroblast and the optimisation was performed by referring the literature.

3.3.6.1 Optimization of H₂O₂ dose to induce oxidative stress in fibroblast cells

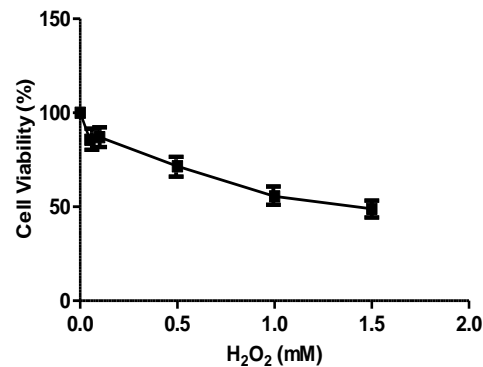


Figure 3.26. Exploring the impact of different doses of H₂O₂ for 15 mins to induce oxidative stress in fibroblast cells. Non-AD fibroblast, AG80125 cell line was used to obtain the EC₅₀ value of H₂O₂ induced oxidative stress with 15 mins incubation. The H₂O₂ doses between 0.05-1.5mM was used and showed gradual decrease in cell viability and 1mM dose was calculated as EC₅₀ for H₂O₂ doses in comparison to the untreated fibroblast cells. MTT assay was used as cytotoxic assay and data was analysed by GraphPad Prism 5. Each point of dose are presented as mean \pm SEM (n=3).

To obtain a specific H₂O₂ dose for induced oxidative stress in the fibroblast cells, optimization using different doses of H₂O₂ for 15 mins was performed (Uberti et al., 2002). The human skin derived fibroblast cell line, AG08125, from non-AD donor were used and investigated the cytotoxic effect of H₂O₂ induced oxidative stress using doses: 0.05, 0.1, 0.5, 1 and 1.5mM. As shown in figure 3.26, when 0.05mM and 0.1mM H₂O₂ doses were incubated for 15 mins, no significant change in cell viability was measured in comparison to the untreated fibroblast cells (without H₂O₂ treatment). The 0.5mM H₂O₂ dose showed decrease in cell viability in comparison to the untreated fibroblast cells. In addition, the doses using 1 and 1.5mM, H₂O₂ showed reduced cell viability. The H₂O₂ dose concentration of 1mM for 15 mins was obtained as EC₅₀ value (57.2 ± 3.01) and considered as final dose concentration for further experiments to induce oxidative stress in fibroblast cells from AD and non-AD skin donors.

Data was analysed by GraphPad Prism5 using non-linear regression for EC50. Each point of dose are presented as mean \pm SEM (% viability) (experiments performed in triplicate, n=3, detailed in section 2.3).

3.3.6.2 Comparing the effect of chemerin (10nM) on non-AD and AD donors skin derived fibroblasts under H₂O₂ induced oxidative stress

To understand the protective effect of commercially available chemerin on AD patient skin derived fibroblasts, a 10nM dose of chemerin was incubated with fibroblast cells with and without H₂O₂. The cell lines: AG08125, AG08517 and AG08509 were used as non-AD fibroblasts and for AD fibroblasts cell lines: AG07872, AG05809 and AG06869 were used. The co-treatment with chemerin and H₂O₂ caused a significant decrease in viability of fibroblast cells in AD patients (57.14 ± 0.07) in comparison to with the non-AD fibroblasts (79.46 ± 2.09) and suggested that chemerin had no protective impact on the viability of AD group.

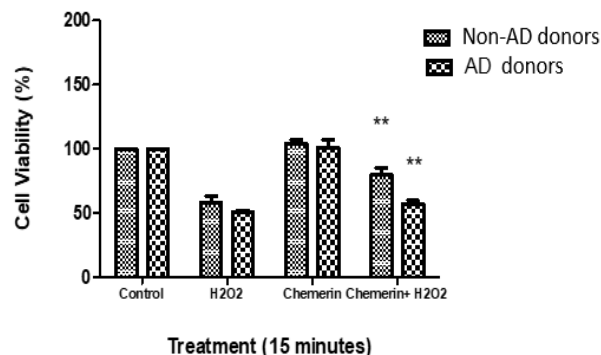


Figure 3.27. Exploring the impact of chemerin with and without H₂O₂ induced oxidative stress for 15 mins using AD patient derived and non-AD fibroblast cells. Chemerin showed protective effect in the non-AD donors in comparison to the AD patients (**p<0.01). Data was statistically analysed by GraphPad Prism5. Each experiment was performed in triplicate (n=3) and data are presented as mean \pm SEM.

The results shown in figure 3.27 confirmed that protective effect of chemerin was only present in the non-AD donors in relation to increased cell viability in comparison to the AD donors derived skin fibroblast cells under H₂O₂ induced oxidative stress. The results were statistically analysed by GraphPad-Prism5 using two-way ANOVA (section 2.3, discussed in detail). Each experiment was performed in triplicate (n=3) and data are presented as mean \pm SEM (% viability).

3.3.6.3 Comparing the effect of chemerin (20nM) on non-AD and AD patient skin derived fibroblasts under H₂O₂ induced oxidative stress

To understand the protective effect of commercially available chemerin on non-AD and AD donors skin derived fibroblasts, 20nM dose of chemerin was used and incubated with fibroblast cells with and without H₂O₂. The cell lines: AG08125, AG08517 and AG08509 were used as non-AD control fibroblast and for AD patients' fibroblasts cell lines: AG07872, AG05809 and AG6869 were used.

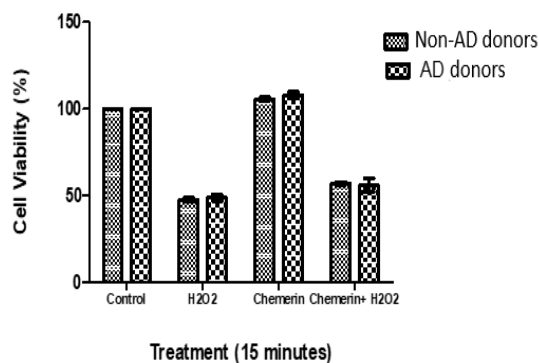


Figure 3.28. Exploring the impact of chemerin with and without H₂O₂ induced oxidative stress for 15 mins using AD patient derived and non-AD fibroblast cells. Chemerin showed no protective effect in the non-AD patients in comparison to the AD patient ($p > 0.05$) with and without H₂O₂ induced oxidative stress. Data are presented as mean \pm SEM and was statistically analysed by GraphPad-Prism5. Each experiment was performed in triplicate ($n=3$) and data are presented as mean \pm SEM.

The results shown in figure 3.28 demonstrated that the cell viability of AD and non-AD patients are similar and there was no statistically significant difference in cell viability of AD donors fibroblasts in comparison to the non-AD donor cells when treated with chemerin in the presence and absence of H₂O₂ induced oxidative stress ($p > 0.05$). The results were statistically analysed using GraphPad-Prism5 using two-way ANOVA (discussed in detail in section 2.3). Each experiment was performed in triplicate ($n=3$) and data are presented as mean \pm SEM (% viability). The results suggested that chemerin showed protective effect under H₂O₂ oxidative stress conditions using slightly higher dose of 20nM whereas no protective effect was observed in 10nM of chemerin, as shown in figure 3.26.

Chapter 4. DISCUSSION

Alzheimer's disease is the most common form of dementia in elderly people and its prevalence will increase to 152 million by 2050 (WHO, 2017). Its pathogenesis is underpinned by a raft of complex molecular mechanisms resulting in the accumulative neuronal damage, synaptic dysfunctional and subsequent cell death (Cohen et al., 2016). At present there is no cure for this debilitating condition and therefore understanding the contributing factors to disease progression is important. Midlife obesity is known to be a risk factor for the development of AD (Peditizi et al., 2016). The prevalence of obesity is increasing globally, and it is a significant burden to healthcare providers. As we are faced with an ever-increasing ageing population who are more likely to be obese, it is more important than ever to understand how obesity contributes do the progression of AD. Only in understanding the interface of these two debilitating diseases the time bomb can be disarmed facing society.

Adipose tissues/adipocytes are vital for the regulation of various physiobiological functions, primarily lipid and glucose homeostasis. The white adipose tissues are essentially involved with the energy storage and distribution whereas brown adipose tissues are responsible for thermogenesis. Apart from these roles the adipocytes secrete various adipokines and hormones such as leptin, chemerin, resistin, adiponectin, fibroblast growth factors 21 and others (Cuevas Ramos et al., 2009; Farooqi & O' Rahilly, 2014; Chait et al., 2020).

Obesity is associated with the accumulation of white adipose tissue and is accompanied by a change in the circulating levels of several adipokines which have the capacity to influence a raft of physiological processes including satiety, blood pressure and mood. Furthermore, adipocyte dysfunction link to obesity has been shown to alter brain metabolism, induced neuroinflammation, neuronal dysfunction, brain atrophy, impaired mood and cognitive decline (Luppino et al., 2010; Chellappa et al., 2019; Uddin et al., 2021) suggesting that there is a close relationship between the brain and the negative effects of obesity. It is thought that perhaps adipokines are key molecules in mediating this cross talk.

A cross sectional study has shown that hyper adiponectin and leptin secretion can modulate the early rheumatoid arthritis (eRA) disease development and can be considered as diagnostic measure (Chaparro-Sanabria et al., 2019). Another study on mice (fed with controlled diet) has shown that after 60 days of stroke, adipokine levels were disturbed significantly. In addition, resistin and adiponectin levels were highly increased whereas leptin levels were found to be unaffected (Haley et al., 2020). A similar study using diet induced obesity in animal models showed that harmful impact of obesity on stroke depends on the prolongation of ischemic condition and remodelling of inflammatory factors due to obesity which could impact negatively on stroke (Maysami et al., 2015). Interestingly, a recent patient study has shown that the maternal obesity can potentially increase the risk of neuropsychiatric disorders, development of cognitive impairment and can negatively influence on the fetal brain development (Letra & Santana, 2017).

Finally, oxidative stress is common to both obesity and AD. In obesity, it is thought that adipocytes become enlarged to an extent that oxygen cannot diffuse efficiently across the adipocyte resulting in oxidative stress, dysregulated adipokine profiles and low-grade chronic inflammation (Parimisetty et al., 2016). The changes in adipokines and immune response, alongside lipid and glucose handling are all thought to be contributory to many diseases. Interestingly, oxidative stress has also been linked to pathogenesis of AD, evident by a study that confirmed the presence of protein, lipid, and DNA oxidation in the brain tissues of AD patients due to oxidative stress (Gella & Durany, 2009). Studies related to conserved kinase consensus sequences confirmed that the protein hyperphosphorylation in neurofibrillary tangles and senile plaques due to the cellular oxidative damage in the AD pathogenesis (Perry et al., 2002). During the AD progression, various sources were considered to be the contributing factors in inducing neuronal oxidative damage leading to neuronal death such as iron induced lipid peroxidation, activated microglia forming peroxy-nitrite, ROS generated by A β itself and advanced glycation of redox end products resulting in the dysfunctional mitochondria which is leading source of ROS release in AD (Smith et al., 2000; Youssef et al., 2018; Ton et al., 2020). Therefore, understanding how adipocytes have the capacity to influence neuronal functioning under oxidative stress in relation to AD forms the basis of this study.

We hypothesized that adipocyte-derived adipokines and specific named adipokines i.e., chemerin, leptin and resistin possess the ability to restore the neuronal proliferation under oxidative stress.

In order for us to address this hypothesis, we:

1. Generated and validated cell culture models of AD and obesity using SHSY5Y cells and 3T3-L1 cells, respectively.
2. Optimised the treatment of our cell models with hydrogen peroxide to recreate the oxidative stress environment associated with AD and obesity.
3. Used conditioned media technique to evaluate the role of an adipokine rich environment on cultured neuronal cell viability in response to oxidative stress.
4. Investigated the effect of specific individual adipokines (chemerin, leptin and resistin) on cultured neuronal cells.
5. Explored the role of chemerin using skin-derived fibroblast of AD and non-AD human patients.

The results described in this thesis demonstrated that the differentiation of SHSY5Y and 3T3-L1 cells was successfully achieved by using specific chemical inducers and confirmed the maturation by ICC and Oil Red-O staining, respectively. In addition, optimal H₂O₂ dose in the SHSY5Y and fibroblast cells was attained by dose-dependent response cell viability and the EC₅₀ dose was obtained to induce oxidative stress. Moreover, in the presence of adipokine rich CM from adipocyte-like demonstrated rescue effect on the neuronal cell viability under oxidative stress. Furthermore, the incubation of chemerin, leptin and resistin with the SHSY5Y and fibroblast cells showed protective effect under oxidative stress. These key findings will be explored in the following sections but first, the selected cell culture models used in this study will be considered.

4.1. Consideration of the cellular models used in this study

In the present study, 3T3-L1, SHSY5Y and skin derived fibroblast cells were used as cellular models. To make 3T3-L1 and SHSY5Y cell lines more relevant as adipocytes and neuronal cells, differentiation of 3T3-L1 and SHSY5Y cells was performed.

There are a number of different pre-adipocyte cells which could have been chosen for this study. The most common of which come from rats and mice, although other animal sources are available and all these models exist as pre-adipocytes which can be differentiated into mature adipocytes once they are provided with correct chemical signals (Armani et al., 2010; Lee et al., 2019). Despite the advantages of using cells from different animal sources there are some limitations in using cellular models such as 3T3F442A cells, which are more commonly utilized for the estimation of potential effect of a compound of interest in an adipogenic study (Torabi et al., 2016). In addition, the TA1 cell line is more useful for adipocytes lineage study i.e., to investigate the expression of pre-existing and new genes during differentiation process in comparison to any other cell lines, making this cell line more suitable for research in identification of adipogenic markers, effective agents screening and others (Vohra et al., 2020). Our study used widely available 3T3-L1 cells which are derived from Murine Swiss 3T3-L1 cells from embryos and are relatively easy and convenient to use compared with freshly isolated cells. They can withstand a high number of passages and they produce a homogeneous response in experiments which makes them particularly suitable to address our hypothesis (Ruiz-Ojeda et al., 2016) to understand the impact of adipocytes secreted adipokines on the neuronal cell proliferation under oxidative stress. In literature it has been shown that the differentiation of 3T3-L1 cells is important to understand the pathology of molecular mechanism in obesity (Pacifci et al., 2020). The 3T3-L1 cells were differentiated into adipocytes-like by following chemically induced protocol with persistent insulin incubation for 3 weeks. During the differentiation progression from pre-adipocytes to mature adipocytes, the majority of genes are up or down regulated at transcriptional level in the initial 4 days, for example transient receptor potential, or TRP (*trpv1* and *trpv3* mRNA levels significantly decreases and *trpv2* and *trpv4* mRNA levels significantly increases) and signalling pathway alteration, release of lipids and proliferation occurs in later stage of differentiation (Sun et al., 2020).

In line with many studies, our 3T3-L1 cells differentiated from day1 and had achieved full differentiation by day21. Because the differentiation of 3T3-L1 cells into adipocyte-like cells is based on the increased synthesis and accumulation of triglycerides (Rizzatti et al., 2013), we used Oil Red-O to confirm that the cells presented were indeed adipocyte-like. Oil Red-O staining has been used by many studies (Blanco et al., 2020) and is a dye that strongly stains the lipids helping to identify adipocyte-like (Kraus et al., 2016). On day21, differentiated cells were used for further experiments. Recent studies have confirmed that the use of 3T3-L1 cells for obesity related studies is useful. A study on adipogenesis used 3T3-L1 cells to understand the factors affecting insulin signalling pathway as well as adipokine secretion and demonstrated that the site-specific methylation of DNA impairs the insulin signalling pathway (Malgorzata et al., 2019). Obesity is chronic disease, associated with multifactorial risk factors which contributes to the increase in body mass and excess accumulation of body fat (Pollin et al., 2008; Zhang & Wang, 2012). Research studies have confirmed that obesity, adipose dysfunction, and oxidative stress are closely related and impairment in adipogenesis or increased levels of reactive oxygen species could be the major cause of obesity (Manna & Jain, 2015). In this study we have used the 3T3-L1 cells which are commercially available in pre-adipocytes state and can be differentiated into mature adipocytes by chemical induction of dexamethasone, IBMX and insulin to attain the adipocyte-like cellular model.

Similar study for 3T3-L1 cell differentiation used rosiglitazone as an additional inducing factor to achieve complete differentiation within 10-12 days (Zebisch et al., 2012). The differentiated 3T3-L1 cells were appeared as matured and differentiated fat cells with higher lipid (triglycerides) presence confirmed by Oil Red-O staining. The Oil Red-O staining is widely accepted to confirm successful 3T3-L1 cells differentiation (Uto-Kondo et al., 2008; Kong et al., 2017). For the investigation of AD pathology in-vivo models are being used in research studies with limitations of success rate in understanding of progression of AD due to the only availability of brain tissue as post-mortem extraction at the later stages of AD (Arber et al., 2017). Therefore, the in-vitro cellular models are becoming increasingly popular for better understanding of translational and detailed mechanism of AD pathology. Various cellular models based on different source of origin are being used such as human brain microvascular endothelial cells (HBMEC), mouse brain endothelial cells (MBEC), induced pluripotent stem cells (iPSC),

pheochromocytoma cell line (PC-12) and others (Wang et al., 2002; Dubey et al., 2019; Penney et al., 2020).

In our study, SHSY5Y cells were used (human neuroblastoma), the differentiation of SHSY5Y cells was carried out to obtain neuronal-like cells. Studies have confirmed that it is vital to differentiate the cells because the mature neuronal-like cells show adrenergic, cholinergic, or dopaminergic characteristics which are absent in undifferentiated cells (Xie et al., 2010). During differentiation, retinoic acid induced reactive species play vital role in regulation of mitochondrial NADH oxidation and expression of various markers which is important for the full differentiation of neuronal cells (Kunzler et al., 2017). In addition, a knockout study has shown that decreased level of Dicer (a ribonuclease crucial for microRNA biogenesis) and increased expression of p53 is important for the regulation of proteins during differentiation progression (Jauhari et al., 2017). In our lab by following 10-and 21-day protocol, the undifferentiated SHSY5Y (continuously dividing, small projections with no networking characteristics) cells were differentiated into mature SHSY5Y cells (non-dividing cells, with extended axonal projections with visible interconnections characteristics). The differentiation was confirmed by ICC to detect the specific neuronal markers i.e., NF, NSE and MAP2.

Alzheimer's disease is a progressive neurodegenerative disorder and the most common cause of dementia affecting majorly the elderly people (Weller et al., 2018). Two hallmarks of AD are A β accumulation and neurofibrillary tangles (Crews & Masliah, 2010). In various neurodegenerative disorders SHSY5Y cells have been used to understand the underlying molecular mechanisms. Differentiated SHSY5Y cells, in the presence of various inducing factors such as BDNF, and RA exhibit neuronal-like characteristics due to which this cell line is ideal for this study (Arosio et al., 2021; de Medeiros, 2019). Various methods are used to distinguish the undifferentiated and differentiated SHSY5Y cells such as electrophysiology and measuring the elasticity by atomic force microscopy to identify the presence of K⁺ channels in undifferentiated and Na⁺ channels in differentiated SHSY5Y cells (Şahin et al., 2021). Studies have confirmed that the oxidative stress is considered as major risk factor for the developing neurodegenerative disorders including AD due to increased level of free radicals released (Chen et al., 2018). In our study, SHSY5Y cells were cultured and differentiated into neuronal-like cells using all-trans RA.

These neuronal-like cells were used as cellular model for experimental use to understand the neuroprotective effect of adipocytes secreted adipokines and other growth factors under oxidative stress condition. The differentiation of SHSY5Y cells was confirmed by using ICC by using neurofilament, neuron specific enolase and microtubule associated protein. The differentiated cells showed presence of above-mentioned markers after following 10- and 21-day differentiation protocol in comparison to the undifferentiated SHSY5Y cells (non-neuronal) and IgG Ab incubated with differentiated cells (negative controls).

AD patient derived fibroblast cells were used as relevant model for understanding the pathology of AD. Studies have shown that the skin derived fibroblast cells from non-AD and AD donors can potentially be induced to develop into an induced neuronal-like cell line which can give very useful cell therapeutics in relation to neuronal diseases (Qiang et al., 2011). In very early studies it has been established that the dysregulation of signal transduction pathway and protein kinase C isoform availability was measured in the AD patient's neuronal as well as fibroblast cells, which makes these fibroblast cells (derived from AD donors) very useful model of study. Interestingly, bradykinin (BK) a neuropeptide mediated by G protein coupled receptors was found to be expressed in brain under induced conditions that contributes towards the AD such as stroke or severe head injury. The modulation of these receptors demonstrated that A β - rich environment in the skin derived fibroblast cell is possibly responsible for the dysregulated expression of BK receptors via disrupted signal transduction mechanism and may lead to the characteristic Alzheimer's plaque lesion in the brain (Jong et al., 2002; Jong et al., 2003). Traditionally, AD has been considered as a CNS related disorder, but new investigations have demonstrated that AD is a systemic disorder, multiple interconnected pathways extend from the AD-affected brain whereby other organs or peripheral tissues, demonstrate similar characteristics to the AD affected brain, such as defect in calcium homeostasis, membrane trafficking or glucose oxidation. A study using AD patient's skin derived fibroblast cells recapitulated similar dysfunctional mitochondrial biogenesis and morphology as in AD brain (Pérez et al., 2017; Trushina, 2019).

With this in mind, it is proposed that peripheral tissues and the cells making these tissues, such as skin fibroblasts, could be considered as a reliable model of the dysregulated neurological

diagnosis (Ambrosi et al., 2014). An in-vitro study using embryonic fibroblast and endometrial mesenchymal stem cells has shown that the high doses of H₂O₂ induced oxidative stress alters the cellular responses leading to cell death or early senescence (Kornienko et al., 2019). In our study, we used non-AD and AD donors skin fibroblast cells. All the cell lines used were obtained from unrelated individuals between age range 50-75 years and the age was matched as close as possible between the non-AD and AD donors to maintain the comparative study more reliable. In an animal study, used AG07872 and AG08509 cell lines (same as our cell lines) alongside the mutation of presenilin (PSEN) in the *C.elegans* to understand the mitochondrial dysfunction mechanism mediated by Ca⁺ signalling, confirms that the mitochondrial defect increases the release of reactive superoxide species which leads to defective metabolic activity causing neurodegenerative diseases (Sarasija et al., 2018). Skin derived fibroblasts were used for the preliminary neurodegeneration studies as they are considered as good source of understanding of AD patients due to the fact that studies have shown that similar effects are shown on the ectoderm and brain cells in AD (Forster et al., 2016). A similar study has used the for the mitochondrial dysfunction and oxidative stress, the results of this study showed mitophagy dysfunction due to impaired autophagy process (Martín-Maestro et al., 2017). In this study, human skin derived fibroblast cells were used from non-AD and AD donors to compare the protective effect of chemerin on the cell survival in with and without H₂O₂ induced oxidative stress. The results obtained from the experimental study will be explored later in this section. A recent study on correlation of aldehyde dehydrogenase 2 (ALDH2) as AD risk factor used human skin derived fibroblast as useful tool to understand the expression of ALDH2 in AG05809 (AD patient derived) showed oxidative stress lead mitochondrial dysfunction and aldehyde load when exposed to ethanol (Joshi et al., 2019).

4.2. Consideration of different concentrations of H₂O₂ to induce oxidative stress

The induction of oxidative stress in cellular model can be achieved by using various agents such as nitric oxide, nonsteroidal inflammatory drugs, n-3-polyunsaturated fatty acids and others (Rigas et al., 2008). H₂O₂ is efficient and permeable to membrane which means the intracellular H₂O₂ levels can induce functional alteration in adjacent cells (Konyalioglu et al., 2013).

Therefore, H₂O₂ was used as oxidising agent to induce oxidative stress in growing cultures of 3T3-L1 cells, SHSY5Y cells and fibroblast cells to investigate the neuroprotective effect of adipokines or growth factors in adipocytes derived conditioned media and commercially available chemerin, leptin and resistin under H₂O₂ induced oxidative stress and the rescue effect of chemerin on skin derived non-AD and AD donor's fibroblast cells under H₂O₂ induced oxidative stress. The results obtained will be discussed in the following section of this chapter. The neuronal-like (differentiated SHSY5Y) cells exhibit cholinergic, adrenergic, and dopaminergic characteristics and these neurotransmitter factors were observed to be disturbed or modulated in AD research in relation to A β modulation by incubating SHSY5Y cells with H₂O₂ confirming the influence of H₂O₂ on cholinergic, acetylcholinesterase and dopamine transmission (Nagpure & Bian, 2014; de Medeiros et al., 2019; Garcimartín et al., 2017).

Numerous research studies have confirmed the relation of oxidative stress as major risk factor in various diseases including age-related neurodegeneration including AD, CVD, obesity, cancer and others (Donato et al., 2007; Arandis et al., 2018; Liguori et al., 2018;). Different research studies use different oxidising agents to induce oxidative stress depending on their availability and types of study model such nitric oxide, H₂O₂, bacterial endotoxins hypoxia condition and others (Ridnour et al., 2005; Safaeian et al., 2020; Spitzer et al., 2020). We used H₂O₂ to induce oxidative stress with different concentrations and attained the optimal H₂O₂ dose, after optimization was performed. A similar study was carried out, using H₂O₂ induced oxidative stress to induce neuronal apoptosis in differentiated and undifferentiated PC-12 and SHSY5Y cells in a concentration and time dependent manner, the results showed that downregulation of the mitogen activated kinases (MAPK) inhibitors and activation of serine/threonine phosphatases or anti-oxidants possess the potential to prevent the neurodegenerative disorders (Chen et al., 2009). In another study, where 100 μ M of H₂O₂ was used for 24 hrs to induce oxidative stress in differentiated SHSY5Y cells demonstrated protective effect of insulin on neuronal viability in comparison to the lactate dehydrogenase, ROS, nitric oxide, and calcium ions (Ramalingam et al., 2014). Our study used different concentrations of H₂O₂ ranging between 50-500 μ M for 12 and 24 hrs. The dose dependent assay for H₂O₂ dose optimisation showed that EC₅₀ (H₂O₂) in non-neuronal cells was 100 μ M of H₂O₂ and in neuronal-like cells was 150 μ M of H₂O₂ for 24hrs.

However, to induce the oxidative stress in the 3T3-L1 cells, 150 μ M of H₂O₂ was used so that the level of oxidation induced in the neuronal-like and adipocyte-like remained with same concentration, this could be one of the factors that can be considered in the future work where the EC₅₀ value of the adipocytes should be optimised to confirm the optimal dose of H₂O₂ required to induce oxidative stress in relation to cell viability reduction. A cellular model study using differentiated 3T3-L1 cells has shown that using 100 μ M of H₂O₂ for 2 hrs with every passage for period of 14 days in serum free medium to induce oxidative stress resulted in cell senescence in comparison to the control evidenced by SA- β -gal staining (Monickaraj et al., 2013). Interestingly, a study has been reported which demonstrates that the resistance against oxidative stress was observed with the progression of 3T3-L1 cells differentiation from pre-adipocytes to adipocytes (Muraoka et al., 2017).

4.3. Considering use of conditioned media technique to evaluate the role of an adipokine rich environment on cultured neuronal cell viability under H₂O₂ induced oxidative stress

Studies have shown that, the conditioned media technique is very useful in-vitro method to understand underlying effect on continued cultured cells, when incubated with multiple factors containing media (from another cell culture) as conditioned media and investigate the altered cellular and molecular mechanisms of growing cells (Sagaradze et al., 2019). Specifically, in relation to our work, the CM of differentiated 3T3-L1 cells has been shown to contain adipokines as well as various other growth factors and could induce remodelling of extracellular matrix that regulates the growth (Wang et al., 2004). Due to the complexities around the co-culture of two cell lines which require differentiation to become functional mature cells (Pawitan et al., 2014). This technique was chosen to allow us to investigate the impact of adipokine containing CM from differentiated 3T3-L1 cells (adipocyte-like) on differentiated SHSY5Y (neuronal-like) and undifferentiated SHSY5Y (non-neuronal) cells under oxidative stress condition. Different manoeuvres were carried out using non-neuronal and neuronal-like cells by co-incubating complete growing culture media replaced with CM, replacing the growing culture media with pre-stressed CM from adipocyte-like and replacing half of the growing culture media with the pre-stressed CM, which will be discussed in the following sections.

4.3.1. Does conditioned media from adipocyte-like possess neuroprotective effects against H₂O₂ induced oxidative stress in neuronal -like cells?

The CM technique is considered as very useful in-vitro study in understanding the interaction and cellular behaviour of two different cell lines in very closed environment. An investigative study on wound healing used adipocytes and pre-adipocytes CM to understand the impact on fibroblast conversion into myofibroblast cells, interestingly, the results showed that both adipocyte and pre-adipocytes have proliferative effect on the fibroblast cells but only with adipocytes derived CM possess the ability to induce the conversion of fibroblast to the myofibroblast cells mediated by TGF- β (El-Hattab et al., 2020). This is suggestive that CM from adipocytes does have positive impact on the regulation of TGF- β , which is multifunctional cytokines. In our experimental study, we used CM from adipocyte-like and pre-adipocytes on the neuronal-like and non-neuronal cells under oxidative stress condition. Our results had shown that in H₂O₂ only treatment, reduction in non-neuronal cell viability was measured. Although we have not confirmed this, but it was likely that was occurred due to oxidative stress as evidenced in literature where H₂O₂ was used as inducer of oxidative stress in SHSY5Y cells and the molecular and oxidative stress markers identification were confirmed that ensures the H₂O₂ induced oxidative stress (Alvariño et al., 2017; El-Hattab et al., 2020).

Co-incubation of CM from adipocyte-like and pre-adipocytes with the non-neuronal cells under oxidative stress showed an overall reduced cell viability in comparison to without H₂O₂ treated cells, indicated that the factors secreted from these cells were unable to protect or rescue from the effect of oxidative stress. Other possibility was may be the non-neuronal cells do not have or expressed the necessary receptors for the proliferation and resulted in cell death due to an immediate and complete change in the culture environment. However, it was interesting to note that the adipocyte-like derived CM was able to rescue at least 50% cell population without H₂O₂ when compared to H₂O₂ only treated cells. Whereas, when we investigated the impact of CM in neuronal-like cells, the results were found to be very resistant and proliferative outcome after co-incubation with adipocyte-like derived CM under oxidative stress. The viability was almost fully restored when neuronal-like cells were co-incubated with the CM from adipocytes with H₂O₂ in comparison to CM from adipocytes without H₂O₂ treated cells.

A comparative study has shown that the neuronal-like cells express the Unc5D, neuropilin-1 in comparison to the non-neuronal cells, which is a multifunctional transmembrane protein with many ligands and play vital role in the cell survival and neural innervation and vascularisation (Gu et al., 2003). The CM from pre-adipocytes incubated with neuronal-like cells did not show protective effect under oxidative stress condition when compared with only H₂O₂ treated cells and indicated that the CM from pre-adipocytes cells do not contain essential factors required by the neuronal-like cells to proliferate or the neuronal-like cells were unable to express required receptors for the factors in the CM of pre-adipocytes that could have rescued the cells under oxidative stress.

As a limitation, both cell lines (3T3-L1 and SHSY5Y cells) were from different sources i.e., murine, and human due to which maybe it is possible that if the cell lines from similar source were used i.e., human-human, or murine-murine, the cell viability assay might had shown different results under oxidative stress. Also, only one incubation time was used to understand the cellular behaviour. In future, for further and more evident understanding of the neuronal-like cells rescuing effect from CM of adipocytes different time of incubation should be performed. In addition, expression of adipokine receptors could be explored to understand the responsiveness of a particular adipokine under oxidative stress. Studies have shown that the expression of adipokine receptor changes during the neuronal differentiation, for instance, SHSY5Y cells expresses functional leptin and insulin receptors upon differentiation, which could be further explored to investigate leptin and insulin resistance at neuronal level (Benomar et al., 2005).

Work from our peer group identified elevated adiponectin within CM extracted from adipocyte-like cells using an adipokine profile assay, it is possible that adiponectin mediated the neuroprotective effect, as discussed above. A previous study has shown that adiponectin is protective against oxidative stress induced cytotoxicity in amyloid beta neurotoxicity using the same SHSY5Y model (Chan et al., 2012). Furthermore, a study using the secreted CM of cultured adipose tissue from lean and obese patients, showed neuroprotective effects only in CM obtained from the lean patients. This suggests that obesity-related dysregulation of growth factor or adipokine expression may be linked with loss of neuroprotective capabilities (Wan et al., 2015).

4.3.2. What is the effect of conditioned media from H₂O₂ stressed-adipocyte-like on the viability of neuronal-like cells under oxidative stress?

The treatment with stressed conditioned media has been used in other neurodegenerative studies which is helpful to determine the rescue effect of a drug against the pathological effect of causative agent (Pokrishevsky et al., 2016). One of the hallmarks of obesity is systemic oxidative stress due to increased free radical and hydrogen peroxide (Bausenwein et al., 2010). In section 4.3.1, we discussed the results when neuronal-like cells were stressed with H₂O₂ to imitate the AD-like condition, whereas, in this section both obesity-like and AD-like conditions were mimicked by H₂O₂ induced oxidative stress in adipocyte-like (incubated or stressed with H₂O₂ for 24 hrs before the experiment) and in the neuronal-like cell.

Our data demonstrated that no neuroprotective effect was measured in neuronal-like and non-neuronal cells in stressed CM with H₂O₂, this observation strongly suggested that the CM from adipocyte-like did not contain vital growth factors or adipokines that holds synergic effect on neuronal cell viability under oxidative stress (Arnoldussen et al., 2014). It was perhaps unsurprising that there was no neuroprotection under these conditions; oxidative stress has been shown to change the profile of adipokines secreted by cultured adipocyte-like such that the intracellular signalling is altered which leads to the metabolic dysregulation related pathogenesis. Another impact of adipokines secretion disruption is gradual development of insulin resistance and higher level of ROS production due to mitochondrial dysfunction (Maslov et al., 2019). Perhaps what startled was that the CM from stressed adipocyte-like with and without H₂O₂ had no further increase on the neuronal-like viability; if midlife obesity is a risk factor for AD, it may be intuitive to think that this was due to dysregulated adipokines impacting neuronal survival. However, as our models is a homogeneous culture of adipocyte-like, we are not truly reflecting the complexities and the heterogeneity of adipose tissue in-situ, in that there are no changes to immune populations or sympathetic nerve activity which could be linked pathogenesis of AD (Parimisetty et al., 2016; Zhou et al., 2021). There are some recent studies which suggests that oxidative stress may elicit neuroprotective effects; one study evaluated the therapeutic potential of human adipocyte derived mesenchymal cell (hASCs) preconditioned with low doses of H₂O₂ to overcome the deleterious effects of oxidative stress in an in-vitro model of oligodendrocyte-

like cells (HOGd) and found reparative effects associated with the co-culture (Garrido-Pascual et al., 2020). Whilst our experiments did not show any restorative effects, our models are distinctly different ranging from progenitor-like nature of the cells used and the low level of H₂O₂ that the cells were exposed to. Interestingly, non-neuronal cells were able to restore at least half of the viability (and maximum in comparison to all other conditions) in presence of pre-adipocytes derived CM with and without H₂O₂. The minor rescued effect by the pre-adipocytes towards the non-neuronal cells (which is neuroblastoma or cancerous in nature) suggested that maybe the pre-adipocytes secreted factors are beneficial for the cancerous like cells instead of neuronal-like cells, this intention is supported by a research study where it has been confirmed that the hASCs secretome possess the ability to promote the differentiation of neuroblastoma cells mediated by AMPK pathway activation. In addition, another study has confirmed that the CM from the hASCs can protect the neuroblastoma cells against the arsenic toxicity and oxidative stress induced by arsenic toxicity (Tan et al., 2011; Choi et al., 2015; Curtis et al., 2018). The reduction in cell viability under oxidative stress indicated that the CM from adipocyte-like do not possess the ability to support non- neuronal cell proliferation , especially the stressed CM from adipocyte-like, although the CM from pre-adipocytes showed some protective effect under H₂O₂ induced oxidative stress suggested that maybe both immature cell lines (non-neuronal and pre-adipocytes) shared some common growth factors which had synergic effect on the cell survival in comparison to the only H₂O₂ treated cell viability.

We limited this study to understand the behaviour of adipocyte-like under oxidative stress and did not pre-stressed the pre-adipocytes, however, what could be interesting is to assess whether pre- adipocytes exposed to low H₂O₂ have the potential to be protective and furthermore why. Taken together, our findings suggested that possibly stressed CM has a fluctuation in the accessibility of certain growth factors/adipokines due to which minor but not effective neuroprotection effect from stressed CM was observed in the neuronal-like cells under with and without H₂O₂ induced oxidative stress. To understand, if the reduction in cell viability was exclusively due to the complete replacement of growing culture media from SHSY5Y cells with CM from 3T3-L1 cells or not, the half media change technique was explored and only half volume of growing culture media from SHSY5Y cells was replaced with CM from 3T3-L1 cells.

4.3.3 Do adipokines in half condition media change from adipocyte-like possess neuroprotective effect in co-treatment with neuronal-like cells under oxidative stress?

The co-culturing and 1:1 ratio mixing of culture media is becoming increasingly popular among research groups and especially in neurobiological studies which helps in the reshuffling of different ingredients without changing the basic components (Jordan et al., 2013; Ray et al., 2014) as well as obesity-related research designed to understand the underlying molecular mechanisms underpinning cell viability, whilst excluding cell death which may have resulted from the complete change of growing culture condition (Bechor et al., 2017). Experiments in which half of the media volume was replaced were performed.

Our results were such that non-neuronal cells showed an increase in viability when half of the growth media was replaced with that CM from adipocyte-like, which had not been observed previously. Perhaps adipokines in CM could be supporting increased proliferation of non-neuronal cells, an observation seen in other research where it has been confirmed that the adipocytes could promote proliferation and migration of cancerous cells (Ko et al., 2019), this may be supported by the observation that there was little impact of pre-adipocyte CM on the non-neuronal cell viability.

Whereas non-neuronal cells co-incubated with stressed CM from adipocyte-like did not showed neuroprotective effect under oxidative stress condition after half media change, which further affirmed the above stated study and probably the pre-stressed condition affected the release of some essential growth factors or adipokines into the CM which was further disturbed by H₂O₂ induced oxidative stress. Why this was not seen in the full media replacement is uncertain. Perhaps most striking was, the co-incubation of CM from pre-adipocytes on non-neuronal cells produced contrasting results to those observed in full CM change experiments and cell viability was found to be increased, perhaps the presence of key growth factors in the remaining SHSY5Y media promoted the cell cycle progression, instead of directing cells down a cell death pathway. For example, adiponectin itself can behave as an anti-proliferative signal in some cells (Alanteet et al., 2021).

Furthermore, metformin, which can act via same AMPK pathway as adiponectin, has been shown to promote neuronal differentiation via ROS (Binlath et al., 2019). This raises the question, could the combination of conditions here be driving our non-neuronal cells down a differentiation pathway, even though the exposure is relatively brief? Also, how the non-neuronal cells responded to H₂O₂ treatment with half media change at molecular level is not clear.

No neuroprotection and decrease in cell viability was measured when neuronal-like cells in stressed CM from adipocyte-like with H₂O₂ induced oxidative stress were compared to CM from adipocyte-like and pre-adipocytes with H₂O₂, may be an increased level of released reactive free radicals in the incubated media caused the neurotoxicity, which was supported by a peer group research study confirming neurotoxic effects of an increased free radicals due to oxidative stress (Ferraro et al., 2020). Similarly, no neuroprotection with decreased neuronal-like viability was measured when co-incubated with stressed CM from adipocytes without H₂O₂ in comparison to CM from the adipocytes and pre-adipocytes without H₂O₂, indicated that maybe with pre-oxidised CM and continuous growth media mixing (because of half media change) had made the neuronal-like cells to shift the transcription of existing neuronal growth promoting factors to the required neuronal survival factors due to change in environment or may be pre-oxidised CM had inhibited some receptors essential for the neuronal proliferation, which was supported by a research. It has been discussed that due to oxidative stress the antioxidant defences mechanism gets disrupted and various proteins and lipids undergo modifications responsible for the cell death (Shi et al., 2007).

It was observed that this experimental study was limited to the positive or negative impact of stressed CM from adipocyte-like on the neuronal-like and non-neuronal cells (mimicking the obesity-like and AD-like models) after half media change, further investigations on this baseline experiment could potentially reveal the down regulating factors involved during the hyper oxidative stress environment by using adipokine antagonists or performing the RNA based PCR for the expression of adipokine or growth related factors such as chemerin, resistin or leptin receptors, which will be explored in detail in later section in relation to neuronal cell viability under oxidative stress.

4.4 Do commercial adipokines have neuroprotective potential under oxidative stress?

Research studies have shown that the circulating adipokines secreted from adipocytes vary in obesity which was supported by a clinical study where non-obese, type-2 diabetes male- patients were examined and found that the positive co-relation between circulating adipokines (adiponectin and chemerin) secretions vary due to glucose tolerance (or insulin sensitivity) without any change in the size of adipocytes (Supriya et al., 2018; Andersson et al., 2016). In an in-vitro study using epithelial cells of mammary gland, chemerin was also found to have positive impact on the autophagy and apoptosis by regulation of various physiological and pathological processes such as immune response and lipid metabolism (Hu et al., 2019). Leptin is one of most studied adipokines and directly proportional to chemerin circulating levels (Coimbra et al., 2014), although its mechanisms are complicated and information regarding leptin resistance is still limited, especially its inability to cross blood brain barrier to reach hypothalamus to exert anorexigenic effect in obesity (Izquierdo et al., 2019). Another adipokine, resistin, which is considered as adipose specific newly discovered hormone was measured to have positive correlation with insulin resistance leading to higher circulating levels in the type-2 diabetes and obese patients (Su et al., 2019). The accurate expression and site of secretion of resistin is still unclear as studies have shown its secretion by the blood cells especially monocytes which supports the fact that resistin is involved in metabolic and inflammatory diseases (Kumar et al., 2019). In the previous sections so far, we discussed the role of adipocytes secreted adipokines, as strongly supported in literature, on the neuronal-like and non-neuronal cells under oxidative stress. To investigate the adipokines impact further and specifically, chemerin, resistin and leptin were co-incubated with neuronal-like and non-neuronal cells under H₂O₂ induced oxidative stress and will be discussed in this section. Our data suggested that the presence of all 3 adipokines i.e., chemerin, leptin and resistin showed neuroprotective effect in neuronal-like cells under oxidative stress and furthermore, in the absence of oxidative stress, promoted neuronal viability. Although this would seem to contradict our hypothesis, as it would be fair to predict that an adipokine which is positively associated with obesity and has a vast number of studies demonstrating its role in inflammation (Martin et al., 2008; Landgraf et al., 2012; Tripathi et al., 2020) would lead to further cell death.

However, other studies have shown that chemerin can have a neuroprotective effect, for example, it has been shown to reverse neurological impairments and ameliorate neuronal apoptosis through a ChemR23/CAMKK2/AMPK pathway (Zhang et al., 2019). We cannot move away from our system being a homogenous cell culture and perhaps the complexity of the in-vivo situation is not recreated in the present study. Neuroprotection is priority of an organ, perhaps the mechanisms behind this are designed to protect the brain function when challenged by disease which was supported by an engaging research study, where the directed and self-repair of neuronal damaged tissue was measured via infrared light induced mitochondrial activation for neuroprotection (Johnstone et al., 2015). Interestingly, the chemerin receptor CMKLR1 is a functional receptor for Amyloid- β peptide which further points to an important role within AD progression. Perhaps receptor expression changes in those more susceptible to disease and maybe an interesting new avenue to explore further (Peng et al., 2015). On the contrary to the neuronal protection by chemerin under oxidative stress the same protection was not observed in most treated non-neuronal cells under oxidative stress. This study was limited to examining the impact of chemerin under oxidative stress on neuronal-like cells, for further investigation and better understanding of chemerin receptor role, the knocking down of ChemR23/ CMKLR1 gene would be an advantage.

A study on endothelial cells from human aorta has shown that knock down of ChemR23 resulted in decreased chemerin associated ROS production and upregulation of autophagy related genes (Shen et al., 2012). In research studies it was shown that the chemerin is closely linked with obesity and the levels of chemerin evidently increases during 3T3-L1 cells differentiation (Bozaoglu et al., 2007). Research studies have confirmed that the expression of leptin receptors in the hypothalamus and it has direct correlation with learning and memory which can be observed during the AD progression due to dysregulation in leptin expression being severely affected (Marwarha & Ghribi, 2012). Leptin is one of the most studied adipokines and directly proportional to the chemerin circulating levels (Coimbra et al., 2014). In literature it has been shown that the pre- adipocytes did not expressed leptin but progression towards differentiation of 3T3-L1 cells increases leptin expression in the mature adipocytes (Kuroda et al., 2016).

An insulin related study has shown that the insulin enhances the leptin action via GRP78 (glucose regulated protein) using SHSY5Y cellular model (Thon et al., 2016). In a leptin related study increase in cell viability and decrease in apoptotic cells were recorded when neuroblastoma SHSY5Y cells were incubated with toxic methylglyoxal (Zmeskalova et al., 2020). In this study, as expected the data suggested that leptin possesses neuroprotective ability in neuronal-like cells under oxidative stress condition, although, no neuroprotection was observed in non-neuronal cells under oxidative stress which can be further supported by a similar research to measure neurotoxicity in the presence of 1-methyl-4-pyridinium, the neuronal-like cells expressed functional leptin receptors and the non-neuronal cells showed very low levels of leptin receptor. Resistin is another type of adipokine and the circulating levels of resistin varies in obesity (Liu et al., 2020). A research study on cellular mechanism of resistin on neuronal autophagy using neuroblastoma SHSY5Y cells under neuroinflammatory condition, showed that significant reduction in the LC3 marker indicating its role as novel regulatory pathway in neuronal autophagy (Miao et al., 2018).

Our results showed that the incubation of neuronal-like cells with resistin has enhanced neuronal proliferation in the absence of oxidative stress and neuroprotection when subjected to oxidative stress. However, in non-neuronal cells, resistin showed no neuroprotective effect, may be the non-neuronal cells did not express relevant receptors or in the presence of oxidative stress the non-neuronal cells activates autophagy or other apoptotic pathway which leads to cell death. In a resistin related research, human coronary artery endothelial cells were used and co-incubated with human recombinant resistin for 24 hrs which resulted in the inhibitory effect on the endothelial nitric oxide synthase leading to dysregulation in redox enzymes distribution (Chen et al., 2010). Interestingly, in recent study, it has been shown that when non-neuronal cells were treated with resistin, it induced the neuroinflammation via increasing the levels of IL6, TNF α and other proinflammatory mediators (Aminse et al., 2021). May be the additive impact of neuroinflammation and increased ROS production due to oxidative stress enhanced the cell death in the non-neuronal cells but not in the neuronal-like cells. Further, understanding of resistin receptor expression on the neuronal-like cells could be a very useful investigation as this adipokine is new and there is much more to explore in relation to its specific secretion, mechanism of action and involvement with various pathways.

Considering the results obtained from the individual adipokine impact on the neuroprotection, chemerin was used to understand its impact on the AD patient derived fibroblast cells, which will be discussed in the following section.

4.5. Does commercial chemerin have protective effect in AD-like condition under oxidative stress?

Use of peripheral cells for the examination and understanding of AD is very reliable and convenient for the research, accumulating evidence have confirmed that AD is a systemic disorder and patient derived RBCs, skin derived fibroblasts, lymphocytes can be used as relevant model because the impact of AD is connected to guts, cardiac and metabolic abnormalities leading to sporadic AD development (Trushina et al., 2019). Recent studies have shown that chemerin is closely associated with oxidative stress and autophagy (An et al., 2021). Our data using SHSY5Y cells suggested that the protective role of chemerin in neuronal-like cells which is in line with other studies. Peer researcher groups have used skin derived fibroblast cells from AD patients to understand the mitochondrial pathology and proteasomal alterations (Auburger et al., 2012). We used the patient derived skin fibroblasts to see whether our findings would be similar in AD patient derived and non-AD donor's fibroblast cells using chemerin under oxidative stress. No study has focussed on the impact and underlying molecular mechanism of chemerin in AD using patient derived skin sample. Our data showed no protective effect by chemerin on AD patient skin derived cell using 10nM dose under oxidative stress condition in comparison to the non-AD donors. In addition, the increased dose of chemerin i.e., 20nM showed no protective effect evident with no change in AD donor skin derived fibroblast viability under oxidative stress condition in comparison to the non-AD donors. From the results it can be estimated that may be chemerin does not possess any rescuing effect on the fibroblast cells. It is may be possible that higher doses of chemerin is required to show any protective effect under oxidative stress, whereas in our study only two different doses were used. This hypothesis can be supported by carcinoma related patient study where role of chemerin was explored using senescent dermal fibroblast from the elder patients, interestingly, the results showed increased expression of CCLR2, a chemerin receptor that promotes the cell migration via MAPK and GPR1 receptor signalling (Farsam et al., 2016).

The fibroblast cell lines we used are from the elderly patients (above 50 years) and the AD is age-related syndrome which enhances the possibility that may be the senescent cell lines used had certain minimum chemerin concentration requirement to trigger the signalling pathway, however, both doses used in our study did not showed rescue effect in AD donor cells under oxidative stress. However, it needs further chemerin receptor/expression targeted investigation which can achieved by using a broad range of chemerin doses and estimation of ROS generated in each dose in comparison to the non-AD donors. In an animal study, it has been shown that the chemerin receptors (CMKLR1) were upregulated in the AD patient brain suggesting their vital role in A β -42 clearance (Li et al., 2014), therefore, it is quite possible that these patients derived cells also express CMKLR1 and prevent cellular damage under oxidative stress.

In another patient based research confirmed that chemerin and obesity are directly co-related, as the results showed that the obese patients with increased chemerin levels higher oxidative stress and increased recruitment of pro-inflammatory factors was measured via c-reactive proteins and oxidised low density lipoproteins as mediators (Fülöp et al., 2014; Li et al., 2020) and may be based on this oxidative stress theory it is possible that the inflammatory receptors are also involved in the protecting effect by chemerin, because of chemerin and pro-inflammatory positive co-relation. An epithelial cell-based research has shown that chemerin play vital role in autophagy and apoptosis pathway regulation and an increased reactive oxygen species alter the mitochondrial functioning and hence autophagy (Goralski et al., 2019; Hu et al., 2019), the co-relation between chemerin and autophagy markers can be explored by using autophagy associated markers such LC3/2. Based on the AD patient derived fibroblast study under oxidative stress condition there are many more questions to be answered. From our study, the cell viability assay has shown that the chemerin lack the ability to protect the cells under oxidative stress and different dose range should be used with minimum 20nM dose and above, however, it is possible that maybe these AD patients were non-obese or suffering from any other physiological complications or whether the patients were on any prescribed medicine that had any relation with lowering/increasing the oxidative stress or inflammation. The other conditions were not considered in this study because the aim of study was to understand the role of chemerin on the AD derived fibroblasts only in relation to the cell viability, but for the future research it has been confirmed that these doses were not effective and other conditions should also be considered.

Future Work

On the basis of preliminary study which includes the understanding of neuronal-like cell behaviour in the presence of pooled and individual adipokine environment under oxidative stress condition. The results obtained from the analysis of cell viability gave better understanding of adipokines impact in relation to neuroprotection. This study holds huge potential in future research because modulation in adipokines can potentially be used as novel therapeutic method to prevent the Alzheimer's disease in mid-life obese patients. From the present study findings, further exploration of the followings may be useful:

1. Adipokine profiling: A comparative adipokine array can be performed between the stressed CM and unstressed CM from adipocyte-like and pre-adipocytes which can provide an insight in the changed factors secreted into the CM.
2. Receptor expression: Expression of chemerin, leptin and resistin receptors could be investigated in neuronal-like cells to understand the underlying molecular/ signalling pathway mediators involvement using mRNA expression assays or immunostaining with receptor specific antagonist.
3. Different doses of adipokine: In this study only 3 doses of chemerin, resistin and leptin were investigated. To better understand the impact of individual adipokines wide range of doses can be explored.
4. Different adipokine investigation: There are wide range of adipokines present in the CM. After the adipokine array analysis, more adipokines can be used to understand their effect on neuronal cell viability.
5. Exploring different adipokines: There are various adipokines available commercially which can be used with different concentrations, and treatment conditions.
6. Human adipocytes use: In the present study mouse adipocyte model was used on the human neuronal model. It would be an advantage and interesting to use human adipocytes on human neuronal cellular model. In addition, the adipokine array profiling would confirm the participation of adipokines present during incubation.

Overall, the present study had given preliminary evidence that the adipocyte-like secreted adipokines and individual adipokines (chemerin, leptin and resistin) have the ability of neuroprotection under oxidative stress. In addition, chemerin doses with 10 and 20nM does not have protective effect on the AD derived fibroblast cells. Based on this preliminary findings, further exploration of underlying molecular mechanisms can be explored for better understanding and connecting the broken links between AD, midlife obesity, and adipokines.

APPENDIX

5.1. Understanding the impact of H₂O₂ on cell viability in oxidative stress

The cell viability of differentiated SHSY5Y cells in H₂O₂ induced oxidative stress condition was observed. To understand the effect of CM obtained from adipocyte-like and pre-adipocytes (differentiated and undifferentiated 3T3-L1 cells, respectively) on differentiated SHSY5Y cells, three different treatment conditions were considered during initial phase of research and 150µM of H₂O₂ was used to induce oxidative stress (see result section 3.3.1.1). First treatment was pre-treatment of differentiated SHSY5Y cells with H₂O₂ and then CM was added after 24 hrs. Second treatment was co-treatment of differentiated SHSY5Y cells with H₂O₂ and CM and last treatment was post-treatment of differentiated SHSY5Y cells with H₂O₂ after 24 hrs of CM treatment.

Research studies have shown that cells can be exposed to H₂O₂ in various ways to obtain a quantitative response or observation (Sobotta et al., 2013). Co-treatment was considered as reliable treatment condition on the basis of results obtained (discussed in results section 3.3) and all the experiments were performed using concurrent treatment with CM and H₂O₂ to avoid 48 hrs (total incubation period of pre- and post-treatment). In the following sections pre-treatment, post-treatment and after effect of CM treatment will be discussed (which were not included as main experiments). The differentiated SHSY5Y cells were incubated with the CM from the differentiated and undifferentiated 3T3-L1 cells for 24 hrs and then MTT assay was performed.

The data was analysed by GraphPad-Prism5 using one-way ANOVA by parametric test and tested for normal distribution and post hoc Bonferroni multiple comparison test. Each experiment was performed in triplicate (n=3) and data are presented as mean ± SEM (% viability). The data was considered significant with p<0.05.

5.1.1. Pre-treatment:

Research condition: In the present set of experiment with differentiated SHSY5Y cells, pre-treatment with 150 μ M of H₂O₂ for 24 hrs was used to induce oxidative stress and then incubated with CM from differentiated/undifferentiated 3T3-L1 cells for another 24 hrs.

Research question: Does CM possess the neuroprotective ability to protect already oxidised differentiated SHSY5Y cells under H₂O₂ induced oxidative stress?

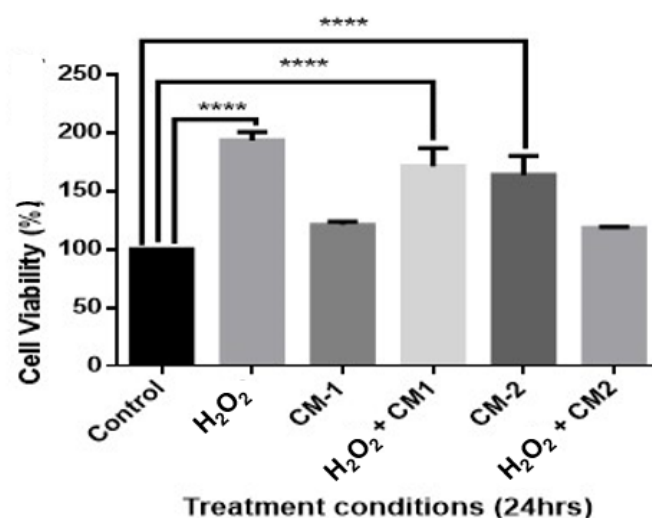


Figure 5.1 Impact on SHSY5Y cell viability after induction of oxidative stress H₂O₂ as pre-treatment and CM was added after 24 hrs. Significant increase in cell viability was measured in H₂O₂, H₂O₂+CM1 and CM-2 treatments in comparison to the control. Control- no treatment, H₂O₂ –only H₂O₂ treatment, CM-1- CM from differentiated 3T3-L1 cells, H₂O₂+CM-1- H₂O₂ and CM from differentiated 3T3-L1 cells, CM-2- CM from undifferentiated 3T3-L1 cells, H₂O₂+CM-2- H₂O₂ and CM from undifferentiated 3T3-L1 cells (data are presented as mean \pm SEM and experiments were repeated in triplicate, n=3, ****p <0.0001).

Result: Significant increase in cell viability was obtained with and without H₂O₂ (186 \pm 1.3), H₂O₂ + CM-1 (H₂O₂ and CM from differentiated 3T3-L1 cells) (166 \pm 3.03) and CM-2 (CM from undifferentiated 3T3-L1 cells) (154 \pm 3.53) treatments in comparison to the control (figure 5.1). Overall, increased cell viability was measured in all treatment conditions in comparison to the control. Data are presented as mean \pm SEM (% viability) and experiments were repeated in triplicate, n=3. Data was considered statistically significant with ****p <0.0001).

Conclusion: Results obtained did not answer our research question because in the H₂O₂ treated differentiated SHSY5Y cell viability was not decreased. Therefore, it was uncertain that oxidative stress was induced or not. Further investigation using pre-treatment of H₂O₂ was discontinued.

5.1.2. Post-treatment

Research condition: The differentiated SHSY5Y cells were incubated with the CM from differentiated and undifferentiated 3T3-L1 cells for 24 hrs and then 150μM of H₂O₂ was added for another 24 hrs. The MTT was performed, and data was analysed using GraphPad-Prism5 (detailed in section 5.1).

Research question: How CM affect cell viability of differentiated SHSY5Y cells under H₂O₂ induced oxidative stress after 24 hrs of CM treatment?

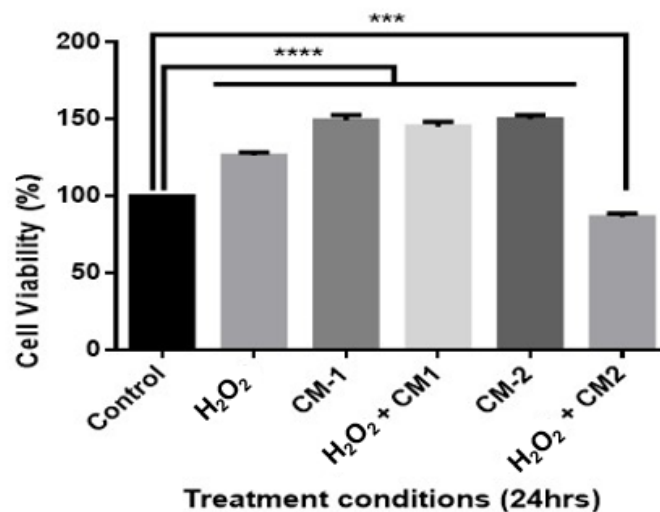


Figure 5.2 Impact on SHSY5Y cell viability using CM (added before 24 hrs) and subsequent induction of oxidative stress as post-treatment with H₂O₂. Significant increase in cell viability was measured in all given treatments in comparison to the control. Control- no treatment, H₂O₂-only H₂O₂ treatment, CM-1- CM from differentiated 3T3-L1 cells, H₂O₂+CM-1- H₂O₂ and CM from differentiated 3T3-L1 cells, CM-2- CM from undifferentiated 3T3-L1 cells, H₂O₂+CM-2- H₂O₂ and CM from undifferentiated 3T3-L1 cells (data are presented as mean ± SEM and experiments were repeated in triplicate, n=3, ***p<0.001, ****p <0.0001).

Result: Significant increase in cell viability was obtained with and without H₂O₂, H₂O₂ (123.3 ± 0.03), CM-1 (CM from differentiated 3T3-L1 cells) (145.9 ± 0.09), H₂O₂ + CM-1 (142.6 ± 0.07) and CM-2 (CM from undifferentiated 3T3-L1 cells) (145.4 ± 0.03) in comparison to the control (figure 5.2). Significantly reduced cell viability was obtained with H₂O₂ + CM-2 (67.4 ± 0.06) treatments in comparison to the control. Overall, all treatment conditions showed increased cell viability except the undifferentiated 3T3-L1 cells derived CM + H₂O₂ in comparison to the control. Data are presented as mean ± SEM (% viability) and experiments were repeated in triplicate, n=3. Data was considered significantly different with ***p <0.001, ****p <0.0001).

Conclusion: Similar results were obtained (as pre-treatment of H₂O₂ results) with post treatment of H₂O₂ and the cell viability of differentiated SHSY5Y was not decreased using H₂O₂ only treated cells. Therefore, it was uncertain that oxidative stress was induced or not. Further investigation using post-treatment of H₂O₂ was discontinued.

5.1.3 Understanding the effect of CM from differentiated 3T3-L1 cells after recovery from H₂O₂ induced stressed on the differentiated SHSY5Y cells.

The effect of CM from differentiated 3T3-L1 cells after being recovered from H₂O₂ induced oxidative stress on the differentiated SHSY5Y cells was investigated. To explore if the CM secreted growth factors or adipokines were restored after oxidation or become worst and what is the impact on the differentiated SHSY5Y cells (neuronal-like cells)? This experiment was performed after the results obtained from co-treated stressed CM from differentiated 3T3-L1 cells on SHSY5Y cells (section 3.3.3 and 3.3.4).

Research condition: In this experiment, the differentiated 3T3-L1 cells were incubated with 150µM of H₂O₂ for 24 hrs and then the media was removed and replaced with pre-warmed fresh differentiation media on mature 3T3-L1 cells for 24 hrs. After 24 hrs of incubation the media was removed and used as CM from the oxidation recovered 3T3-L1 cells and incubated on the differentiated SHSY5Y cells for another 24 hrs as treatment condition.

Research question: What is the impact of CM on the differentiated SHSY5Y cell viability after being recovered from 24 hrs of oxidative stress?

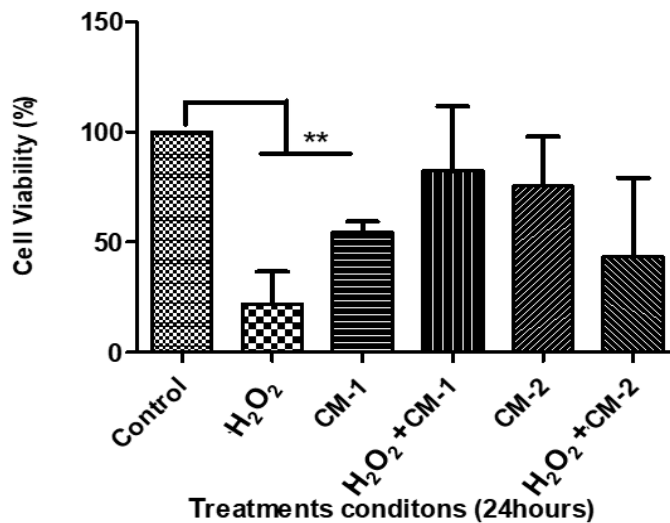


Figure 5.3 The impact of recovered CM after being oxidised with H₂O₂ for 24 hrs on the differentiated SHSY5Y cells in comparison to the control. Significantly decreased cell viability was measured in H₂O₂ and CM-1 treatments in comparison to the control. Control- no treatment, H₂O₂—only H₂O₂ treatment, CM-1- CM from differentiated 3T3-L1 cells, H₂O₂+CM-1- H₂O₂ and CM from differentiated 3T3-L1 cells, CM-2- CM from undifferentiated 3T3-L1 cells, H₂O₂+CM-2- H₂O₂ and CM from undifferentiated 3T3-L1 cells (data are presented as mean ± SEM and experiments were repeated in triplicate, n=3, **p<0.01).

Result: Significant decrease in cell viability was obtained with and without H₂O₂, H₂O₂ (26.06 ± 11.03), CM-1 (CM from differentiated 3T3-L1 cells) (59.07 ± 6.09) in comparison to the control (figure 5.3). Overall, an inconsistent cell viability was measured in comparison to the control. Data are presented as mean ± SEM (% viability) and experiments were repeated in triplicate, n=3. Data was considered statistically significant difference with **p <0.01).

Conclusion: Results obtained were informative but due to higher difference within the experimental repeats higher SEM was obtained in differentiated SHSY5Y cell viability and statistical significance was not measured. Therefore, further investigation using stressed recovered CM and H₂O₂ was discontinued.

5.2 To estimate the cytometric responsiveness of chemerin on SHSY5Y cells

FACS analysis is based on the principle of fluorescence emission and detection by following three stages which are fluidics, optics and electronics. The single cell suspension preparation was accomplished by sheath fluid and core hydrodynamic focusing as single file detected by focused laser beam adjusted at defined wavelength for excitation and emission to emit fluorescence, which is converted to electronic signals, further processed by computer for visualization at computer screen for data interpretation and gating (Menon et al.,2011).

Research Question: Does chemerin (5nM) possess anti-apoptotic ability under H₂O₂ (100µM) induced oxidative stress in undifferentiated SHSY5Y cells?

Research Condition: This experiment was performed to understand the effect of chemerin dose of 5nM in the presence and absence of H₂O₂ induced oxidative stress after 24 hrs of incubation in undifferentiated SHSY5Y cells. This was experimented to further explore the impact of chemerin in relation to anti-apoptotic property, on the basis of results obtained by MTT assay and showed slight but significant increased cell viability on undifferentiated SHSY5Y cells (section 3.3.5.1, C and D). The SHSY5Y cells were cultured in T75 flask. The cells were harvested from T75 flask (70-80% confluency) after being trypsinized using EDTA-trypsin. The cells were collected in falcon and centrifuged, the cell pellet obtained was resuspended in complete media and seeded with 5×10^4 cell density per well in 24 well plate. The cells in 24 well plate was placed in the humid incubator, 37°C and 5% CO₂ for 24 hrs to allow the cells adhere and adjust in each well. Next day, the plate was taken out in sterile hood for dosing with H₂O₂ and chemerin. Four conditions were prepared, and the plate was placed back in the incubator for further 24 hrs incubation, 37°C and 5% CO₂:

1. Control with no treatment
2. Chemerin with 5nM concentration
3. H₂O₂ with 100µM to induce oxidative stress
4. Chemerin (5nM) + H₂O₂ (100µM)

After the incubation, the cells from respective treatments were harvested by using EDTA-trypsinization. The detached cells were added in the different 1.5ml labelled eppendorfs and centrifuged for 10 mins at 1000rpm. The collected pellet was washed with PBS and the cells were centrifuged again for 10 mins at 1000 rpm. The collected pellet was washed with PBS again and centrifuged for 10 mins at 1000 rpm. After the final centrifuge, the cell pellet in each eppendorfs, 0.5ml of 1% Annexin binding buffer was added and pipetted gently to prevent the cell lyses. The resuspended cells were then incubated with 5µl of APC ready flow™ reagent and 5µl of propidium iodide. The samples were incubated in dark for 15 mins. The samples were analysed using BD FACS verse instrument with BD FACSuite v1.0.6 software. After incubation, each sample was added to the reaction tube one by one. Each data was recorded as cell distribution/scattering within the gates. Gating (divided the cells that are scattered into groups) was made by testing individual dyes to measure the range for excitation and emission for the cells. After each sample analysis, the data was analysed using FACSuite software to obtain the percentage of treated cells going through the stages of apoptosis.

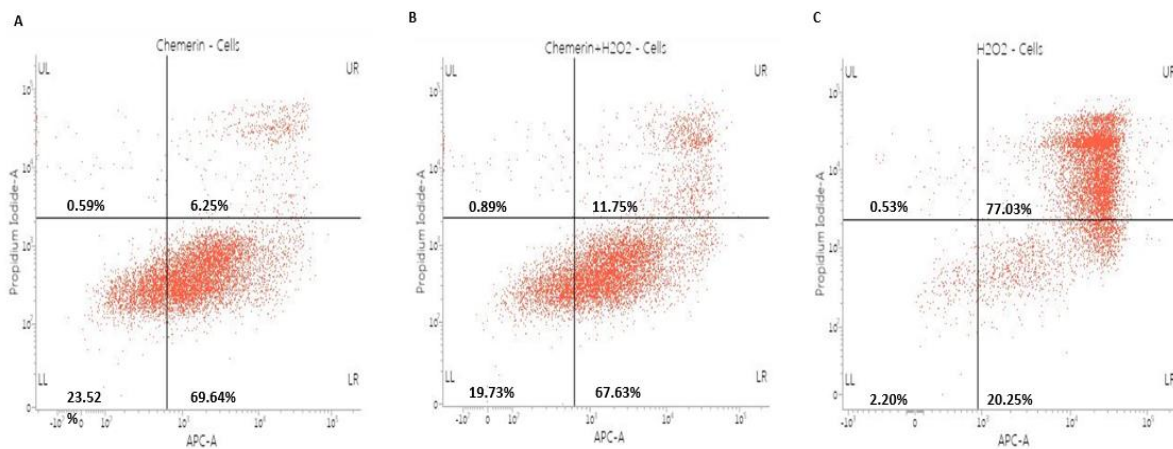


Figure 5.4 The anti-apoptotic properties of chemerin (5nM) was explored. **A.** The undifferentiated SHSY5Y cells were incubated with chemerin only and showed 69.64% cells in the early apoptotic stage (LR). **B.** Chemerin+ H₂O₂ incubated undifferentiated SHSY5Y cells demonstrated 67.63% of cells in early apoptotic phase (LR) and 11.75% in late apoptotic phase (UR). **C.** In the presence of only H₂O₂, the undifferentiated SHSY5Y cells demonstrated that majority of cell population was in late apoptotic phase with 77.03% (UR). No statistical analysis was performed because the experiment was completed once (n=1). The data are presented as obtained by FACSuite software during the experimental run as basic statistics on the cell population run. LL- lower left represents live cells, LR-lower right-represents early apoptosis, UR-upper right-represents late apoptosis, UL- Upper left- represents necrosis.

To investigate the underlying anti-apoptotic ability of chemerin with and without H₂O₂ induced oxidative stress in undifferentiated SHSY5Y cells, FACS analysis was performed. 5nM dose of chemerin was used on the basis of MTT assay results obtained, as discussed in section 3.3.5.1. The results obtained from only chemerin (5nM) treated undifferentiated cells, demonstrated that higher percentage of cell population was in early apoptotic phase with 69.64% and 23.52% in live phase (figure 5.4. A-LR, LL, respectively). As expected, the neuroprotective effect of chemerin with H₂O₂ was recorded as the higher percentage of cell population was in early apoptotic phase with 67.63% (figure 5.4. B-LR) and in comparison, to the only H₂O₂ treated cells with higher levels of late apoptotic cell population with 77.03% and 20.25 % in early apoptotic stage (figure 5.4. C-UR, LR, respectively). The statistical analysis was performed by the FACS suite software analyser during the sample run. No statistical analysis was performed to obtain the concluded results using n=3, because the experiment was performed once and completion of n=3 and data analysis should be performed as future work.

Conclusion: Chemerin possess the ability to delay the apoptosis in 24 hrs treatment, however, the cells were observed to be inclined in the progressive direction of apoptotic pathway, which means, the cells will eventually reach late apoptosis and finally necrosis or cell death. In addition, the experiment was performed once, therefore, no concluded result can be estimated, but further experiment should be performed in triplicate (n=3) for statistical analysis.

5.3 Impact of H₂O₂ induced oxidative stress on mitochondrial function using dichlorodihydrofluorescein diacetate (DCFDA) assay in undifferentiated SHSY5Y cells.

Research question: Does the cell viability results obtained from MTT assay (section 3.3) are due to mitochondrial dysfunction related cellular ROS production under H₂O₂ induced oxidative stress in undifferentiated SHSY5Y cells?

Research condition: To explore the cellular ROS production which is specific to mitochondrial dysfunction under H₂O₂ induced oxidative stress in undifferentiated SHSY5Y cells by DCFDA assay kit. The cells were cultured in 96 well plate using 5×10^4 per well for 24 hrs.

Next day, the cells were washed for twice with PBS. Diluted DCFDA solution was added and incubated with for 45 mins at 37°C in the dark. After incubation, cells were washed for twice with PBS. Cell microscopy was performed with filter set for fluorescein (FITC). Maintained low light conditions to avoid photo-bleaching and photo oxidation of dichlorodihydrofluorescein.

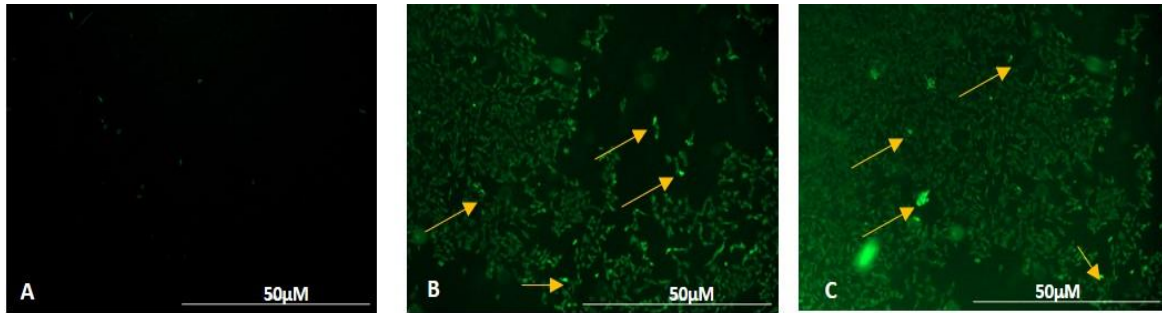


Figure 5.5. Fluorescence images of undifferentiated cells using DCFDA assay. **A.** No DCFDA solution incubated with the SHSY5Y cells. **B.** ROS specific DCFDA solution showed bright green fluorescence (indicated by arrows) in the presence of chemerin. **C.** In the presence of chemerin + H₂O₂, strong bright green fluorescence was measured (indicated by the arrows). No clear difference was concluded between bright green and less green fluorescence images obtained. The images were taken using Cytation3 with FITC filter and the experiment was performed once, so, no statistics was performed.

In the figure 5.5.A, the fluorescence images obtained from undifferentiated SHSY5Y cells using DCFDA assay did not showed green fluorescence in the absence of DCFDA solution. Few bright green fluorescence undifferentiated SHSY5Y cells were observed (shown by arrows, figure 5.5.B) in the presence of chemerin (5nM) without H₂O₂. In addition, in the presence of chemerin (5nM) + H₂O₂ treatment, the results showed that few very dominant bright green fluorescence was visible due to the presence of higher ROS production (indicated by arrows, figure 5.5.C). The experiment was performed once, so image analysis was performed.

Conclusion: The results obtained from incubated chemerin (5nM) and chemerin (5nM) + H₂O₂ was not very conclusive in relation to the ROS production in undifferentiated SHSY5Y cells. However, presence of minor but dominant green fluorescence confirmed that under H₂O₂ induced oxidative stress chemerin with dose of 5nM was ineffective to reduce the ROS production.

REFERENCES

- ABDULWANIS MOHAMED, Z., MOHAMED ELIASER, E., JAAFARU, M. S., NORDIN, N., IOANNIDES, C. & ABDULL RAZIS, A. F. 2020. Neuroprotective Effects of 7-Geranyloxycinnamic Acid from *Melicope lunu ankenda* Leaves. *Molecules (Basel, Switzerland)*, 25, 3724.
- AGHA, M. & AGHA, R. 2017. The rising prevalence of obesity: part A: impact on public health. *International journal of surgery. Oncology*, 2, e17-e17.
- AGHOLME, L., LINDSTRÖM, T., KÅGEDAL, K., MARCUSSEON, J. & HALLBECK, M. 2010. An in-vitro model for neuroscience: differentiation of SH-SY5Y cells into cells with morphological and biochemical characteristics of mature neurons. *J Alzheimers Dis*, 20, 1069-82.
- AGOSTINHO, P., CUNHA, R. A. & OLIVEIRA, C. 2010. Neuroinflammation, oxidative stress and the pathogenesis of Alzheimer's disease. *Curr Pharm Des*, 16, 2766-78.
- ALFORD, S., PATEL, D., PERAKAKIS, N. & MANTZOROS, C. S. 2018. Obesity as a risk factor for Alzheimer's disease: weighing the evidence. *Obesity Reviews*, 19, 269-280.
- AL HAZZOURI, A. Z., HAAN, M., STONE, K. & YAFFE, K. 2012. Leptin, mild cognitive impairment (MCI) and dementia among elderly women. *Alzheimer's & Dementia: The Journal of the Alzheimer's Association*, 8, P134.
- ALAM, Q., ALAM, M. Z., MUSHTAQ, G., DAMANHRI, G. A., RASOOL, M., KAMAL, M. A. & HAQUE, A. 2016. Inflammatory Process in Alzheimer's and Parkinson's Diseases: Central Role of Cytokines. *Curr Pharm Des*, 22, 541-8.
- ALMATHHUR, R., YAKUBOV, R., DONKOR, I., SUH, C., CHAKRABORTY, S. & CHAKRABORTY, T. R. 2018. Neuroprotective effects of estrogen on Alzheimer induced SH-SY5Y neuroblastoma cells and N38 hypothalamic neuronal cells. *The FASEB Journal*, 32, 782.17-782.17.
- ALANTEET, A. A., ATTIA, H. A., SHAHEEN, S., ALFAYEZ, M. & ALSHANAWANI, B. 2021. Anti-Proliferative Activity of Glucagon-Like Peptide-1 Receptor Agonist on Obesity-Associated Breast Cancer: The Impact on Modulating Adipokines' Expression in Adipocytes and Cancer Cells. *Dose-Response*, 19, 1559325821995651.

- ALVARIÑO, R., ALONSO, E., TRIBALAT, M. A., GEGUNDE, S., THOMAS, O. P. & BOTANA, L. M. 2017. Evaluation of the Protective Effects of Sarains on H(2)O(2)-Induced Mitochondrial Dysfunction and Oxidative Stress in SH-SY5Y Neuroblastoma Cells. *Neurotox Res*, 32, 368-380.
- ALZHEIMER'S SOCIETY (2016) Alzheimer's society view on demography. Available at: <https://www.alzheimers.org.uk/about-us/policy-and-influencing/what-we-think/demography> (Accessed on 23 March 2018).
- AMBROSI, G., GHEZZI, C., SEPE, S., MILANESE, C., PAYAN-GOMEZ, C., BOMBARDIERI, C. R., ARMENTERO, M.-T., ZANGAGLIA, R., PACCHETTI, C., MASTROBERARDINO, P. G. & BLANDINI, F. 2014. Bioenergetic and proteolytic defects in fibroblasts from patients with sporadic Parkinson's disease. *Biochimica et Biophysica Acta (BBA) - Molecular Basis of Disease*, 1842, 1385-1394.
- AMINSE, H., BENOMAR, Y. & TAOUIS, M. 2021. Palmitic acid promotes resistin-induced insulin resistance and inflammation in SH-SY5Y human neuroblastoma. *Scientific Reports*, 11, 5427.
- AMIRHAKIMI, A., KARAMIFAR, H., MORAVEJ, H. & AMIRHAKIMI, G. 2011. Serum Resistin Level in Obese Male Children. *Journal of Obesity*, 2011, 953410.
- AN, X., LIU, J., LI, Y., DOU, Z., LI, N., SUO, Y., MA, Y., SUN, M., TIAN, Z. & XU, L. 2021. Chemerin/CMKLR1 ameliorates nonalcoholic steatohepatitis by promoting autophagy and alleviating oxidative stress through the JAK2-STAT3 pathway. *Peptides*, 135, 170422.
- ANDERSSON, D. P., LAURENCIKIENE, J., ACOSTA, J. R., RYDÉN, M. & ARNER, P. 2016. Circulating and Adipose Levels of Adipokines Associated With Insulin Sensitivity in Nonobese Subjects With Type 2 Diabetes. *The Journal of clinical endocrinology and metabolism*, 101, 3765-3771.
- ANDRADE-OLIVEIRA, V., #XED, CIUS, #XE2, MARA, N. O. S. & MORAES-VIEIRA, P. M. 2015. Adipokines as Drug Targets in Diabetes and Underlying Disturbances. *Journal of Diabetes Research*, 2015, 11.
- APOVIAN, C. M. 2016. Obesity: definition, comorbidities, causes, and burden. *The American journal of managed care*, 22, s176-85.
- ARBER, C., LOVEJOY, C. & WRAY, S. 2017. Stem cell models of Alzheimer's disease: progress and challenges. *Alzheimer's Research & Therapy*, 9, 42.

- ARMSTRONG, J. L., RUIZ, M., BODDY, A. V., REDFERN, C. P. F., PEARSON, A. D. J. & VEAL, G. J. 2005. Increasing the intracellular availability of all-trans retinoic acid in neuroblastoma cells. *British Journal of Cancer*, 92, 696-704.
- ARMANI, A., MAMMI, C., MARZOLLA, V., CALANCHINI, M., ANTELM, A., ROSANO, G. M. C., FABBRI, A. & CAPRIO, M. 2010. Cellular models for understanding adipogenesis, adipose dysfunction, and obesity. *Journal of Cellular Biochemistry*, 110, 564-572.
- ARNOLDUSSEN, I. A., KILIAAN, A. J. & GUSTAFSON, D. R. 2014. Obesity and dementia: adipokines interact with the brain. *Eur Neuropsychopharmacol*, 24, 1982-99.
- ARNANDIS, T., MONTEIRO, P., ADAMS, S. D., BRIDGEMAN, V. L., RAJEEVE, V., GADALETA, E., MARZEC, J., CHELALA, C., MALANCHI, I., CUTILLAS, P. R. & GODINHO, S. A. 2018. Oxidative Stress in Cells with Extra Centrosomes Drives Non-Cell-Autonomous Invasion. *Dev Cell*, 47, 409-424.e9.
- AROSIO, B., GUERINI, F. R., VOSHAAR, R. C. O. & APRAHAMIAN, I. 2021. Blood Brain-Derived Neurotrophic Factor (BDNF) and Major Depression: Do We Have a Translational Perspective? *Frontiers in behavioral neuroscience*, 15, 626906-626906.
- ARVANITAKIS, Z., SHAH, R. C. & BENNETT, D. A. 2019. Diagnosis and Management of Dementia: Review. *JAMA*, 322, 1589-1599.
- ATHAR, T., AL BALUSHI, K. & KHAN, S. A. 2021. Recent advances on drug development and emerging therapeutic agents for Alzheimer's disease. *Molecular biology reports*, 1-17.
- ATCC (2014) ATCC, cell lines. Available at <https://www.atcc.org/products/cl-173> Accessed on 10 June -15
- ATCC (2019) ATCC, cell lines. Available at <https://www.atcc.org/products/cl-173> Accessed on 4 Julye -20
- AUBURGER, G., KLINKENBERG, M., DROST, J., MARCUS, K., MORALES-GORDO, B., KUNZ, W. S., BRANDT, U., BROCCOLI, V., REICHMANN, H., GISPERT, S. & JENDRACH, M. 2012. Primary skin fibroblasts as a model of Parkinson's disease. *Molecular neurobiology*, 46, 20-27.
- AYODELE, T., ROGAEVA, E., KURUP, J. T., BEECHAM, G. & REITZ, C. 2021. Early-Onset Alzheimer's Disease: What Is Missing in Research? *Current Neurology and Neuroscience Reports*, 21, 4.

- BAGYINSZKY, E., YOUN, Y. C., AN, S. S. A. & KIM, S. 2014. The genetics of Alzheimer's disease. *Clinical interventions in aging*, 9, 535-551.
- BANJARE, J., RAINA, P., MANSARA, P., GHANEKAR, R. K. & BHALERAO, S. 2018. Triphala, Regulates Adipogenesis through Modulation of Expression of Adipogenic Genes in 3T3-L1 Cell Line. *Pharmacognosy magazine*, 13, S834-S839.
- BAUSENWEIN, J., SERKE, H., EBERLE, K., HIRRLINGER, J., JOGSCHIES, P., HMEIDAN, F. A., BLUMENAUER, V. & SPANEL-BOROWSKI, K. 2010. Elevated levels of oxidized low-density lipoprotein and of catalase activity in follicular fluid of obese women. *Mol Hum Reprod*, 16, 117-24.
- BECHOR, S., NACHMIAS, D., ELIA, N., HAIM, Y., VATARESCU, M., LEIKIN-FRENKEL, A., GERICKE, M., TARNOVSKI, T., LAS, G. & RUDICH, A. 2017. Adipose tissue conditioned media support macrophage lipid-droplet biogenesis by interfering with autophagic flux. *Biochim Biophys Acta Mol Cell Biol Lipids*, 1862, 1001-1012.
- BEKRIS, L. M., YU, C.-E., BIRD, T. D. & TSUANG, D. W. 2010. Genetics of Alzheimer disease. *Journal of geriatric psychiatry and neurology*, 23, 213-227.
- BENOMAR, Y., ROY, A.-F., AUBOURG, A., DJIANE, J. & TAOUIS, M. 2005. Cross down-regulation of leptin and insulin receptor expression and signalling in a human neuronal cell line. *The Biochemical journal*, 388, 929-939.
- BELL, M., BACHMANN, S., KLIMEK, J., LANGERSCHEIDT, F. & ZEMPEL, H. 2020. Axonal TAU sorting in SH-SY5Y-derived neurons requires the C-terminus of TAU but is independent of Ankyrin G. *bioRxiv*, 2020.06.26.173526.
- BEST, B. P. 2015. Cryoprotectant Toxicity: Facts, Issues, and Questions. *Rejuvenation Res*, 18, 422-36.
- BETTERIDGE, D. J. 2000. What is oxidative stress? *Metabolism*, 49, 3-8.
- BINLATEH, T., TANASAWET, S., RATTANAPORN, O., SUKKETSIRI, W. & HUTAMEKALIN, P. 2019. Metformins Promotes Neuronal Differentiation via Crosstalk between Cdk5 and Sox6 in Neuroblastoma Cells. *Evidence-Based Complementary and Alternative Medicine*, 2019, 1765182.

- BIRBEN, E., SAHINER, U. M., SACKESEN, C., ERZURUM, S. & KALAYCI, O. 2012. Oxidative stress and antioxidant defense. *The World Allergy Organization journal*, 5, 9-19.
- BIRD T.D. (2020) Alzheimer Disease Overview. Available at: <https://www.ncbi.nlm.nih.gov/books/NBK1161/> (Accessed on 04 July 2021)
- BLANCO, J., GUARDIA-ESCOTE, L., MULERO, M., BASAURE, P., BIOSCA-BRULL, J., CABRÉ, M., COLOMINSA, M. T., DOMINGO, J. L. & SÁNCHEZ, D. J. 2020. Obesogenic effects of chlorpyrifos and its metabolites during the differentiation of 3T3-L1 pre-adipocytes. *Food and Chemical Toxicology*, 137, 111171.
- BONDI, M. W., EDMONDS, E. C. & SALMON, D. P. 2017. Alzheimer's Disease: Past, Present, and Future. *Journal of the International Neuropsychological Society : JINS*, 23, 818-831.RA
- BOMFIM, T. R., FORNY-GERMANO, L., SATHLER, L. B., BRITO-MOREIRA, J., HOUZEL, J. C., DECKER, H., SILVERMAN, M. A., KAZI, H., MELO, H. M., MCCLEAN, P. L., HOLSCHER, C., ARNOLD, S. E., TALBOT, K., KLEIN, W. L., MUNOZ, D. P., FERREIRA, S. T. & DE FELICE, F. G. 2012. An anti-diabetes agent protects the mouse brain from defective insulin signaling caused by Alzheimer's disease- associated A β oligomers. *J Clin Invest*, 122, 1339-53.
- BOZAOGLU, K., BOLTON, K., MCMILLAN, J., ZIMMET, P., JOWETT, J., COLLIER, G., WALDER, K. & SEGAL, D. 2007. Chemerin Is a Novel Adipokine Associated with Obesity and Metabolic Syndrome. *Endocrinology*, 148, 4687-4694.
- BRAND, M. D. 2010. The sites and topology of mitochondrial superoxide production. *Experimental gerontology*, 45, 466-472.
- BRIGGS, R., KENNELLY, S. P. & O'NEILL, D. 2016. Drug treatments in Alzheimer's disease. *Clin Med (Lond)*, 16, 247-53.
- BROTHERS, H. M., GOSZTYLA, M. L. & ROBINSON, S. R. 2018. The Physiological Roles of Amyloid- β Peptide Hint at New Ways to Treat Alzheimer's Disease. *Frontiers in aging neuroscience*, 10, 118-118.

- BRUNETTI, L., ORLANDO, G., FERRANTE, C., RECINELLA, L., LEONE, S., CHIAVAROLI, A., DI NISIO, C., SHOHREH, R., MANIPPA, F., RICCIUTI, A. & VACCA, M. 2014. Peripheral chemerin administration modulates hypothalamic control of feeding. *Peptides*, 51, 115-121.
- CACACE, R., SLEEGERS, K. & VAN BROECKHOVEN, C. 2016. Molecular genetics of early-onset Alzheimer's disease revisited. *Alzheimers Dement*, 12, 733-48.
- CAI, W., URIBARRI, J., ZHU, L., CHEN, X., SWAMY, S., ZHAO, Z., GROSJEAN, F., SIMONARO, C., KUCHEL, G. A., SCHNAIDER-BEERI, M., WOODWARD, M., STRIKER, G. E. & VLASSARA, H. 2014. Oral glycotoxins are a modifiable cause of dementia and the metabolic syndrome in mice and humans. *Proc Natl Acad Sci U S A*, 111, 4940-5.
- CAWTHORN, W. P. & SETHI, J. K. 2008. TNF-alpha and adipocyte biology. *FEBS Lett*, 582, 117-31.
- CHAIT, A. & DEN HARTIGH, L. J. 2020. Adipose Tissue Distribution, Inflammation and Its Metabolic Consequences, Including Diabetes and Cardiovascular Disease. *Frontiers in cardiovascular medicine*, 7, 22-22.
- CHAN, K.-H., LAM, K. S.-L., CHENG, O.-Y., KWAN, J. S.-C., HO, P. W.-L., CHENG, K. K.-Y., CHUNG, S. K., HO, J. W.-M., GUO, V. Y. & XU, A. 2012. Adiponectin is Protective against Oxidative Stress Induced Cytotoxicity in Amyloid-Beta Neurotoxicity. *PLOS ONE*, 7, e52354.
- CHANDRASEKARAN, A., IDELCHIK, M. & MELENDEZ, J. A. 2017. Redox control of senescence and age-related disease. *Redox Biol*, 11, 91-102.
- CHAPARRO-SANABRIA, J. A., BAUTISTA-MOLANO, W., BELLO-GUALTERO, J. M., CHILA-MORENO, L., CASTILLO, D. M., VALLE-OÑATE, R., CHALEM, P. & ROMERO-SÁNCHEZ, C. 2019. Association of adipokines with rheumatic disease activity indexes and periodontal disease in patients with early rheumatoid arthritis and their first-degree relatives. *Int J Rheum Dis*, 22, 1990-2000.
- CHATTERJEE, S. & MUDHER, A. 2018. Alzheimer's Disease and Type 2 Diabetes: A Critical Assessment of the Shared Pathological Traits. *Front Neurosci*, 12, 383.
- CHEIGNON, C., TOMAS, M., BONNEFONT-ROUSSELOT, D., FALLER, P., HUREAU, C. & COLLIN, F. 2017. Oxidative stress and the amyloid beta peptide in Alzheimer's disease. *Redox Biol*, 14, 450-464.

- CHELLAPPA, K., PERRON, I. J., NAIDOO, N. & BAUR, J. A. 2019. The leptin sensitizer celastrol reduces age-associated obesity and modulates behavioral rhythms. *Aging Cell*, 18, e12874.
- CHEUNG, K., LAU, W., YU, M.-S., LAI, C., YEUNG, S.-C., SO, K.-F. & CHANG, R. 2008. Effects of all-trans-retinoic acid on human SH-SY5Y neuroblastoma as in-vitro model in neurotoxicity research. *Neurotoxicology*, 30, 127-35.
- CHEN, L., LIU, L., YIN, J., LUO, Y. & HUANG, S. 2009. Hydrogen peroxide-induced neuronal apoptosis is associated with inhibition of protein phosphatase 2A and 5, leading to activation of MAPK pathway. *The International Journal of Biochemistry & Cell Biology*, 41, 1284-1295.
- CHEN, C., JIANG, J., LÜ, J. M., CHAI, H., WANG, X., LIN, P. H. & YAO, Q. 2010. Resistin decreases expression of endothelial nitric oxide synthase through oxidative stress in human coronary artery endothelial cells. *Am J Physiol Heart Circ Physiol*, 299, H193-201.
- CHEN, C., LI, B., CHENG, G., YANG, X., ZHAO, N. & SHI, R. 2018. Amentoflavone Ameliorates A β 1–42-Induced Memory Deficits and Oxidative Stress in Cellular and Rat Model. *Neurochemical Research*, 43, 857-868.
- CHEN, Y.-Z., ZHOU, S.-Q., CHEN, Y.-Q., PENG, H. & ZHUANG, Y.-G. 2020. Plasma Adipokines in Patients Resuscitated from Cardiac Arrest: Difference of Visfatin between Survivors and Nonsurvivors. *Disease Markers*, 2020, 9608276.
- CHEW, W. F., MASYITA, M., LEONG, P. P., BOO, N. Y., ZIN, T., CHOO, K. B. & YAP, S. F. 2014. Prevalence of obesity and its associated risk factors among Chinese adults in a Malaysian suburban village. *Singapore medical journal*, 55, 84-91.
- CHI, H., CHANG, H. Y. & SANG, T. K. 2018. Neuronal Cell Death Mechanisms in Major Neurodegenerative Diseases. *Int J Mol Sci*, 19.
- CHOE, S. S., HUH, J. Y., HWANG, I. J., KIM, J. I. & KIM, J. B. 2016. Adipose Tissue Remodeling: Its Role in Energy Metabolism and Metabolic Disorders. *Frontiers in Endocrinology*, 7.
- CHOI, S. A., LEE, J. Y., KWON, S. E., WANG, K.-C., PHI, J. H., CHOI, J. W., JIN, X., LIM, J. Y., KIM, H. & KIM, S.-K. 2015. Human Adipose Tissue-Derived Mesenchymal Stem Cells Target Brain Tumor-Initiating Cells. *PLOS ONE*, 10, e0129292.

- CLARKE, J. R., LYRA, E. S. N. M., FIGUEIREDO, C. P., FROZZA, R. L., LEDO, J. H., BECKMAN, D., KATASHIMA, C. K., RAZOLLI, D., CARVALHO, B. M., FRAZAO, R., SILVEIRA, M. A., RIBEIRO, F. C., BOMFIM, T. R., NEVES, F. S., KLEIN, W. L., MEDEIROS, R., LAFERLA, F. M., CARVALHEIRA, J. B., SAAD, M. J., MUNOZ, D. P., VELLOSO, L. A., FERREIRA, S. T. & DE FELICE, F. G. 2015. Alzheimer-associated Abeta oligomers impact the central nervous system to induce peripheral metabolic deregulation. *EMBO Mol Med*, 7, 190-210.
- CODOÑER-FRANCH, P. & ALONSO-IGLESIAS, E. 2015. Resistin: Insulin resistance to malignancy. *Clinica Chimica Acta*, 438, 46-54.
- COHEN, P. & SPIEGELMAN, B. M. 2016. Cell biology of fat storage. *Molecular biology of the cell*, 27, 2523-2527.
- COELHO, M., OLIVEIRA, T. & FERNANDES, R. 2013. Biochemistry of adipose tissue: an endocrine organ. *Arch Med Sci*, 9, 191-200.
- COIMBRA, S., BRANDÃO PROENÇA, J., SANTOS-SILVA, A. & NEUPARTH, M. J. 2014. Adiponectin, leptin, and chemerin in elderly patients with type 2 diabetes mellitus: a close linkage with obesity and length of the disease. *Biomed Res Int*, 2014, 701915.
- CORRÊA, L. H., HEYN, G. S. & MAGALHAES, K. G. 2019. The Impact of the Adipose Organ Plasticity on Inflammation and Cancer Progression. *Cells*, 8.
- CONGDON, E. E. & SIGURDSSON, E. M. 2018. Tau-targeting therapies for Alzheimer disease. *Nat Rev Neurol*, 14, 399-415.
- COYLE, C. H., MARTINEZ, L. J., COLEMAN, M. C., SPITZ, D. R., WEINTRAUB, N. L. & KADER, K. N. 2006. Mechanisms of H₂O₂-induced oxidative stress in endothelial cells. *Free Radic Biol Med*, 40, 2206-13.
- CREHAN, H. & LEMERE, C. A. 2016. Chapter 7 - Anti-Amyloid- β Immunotherapy for Alzheimer's Disease. In: WOLFE, M. S. (ed.) *Developing Therapeutics for Alzheimer's Disease*. Boston: Academic Press.
- CREWS, L. & MASLIAH, E. 2010. Molecular mechanisms of neurodegeneration in Alzheimer's disease. *Hum Mol Genet*, 19, R12-20.

- CUEVAS-RAMOS, D., ALMEDA-VALDES, P., AGUILAR-SALINAS, C. A., CUEVAS-RAMOS, G., CUEVAS-SOSA, A. A. & GOMEZ-PEREZ, F. J. 2009. The role of fibroblast growth factor 21 (FGF21) on energy balance, glucose and lipid metabolism. *Curr Diabetes Rev*, 5, 216-20.
- CURTIS, T. M., HANNETT, J. M., HARMAN, R. M., PUOPLO, N. A. & VAN DE WALLE, G. R. 2018. The secretome of adipose-derived mesenchymal stem cells protects SH-SY5Y cells from arsenic-induced toxicity, independent of a neuron-like differentiation mechanism. *NeuroToxicology*, 67, 54-64.
- DAI, M.-H., ZHENG, H., ZENG, L.-D. & ZHANG, Y. 2017. The genes associated with earlyonset Alzheimer's disease. *Oncotarget*, 9, 15132-15143.
- DAMAL VILLIVALAM, S., YOU, D., KIM, J., LIM, H. W., XIAO, H., ZUSHIN, P.-J. H., OGURI, Y., AMINS, P. & KANG, S. 2020. TET1 is a beige adipocyte-selective epigenetic suppressor of thermogenesis. *Nature Communications*, 11, 4313.
- DATKI, Z., JUHÁSZ, A., GÁLFI, M., SOÓS, K., PAPP, R., ZÁDORI, D. & PENKE, B. 2003. Method for measuring neurotoxicity of aggregating polypeptides with the MTT assay on differentiated neuroblastoma cells. *Brain Res Bull*, 62, 223-9.
- DARDENO, T. A., CHOU, S. H., MOON, H.-S., CHAMBERLAND, J. P., FIORENZA, C. G. & MANTZOROS, C. S. 2010. Leptin in human physiology and therapeutics. *Frontiers in Neuroendocrinology*, 31, 377-393.
- DE MEDEIROS, L. M., DE BASTIANI, M. A., RICO, E. P., SCHONHOFEN, P., PFAFFENSELLER, B., WOLLENHAUPT-AGUIAR, B., GRUN, L., BARBÉTUANA, F., ZIMMER, E. R., CASTRO, M. A. A., PARSONS, R. B. & KLAMT, F. 2019. Cholinergic Differentiation of Human Neuroblastoma SH-SY5Y Cell Line and Its Potential Use as an In-vitro Model for Alzheimer's Disease Studies. *Molecular Neurobiology*, 56, 7355-7367.
- DEMIRCI, S., AYNALI, A., DEMIRCI, K., DEMIRCI, S. & ARIDOĞAN, B. C. 2017. The Serum Levels of Resistin and Its Relationship with Other Proinflammatory Cytokines in Patients with Alzheimer's Disease. *Clinical psychopharmacology and neuroscience : the official scientific journal of the Korean College of Neuropsychopharmacology*, 15, 59-63.
- DEMENTIAUK (2017) Types of Dementia. Available at: dementiauk.org/about-dementia/types-of-dementia/ (Accessed on 01 March 2021).

DEMENTIASTATISTICS (2021) Statistics about dementia. Available at: <https://www.dementiastatistics.org/statistics-about-dementia/> (Accessed on 19 February 2021).

DUAN, L., BHATTACHARYYA, B. J., BELMADANI, A., PAN, L., MILLER, R. J. & KESSLER, J. A. 2014. Stem cell derived basal forebrain cholinergic neurons from Alzheimer's disease patients are more susceptible to cell death. *Molecular Neurodegeneration*, 9, 3.

DUBEY, S. K., RAM, M. S., KRISHNA, K. V., SAHA, R. N., SINGHVI, G., AGRAWAL, M., AJAZUDDIN, SARAF, S., SARAF, S. & ALEXANDER, A. 2019. Recent Expansions on Cellular Models to Uncover the Scientific Barriers Towards Drug Development for Alzheimer's Disease. *Cellular and Molecular Neurobiology*, 39, 181-209.

DUBOIS, B., HAMPEL, H., FELDMAN, H. H., SCHELTENS, P., AISEN, P., ANDRIEU, S., BAKARDJIAN, H., BENALI, H., BERTRAM, L., BLENNOW, K., BROICH, K., CAVEDO, E., CRUTCH, S., DARTIGUES, J. F., DUYSKAERTS, C., EPELBAUM, S., FRISONI, G. B., GAUTHIER, S., GENTHON, R., GOUW, A. A., HABERT, M. O., HOLTZMAN, D. M., KIVIPELTO, M., LISTA, S., MOLINUEVO, J. L., O'BRYANT, S. E., RABINOVICI, G. D., ROWE, C., SALLOWAY, S., SCHNEIDER, L. S., SPERLING, R., TEICHMANN, M., CARRILLO, M. C., CUMMINGS, J. & JACK, C. R., JR. 2016. Preclinical Alzheimer's disease: Definition, natural history, and diagnostic criteria. *Alzheimers Dement*, 12, 292-323.

DUNN, B., STEIN, P. & CAVAZZONI, P. 2021. Approval of Aducanumab for Alzheimer Disease—the FDA's Perspective. *JAMA Internal Medicine*.

DULLOO, A. G., JACQUET, J., SOLINAS, G., MONTANI, J. P. & SCHUTZ, Y. 2010. Body composition phenotypes in pathways to obesity and the metabolic syndrome. *Int J Obes (Wiseman et al.)*, 34 Suppl 2, S4-17.

DORJGOCHOO, T., GAO, Y. T., CHOW, W. H., SHU, X. O., YANG, G., CAI, Q., ROTHMAN, N., CAI, H., LI, H., DENG, X., SHRUBSOLE, M. J., MURFF, H., MILNE, G., ZHENG, W. & DAI, Q. 2011. Obesity, age, and oxidative stress in middle-aged and older women. *Antioxid Redox Signal*, 14, 2453-60.

DONATO, A. J., ESKURZA, I., SILVER, A. E., LEVY, A. S., PIERCE, G. L., GATES, P. E. & SEALS, D. R. 2007. Direct evidence of endothelial oxidative stress with aging in humans: relation to impaired endothelium-dependent dilation and upregulation of nuclear factor-kappaB. *Circ Res*, 100, 1659-66.

- DWANE, S., DURACK, E. & KIELY, P. A. 2013. Optimising parameters for the differentiation of SH-SY5Y cells to study cell adhesion and cell migration. *BMC Research Notes*, 6, 366.
- EDWARDS III, G. A., GAMEZ, N., ESCOBEDO, G., JR., CALDERON, O. & MORENO-GONZALEZ, I. 2019. Modifiable Risk Factors for Alzheimer's Disease. *Frontiers in aging neuroscience*, 11, 146-146.
- EFEOGLU, E., CASEY, A. & BYRNE, H. J. 2016. In-vitro monitoring of time and dose dependent cytotoxicity of aminated nanoparticles using Raman spectroscopy. *Analyst*, 141, 5417-5431.
- EL-HATTAB, M. Y., NAGUMO, Y., GOURRONC, F. A., KLINGELHUTZ, A. J., ANKRUM, J. A. & SANDER, E. A. 2020. Human Adipocyte Conditioned Medium Promotes In-vitro Fibroblast Conversion to Myofibroblasts. *Scientific Reports*, 10, 10286.
- ELLIS, J. M. 2005. Cholinesterase inhibitors in the treatment of dementia. *J Am Osteopath Assoc*, 105, 145-58.
- ENCINAS, M., IGLESIAS, M., LIU, Y., WANG, H., MUHAISEN, A., CEÑA, V., GALLEGRO, C. & COMELLA, J. X. 2000. Sequential treatment of SH-SY5Y cells with retinoic acid and brain-derived neurotrophic factor gives rise to fully differentiated, neurotrophic factor-dependent, human neuron-like cells. *J Neurochem*, 75, 991-1003.
- ERNST, M. C. & SINAL, C. J. 2010. Chemerin: at the crossroads of inflammation and obesity. *Trends in Endocrinology & Metabolism*, 21, 660-667
- EVANS, P. H. 1993. Free radicals in brain metabolism and pathology. *Br Med Bull*, 49, 57787.
- EVIN, G. & WEIDEMANN, A. 2002. Biogenesis and metabolism of Alzheimer's disease A β amyloid peptides. *Peptides*, 23, 1285-1297.
- FARSAM, V., BASU, A., GATZKA, M., TREIBER, N., SCHNEIDER, L. A., MULAW, M. A., LUCAS, T., KOCHANNEK, S., DUMMER, R., LEVESQUE, M. P., WLASCHEK, M. & SCHARFFETTER-KOCHANNEK, K. 2016. Senescent fibroblast-derived Chemerin promotes squamous cell carcinoma migration. *Oncotarget*, 7, 83554-83569.

FAROOQI, I. S. & O'RAHILLY, S. 2014. 20 years of leptin: human disorders of leptin action. *J Endocrinol*, 223, T63-70

FDA (2021) FDA's Decision to Approve New Treatment for Alzheimer's Disease. Available at: <https://www.fda.gov/drugs/news-events-human-drugs/fdas-decision-approve-new-treatment-alzheimers-disease> (Accessed on 04 August 2021).

FERNÁNDEZ-SÁNCHEZ, A., MADRIGAL-SANTILLÁN, E., BAUTISTA, M., ESQUIVEL-SOTO, J., MORALES-GONZÁLEZ, A., ESQUIVEL-CHIRINO, C., DURANTE-MONTIEL, I., SÁNCHEZ-RIVERA, G., VALADEZ-VEGA, C. & MORALES-GONZÁLEZ, J. A. 2011a. Inflammation, oxidative stress, and obesity. *International journal of molecular sciences*, 12, 3117-3132.

FERNÁNDEZ-SÁNCHEZ, A., MADRIGAL-SANTILLÁN, E., BAUTISTA, M., ESQUIVEL-SOTO, J., MORALES-GONZÁLEZ, Á., ESQUIVEL-CHIRINO, C., DURANTE-MONTIEL, I., SÁNCHEZ-RIVERA, G., VALADEZ-VEGA, C. & MORALES-GONZÁLEZ, J. A. 2011b. Inflammation, Oxidative Stress, and Obesity. *Int J Mol Sci*, 12, 3117-32.

FERNANDEZ, A. M. & TORRES-ALEMÁN, I. 2012. The many faces of insulin-like peptide signalling in the brain. *Nat Rev Neurosci*, 13, 225-39.

FERRARO, S. A., DOMINGO, M. G., ETCHEVERRITO, A., OLMEDO, D. G. & TASAT, D. R. 2020. Neurotoxicity mediated by oxidative stress caused by titanium dioxide nanoparticles in human neuroblastoma (SH-SY5Y) cells. *J Trace Elem Med Biol*, 57, 126413.

FISHER CENTRE FOR ALZHEIMERS RESEARCH FOUNDATION (2021) The difference between Alzheimer's and dementia. Available at: <https://www.alzinfo.org/treatment-care/blogs/2010/08/the-difference-between-alzheimers-and-dementia/> (Accessed on 21 July 2021).

FIUZA-LUCES, C., VALENZUELA, P. L., LAINE-MENÉNDEZ, S., FERNÁNDEZ-DE LA TORRE, M., BERMEJO-GÓMEZ, V., RUFÍAN-VÁZQUEZ, L., ARENAS, J., MARTÍN, M. A., LUCIA, A. & MORÁN, M. 2019. Physical Exercise and Mitochondrial Disease: Insights From a Mouse Model. *Frontiers in Neurology*, 10.

FÜLÖP, P., SERES, I., LÓRINCZ, H., HARANGI, M., SOMODI, S. & PARAGH, G. 2014. Association of chemerin with oxidative stress, inflammation and classical adipokines in non-diabetic obese patients. *J Cell Mol Med*, 18, 1313-20.

- FORSBY, A. 2011. Neurite Degeneration in Human Neuronal SH-SY5Y Cells as an Indicator of Axonopathy. *In: ASCHNER, M., SUÑOL, C. & BAL-PRICE, A. (eds.) Cell Culture Techniques*. Totowa, NJ: Humana Press.
- FORSTER, J. I., KÖGLSBERGER, S., TREFOIS, C., BOYD, O., BAUMURATOV, A. S., BUCK, L., BALLING, R. & ANTONY, P. M. 2016. Characterization of Differentiated SH-SY5Y as Neuronal Screening Model Reveals Increased Oxidative Vulnerability. *J Biomol Screen*, 21, 496-509.
- FRACASSI, A., MARCATTI, M., ZOLOCHEVSKA, O., TABOR, N., WOLTJER, R., MORENO, S. & TAGLIALATELA, G. 2021. Oxidative Damage and Antioxidant Response in Frontal Cortex of Demented and Nondemented Individuals with Alzheimer's Neuropathology. *The Journal of Neuroscience*, 41, 538-554.
- GABIN, J. M., TAMBS, K., SALTVEDT, I., SUND, E. & HOLMEN, J. 2017. Association between blood pressure and Alzheimer disease measured up to 27 years prior to diagnosis: the HUNT Study. *Alzheimer's Research & Therapy*, 9, 37.
- GARCÍA-SÁNCHEZ, A., MIRANDA-DÍAZ, A. G. & CARDONA-MUÑOZ, E. G. 2020. The Role of Oxidative Stress in Physiopathology and Pharmacological Treatment with Pro- and Antioxidant Properties in Chronic Diseases. *Oxidative Medicine and Cellular Longevity*, 2020, 2082145.
- GARCIMARTÍN, A., LÓPEZ-OLIVA, M. E., GONZÁLEZ, M. P., SÁNCHEZ-MUNIZ, F. J. & BENEDÍ, J. 2017. Hydrogen peroxide modifies both activity and isoforms of acetylcholinesterase in human neuroblastoma SH-SY5Y cells. *Redox Biology*, 12, 719-726.
- GARRIDO-PASCUAL, P., ALONSO-VARONA, A., CASTRO, B., BURÓN, M. & PALOMARES, T. 2020. Hydrogen Peroxide-Preconditioned Human Adipose-Derived Stem Cells Enhance the Recovery of Oligodendrocyte-Like Cells after Oxidative Stress-Induced Damage. *Int J Mol Sci*, 21.
- GIBSON, G. E. & HUANG, H.-M. 2005. Oxidative stress in Alzheimer's disease. *Neurobiology of Aging*, 26, 575-578.
- GEJL, M., GJEDDE, A., EGEFJORD, L., MØLLER, A., HANSEN, S. B., VANG, K., RODELL, A., BRÆNDGAARD, H., GOTTRUP, H., SCHACHT, A., MØLLER, N., BROCK, B. & RUNGBY, J. 2016. In Alzheimer's Disease, 6-Month Treatment with GLP-1 Analog Prevents Decline of Brain Glucose Metabolism: Randomized, Placebo-Controlled, Double-Blind Clinical Trial. *Front Aging Neurosci*, 8.

- GELLA, A. & DURANY, N. 2009. Oxidative stress in Alzheimer disease. *Cell adhesion & migration*, 3, 88-93.
- GETACHEW, B., CSOKA, A. B., BHATTI, A., COPELAND, R. L. & TIZABI, Y. 2020. Butyrate Protects Against Salsolinol-Induced Toxicity in SH-SY5Y Cells: Implication for Parkinson's Disease. *Neurotoxicity Research*, 38, 596-602.
- GOLDIE, B. J., BARNETT, M. M. & CAIRNS, M. J. 2014. BDNF and the maturation of posttranscriptional regulatory networks in human SH-SY5Y neuroblast differentiation. *Frontiers in cellular neuroscience*, 8, 325-325.
- GORALSKI, K. B., JACKSON, A. E., MCKEOWN, B. T. & SINAL, C. J. 2019. More Than an Adipokine: The Complex Roles of Chemerin Signaling in Cancer. *International journal of molecular sciences*, 20, 4778.
- GRATUZE, M., LEYNS, C. E. G. & HOLTZMAN, D. M. 2018. New insights into the role of TREM2 in Alzheimer's disease. *Molecular Neurodegeneration*, 13, 66.
- GREENBERG, A. S. & OBIN, M. S. 2006. Obesity and the role of adipose tissue in inflammation and metabolism. *Am J Clin Nutr*, 83, 461s-465s.
- GREENE, A. N., PARKS, L. G., SOLOMON, M. B. & PRIVETTE VINNEDGE, L. M. 2020. Loss of DEK Expression Induces Alzheimer's Disease Phenotypes in Differentiated SH-SY5Y Cells. *Frontiers in Molecular Neuroscience*, 13.
- GRUTZENDLER, J., HELMINS, K., TSAI, J. & GAN, W. B. 2007. Various dendritic abnormalities are associated with fibrillar amyloid deposits in Alzheimer's disease. *Ann N Y Acad Sci*, 1097, 30-9.
- GU, L., SU, L., CHEN, Q., LIANG, B., QIN, Y., XIE, J., WU, G., YAN, Y., LONG, J., WU, H., TAN, J., DOU, W., CHEN, W., WU, P. & WANG, J. 2013. Association between the apolipoprotein E gene polymorphism and ischemic stroke in Chinese populations: New data and meta-analysis. *Experimental and therapeutic medicine*, 5, 853-859.
- GU, Y., NIEVES, J. W., STERN, Y., LUCHSINGER, J. A. & SCARMEAS, N. 2010. Food combination and Alzheimer disease risk: a protective diet. *Arch Neurol*, 67, 699-706.

- GUGLIELMOTTO, M., GILIBERTO, L., TAMAGNO, E. & TABATON, M. 2010. Oxidative stress mediates the pathogenic effect of different Alzheimer's disease risk factors. *Frontiers in Aging Neuroscience*, 2.
- GUO, T., ZHANG, D., ZENG, Y., HUANG, T. Y., XU, H. & ZHAO, Y. 2020. Molecular and cellular mechanisms underlying the pathogenesis of Alzheimer's disease. *Molecular Neurodegeneration*, 15, 40.
- GUO, Z., TANG, J., WANG, J., ZHENG, F., ZHANG, C., WANG, Y.-L., CAI, P., SHAO, W., YU, G., WU, S. & LI, H. 2021. The negative role of histone acetylation in cobalt chloride-induced neurodegenerative damages in SHSY5Y cells. *Ecotoxicology and Environmental Safety*, 209, 111832.
- GUPTA, A. & GOYAL, R. 2016. Amyloid beta plaque: a culprit for neurodegeneration. *Acta Neurologica Belgica*, 116, 445-450.
- HAHN, H. J., KIM, K. B., AN, I. S., AHN, K. J. & HAN, H. J. 2017. Protective effects of rosmarinic acid against hydrogen peroxide-induced cellular senescence and the inflammatory response in normal human dermal fibroblasts. *Mol Med Rep*, 16, 9763-9769.
- HADARI, F., MOHAMMADSHAHI, M., ZAREI, M. & FATHI, M. 2019. Protective effect of citrus lemon on inflammation and adipokine levels in acrylamide-induced oxidative stress in rats. *Brazilian Journal of Pharmaceutical Sciences*, 55.
- HAMELIN, L., LAGARDE, J., DOROTHÉE, G., LEROY, C., LABIT, M., COMLEY, R. A., DE SOUZA, L. C., CORNE, H., DAUPHINOT, L., BERTOUX, M., DUBOIS, B., GERVAIS, P., COLLIOT, O., POTIER, M. C., BOTTLAENDER, M. & SARAZIN, M. 2016. Early and protective microglial activation in Alzheimer's disease: a prospective study using 18F-DPA-714 PET imaging. *Brain*, 139, 1252-64.
- HANAFY, D. M., PRENZLER, P. D., BURROWS, G. E., GURUSINGHE, S., THEJER, B. M., OBIED, H. K. & HILL, R. A. 2020. Neuroprotective Activity of Mentha Species on Hydrogen Peroxide-Induced Apoptosis in SH-SY5Y Cells. *Nutrients*, 12, 1366.
- HALEY, M. J., MULLARD, G., HOLLYWOOD, K. A., COOPER, G. J., DUNN, W. B. & LAWRENCE, C. B. 2017. Adipose tissue and metabolic and inflammatory responses to stroke are altered in obese mice. *Disease Models & Mechanisms*, 10, 1229-1243.

- HALEY, M. J., WHITE, C. S., ROBERTS, D., O'TOOLE, K., CUNNINGHAM, C. J., RIVERS-AUTY, J., O'BOYLE, C., LANE, C., HEANEY, O., ALLAN, S. M. & LAWRENCE, C. B. 2020. Stroke Induces Prolonged Changes in Lipid Metabolism, the Liver and Body Composition in Mice. *Translational stroke research*, 11, 837-850.
- HALL-ROBERTS, H., AGARWAL, D., OBST, J., SMITH, T. B., MONZÓN-SANDOVAL, J., DI DANIEL, E., WEBBER, C., JAMES, W. S., MEAD, E., DAVIS, J. B. & COWLEY, S. A. 2020. TREM2 Alzheimer's variant R47H causes similar transcriptional dysregulation to knockout, yet only subtle functional phenotypes in human iPSC-derived macrophages. *Alzheimer's Research & Therapy*, 12, 151.
- HAROLD, D., ABRAHAM, R., HOLLINGWORTH, P., SIMS, R., GERRISH, A., HAMSHERE, M. L., PAHWA, J. S., MOSKVINA, V., DOWZELL, K., WILLIAMS, A., JONES, N., THOMAS, C., STRETTON, A., MORGAN, A. R., LOVESTONE, S., POWELL, J., PROITSI, P., LUPTON, M. K., BRAYNE, C., RUBINSZTEIN, D. C., GILL, M., LAWLOR, B., LYNCH, A., MORGAN, K., BROWN, K. S., PASSMORE, P. A., CRAIG, D., MCGUINNESS, B., TODD, S., HOLMES, C., MANN, D., SMITH, A. D., LOVE, S., KEHOE, P. G., HARDY, J., MEAD, S., FOX, N., ROSSOR, M., COLLINGE, J., MAIER, W., JESSEN, F., SCHURMANN, B., HEUN, R., VAN DEN BUSSCHE, H., HEUSER, I., KORNUBER, J., WILTFANG, J., DICHGANS, M., FROLICH, L., HAMPEL, H., HULL, M., RUJESCU, D., GOATE, A. M., KAUWE, J. S., CRUCHAGA, C., NOWOTNY, P., MORRIS, J. C., MAYO, K., SLEEGERS, K., BETTENS, K., ENGELBORGH, S., DE DEYN, P. P., VAN BROECKHOVEN, C., LIVINGSTON, G., BASS, N. J., GURLING, H., MCQUILLIN, A., GWILLIAM, R., DELOUKAS, P., AL-CHALABI, A., SHAW, C. E., TSOLAKI, M., SINGLETON, A. B., GUERREIRO, R., MUHLEISEN, T. W., NOTHEN, M. M., MOEBUS, S., JOCKEL, K. H., KLOPP, N., WICHMANN, H. E., CARRASQUILLO, M. M., PANKRATZ, V. S., YOUNKIN, S. G., HOLMANS, P. A., O'DONOVAN, M., OWEN, M. J. & WILLIAMS, J. 2009. Genome-wide association study identifies variants at CLU and PICALM associated with Alzheimer's disease. *Nat Genet*, 41, 1088-93.
- HARDY, J. A. & HIGGINS, G. A. 1992. Alzheimer's disease: the amyloid cascade hypothesis. *Science*, 256, 184-5.
- HELPER, G., ROSS, A. W., THOMSON, L. M., MAYER, C. D., STONEY, P. N., MCCAFFERY, P. J. & MORGAN, P. J. 2016a. A neuroendocrine role for chemerin in hypothalamic remodelling and photoperiodic control of energy balance. *Sci Rep*, 6, 26830.

- HELPER, G., ROSS, A. W., THOMSON, L. M., MAYER, C. D., STONEY, P. N., MCCAFFERY, P. J. & MORGAN, P. J. 2016b. A neuroendocrine role for chemerin in hypothalamic remodelling and photoperiodic control of energy balance. *Scientific Reports*, 6, 26830.
- HIPPIUS, H. & NEUNDÖRFER, G. 2003. The discovery of Alzheimer's disease. *Dialogues in clinical neuroscience*, 5, 101-108.
- HONG, S., DISSING-OLESEN, L. & STEVENS, B. 2016. New insights on the role of microglia in synaptic pruning in health and disease. *Current Opinion in Neurobiology*, 36, 128-134.
- HRUBY, A. & HU, F. B. 2015a. The Epidemiology of Obesity: A Big Picture. *Pharmacoeconomics*, 33, 673-689.
- HRUBY, A. & HU, F. B. 2015b. The Epidemiology of Obesity: A Big Picture. *Pharmacoeconomics*, 33, 673-89.
- HU, K., LIU, F. & GONG, C.-X. 2016. Tau and neurodegenerative disease: the story so far. *Nature Reviews Neurology*, 12, 15-27.
- HU, B., SONG, W., TANG, Y., SHI, M., LI, H. & YU, D. 2019. Induction of Chemerin on Autophagy and Apoptosis in Dairy Cow Mammary Epithelial Cells. *Animals*, 9, 848.
- HUANG, W. J., ZHANG, X. & CHEN, W. W. 2016. Role of oxidative stress in Alzheimer's disease. *Biomed Rep*, 4, 519-522.
- HUANG, H., ULLAH, F., ZHOU, D.-X., YI, M. & ZHAO, Y. 2019. Mechanisms of ROS Regulation of Plant Development and Stress Responses. *Frontiers in Plant Science*, 10.
- HUANG, B., LIU, J., FU, S., ZHANG, Y., LI, Y., HE, D., RAN, X., YAN, X., DU, J., MENG, T., GAO, X. & LIU, D. 2020. α -Cyperone Attenuates H₂O₂-Induced Oxidative Stress and Apoptosis in SH-SY5Y Cells via Activation of Nrf2. *Frontiers in Pharmacology*, 11.
- ISGRÒ, M. A., BOTTONI, P. & SCATENA, R. 2015. Neuron-Specific Enolase as a Biomarker: Biochemical and Clinical Aspects. *Adv Exp Med Biol*, 867, 125-43.

- ISMAIL, N., ISMAIL, M., AZMI, N. H., ABU BAKAR, M. F., BASRI, H. & ABDULLAH, M. A. 2016. Modulation of Hydrogen Peroxide-Induced Oxidative Stress in Human Neuronal Cells by Thymoquinone-Rich Fraction and Thymoquinone via Transcriptomic Regulation of Antioxidant and Apoptotic Signaling Genes. *Oxid Med Cell Longev*, 2016, 2528935.
- IQBAL, K., LIU, F. & GONG, C.-X. 2014. Alzheimer disease therapeutics: focus on the disease and not just plaques and tangles. *Biochemical pharmacology*, 88, 631-639.
- IQBAL, K., LIU, F. & GONG, C.-X. 2016. Tau and neurodegenerative disease: the story so far. *Nature Reviews Neurology*, 12, 15-27.
- IQBAL, T., ZHANG, D., ZENG, Y., HUANG, T. Y., XU, H. & ZHAO, Y. 2020. Molecular and cellular mechanisms underlying the pathogenesis of Alzheimer's disease. *Molecular Neurodegeneration*, 15, 40.
- IZQUIERDO, A. G., CRUJEIRAS, A. B., CASANUEVA, F. F. & CARREIRA, M. C. 2019. Leptin, Obesity, and Leptin Resistance: Where Are We 25 Years Later? *Nutrients*, 11, 2704.
- JAMALUDDIN, M. S., WEAKLEY, S. M., YAO, Q. & CHEN, C. 2012. Resistin: functional roles and therapeutic considerations for cardiovascular disease. *British journal of pharmacology*, 165, 622-632.
- JANTAS, D., CHWASTEK, J., GRYGIER, B. & LASON, W. 2020. Neuroprotective Effects of Necrostatin-1 Against Oxidative Stress-Induced Cell Damage: an Involvement of Cathepsin D Inhibition. *Neurotoxicity Research*.
- JÄKEL, S. & DIMOU, L. 2017. Glial Cells and Their Function in the Adult Brain: A Journey through the History of Their Ablation. *Frontiers in Cellular Neuroscience*, 11.
- JAUHARI, A., SINGH, T., PANDEY, A., SINGH, P., SINGH, N., SRIVASTAVA, A. K., PANT, A. B., PARMAR, D. & YADAV, S. 2017. Differentiation Induces Dramatic Changes in miRNA Profile, Where Loss of Dicer Diverts Differentiating SH-SY5Y Cells Toward Senescence. *Mol Neurobiol*, 54, 4986-4995.

- JIANG, J. & JIANG, H. 2015. Efficacy and adverse effects of memantine treatment for Alzheimer's disease from randomized controlled trials. *Neurological Sciences*, 36, 1633-1641.
- JIE, M., YACIR, B., SARAH AL, R., GHISLAINE, P., LAURE, R., DELPHINE, C. & MOHAMMED, T. 2018. Resistin inhibits neuronal autophagy through Toll-like receptor 4. *Journal of Endocrinology*, 238, 77-89.
- JO, D. G., ARUMUGAM, T. V., WOO, H. N., PARK, J. S., TANG, S. C., MUGHAL, M., HYUN, D. H., PARK, J. H., CHOI, Y. H., GWON, A. R., CAMANDOLA, S., CHENG, A., CAI, H., SONG, W., MARKESBERY, W. R. & MATTSON, M. P. 2010. Evidence that gamma-secretase mediates oxidative stress-induced beta-secretase expression in Alzheimer's disease. *Neurobiol Aging*, 31, 917-25.
- JOHNSTONE, D. M., MITROFANIS, J. & STONE, J. 2015. Targeting the body to protect the brain: inducing neuroprotection with remotely-applied near infrared light. *Neural regeneration research*, 10, 349-351.
- JONES, N. S. & REBECK, G. W. 2018. The Synergistic Effects of APOE Genotype and Obesity on Alzheimer's Disease Risk. *Int J Mol Sci*, 20.
- JONG, Y. J. I., DALEMAR, L. R., SEEHRA, K. & BAENZIGER, N. L. 2002. Bradykinin receptor modulation in cellular models of aging and Alzheimer's disease. *International Immunopharmacology*, 2, 18.
- JONG, Y.-J. I., FORD, S. R., SEEHRA, K., MALAVE, V. B. & BAENZIGER, N. L. 2003. Alzheimer's disease skin fibroblasts selectively express a bradykinin signaling pathway mediating tau protein Ser phosphorylation. *The FASEB Journal*, 17, 2319-232.
- JORDAN, M., VOISARD, D., BERTHOUD, A., TERCIER, L., KLEUSER, B., BAER, G. & BROLY, H. 2013. Cell culture medium improvement by rigorous shuffling of components using media blending. *Cytotechnology*, 65, 31-40.
- JOSHI, A. U., VAN WASSENHOVE, L. D., LOGAS, K. R., MINSHAS, P. S., ANDREASSON, K. I., WEINBERG, K. I., CHEN, C. H. & MOCHLY-ROSEN, D. 2019. Aldehyde dehydrogenase 2 activity and aldehydic load contribute to neuroinflammation and Alzheimer's disease related pathology. *Acta Neuropathol Commun*, 7, 190.

- KAEIDI, A., HAJIALIZADEH, Z., JAHANDARI, F. & FATEMI, I. 2019. Leptin attenuates oxidative stress and neuronal apoptosis in hyperglycemic condition. *Fundamental & Clinical Pharmacology*, 33, 75-83.
- PENNEY, J., RALVENIUS, W. T. & TSAI, L.-H. 2020. Modeling Alzheimer's disease with iPSC-derived brain cells. *Molecular Psychiatry*, 25, 148-167.
- KAMETANI, F. & HASEGAWA, M. 2018. Reconsideration of Amyloid Hypothesis and Tau Hypothesis in Alzheimer's Disease. *Front Neurosci*, 12, 25.
- KAMIGAKI, M., SAKAUE, S., TSUJINO, I., OHIRA, H., IKEDA, D., ITOH, N., ISHIMARU, S., OHTSUKA, Y. & NISHIMURA, M. 2006. Oxidative stress provokes atherogenic changes in adipokine gene expression in 3T3-L1 adipocytes. *Biochemical and Biophysical Research Communications*, 339, 624-632.
- KARCZEWSKA-KUPCZEWSKA, M., NIKOŁAJUK, A., STEFANOWICZ, M., MATULEWICZ, N., KOWALSKA, I. & STRĄCZKOWSKI, M. 2020. Serum and adipose tissue chemerin is differentially related to insulin sensitivity. *Endocr Connect*, 9, 360-369.
- KASSOTIS, C. D., MASSE, L., KIM, S., SCHLEZINGER, J. J., WEBSTER, T. F. & STAPLETON, H. M. 2017. Characterization of Adipogenic Chemicals in Three Different Cell Culture Systems: Implications for Reproducibility Based on Cell Source and Handling. *Scientific Reports*, 7, 42104.
- KERN, D. M., CEPEDA, M. S., FLORES, C. M. & WITTENBERG, G. M. 2021. Application of Real-World Data and the REWARD Framework to Detect Unknown Benefits of Memantine and Identify Potential Disease Targets for New NMDA Receptor Antagonists. *CNS Drugs*.
- KHEMKA, V. K., BAGCHI, D., BANDYOPADHYAY, K., BIR, A., CHATTOPADHYAY, M., BISWAS, A., BASU, D. & CHAKRABARTI, S. 2014. Altered serum levels of adipokines and insulin in probable Alzheimer's disease. *J Alzheimers Dis*, 41.
- KIM, M.-H. & KIM, H. 2021. Role of Leptin in the Digestive System. *Frontiers in Pharmacology*, 12.

- KO, J.-H., UM, J.-Y., LEE, S.-G., YANG, W. M., SETHI, G. & AHN, K. S. 2019. Conditioned media from adipocytes promote proliferation, migration, and invasion in melanoma and colorectal cancer cells. *Journal of Cellular Physiology*, 234, 18249-18261.
- KONDO, T., ASAI, M., TSUKITA, K., KUTOKU, Y., OHSAWA, Y., SUNADA, Y., IMAMURA, K., EGAWA, N., YAHATA, N., OKITA, K., TAKAHASHI, K., ASAKA, I., AOI, T., WATANABE, A., WATANABE, K., KADOYA, C., NAKANO, R., WATANABE, D., MARUYAMA, K., HORI, O., HIBINO, S., CHOSHI, T., NAKAHATA, T., HIOKI, H., KANEKO, T., NAITOH, M., YOSHIKAWA, K., YAMAWAKI, S., SUZUKI, S., HATA, R., UENO, S., SEKI, T., KOBAYASHI, K., TODA, T., MURAKAMI, K., IRIE, K., KLEIN, W. L., MORI, H., ASADA, T., TAKAHASHI, R., IWATA, N., YAMANAKA, S. & INOUE, H. 2013. Modeling Alzheimer's disease with iPSCs reveals stress phenotypes associated with intracellular A β and differential drug responsiveness. *Cell Stem Cell*, 12, 487-96.
- KONYALIOGLU, S., ARMAGAN, G., YALCIN, A., ATALAYIN, C. & DAGCI, T. 2013. Effects of resveratrol on hydrogen peroxide-induced oxidative stress in embryonic neural stem cells. *Neural regeneration research*, 8, 485-495.
- KONG, S., DING, C., HUANG, L., BAI, Y., XIAO, T., GUO, J. & SU, Z. 2017. The effects of COST on the differentiation of 3T3-L1 pre-adipocytes and the mechanism of action. *Saudi journal of biological sciences*, 24, 251-255.
- KORNIENKO, J. S., SMIRNOVA, I. S., PUGOVKINA, N. A., IVANOVA, J. S., SHILINA, M. A., GRINCHUK, T. M., SHATROVA, A. N., AKSENOV, N. D., ZENIN, V. V., NIKOLSKY, N. N. & LYUBLINSKAYA, O. G. 2019. High doses of synthetic antioxidants induce premature senescence in cultivated mesenchymal stem cells. *Scientific Reports*, 9, 1296.
- KORECKA, J. A., VAN KESTEREN, R. E., BLAAS, E., SPITZER, S. O., KAMSTRA, J. H., SMIT, A. B., SWAAB, D. F., VERHAAGEN, J. & BOSSERS, K. 2013. Phenotypic characterization of retinoic acid differentiated SH-SY5Y cells by transcriptional profiling. *PloS one*, 8, e63862-e63862.
- KOTH, L. L., CAMBIER, C. J., ELLWANGER, A., SOLON, M., HOU, L., LANIER, L. L., ABRAM, C. L., HAMERMAN, J. A. & WOODRUFF, P. G. 2010. DAP12 Is Required for Macrophage Recruitment to the Lung in Response to Cigarette Smoke and Chemotaxis toward CCL2. *The Journal of Immunology*, 184, 6522-6528.

- KOVALEVICH, J. & LANGFORD, D. 2013a. Considerations for the use of SH-SY5Y neuroblastoma cells in neurobiology. *Methods Mol Biol*, 1078, 9-21.
- KOVALEVICH, J. & LANGFORD, D. 2013b. Considerations for the use of SH-SY5Y neuroblastoma cells in neurobiology. *Methods in molecular biology (Clifton, N.J.)*, 1078, 9-21.
- KUNCHALA, S. R., SUZUKI, T. & MURAYAMA, A. 2000. Photoisomerization of retinoic acid and its influence on regulation of human keratinocyte growth and differentiation.
- KRAUS, N. A., EHEBAUER, F., ZAPP, B., RUDOLPHI, B., KRAUS, B. J. & KRAUS, D. 2016. Quantitative assessment of adipocyte differentiation in cell culture. *Adipocyte*, 5, 351-358.
- KUMAR, P., NAGARAJAN, A. & UCHIL, P. D. 2018. Analysis of Cell Viability by the MTT Assay. *Cold Spring Harb Protoc*, 2018.
- KUMAR, D., LEE, B., PUAN, K. J., LEE, W., LUIS, B. S., YUSOF, N., ANDIAPPAN, A. K., DEL ROSARIO, R., POSCHMANN, J., KUMAR, P., DELIBERO, G., SINGHAL, A., PRABHAKAR, S., DE YUN, W., POIDINGER, M. & RÖTZSCHKE, O. 2019. Resistin expression in human monocytes is controlled by two linked promoter SNPs mediating NFkB p50/p50 binding and C-methylation. *Scientific Reports*, 9, 15245.
- KUNCHALA, S. R., SUZUKI, T. & MURAYAMA, A. 2000. Photoisomerization of retinoic acid and its influence on regulation of human keratinocyte growth and differentiation.
- KURODA, M., TOMINSAGA, A., NAKAGAWA, K., NISHIGUCHI, M., SEBE, M., MIYATAKE, Y., KITAMURA, T., TSUTSUMI, R., HARADA, N., NAKAYA, Y. & SAKAUE, H. 2016. DNA Methylation Suppresses Leptin Gene in 3T3-L1 Adipocytes. *PloS one*, 11, e0160532-e0160532.
- KUSMINSSKI, C. M., MCTERNAN, P. G. & KUMAR, S. 2005. Role of resistin in obesity, insulin resistance and Type II diabetes. *Clin Sci (Wiseman et al.)*, 109, 243-56.
- KWON, H. & PESSIN, J. E. 2013. Adipokines mediate inflammation and insulin resistance. *Front Endocrinol (Lausanne)*, 4, 71.

- LACE, G., SAVVA, G. M., FORSTER, G., DE SILVA, R., BRAYNE, C., MATTHEWS, F. E., BARCLAY, J. J., DAKIN, L., INCE, P. G., WHARTON, S. B. & MRC-CFAS, O. B. O. 2009. Hippocampal tau pathology is related to neuroanatomical connections: an ageing population-based study. *Brain*, 132, 1324-1334.
- LANDGRAF, K., FRIEBE, D., ULLRICH, T., KRATZSCH, J., DITTRICH, K., HERBERTH, G., ADAMS, V., KIESS, W., ERBS, S. & KÖRNER, A. 2012. Chemerin as a mediator between obesity and vascular inflammation in children. *J Clin Endocrinol Metab*, 97, E556-64.
- LANOISELÉE, H. M., NICOLAS, G., WALLON, D., ROVELET-LECRUX, A., LACOUR, M., ROUSSEAU, S., RICHARD, A. C., PASQUIER, F., ROLLIN-SILLAIRE, A., MARTINAUD, O., QUILLARD-MURAINÉ, M., DE LA SAYETTE, V., BOUTOLEAU-BRETONNIERE, C., ETCHARRY-BOUYX, F., CHAUVIRÉ, V., SARAZIN, M., LE BER, I., EPELBAUM, S., JONVEAUX, T., ROUAUD, O., CECCALDI, M., FÉLICIAN, O., GODEFROY, O., FORMAGLIO, M., CROISILE, B., AURIACOMBE, S., CHAMARD, L., VINCENT, J. L., SAUVÉE, M., MARELLI-TOSI, C., GABELLE, A., OZSANCAK, C., PARIENTE, J., PAQUET, C., HANNEQUIN, D. & CAMPION, D. 2017. APP, PSEN1, and PSEN2 mutations in early-onset Alzheimer disease: A genetic screening study of familial and sporadic cases. *PLoS Med*, 14, e1002270.
- LAURENT, C., BUÉE, L. & BLUM, D. 2018. Tau and neuroinflammation: What impact for Alzheimer's Disease and Tauopathies? *Biomedical Journal*, 41, 21-33.
- LAWRENCE, T. & NATOLI, G. 2011. Transcriptional regulation of macrophage polarization: enabling diversity with identity. *Nature Reviews Immunology*, 11, 750-761.
- LEE, S. Y., PARK, S. B., KIM, Y. E., YOO, H. M., HONG, J., CHOI, K.-J., KIM, K. Y. & KANG, D. 2019. iTRAQ-Based Quantitative Proteomic Comparison of 2D and 3D Adipocyte Cell Models Co-cultured with Macrophages Using Online 2D-nanoLC-ESI-MS/MS. *Scientific Reports*, 9, 16746.
- LEFRANC, C., FRIEDERICH-PERSSON, M., PALACIOS-RAMIREZ, R. & NGUYEN DINH CAT, A. 2018. Mitochondrial oxidative stress in obesity: role of the mineralocorticoid receptor. *Journal of Endocrinology*, 238, R143-R159.
- LESZEK, J., TRYPKA, E., TARASOV, V. V., ASHRAF, G. M. & ALIEV, G. 2017. Type 3 Diabetes Mellitus: A Novel Implication of Alzheimers Disease. *Curr Top Med Chem*, 17, 1331-1335.

- LETRA, L. & SANTANA, I. 2017. The Influence of Adipose Tissue on Brain Development, Cognition, and Risk of Neurodegenerative Disorders. *Adv Neurobiol*, 19, 151-161.
- LEVINE, M. E., LU, A. T., BENNETT, D. A. & HORVATH, S. 2015. Epigenetic age of the pre-frontal cortex is associated with neuritic plaques, amyloid load, and Alzheimer's disease related cognitive functioning. *Aging (Albany NY)*, 7, 1198-211.
- LI, L., MA, P., HUANG, C., LIU, Y., ZHANG, Y., GAO, C., XIAO, T., REN, P.-G., ZABEL, B. A. & ZHANG, J. V. 2014. Expression of chemerin and its receptors in rat testes and its action on testosterone secretion. *The Journal of endocrinology*, 220, 155-163.
- LI, R. & LIU, Y. 2016. Physical activity and prevention of Alzheimer's disease. *Journal of Sport and Health Science*, 5, 381-382.
- LI, J. & SHEN, X. 2019. Oxidative stress and adipokine levels were significantly correlated in diabetic patients with hyperglycemic crises. *Diabetology & metabolic syndrome*, 11, 13-13.
- LI, J., LU, Y., LI, N., LI, P., WANG, Z., TING, W., LIU, X. & WU, W. 2020. Chemerin: A Potential Regulator of Inflammation and Metabolism for Chronic Obstructive Pulmonary Disease and Pulmonary Rehabilitation. *BioMed Research International*, 2020, 4574509.
- LI, J., VAN VRANKEN, J. G., PONTANO VAITES, L., SCHWEPPE, D. K., HUTTLIN, E. L., ETIENNE, C., NANDHIKONDA, P., VINER, R., ROBITAILLE, A. M., THOMPSON, A. H., KUHN, K., PIKE, I., BOMGARDEN, R. D., ROGERS, J. C., GYGI, S. P. & PAULO, J. A. 2020. TMTpro reagents: a set of isobaric labeling mass tags enables simultaneous proteome-wide measurements across 16 samples. *Nat. Methods*, 17, 399.
- LIGUORI, I., RUSSO, G., CURCIO, F., BULLI, G., ARAN, L., DELLA-MORTE, D., GARGIULO, G., TESTA, G., CACCIATORE, F., BONADUCE, D. & ABETE, P. 2018. Oxidative stress, aging, and diseases. *Clinical interventions in aging*, 13, 757772.
- LITTLE, J. P. & SAFDAR, A. 2015. Adipose-brain crosstalk: do adipokines have a role in neuroprotection? *Neural regeneration research*, 10, 1381-1382.
- LIU, C.-C., LIU, C.-C., KANEKIYO, T., XU, H. & BU, G. 2013. Apolipoprotein E and Alzheimer disease: risk, mechanisms and therapy. *Nature reviews. Neurology*, 9, 106118.

- LIU, W., ZHOU, X., LI, Y., ZHANG, S., CAI, X., ZHANG, R., GONG, S., HAN, X. & JI, L. 2020. Serum leptin, resistin, and adiponectin levels in obese and non-obese patients with newly diagnosed type 2 diabetes mellitus: A population-based study. *Medicine*, 99, e19052-e19052.
- LIVINGSTON, G., SOMMERLAD, A., ORGETA, V., COSTAFREDA, S. G., HUNTLEY, J., AMES, D., BALLARD, C., BANERJEE, S., BURNS, A., COHEN-MANSFIELD, J., COOPER, C., FOX, N., GITLIN, L. N., HOWARD, R., KALES, H. C., LARSON, E. B., RITCHIE, K., ROCKWOOD, K., SAMPSON, E. L., SAMUS, Q., SCHNEIDER, L. S., SELBÆK, G., TERI, L. & MUKADAM, N. 2017. Dementia prevention, intervention, and care. *Lancet*, 390, 2673-2734.
- LIZARBE, B., SOARES, A. F., LARSSON, S. & DUARTE, J. M. N. 2018. Neurochemical Modifications in the Hippocampus, Cortex and Hypothalamus of Mice Exposed to Long-Term High-Fat Diet. *Front Neurosci*, 12, 985.
- LLANOS-GONZÁLEZ, E., HENARES-CHAVARINO, Á. A., PEDRERO-PRIETO, C. M., GARCÍA-CARPINTERO, S., FRONTIÑÁN-RUBIO, J., SANCHO-BIELSA, F. J., ALCAIN, F. J., PEINADO, J. R., RABANAL-RUIZ, Y. & DURÁN-PRADO, M. 2020. Interplay Between Mitochondrial Oxidative Disorders and Proteostasis in Alzheimer's Disease. *Frontiers in Neuroscience*, 13.
- LLORET, A., MONLLOR, P., ESTEVE, D., CERVERA-FERRI, A. & LLORET, A. 2019. Obesity as a Risk Factor for Alzheimer's Disease: Implication of Leptin and Glutamate. *Frontiers in Neuroscience*, 13.
- LOVESTONE, S. & SMITH, U. 2014. Advanced glycation end products, dementia, and diabetes. *Proc Natl Acad Sci U S A*, 111, 4743-4.
- LOPES, F. M., SCHRÖDER, R., JÚNIOR, M. L. C. D. F., ZANOTTO-FILHO, A., MÜLLER, C. B., PIRES, A. S., MEURER, R. T., COLPO, G. D., GELAIN, D. P., KAPCZINSKI, F., MOREIRA, J. C. F., FERNANDES, M. D. C. & KLAMT, F. 2010. Comparison between proliferative and neuron-like SH-SY5Y cells as an in-vitro model for Parkinson disease studies. *Brain Research*, 1337, 85-94.
- LOPEZ-CARBALLO, G., MORENO, L., MASIA, S., PEREZ, P. & BARETTINO, D. 2002.

Activation of the phosphatidylinositol 3-kinase/Akt signaling pathway by retinoic acid is required for neural differentiation of SH-SY5Y human neuroblastoma cells. *J Biol Chem*, 277, 25297-304.

LU, J., PARK, C. S., LEE, S. K., SHIN, D. W. & KANG, J. H. 2006. Leptin inhibits 1-methyl-4-phenylpyridinium-induced cell death in SH-SY5Y cells. *Neurosci Lett*, 407, 240-3.

LUMENG, C. N., BODZIN, J. L. & SALTIEL, A. R. 2007. Obesity induces a phenotypic switch in adipose tissue macrophage polarization. *The Journal of Clinical Investigation*, 117, 175-184.

LUO, L. & LIU, M. 2016. Adipose tissue in control of metabolism. *J Endocrinol*, 231, R77-r99.

LUPIEN, S. J., MCEWEN, B. S., GUNNAR, M. R. & HEIM, C. 2009. Effects of stress throughout the lifespan on the brain, behaviour and cognition. *Nat Rev Neurosci*, 10, 434-45.

LUPPINO, F. S., DE WIT, L. M., BOUVY, P. F., STIJNEN, T., CUIJPERS, P., PENNINX, B. W. & ZITMAN, F. G. 2010. Overweight, obesity, and depression: a systematic review and meta-analysis of longitudinal studies. *Arch Gen Psychiatry*, 67, 220-9.

MA, Y., AJNAKINA, O., STEPTOE, A. & CADAR, D. 2020. Higher risk of dementia in English older individuals who are overweight or obese. *International Journal of Epidemiology*, 49, 1353-1365.

MACCIONI, R. B., FARÍAS, G., MORALES, I. & NAVARRETE, L. 2010. The Revitalized Tau Hypothesis on Alzheimer's Disease. *Archives of Medical Research*, 41, 226-231.

MAGALINGAM, K. B., RADHAKRISHNAN, A. K., SOMANATH, S. D., MD, S. & HALEAGRAHARA, N. 2020. Influence of serum concentration in retinoic acid and phorbol ester induced differentiation of SH-SY5Y human neuroblastoma cell line. *Mol Biol Rep*, 47, 8775-8788.

MAHASE, E. 2021. FDA approves controversial Alzheimer's drug despite uncertainty over effectiveness. *BMJ*, 373, n1462.

- MAŁODOBRA-MAZUR, M., CIERZNIAK, A., MYSZCZYSZYN, A., KALISZEWSKI, K. & DOBOSZ, T. 2021. Histone modifications influence the insulin-signaling genes and are related to insulin resistance in human adipocytes. *The International Journal of Biochemistry & Cell Biology*, 137, 106031.
- MANNA, P. & JAIN, S. K. 2015. Obesity, Oxidative Stress, Adipose Tissue Dysfunction, and the Associated Health Risks: Causes and Therapeutic Strategies. *Metabolic syndrome and related disorders*, 13, 423-444.
- MARKESBERY, W. R. 1997. Oxidative Stress Hypothesis in Alzheimer's Disease. *Free Radical Biology and Medicine*, 23, 134-147.
- MARSEGLIA, L., MANTI, S., D'ANGELO, G., NICOTERA, A., PARISI, E., DI ROSA, G., GITTO, E. & ARRIGO, T. 2014. Oxidative stress in obesity: a critical component in human diseases. *International journal of molecular sciences*, 16, 378-400.
- MARTIN, S. S., QASIM, A. & REILLY, M. P. 2008. Leptin Resistance. *Journal of the American College of Cardiology*, 52, 1201-1210.
- MARTÍN-MAESTRO, P., GARGINI, R., A. SPROUL, A., GARCÍA, E., ANTÓN, L. C., NOGGLE, S., ARANCIO, O., AVILA, J. & GARCÍA-ESCUADERO, V. 2017. Mitophagy Failure in Fibroblasts and iPSC-Derived Neurons of Alzheimer's Disease-Associated Presenilin 1 Mutation. *Frontiers in Molecular Neuroscience*, 10.
- MARTIN-JIMÉNEZ, C. A., GAITÁN-VACA, D. M., ECHEVERRIA, V., GONZÁLEZ, J. & BARRETO, G. E. 2017. Relationship Between Obesity, Alzheimer's Disease, and Parkinson's Disease: an Astrocentric View. *Molecular Neurobiology*, 54, 7096-7115.
- MASLOV, L. N., NARYZHAYAYA, N. V., BOSHCHENKO, A. A., POPOV, S. V., IVANOV, V. V. & OELTGEN, P. R. 2019. Is oxidative stress of adipocytes a cause or a consequence of the metabolic syndrome? *Journal of Clinical & Translational Endocrinology*, 15, 1-5.
- MAURO, L., NAIMO, G. D., RICCHIO, E., PANNO, M. L. & ANDÒ, S. 2015. Cross-talk between Adiponectin and IGF-IR in Breast Cancer. *Frontiers in Oncology*, 5.
- MARWARHA, G. & GHRIBI, O. 2012. Leptin signaling and Alzheimer's disease. *Am J Neurodegener Dis*, 1, 245-65.

- MAYSAMI, S., HALEY, M. J., GORENKOVA, N., KRISHNAN, S., MCCOLL, B. W. & LAWRENCE, C. B. 2015. Prolonged diet-induced obesity in mice modifies the inflammatory response and leads to worse outcome after stroke. *Journal of Neuroinflammation*, 12, 140.
- MAZANETZ, M. P. & FISCHER, P. M. 2007. Untangling tau hyperphosphorylation in drug design for neurodegenerative diseases. *Nature Reviews Drug Discovery*, 6, 464-479.
- MAZEN, I., EL-GAMMAL, M., ABDEL-HAMID, M. & AMR, K. 2009. A novel homozygous missense mutation of the leptin gene (N103K) in an obese Egyptian patient. *Molecular Genetics and Metabolism*, 97, 305-308.
- MCGUIRE, M. J. & ISHII, M. 2016. Leptin Dysfunction and Alzheimer's Disease: Evidence from Cellular, Animal, and Human Studies. *Cell Mol Neurobiol*, 36, 203-17.
- MENON, M. B., KOTLYAROV, A. & GAESTEL, M. 2011. SB202190-Induced Cell Type-Specific Vacuole Formation and Defective Autophagy Do Not Depend on p38 MAP Kinase Inhibition. *PLOS ONE*, 6, e23054.
- MIAO, J., BENOMAR, Y., AL RIFAI, S., POIZAT, G., RIFFAULT, L., CRÉPIN, D. & TAOUIS, M. 2018. Resistin inhibits neuronal autophagy through Toll-like receptor 4. *Journal of Endocrinology*, 238, 77-89.
- MIAO, J., SHI, R., LI, L., CHEN, F., ZHOU, Y., TUNG, Y. C., HU, W., GONG, C.-X., IQBAL, K. & LIU, F. 2019. Pathological Tau From Alzheimer's Brain Induces Site-Specific Hyperphosphorylation and SDS- and Reducing Agent-Resistant Aggregation of Tau in vivo. *Frontiers in Aging Neuroscience*, 11.
- MICHAEL J. HALEY, GRAHAM MULLARD, KATHERINE A. HOLLYWOOD, GARTH J. COOPER, WARWICK B. DUNN, CATHERINE B. LAWRENCE (2017) Adipose tissue and metabolic and inflammatory responses to stroke are altered in obese mice. *Dis Model Mech*, 10 (10): 1229–1243.
- MISRANI, A., TABASSUM, S. & YANG, L. 2021. Mitochondrial Dysfunction and Oxidative Stress in Alzheimer's Disease. *Frontiers in Aging Neuroscience*, 13.

- MOHANDAS, E., RAJMOHAN, V. & RAGHUNATH, B. 2009. Neurobiology of Alzheimer's disease. *Indian journal of psychiatry*, 51, 55-61.
- MONICKARAJ, F., ARAVIND, S., NANDHINI, P., PRABU, P., SATHISHKUMAR, C., MOHAN, V. & BALASUBRAMANYAM, M. 2013. Accelerated fat cell aging links oxidative stress and insulin resistance in adipocytes. *Journal of Biosciences*, 38, 113-122.
- MONTESI, L., EL GHOSH, M., BRODOSI, L., CALUGI, S., MARCHESINI, G. & DALLE GRAVE, R. 2016. Long-term weight loss maintenance for obesity: a multidisciplinary approach. *Diabetes Metab Syndr Obes*, 9, 37-46.
- MORRISON, S. & MCGEE, S. L. 2015. 3T3-L1 adipocytes display phenotypic characteristics of multiple adipocyte lineages. *Adipocyte*, 4, 295-302.
- MURAOKA, S., NITTA, Y., YAMADA, T., SAKUMA, Y., ICHIMURA, A. & SAKURAI, K. 2017. [Increase of Anti-oxidative Capacity during Differentiation of 3T3-L1 Pre-adipocytes into Adipocytes]. *Yakugaku Zasshi*, 137, 1137-1145.
- MURILLO, J. R., GOTO-SILVA, L., SÁNCHEZ, A., NOGUEIRA, F. C. S., DOMONT, G. B. & JUNQUEIRA, M. 2017. Quantitative proteomic analysis identifies proteins and pathways related to neuronal development in differentiated SH-SY5Y neuroblastoma cells. *EuPA Open Proteomics*, 16, 1-11.
- MUSTAFA, N. R., DE WINTER, W., VAN IREN, F. & VERPOORTE, R. 2011. Initiation, growth and cryopreservation of plant cell suspension cultures. *Nature Protocols*, 6, 715-742.
- NAGPURE, B. V. & BIAN, J.-S. 2014. Hydrogen Sulfide Inhibits A2A Adenosine Receptor Agonist Induced β -Amyloid Production in SH-SY5Y Neuroblastoma Cells via a cAMP Dependent Pathway. *PLOS ONE*, 9, e88508.
- NAGAEV, I., BOKAREWA, M., TARKOWSKI, A. & SMITH, U. 2006. Human Resistin Is a Systemic Immune-Derived Proinflammatory Cytokine Targeting both Leukocytes and Adipocytes. *PLOS ONE*, 1, e31.
- NHS Digital (2015) Health Survey England 2015. Available at: <https://digital.nhs.uk/data-and-information/publications/statistical/health-survey-for-england/health-survey-for-england-2015> (Accessed on 04 March 2021).

NHS Digital (2021) Statistics on obesity, Physical Activity and Diet, England 2021. Available at: <https://digital.nhs.uk/data-and-information/publications/statistical/statistics-on-obesity-physical-activity-and-diet/england-2021> (Accessed on 04 August 2021).

NIEDZIELSKA, E., SMAGA, I., GAWLIK, M., MONICZEWSKI, A., STANKOWICZ, P., PERA, J. & FILIP, M. 2016. Oxidative Stress in Neurodegenerative Diseases. *Mol Neurobiol*, 53, 4094-4125.

NIRMALADEVI, D., VENKATARAMANA, M., CHANDRANAYAKA, S., RAMESHA, A., JAMEEL, N. M. & SRINIVAS, C. 2014. Neuroprotective Effects of Bikaverin on H₂O₂-Induced Oxidative Stress Mediated Neuronal Damage in SH-SY5Y Cell Line. *Cellular and Molecular Neurobiology*, 34, 973-985.

NISHIDA, N., ARIZUMI, T., TAKITA, M., KITAI, S., YADA, N., HAGIWARA, S., INOUE, T., MINSAMI, Y., UESHIMA, K., SAKURAI, T. & KUDO, M. 2013. Reactive Oxygen Species Induce Epigenetic Instability through the Formation of 8-Hydroxydeoxyguanosine in Human Hepatocarcinogenesis. *Digestive Diseases*, 31, 459-466.

NIKLOWITZ, P., ROTHERMEL, J., LASS, N., BARTH, A. & REINEHR, T. 2018. Link between chemerin, central obesity, and parameters of the Metabolic Syndrome: findings from a longitudinal study in obese children participating in a lifestyle intervention. *Int J Obes*, 42, 1743-1752.

NORDENGEN, K., KIRSEBOM, B.-E., HENJUM, K., SELNES, P., GÍSLADÓTTIR, B., WETTERGREEN, M., TORSETNES, S. B., GRØNTVEDT, G. R., WATERLOO, K. K., AARSLAND, D., NILSSON, L. N. G. & FLADBY, T. 2019. Glial activation and inflammation along the Alzheimer's disease continuum. *Journal of Neuroinflammation*, 16, 46.

NUNOMURA, A. & PERRY, G. 2020. RNA and Oxidative Stress in Alzheimer's Disease: Focus on microRNAs. *Oxidative Medicine and Cellular Longevity*, 2020, 2638130.

NYBO, K. 2012. GFP Imaging in Fixed Cells. *BioTechniques*, 52, 359-360.

O'BRIEN, R. J. & WONG, P. C. 2011. Amyloid precursor protein processing and Alzheimer's disease. *Annual review of neuroscience*, 34, 185-204.

OPATRILOVA, R., CAPRNDA, M., KUBATKA, P., VALENTOVA, V., URAMOVA, S., NOSAL, V., GASPAR, L., ZACHAR, L., MOZOS, I., PETROVIC, D., DRAGASEK,

- J., FILIPOVA, S., BÜSSELBERG, D., ZULLI, A., RODRIGO, L., KRUZLIAK, P. & KRASNIK, V. 2018. Adipokines in neurovascular diseases. *Biomedicine & Pharmacotherapy*, 98, 424-432.
- OTTAVIANI, E., MALAGOLI, D. & FRANCESCHI, C. 2011. The evolution of the adipose tissue: a neglected enigma. *Gen Comp Endocrinol*, 174, 1-4.
- OUCHI, N., PARKER, J. L., LUGUS, J. J. & WALSH, K. 2011. Adipokines in inflammation and metabolic disease. *Nature Reviews Immunology*, 11, 85-97.
- PACIFICI, F., FARIAS, C. L. A., REA, S., CAPUANI, B., FERACO, A., COPPOLA, A., MAMMI, C., PASTORE, D., ABETE, P., ROVELLA, V., SALIMEI, C., LOMBARDO, M., CAPRIO, M., BELLIA, A., SBRACCIA, P., DI DANIELE, N., LAURO, D. & DELLA-MORTE, D. 2020. Tyrosol May Prevent Obesity by Inhibiting Adipogenesis in 3T3-L1 Pre-adipocytes. *Oxidative Medicine and Cellular Longevity*, 2020, 4794780.
- PARIMISETTY, A., DORSEMAN, A.-C., AWADA, R., RAVANAN, P., DIOTEL, N. & LEFEBVRE D'HELLEN COURT, C. 2016. Secret talk between adipose tissue and central nervous system via secreted factors-an emerging frontier in the neurodegenerative research. *Journal of neuroinflammation*, 13, 67-67.
- PAN, X.-D., ZHU, Y.-G., LIN, N., ZHANG, J., YE, Q.-Y., HUANG, H.-P. & CHEN, X.-C. 2011. Microglial phagocytosis induced by fibrillar β -amyloid is attenuated by oligomeric β -amyloid: implications for Alzheimer's disease. *Molecular Neurodegeneration*, 6, 45.
- PANTOJA, C., HUFF, J. T. & YAMAMOTO, K. R. 2008. Glucocorticoid signaling defines a novel commitment state during adipogenesis in-vitro. *Molecular biology of the cell*, 19, 4032-4041.
- PAWITAN, J. A. 2014. Prospect of Stem Cell Conditioned Medium in Regenerative Medicine. *BioMed Research International*, 2014, 965849.
- PEDITIZI, E., PETERS, R. & BECKETT, N. 2016. The risk of overweight/obesity in mid-life and late life for the development of dementia: a systematic review and meta-analysis of longitudinal studies. *Age and Ageing*, 45, 14-21.
- PENNEY, J., RALVENIUS, W. T. & TSAI, L.-H. 2020. Modeling Alzheimer's disease with iPSC-derived brain cells. *Molecular Psychiatry*, 25, 148-167.

- PENG, L., YU, Y., LIU, J., LI, S., HE, H., CHENG, N. & YE, R. D. 2015. The chemerin receptor CMKLR1 is a functional receptor for amyloid-beta peptide. *J Alzheimers Dis*, 43, 227-42.
- PÉREZ, M. J., PONCE, D. P., OSORIO-FUENTEALBA, C., BEHRENS, M. I. & QUINTANILLA, R. A. 2017. Mitochondrial Bioenergetics Is Altered in Fibroblasts from Patients with Sporadic Alzheimer's Disease. *Frontiers in Neuroscience*, 11.
- PEREIRA, A. C., HUDDLESTON, D. E., BRICKMAN, A. M., SOSUNOV, A. A., HEN, R., MCKHANN, G. M., SLOAN, R., GAGE, F. H., BROWN, T. R. & SMALL, S. A. 2007. An *in-vivo* correlate of exercise-induced neurogenesis in the adult dentate gyrus. *Proceedings of the National Academy of Sciences*, 104, 5638.
- PERLSON, E., MADAY, S., FU, M. M., MOUGHAMIAN, A. J. & HOLZBAUR, E. L. 2010. Retrograde axonal transport: pathways to cell death? *Trends Neurosci*, 33, 335-44.
- PERRY, G., CASH, A. D. & SMITH, M. A. 2002. Alzheimer Disease and Oxidative Stress. *Journal of biomedicine & biotechnology*, 2, 120-123.
- PESHADARY, V. & ATLAS, E. 2018. Dexamethasone induced miR-155 up-regulation in differentiating 3T3-L1 pre-adipocytes does not affect adipogenesis. *Scientific Reports*, 8, 1264.
- PIZZINO, G., IRRERA, N., CUCINOTTA, M., PALLIO, G., MANNINO, F., ARCORACI, V., SQUADRITO, F., ALTAVILLA, D. & BITTO, A. 2017. Oxidative Stress: Harms and Benefits for Human Health. *Oxidative medicine and cellular longevity*, 2017, 8416763-8416763.
- PLASCENCIA-VILLA, G. & PERRY, G. 2020. Chapter One - Status and future directions of clinical trials in Alzheimer's disease. In: SÖDERBOM, G., ESTERLINE, R., OSCARSSON, J. & MATTSON, M. P. (eds.) *International Review of Neurobiology*. Academic Press.
- PLOTKIN, S. S. & CASHMAN, N. R. 2020. Passive immunotherapies targeting A β and tau in Alzheimer's disease. *Neurobiology of Disease*, 144, 105010.
- POKRISHEVSKY, E., GRAD, L. I. & CASHMAN, N. R. 2016. TDP-43 or FUS-induced misfolded human wild-type SOD1 can propagate intercellularly in a prion-like fashion. *Scientific Reports*, 6, 22155.

- POLLIN, T. I., DAMCOTT, C. M., SHEN, H., OTT, S. H., SHELTON, J., HORENSTEIN, R. B., POST, W., MCLENITHAN, J. C., BIELAK, L. F., PEYSER, P. A., MITCHELL, B. D., MILLER, M., O'CONNELL, J. R. & SHULDINER, A. R. 2008. A null mutation in human APOC3 confers a favorable plasma lipid profile and apparent cardioprotection. *Science*, 322, 1702-5.
- PRATICÒ, D. 2008. Oxidative stress hypothesis in Alzheimer's disease: a reappraisal. *Trends in Pharmacological Sciences*, 29, 609-615.
- PRESGRAVES, S. P., AHMED, T., BORWEGE, S. & JOYCE, J. N. 2003. Terminally differentiated SH-SY5Y cells provide a model system for studying neuroprotective effects of dopamine agonists. *Neurotoxic. Res.*, 5, 579.
- PRINCE, J. & BUDSON, A. 2014. Current understanding of Alzheimer's disease diagnosis and treatment. *F1000Research*, 7, F1000 Faculty Rev-1161.
- PUBLIC HEALTH ENGLAND (2017) Health matters: obesity and food environment (2017). Available at: <https://www.gov.uk/government/publications/health-matters-obesity-and-the-food-environment/health-matters-obesity-and-the-food-environment--2>. Accessed on 05 March 2021.
- PUBLIC HEALTH ENGLAND (2018) Dementia: Applying to our health. Available at: <https://www.gov.uk/government/publications/dementia-applying-all-our-health/dementia-applying-all-our-health#facts-about-dementia>. Accessed on 08 March 2021.
- PUGAZHENTHI, S., QIN, L. & REDDY, P. H. 2017. Common neurodegenerative pathways in obesity, diabetes, and Alzheimer's disease. *Biochimica et Biophysica Acta (BBA) - Molecular Basis of Disease*, 1863, 1037-1045.
- QIANG, L., FUJITA, R., YAMASHITA, T., ANGULO, S., RHINN, H., RHEE, D., DOEGE, C., CHAU, L., AUBRY, L., VANTI, W. B., MORENO, H. & ABELIOVICH, A. 2011. Directed conversion of Alzheimer's disease patient skin fibroblasts into functional neurons. *Cell*, 146, 359-371.
- QUERFURTH, H. W. & LAFERLA, F. M. 2010. Alzheimer's disease. *N Engl J Med*, 362, 329-44.
- RAKESH, G., SZABO, S. T., ALEXOPOULOS, G. S. & ZANNAS, A. S. 2017. Strategies for dementia prevention: latest evidence and implications. *Therapeutic advances in chronic disease*, 8, 121-136.

- RAMAMOORTHY, M., SYKORA, P., SCHEIBYE-KNUDSEN, M., DUNN, C., KASMER, C., ZHANG, Y., BECKER, K. G., CROTEAU, D. L. & BOHR, V. A. 2012. Sporadic Alzheimer disease fibroblasts display an oxidative stress phenotype. *Free radical biology & medicine*, 53, 1371-1380.
- RAMALINGAM, M. & KIM, S. J. 2014. The role of insulin against hydrogen peroxide-induced oxidative damages in differentiated SH-SY5Y cells. *J Recept Signal Transduct Res*, 34, 212-20.
- RAMOS-CEJUDO, J., WISNIEWSKI, T., MARMAR, C., ZETTERBERG, H., BLENNOW, K., DE LEON, M. J. & FOSSATI, S. 2018. Traumatic Brain Injury and Alzheimer's Disease: The Cerebrovascular Link. *EBioMedicine*, 28, 21-30.
- RAY, B., CHOPRA, N., LONG, J. M. & LAHIRI, D. K. 2014. Human primary mixed brain cultures: preparation, differentiation, characterization and application to neuroscience research. *Molecular brain*, 7, 63-63.
- REITZ, C. & MAYEUX, R. 2014. Alzheimer disease: epidemiology, diagnostic criteria, risk factors and biomarkers. *Biochem Pharmacol*, 88, 640-51.
- REITZ, C., ROGAEVA, E. & BEECHAM, G. W. 2020. Late-onset vs nonmendelian early onset Alzheimer disease: A distinction without a difference? *Neurology. Genetics*, 6, e512-e512.
- RICCIARELLI, R. & FEDELE, E. 2017. The Amyloid Cascade Hypothesis in Alzheimer's Disease: It's Time to Change Our Minsd. *Current neuropharmacology*, 15, 926-935.
- RICHARDS, S. A., MUTER, J., RITCHIE, P., LATTANZI, G. & HUTCHISON, C. J. 2011. The accumulation of un-repairable DNA damage in laminopathy progeria fibroblasts is caused by ROS generation and is prevented by treatment with N-acetyl cysteine. *Human Molecular Genetics*, 20, 3997-4004.
- RICHARD, A.J., WHITE, U., ELKS, C.M., & JACQUELINE, M. S.2020. Adipose Tissue: Physiology to Metabolic Dysfunction. *Endotext*, 2000-2013.
- RIDHA, B.H., & YOUSRY, T.A. (2016) Neurodegeneration: Cerebrum. Available at <https://radiologykey.com/neurodegeneration-cerebrum/#> (Accessed 24th March 2021).

- RIDNOUR, L. A., ISENBERG, J. S., ESPEY, M. G., THOMAS, D. D., ROBERTS, D. D. & WINK, D. A. 2005. Nitric oxide regulates angiogenesis through a functional switch involving thrombospondin-1. *Proceedings of the National Academy of Sciences of the United States of America*, 102, 13147-13152.
- RIGAS, B. & SUN, Y. 2008. Induction of oxidative stress as a mechanism of action of chemopreventive agents against cancer. *British journal of cancer*, 98, 1157-1160.
- RISTOW, M. & ZARSE, K. 2010. How increased oxidative stress promotes longevity and metabolic health: The concept of mitochondrial hormesis (mitohormesis). *Exp Gerontol*, 45, 410-8.
- RIZZATTI, V., BOSCHI, F., PEDROTTI, M., ZOICO, E., SBARBATI, A. & ZAMBONI, M. 2013. Lipid droplets characterization in adipocyte differentiated 3T3-L1 cells: size and optical density distribution. *European journal of histochemistry : EJH*, 57, e24-e24.
- RODRÍGUEZ-PENAS, D., FEIJÓO-BANDÍN, S., GARCÍA-RÚA, V., MOSQUERA-LEAL, A., DURÁN, D., VARELA, A., PORTOLÉS, M., ROSELLÓ-LLETÍ, E., RIVERA, M., DIÉGUEZ, C., GUALILLO, O., GONZÁLEZ-JUANATEY, J. R. & LAGO, F. 2015. The Adipokine Chemerin Induces Apoptosis in Cardiomyocytes. *Cellular Physiology and Biochemistry*, 37, 176-192.
- ROGERS, J., MASTROENI, D., LEONARD, B., JOYCE, J. & GROVER, A. 2007. Neuroinflammation in Alzheimer's disease and Parkinson's disease: are microglia pathogenic in either disorder? *Int Rev Neurobiol*, 82, 235-46.
- ROSENTHAL, S. L. & KAMBOH, M. I. 2014. Late-Onset Alzheimer's Disease Genes and the Potentially Implicated Pathways. *Curr Genet Med Rep*, 2, 85-101.
- RONAN, L., ALEXANDER-BLOCH, A. F., WAGSTYL, K., FAROOQI, S., BRAYNE, C., TYLER, L. K. & FLETCHER, P. C. 2016. Obesity associated with increased brain age from midlife. *Neurobiology of Aging*, 47, 63-70.
- ROSELL, M., KAFOROU, M., FRONTINI, A., OKOLO, A., CHAN, Y.-W., NIKOLOPOULOU, E., MILLERSHIP, S., FENECH, M. E., MACINTYRE, D., TURNER, J. O., MOORE, J. D., BLACKBURN, E., GULLICK, W. J., CINTI, S., MONTANA, G., PARKER, M. G. & CHRISTIAN, M. 2014. Brown and white adipose tissues: intrinsic differences in gene expression and response to cold exposure in mice. *American Journal of Physiology-Endocrinology and Metabolism*, 306, E945-E964.

ROSSOR, M. N., FOX, N. C., MUMMERY, C. J., SCHOTT, J. M. & WARREN, J. D. 2010. The diagnosis of young-onset dementia. *Lancet Neurol*, 9, 793-806.

ROVELET-LECRUX, A., HANNEQUIN, D., RAUX, G., LE MEUR, N., LAQUERRIÈRE, A., VITAL, A., DUMANCHIN, C., FEUILLETTE, S., BRICE, A., VERCELLETTO, M., DUBAS, F., FREBOURG, T. & CAMPION, D. 2006. APP locus duplication causes autosomal dominant early-onset Alzheimer disease with cerebral amyloid angiopathy. *Nat Genet*, 38, 24-6.

RUIZ-OJEDA, F. J., RUPÉREZ, A. I., GOMEZ-LLORENTE, C., GIL, A. & AGUILERA, C. M. 2016. Cell Models and Their Application for Studying Adipogenic Differentiation in Relation to Obesity: A Review. *International journal of molecular sciences*, 17, 1040.

SABBAGH, M. N. 2020. Editorial: Alzheimer's Disease Drug Development Pipeline 2020. *The journal of prevention of Alzheimer's disease*, 7, 66-67.

SAFAEIAN, L., MIRIAN, M. & BAHRIZADEH, S. 2020. Evolocumab, a PCSK9 inhibitor, protects human endothelial cells against H(2)O(2)-induced oxidative stress. *Arch Physiol Biochem*, 1-6.

SADASHIV, TIWARI, S., PAUL, B. N., KUMAR, S., CHANDRA, A., DHANANJAI, S. & NEGI, M. P. 2012. Over expression of resistin in adipose tissue of the obese induces insulin resistance. *World journal of diabetes*, 3, 135-141.

SAELY, C. H., GEIGER, K. & DREXEL, H. 2012. Brown versus white adipose tissue: a mini-review. *Gerontology*, 58, 15-23.

ŞAHİN, M., ÖNCÜ, G., YILMAZ, M. A., ÖZKAN, D. & SAYBAŞILı, H. 2021. Transformation of SH-SY5Y cell line into neuron-like cells: Investigation of electrophysiological and biomechanical changes. *Neuroscience Letters*, 745, 135628.

SAGARADZE, G., GRIGORIEVA, O., NIMIRITSKY, P., BASALOVA, N., KALININA, N., AKOPYAN, Z. & EFIMENKO, A. 2019. Conditioned Medium from Human Mesenchymal Stromal Cells: Towards the Clinical Translation. *Int J Mol Sci*, 20.

SANG, Q., LIU, X., WANG, L., QI, L., SUN, W., WANG, W., SUN, Y. & ZHANG, H. 2018. Curcumins Protects an SH-SY5Y Cell Model of Parkinson's Disease Against Toxic Injury by Regulating HSP90. *Cellular Physiology and Biochemistry*, 51, 681-691.

- SAKURAI, T., IZAWA, T., KIZAKI, T., OGASAWARA, J.-E., SHIRATO, K., IMAIZUMI, K., TAKAHASHI, K., ISHIDA, H. & OHNO, H. 2009. Exercise training decreases expression of inflammation-related adipokines through reduction of oxidative stress in rat white adipose tissue. *Biochemical and Biophysical Research Communications*, 379, 605-609.
- SARMENTO-CABRAL, A., PEINADO, J. R., HALLIDAY, L. C., MALAGON, M. M., CASTAÑO, J. P., KINEMAN, R. D. & LUQUE, R. M. 2017. Adipokines (Leptin, Adiponectin, Resistin) Differentially Regulate All Hormonal Cell Types in Primary Anterior Pituitary Cell Cultures from Two Primate Species. *Scientific Reports*, 7, 43537.
- SARASIJA, S., LABOY, J. T., ASHKAVAND, Z., BONNER, J., TANG, Y. & NORMAN, K. R. 2018. Presenilin mutations deregulate mitochondrial Ca²⁺ homeostasis and metabolic activity causing neurodegeneration in *Caenorhabditis elegans*. *Elife*, 7.
- SARASIJA, S., LABOY, J. T., ASHKAVAND, Z., BONNER, J., TANG, Y. & NORMAN, K. R. 2018. Presenilin mutations deregulate mitochondrial Ca²⁺ homeostasis and metabolic activity causing neurodegeneration in *Caenorhabditis elegans*. *Elife*, 7.
- SAVAGE, D. B., SEWTER, C. P., KLENK, E. S., SEGAL, D. G., VIDAL-PUIG, A., CONSIDINE, R. V. & O'RAHILLY, S. 2001. Resistin / Fizz3 Expression in Relation to Obesity and Peroxisome Proliferator-Activated Receptor- γ Action in Humans. *Diabetes*, 50, 2199-2202.
- SCOTECE, M., PEREZ, T., CONDE, J., ABELLA, V., LOPEZ, V., PINO, J., GONZALEZGAY, M. A., GOMEZ-REINO, J. J., MERA, A., GOMEZ, R. & GUALILLO, O. 2017. Adipokines induce pro-inflammatory factors in activated Cd4+ T cells from osteoarthritis patient. *J Orthop Res*, 35, 1299-1303.
- SELKOE, D. J. & HARDY, J. 2016. The amyloid hypothesis of Alzheimer's disease at 25 years. *EMBO Mol Med*, 8, 595-608.
- SELL, H., LAURENCIKIENE, J., TAUBE, A., ECKARDT, K., CRAMER, A., HERRIGHS, A., ARNER, P. & ECKEL, J. 2009. Chemerin is a novel adipocyte-derived factor inducing insulin resistance in primary human skeletal muscle cells. *Diabetes*, 58, 2731-40.
- SHEN, W., TIAN, C., CHEN, H., YANG, Y., ZHU, D., GAO, P. & LIU, J. 2012. Oxidative Stress Mediates Chemerin Induced Autophagy in Endothelial Cells. *Free radical biology & medicine*, 55.

- SENGOKU, R. 2020. Aging and Alzheimer's disease pathology. *Neuropathology*, 40, 22-29.
- SERIO, R. N., LAURSEN, K. B., URVALEK, A. M., GROSS, S. S. & GUDAS, L. J. 2019. Ethanol promotes differentiation of embryonic stem cells through retinoic acid receptor- γ . *The Journal of biological chemistry*, 294, 5536-5548.
- SERRANO-POZO, A., FROSCHE, M. P., MASLIAH, E. & HYMAN, B. T. 2011. Neuropathological alterations in Alzheimer disease. *Cold Spring Harbor perspectives in medicine*, 1, a006189-a006189.
- SHI, Q. & GIBSON, G. E. 2007. Oxidative stress and transcriptional regulation in Alzheimer disease. *Alzheimer disease and associated disorders*, 21, 276-291.
- SHIPLEY, M. M., MANGOLD, C. A. & SZPARA, M. L. 2016. Differentiation of the SHSY5Y Human Neuroblastoma Cell Line. *Journal of visualized experiments: JoVE*, 53193-53193.
- SHIPLEY, M. M., MANGOLD, C. A., KUNY, C. V. & SZPARA, M. L. 2017. Differentiated Human SH-SY5Y Cells Provide a Reductionist Model of Herpes Simplex Virus 1 Neurotropism. *Journal of virology*, 91, e00958-17.
- SIES, H., BERNDT, C. & JONES, D. P. 2017. Oxidative Stress. *Annu Rev Biochem*, 86, 715-748.
- ŠIMIĆ, G., BABIĆ LEKO, M., WRAY, S., HARRINGTON, C., DELALLE, I., JOVANOVIĆ MILOŠEVIĆ, N., BAŽADONA, D., BUÉE, L., DE SILVA, R., DI GIOVANNI, G., WISCHIK, C. & HOF, P. R. 2016. Tau Protein Hyperphosphorylation and Aggregation in Alzheimer's Disease and Other Tauopathies, and Possible Neuroprotective Strategies. *Biomolecules*, 6, 6.
- SINGH, R. & SADIQ, N. M. 2021. Cholinesterase Inhibitors. *StatPearls*. Treasure Island (FL): StatPearls Publishing Copyright © 2021, StatPearls Publishing LLC.
- SINGH, S. K., SRIVASTAV, S., YADAV, A. K., SRIKRISHNA, S. & PERRY, G. 2016. Overview of Alzheimer's Disease and Some Therapeutic Approaches Targeting A β by Using Several Synthetic and Herbal Compounds. *Oxidative medicine and cellular longevity*, 2016, 7361613-7361613.

SMITH, K. B. & SMITH, M. S. 2016. Obesity Statistics. *Prim Care*, 43, 121-35, ix.

SMITH, M. A., ROTTKAMP, C. A., NUNOMURA, A., RAINA, A. K. & PERRY, G. 2000. Oxidative stress in Alzheimer's disease. *Biochimica et Biophysica Acta (BBA) - Molecular Basis of Disease*, 1502, 139-144.

SOBOTTA, M. C., BARATA, A. G., SCHMIDT, U., MUELLER, S., MILLONIG, G. & DICK, T. P. 2013. Exposing cells to H₂O₂: a quantitative comparison between continuous low-dose and one-time high-dose treatments. *Free Radic Biol Med*, 60, 325-35.

SOLTANI, M. H., PICHARDO, R., SONG, Z., SANGHA, N., CAMACHO, F., SATYAMOORTHY, K., SANGUEZA, O. P. & SETALURI, V. 2005. Microtubule-associated protein 2, a marker of neuronal differentiation, induces mitotic defects, inhibits growth of melanoma cells, and predicts metastatic potential of cutaneous melanoma. *Am J Pathol*, 166, 1841-50.

SONG, J. & LEE, J. E. 2013. Adiponectin as a new paradigm for approaching Alzheimer's disease. *Anat Cell Biol*, 46, 229-34.

SOWERS, J. R. 2008. Endocrine functions of adipose tissue: focus on adiponectin. *Clin Cornerstone*, 9, 32-8; discussion 39-40.

SPILLANTINI, M. G., MURRELL, J. R., GOEDERT, M., FARLOW, M. R., KLUG, A. & GHETTI, B. 1998. Mutation in the tau gene in familial multiple system tauopathy with presenile dementia. *Proc Natl Acad Sci U S A*, 95, 7737-41.

SPITZER, A. J., TIAN, Q., CHOUDHARY, R. K. & ZHAO, F.-Q. 2020. Bacterial Endotoxin Induces Oxidative Stress and Reduces Milk Protein Expression and Hypoxia in the Mouse Mammary Gland. *Oxidative Medicine and Cellular Longevity*, 2020, 3894309.

STEPHAN, C. M., BAILEY, S. T., BHAT, S., BROWN, E. J., BANERJEE, R. R., WRIGHT, C. M., PATEL, H. R., AHIMA, R. S. & LAZAR, M. A. 2001. The hormone resistin links obesity to diabetes. *Nature*, 409, 307-312.

- SUPRIYA, R., TAM, B. T., YU, A. P., LEE, P. H., LAI, C. W., CHENG, K. K., YAU, S. Y., CHAN, L. W., YUNG, B. Y., SHERIDAN, S. & SIU, P. M. 2018. Adipokines demonstrate the interacting influence of central obesity with other cardiometabolic risk factors of metabolic syndrome in Hong Kong Chinese adults. *PloS one*, 13, e0201585-e0201585.
- SU, K.-Z., LI, Y.-R., ZHANG, D., YUAN, J.-H., ZHANG, C.-S., LIU, Y., SONG, L.-M., LIN, Q., LI, M.-W. & DONG, J. 2019. Relation of Circulating Resistin to Insulin Resistance in Type 2 Diabetes and Obesity: A Systematic Review and Meta-Analysis. *Frontiers in Physiology*, 10.
- SUN, W., YU, Z., YANG, S., JIANG, C., KOU, Y., XIAO, L., TANG, S. & ZHU, T. 2020. A Transcriptomic Analysis Reveals Novel Patterns of Gene Expression During 3T3-L1 Adipocyte Differentiation. *Frontiers in Molecular Biosciences*, 7.
- SWERDLOW, R. H., BURNS, J. M. & KHAN, S. M. 2014. The Alzheimer's disease mitochondrial cascade hypothesis: progress and perspectives. *Biochim Biophys Acta*, 1842, 1219-31.
- TAKAHASHI, M., TAKAHASHI, Y., TAKAHASHI, K., ZOLOTARYOV, F. N., HONG, K. S., KITAZAWA, R., IIDA, K., OKIMURA, Y., KAJI, H., KITAZAWA, S., KASUGA, M. & CHIHARA, K. 2008. Chemerin enhances insulin signaling and potentiates insulin-stimulated glucose uptake in 3T3-L1 adipocytes. *FEBS Letters*, 582, 573-578.
- TAN, B., LUAN, Z., WEI, X., HE, Y., WEI, G., JOHNSTONE, B. H., FARLOW, M. & DU, Y. 2011. AMP-activated kinase mediates adipose stem cell-stimulated neurogenesis of PC12 cells. *Neuroscience*, 181, 40-47.
- TAN, C. C., YU, J. T., WANG, H. F., TAN, M. S., MENG, X. F., WANG, C., JIANG, T., ZHU, X. C. & TAN, L. 2014. Efficacy and safety of donepezil, galantamine, rivastigmine, and memantine for the treatment of Alzheimer's disease: a systematic review and meta-analysis. *J Alzheimers Dis*, 41, 615-31.
- TEPPOLA, H., SARKANEN, J.-R., JALONEN, T. O. & LINNE, M.-L. Impacts of laminin and polyethyleneimine surface coatings on morphology of differentiating human SHSY5Y cells and networks. *In*: ESKOLA, H., VÄISÄNEN, O., VIIK, J. & HYTTINEN, J., eds. EMBEC & NBC 2017, 2018// 2018 Singapore. Springer Singapore, 298-301.

- THINAKARAN, G. & KOO, E. H. 2008. Amyloid precursor protein trafficking, processing, and function. *J Biol Chem*, 283, 29615-9.
- THON, M., HOSOI, T. & OZAWA, K. 2016. Insulin enhanced leptin-induced STAT3 signaling by inducing GRP78. *Scientific reports*, 6, 34312-34312.
- TOLLESON, W. H., CHERNG, S.-H., XIA, Q., BOUDREAU, M., YIN, J. J., WAMER, W. G., HOWARD, P. C., YU, H. & FU, P. P. 2005. Photodecomposition and phototoxicity of natural retinoids. *International journal of environmental research and public health*, 2, 147-155.
- TON, A. M. M., CAMPAGNARO, B. P., ALVES, G. A., AIRES, R., CÔCO, L. Z., ARPINI, C. M., GUERRA E OLIVEIRA, T., CAMPOS-TOIMIL, M., MEYRELLES, S. S., PEREIRA, T. M. C. & VASQUEZ, E. C. 2020. Oxidative Stress and Dementia in Alzheimer's Patients: Effects of Synbiotic Supplementation. *Oxidative Medicine and Cellular Longevity*, 2020, 2638703.
- TÖNNIES, E. & TRUSHINA, E. 2017. Oxidative Stress, Synaptic Dysfunction, and Alzheimer's Disease. *Journal of Alzheimer's disease : JAD*, 57, 1105-1121.
- TORABI, S., YEGANEHJOO, H., SHEN, C.-L. & MO, H. 2016. Peroxisome proliferator-activated receptor γ down-regulation mediates the inhibitory effect of d- δ -tocotrienol on the differentiation of murine 3T3-F442A pre-adipocytes. *Nutrition Research*, 36, 1345-1352.
- TSUBAI, T., YOSHIMI, A., HAMADA, Y., NAKAO, M., ARIMA, H., OISO, Y. & NODA, Y. 2017. Effects of clozapine on adipokine secretions/productions and lipid droplets in 3T3-L1 adipocytes. *J Pharmacol Sci*, 133, 79-87.
- TÜMMLER, C., SNAPKOV, I., WICKSTRÖM, M., MOENS, U., LJUNGBLAD, L., MARIA ELFMAN, L. H., WINBERG, J.-O., KOGNER, P., JOHNSEN, J. I. & SVEINBJÖRNSSON, B. 2017. Inhibition of chemerin/CMKLR1 axis in neuroblastoma cells reduces clonogenicity and cell viability in-vitro and impairs tumor growth in-vivo. *Oncotarget*, 8, 95135-95151.
- TRIPATHI, D., KANT, S., PANDEY, S. & EHTESHAM, N. Z. 2020. Resistin in metabolism, inflammation, and disease. *The FEBS Journal*, 287, 3141-3149.

- TRUSHINA, E. 2019. Alzheimer's disease mechanisms in peripheral cells: Promises and challenges. *Alzheimer's & dementia (New York, N. Y.)*, 5, 652-660.
- UBERTI, D., CARSANA, T., BERNARDI, E., RODELLA, L., GRIGOLATO, P., LANNI, C., RACCHI, M., GOVONI, S. & MEMO, M. 2002. Selective impairment of p53-mediated cell death in fibroblasts from sporadic Alzheimer's disease patients. *J Cell Sci*, 115, 3131-8.
- UDDIN, M. S., RAHMAN, M. M., SUFIAN, M. A., JEANDET, P., ASHRAF, G. M., BIN-JUMAH, M. N., MOUSA, S. A., ABDEL-DAIM, M. M., AKHTAR, M. F., SALEEM, A. & AMRAN, M. S. 2021. Exploring the New Horizon of AdipoQ in Obesity-Related Alzheimer's Dementia. *Frontiers in Physiology*, 11.
- UNGER, C., GAO, S., COHEN, M., JACONI, M., BERGSTROM, R., HOLM, F., GALAN, A., SANCHEZ, E., IRION, O., DUBUISSON, J. B., GIRY-LATERRIERE, M., SALMON, P., SIMON, C., HOVATTA, O. & FEKI, A. 2009. Immortalized human skin fibroblast feeder cells support growth and maintenance of both human embryonic and induced pluripotent stem cells. *Human Reproduction*, 24, 2567-2581.
- UPADHYAY, S., VAISH, S. & DHIMAN, M. 2019. Hydrogen peroxide-induced oxidative stress and its impact on innate immune responses in lung carcinoma A549 cells. *Mol Cell Biochem*, 450, 135-147.
- UTO-KONDO, H., OHMORI, R., KIYOSE, C., KISHIMOTO, Y., SAITO, H., IGARASHI, O. & KONDO, K. 2008. Tocotrienol Suppresses Adipocyte Differentiation and Akt Phosphorylation in 3T3-L1 Pre-adipocytes. *The Journal of Nutrition*, 139, 51-57.
- VAN ELDIK, L. J., CARRILLO, M. C., COLE, P. E., FEUERBACH, D., GREENBERG, B. D., HENDRIX, J. A., KENNEDY, M., KOZAUER, N., MARGOLIN, R. A., MOLINUEVO, J. L., MUELLER, R., RANSOHOFF, R. M., WILCOCK, D. M., BAIN, L. & BALES, K. 2016. The roles of inflammation and immune mechanisms in Alzheimer's disease. *Alzheimer's & Dementia: Translational Research & Clinical Interventions*, 2, 99-109.
- VAN DER KANT, R., GOLDSTEIN, L. S. B. & OSSENKOPPELE, R. 2020. Amyloid- β -independent regulators of tau pathology in Alzheimer disease. *Nat Rev Neurosci*, 21, 21-35.
- VAN MEERLOO, J., KASPERS, G. J. & CLOOS, J. 2011. Cell sensitivity assays: the MTT assay. *Methods Mol Biol*, 731, 237-45.

- VEAL, G. J., ERRINGTON, J., REDFERN, C. P., PEARSON, A. D. & BODDY, A. V. 2002. Influence of isomerisation on the growth inhibitory effects and cellular activity of 13-cis and all-trans retinoic acid in neuroblastoma cells. *Biochem Pharmacol*, 63, 207-15.
- VISHWANATH, D., SRINIVASAN, H., PATIL, M. S., SEETARAMA, S., AGRAWAL, S. K., DIXIT, M. N. & DHAR, K. 2013. Novel method to differentiate 3T3 L1 cells in-vitro to produce highly sensitive adipocytes for a GLUT4 mediated glucose uptake using fluorescent glucose analog. *Journal of cell communication and signaling*, 7, 129-140.
- VOHRA, M. S., AHMAD, B., SERPELL, C. J., PARHAR, I. S. & WONG, E. H. 2020. Murine in-vitro cellular models to better understand adipogenesis and its potential applications. *Differentiation*, 115, 62-84.
- WAN, Z., MAH, D., SIMTCHOUK, S., KLUFTINGER, A. & LITTLE, J. P. 2015. Human adipose tissue conditioned media from lean subjects is protective against H₂O₂ induced neurotoxicity in human SH-SY5Y neuronal cells. *International journal of molecular sciences*, 16, 1221-1231.
- WANG, P., MARIMAN, E., KEIJER, J., BOUWMAN, F., NOBEN, J. P., ROBBEN, J. & RENES, J. 2004. Profiling of the secreted proteins during 3T3-L1 adipocyte differentiation leads to the identification of novel adipokines. *Cell Mol Life Sci*, 61, 2405-17.
- WANG, Y., SONG, T. & LU, M. 2002. Setting up Alzheimer disease cell apoptosis model with PC-12 cell induced by A β (25-35). *Journal of Xi'an Medical University*, 23, 129-132.
- WANG, X., HUA, T. C., SUN, D. W., LIU, B., YANG, G. & CAO, Y. 2007. Cryopreservation of tissue-engineered dermal replacement in Me₂SO: Toxicity study and effects of concentration and cooling rates on cell viability. *Cryobiology*, 55, 60-5.
- WANG, Y., ULLAND, T. K., ULRICH, J. D., SONG, W., TZAFERIS, J. A., HOLE, J. T., YUAN, P., MAHAN, T. E., SHI, Y., GILFILLAN, S., CELLA, M., GRUTZENDLER, J., DEMATTOS, R. B., CIRRITO, J. R., HOLTZMAN, D. M. & COLONNA, M. 2016. TREM2-mediated early microglial response limits diffusion and toxicity of amyloid plaques. *Journal of Experimental Medicine*, 213, 667-675.

- WANG, Y., BRANICKY, R., NOË, A. & HEKIMI, S. 2018. Superoxide dismutases: Dual roles in controlling ROS damage and regulating ROS signaling. *Journal of Cell Biology*, 217, 1915-1928.
- WAY, J. M., GÖRGÜN, C. Z., TONG, Q., UYSAL, K. T., BROWN, K. K., HARRINGTON, W. W., OLIVER, W. R., JR., WILLSON, T. M., KLIEWER, S. A. & HOTAMISLIGIL, G. S. 2001. Adipose tissue resistin expression is severely suppressed in obesity and stimulated by peroxisome proliferator-activated receptor gamma agonists. *J Biol Chem*, 276, 25651-3.
- WARING, S. C. & ROSENBERG, R. N. 2008. Genome-wide association studies in alzheimer disease. *Archives of Neurology*, 65, 329-334.
- WASIM, M., AWAN, F. R., NAJAM, S. S., KHAN, A. R. & KHAN, H. N. 2016. Role of Leptin Deficiency, Inefficiency, and Leptin Receptors in Obesity. *Biochemical Genetics*, 54, 565-572.
- WATTMO, C., MINSTHON, L. & WALLIN Å, K. 2016. Mild versus moderate stages of Alzheimer's disease: three-year outcomes in a routine clinical setting of cholinesterase inhibitor therapy. *Alzheimers Res Ther*, 8. WISEMAN, F. K., PULFORD, L. J., BARKUS, C., LIAO, F., PORTELIUS, E., WEBB, R., CHÁVEZ-GUTIÉRREZ, L., CLEVERLEY, K., NOY, S., SHEPPARD, O., COLLINS, T., POWELL, C., SARELL, C. J., RICKMAN, M., CHOONG, X., TOSH, J. L., SIGANPORIA, C., WHITTAKER, H. T., STEWART, F., SZARUGA, M., LONDON DOWN SYNDROME, C., MURPHY, M. P., BLENNOW, K., DE STROOPER, B., ZETTERBERG, H., BANNERMAN, D., HOLTZMAN, D. M., TYBULEWICZ, V. L. J., FISHER, E. M. C. & LONDOWN, S. C. 2018. Trisomy of human chromosome 21 enhances amyloid- β deposition independently of an extra copy of APP. *Brain : a journal of neurology*, 141, 2457-2474.
- WAY, J. M., GÖRGÜN, C. Z., TONG, Q., UYSAL, K. T., BROWN, K. K., HARRINGTON, W. W., OLIVER, W. R., JR., WILLSON, T. M., KLIEWER, S. A. & HOTAMISLIGIL, G. S. 2001. Adipose tissue resistin expression is severely suppressed in obesity and stimulated by peroxisome proliferator-activated receptor gamma agonists. *J Biol Chem*, 276, 25651-3.
- WEI, T., CHEN, C., HOU, J., XIN, W. & MORI, A. 2000. Nitric oxide induces oxidative stress and apoptosis in neuronal cells. *Biochimica et Biophysica Acta (BBA) - Molecular Cell Research*, 1498, 72-79.

- WEILER, M., STIEGER, K. C., LONG, J. M. & RAPP, P. R. 2020. Transcranial Magnetic Stimulation in Alzheimer's Disease: Are We Ready? *eNeuro*, 7.
- WEN, Y., LU, P. & DAI, L. 2013. Association between resistin gene -420 C/G polymorphism and the risk of type 2 diabetes mellitus: a meta-analysis. *Acta Diabetologica*, 50, 267272.
- WENK, G. L. 2006. Neuropathologic changes in Alzheimer's disease: potential targets for treatment. *J Clin Psychiatry*, 67 Suppl 3, 3-7; quiz 23.
- WELLER, J. & BUDSON, A. 2018. Current understanding of Alzheimer's disease diagnosis and treatment. *F1000Res*, 7.
- WITTAMER, V., FRANSSSEN, J. D., VULCANO, M., MIRJOLET, J. F., LE POUL, E., MIGEOTTE, I., BRÉZILLON, S., TYLDESLEY, R., BLANPAIN, C., DETHEUX, M., MANTOVANI, A., SOZZANI, S., VASSART, G., PARMENTIER, M. & COMMUNI, D. 2003. Specific recruitment of antigen-presenting cells by chemerin, a novel processed ligand from human inflammatory fluids. *J Exp Med*, 198, 977-85.
- WORLD HEALTH ORGANISATION (2017) *Alzheimer's Disease International*. Available at: <https://www.alzint.org/about/dementia-facts-figures/dementia-statistics/> (Accessed on 03 March 2021).
- WORLD HEALTH ORGANISATION (2020) *Global dementia Observatory*. Available at: <https://apps.who.int/gho/data/node.dementia> (Accessed on 10 March 2020).
- XICOY, H., WIERINGA, B. & MARTENS, G. J. M. 2017. The SH-SY5Y cell line in Parkinson's disease research: a systematic review. *Molecular Neurodegeneration*, 12, 10.
- XIE, H. R., HU, L. S. & LI, G. Y. 2010. SH-SY5Y human neuroblastoma cell line: in-vitro cell model of dopaminergic neurons in Parkinson's disease. *Chin Med J (Engl)*, 123, 108692.
- XU, W. L., ATTI, A. R., GATZ, M., PEDERSEN, N. L., JOHANSSON, B. & FRATIGLIONI, L. 2011. Midlife overweight and obesity increase late-life dementia risk: a populationbased twin study. *Neurology*, 76, 1568-1574.

- YAGI, T., ITO, D., OKADA, Y., AKAMATSU, W., NIHEI, Y., YOSHIZAKI, T., YAMANAKA, S., OKANO, H. & SUZUKI, N. 2011. Modeling familial Alzheimer's disease with induced pluripotent stem cells. *Hum Mol Genet*, 20, 4530-9.
- YIANNOPOULOU, K. G. & PAPAGEORGIOU, S. G. 2020. Current and Future Treatments in Alzheimer Disease: An Update. *Journal of central nervous system disease*, 12, 1179573520907397-1179573520907397.
- YOON, S.-B., LEE, G., PARK, S. B., CHO, H., LEE, J.-O. & KOH, B. 2020. Properties of differentiated SH-SY5Y grown on carbon-based materials. *RSC Advances*, 10, 19382-19389.
- YOUSSEF, P., CHAMI, B., LIM, J., MIDDLETON, T., SUTHERLAND, G. T. & WITTING, P. K. 2018. Evidence supporting oxidative stress in a moderately affected area of the brain in Alzheimer's disease. *Scientific Reports*, 8, 11553.
- YUAN, Q., REN, C., XU, W., PETRI, B., ZHANG, J., ZHANG, Y., KUBES, P., WU, D. & TANG, W. 2017. PKN1 Directs Polarized RAB21 Vesicle Trafficking via RPH3A and Is Important for Neutrophil Adhesion and Ischemia-Reperfusion Injury. *Cell Rep.*, 19, 2586.
- ZEBISCH, K., VOIGT, V., WABITSCH, M. & BRANDSCH, M. 2012. Protocol for effective differentiation of 3T3-L1 cells to adipocytes. *Analytical Biochemistry*, 425, 88-90.
- ZHANG, Y., PROENCA, R., MAFFEI, M., BARONE, M., LEOPOLD, L. & FRIEDMAN, J. M. 1994. Positional cloning of the mouse obese gene and its human homologue. *Nature*, 372, 425-432.
- ZHANG, Z. Y. & WANG, M. W. 2012. Obesity, a health burden of a global nature. *Acta Pharmacol Sin*, 33, 145-7.
- ZHANG, Z., GUO, M., ZHANG, J., DU, C. & XING, Y. 2016. Leptin Regulates Tau Phosphorylation through Wnt Signaling Pathway in PC12 Cells. *Neurosignals*, 24, 95-101.

- ZHANG, Y., XU, N., DING, Y., DOYCHEVA, D. M., ZHANG, Y., LI, Q., FLORES, J., HAGHIGHIABYANEH, M., TANG, J. & ZHANG, J. H. 2019. Chemerin reverses neurological impairments and ameliorates neuronal apoptosis through ChemR23/CAMKK2/AMPK pathway in neonatal hypoxic–ischemic encephalopathy. *Cell Death & Disease*, 10, 97.
- ZHANG, Q., SIDORENKO, J., COUVY-DUCHESNE, B., MARIONI, R. E., WRIGHT, M. J., GOATE, A. M., MARCORI, E., HUANG, K.-L., PORTER, T., LAWS, S. M., MASTERS, C. L., BUSH, A. I., FOWLER, C., DARBY, D., PERTILE, K., RESTREPO, C., ROBERTS, B., ROBERTSON, J., RUMBLE, R., RYAN, T., COLLINS, S., THAI, C., TROUNSON, B., LENNON, K., LI, Q.-X., UGARTE, F. Y., VOLITAKIS, I., VOVOS, M., WILLIAMS, R., BAKER, J., RUSSELL, A., PERETTI, M., MILICIC, L., LIM, L., RODRIGUES, M., TADDEI, K., TADDEI, T., HONE, E., LIM, F., FERNANDEZ, S., RAINEY-SMITH, S., PEDRINI, S., MARTINS, R., DOECKE, J., BOURGEAT, P., FRIPP, J., GIBSON, S., LEROUX, H., HANSON, D., DORE, V., ZHANG, P., BURNHAM, S., ROWE, C. C., VILLEMAGNE, V. L., YATES, P., PEJOSKA, S. B., JONES, G., AMES, D., CYARTO, E., LAUTENSCHLAGER, N., BARNHAM, K., CHENG, L., HILL, A., KILLEEN, N., MARUFF, P., SILBERT, B., BROWN, B., SOHRABI, H., SAVAGE, G., VACHER, M., SACHDEV, P. S., MATHER, K. A., ARMSTRONG, N. J., THALAMUTHU, A., BRODATY, H., YENGO, L., YANG, J., WRAY, N. R., MCRAE, A. F., VISSCHER, P. M., AUSTRALIAN IMAGING, B. & LIFESTYLE, S. 2020. Risk prediction of late-onset Alzheimer's disease implies an oligogenic architecture. *Nature Communications*, 11, 4799.
- ZHOU, Y., LI, H. & XIA, N. 2021. The Interplay Between Adipose Tissue and Vasculature: Role of Oxidative Stress in Obesity. *Frontiers in Cardiovascular Medicine*, 8.
- ZHU, X.-C., TAN, L., WANG, H.-F., JIANG, T., CAO, L., WANG, C., WANG, J., TAN, C.-C., MENG, X.-F. & YU, J.-T. 2015. Rate of early onset Alzheimer's disease: a systematic review and meta-analysis. *Annals of translational medicine*, 3, 38-38.
- ZEBISCH, K., VOIGT, V., WABITSCH, M. & BRANDSCH, M. 2012. Protocol for effective differentiation of 3T3-L1 cells to adipocytes. *Analytical Biochemistry*, 425, 88-90.
- ŻÓŁKIEWICZ, J., STOCHMAL, A. & RUDNICKA, L. 2019. The role of adipokines in systemic sclerosis: a missing link? *Archives of Dermatological Research*, 311, 251-263.

ZORENA, K., JACHIMOWICZ-DUDA, O., ŚLEZAK, D., ROBAKOWSKA, M. & MRUGACZ, M. 2020. Adipokines and Obesity. Potential Link to Metabolic Disorders and Chronic Complications. *International journal of molecular sciences*, 21, 3570.

ZMEŠKALOVÁ, A., POPELOVÁ, A., EXNEROVÁ, A., ŽELEZNÁ, B., KUNEŠ, J. & MALETÍNSKÁ, L. 2020. Cellular Signaling and Anti-Apoptotic Effects of Prolactin-Releasing Peptide and Its Analog on SH-SY5Y Cells. *International journal of molecular sciences*, 21, 6343.